

Development of a Side Impact Sled Test Method using Multiple Actuators

Akira Kinoshita

Naoki Shigeno

Hiroshi Kuniyuki

Nissan Motor Co., Ltd.

Japan

Hermann Steffan

Dr. Steffan Datentechnik Ges.m.b.H.

Austria

Paper Number 11-0072

ABSTRACT

This paper describes a new test method for predicting Anthropomorphic Test Dummy responses to calculate injury index in side impact tests with a moving deformable barrier (MDB). Sled tests are effective in shortening the development period for more safety vehicle equipped with side impact safety devices and reducing the cost and period needed to prepare prototype test vehicles. To accomplish sled tests successfully, it is necessary to simulate the complex door deformation behavior which changes different in dummy response regions by impacting with a MDB. Conventional sled test methods simulated roughly the intrusion of the entire door using a single actuator. The methods limited the dummy response regions which can be predicted because it was difficult to simulate the door deformation behavior.

The new sled test method using the **Advanced Side Impact Simulator (ASIS)** was developed by identifying the door intrusion behavior needed to predict each dummy response. Multiple actuators were used to simulate door deformation behavior of each dummy response region. High-output actuators were used to simulate the intrusion of the rapidly accelerating door in the initial phase. A feedback control function was used to regulate the door and seat velocities of the actuators so that they would simulate the input velocity profile even if they were acted on by the reaction force of the dummy or other parts. A comparison of dummy responses obtained in ASIS tests and in vehicle tests showed good agreement. This confirmed that the new test method is capable of predicting each dummy response with high accuracy.

INTRODUCTION

There are two principal factors that determine dummy responses in side impact tests. One factor is the body structure of the impacted vehicle. The body structure reducing the body deformation and the crash forces applied to the dummy result in reducing dummy responses. Another factor is side impact

safety devices such as a door trim and a side airbag. The devices reducing the crash forces applied to the dummy result in reducing dummy responses. It is essential that the devices are effective in various types of real-world accident configurations. [1]

Developing more safety vehicle equipped with side impact safety devices involves a process of trial and error in order to find the optimum combination of design variables. If that process could be carried out in sled tests, it would be possible to reduce the cost and period needed to prepare prototype test vehicles. Toward that end, various methods of conducting side impact sled tests have been developed to date. [2] To accomplish sled tests successfully, it is necessary to simulate the complex door deformation behavior which changes different in dummy response regions by impacting with a MDB. Conventional sled test methods simulated roughly the intrusion of the entire door using a single actuator. The methods limited the dummy response regions which can be predicted because it was difficult to simulate the door deformation behavior. Moreover, in order to predict dummy responses with more regions, the input profiles, initial layout and initial door metal shapes must be modified, thereby complicating the design of the sled test and making it difficult to obtain sufficiently reliable test results. [3]

This paper describes a new test method predicting each dummy response region. Vehicle test data are also presented to verify the prediction accuracy of the dummy responses obtained with the proposed method.

TEST METHOD

The key factors used in predicting dummy response in this test method are the door deformation, which applies force to the dummy via the door trim and the side airbag, and the deformation of the seat that houses the side airbag. However, the door deformation is complex, and the intrusion depth toward the interior of the vehicle varies from one part of the door to another. To take such differences into account, ASIS shown in Figures 1 and 2 was developed. Multiple actuators were used to simulate

door deformation behavior of each dummy response region. Each actuator incorporated a hydraulic brake device for simulating the door intrusion velocity. Another actuator was also used to simulate seat behavior in the lateral direction. These multiple actuators were synchronized and controlled based on the operating velocity profile input into each one.

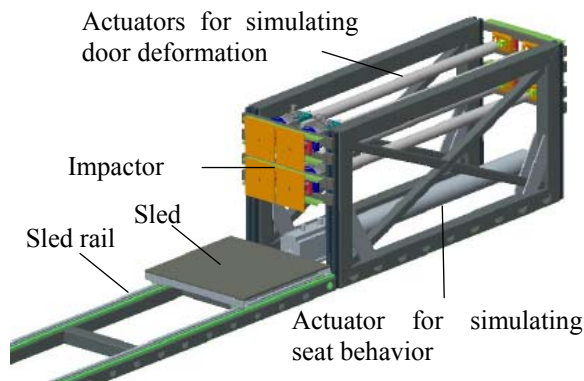


Figure 1. Structure of ASIS.



Figure 2. Photo of ASIS.

1. Simulation of complex door deformation

The principal dummy responses are related to chest deflection, abdominal deflection, abdominal force and pelvic force. The door deformation characteristics needed to predict dummy responses in these regions were summarized, and the optimum positions of the actuators for simulating the characteristics were determined.

In this study, computer simulations of dummy responses by using a FE dummy model were conducted to optimize the number and positions of the actuators. The chest, abdomen, pelvis and knee were selected as typical regions where impact forces are input to a dummy. The door deformation was simulated using from one to four actuators. Then the obtained dummy responses were compared with corresponding data recorded in vehicle tests. Figure 3 shows the input conditions considered in the simulations; Figure 4 presents the input profiles to each region resulted from previously conducted vehicle tests; and Figure 5 shows the relationship

between the dummy responses and the number of actuators used in the computer simulations. The results in Figure 5-a) indicate the difficulty in simulating the dummy responses in all four regions with a conventional approach using only one actuator. Moreover, door deformation extending from the chest to the pelvis must be simulated in order to predict the dummy responses of the chest and abdomen (Figure 5-b), 5-c)). In order to predict the dummy responses of the pelvis, it is necessary to simulate door deformation as far as the knee, in addition to the chest, abdomen and pelvis regions (Figure 5-d)).

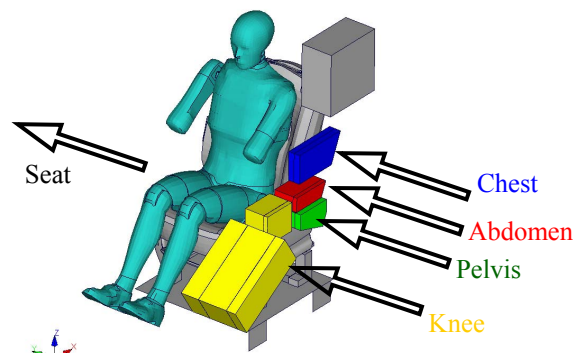


Figure 3. Input conditions of door and seat for computer simulation.

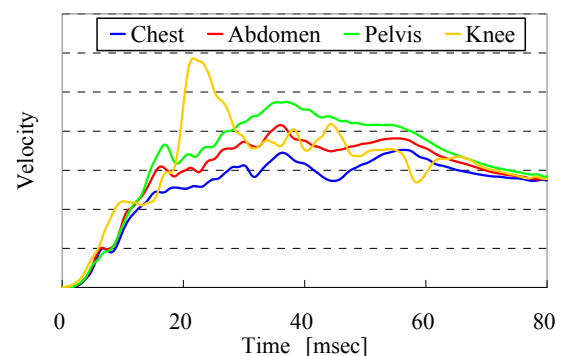


Figure 4. Input profiles for computer simulation.

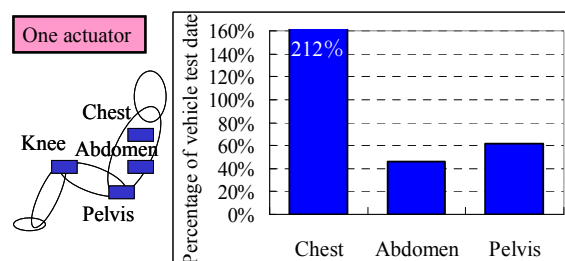


Figure 5-a). One actuator

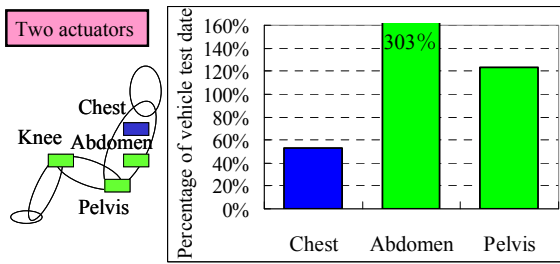


Figure 5-b). Two actuators

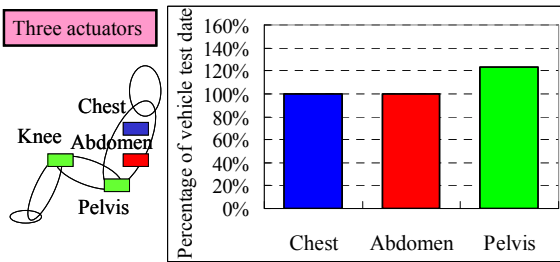


Figure 5-c). Three actuators

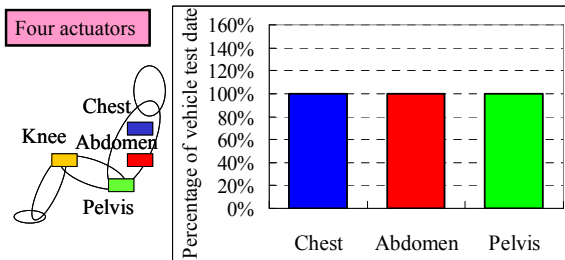


Figure 5-d). Four actuators

Figure 5. Relationship between number of actuators and dummy responses in computer simulation.

However, door deformation in the regions corresponding to the chest, abdomen and pelvis cannot be simulated simply by using three actuators. To simulate intrusion of rapidly accelerating door, it is necessary to use an actuator with a large outer diameter. That would not allow separate intrusion to be applied to the chest, abdomen and pelvis. Accordingly, the actuators for the chest and pelvis regions were used to produce door deformation corresponding to the abdomen region. Two actuators for the chest and pelvis regions were used to apply to the chest, abdomen and pelvis of dummy. In addition, one actuator was used to apply force to the knee region, which contributes substantially to pelvis response.

Figure 6 presents profile of the door deformation in the chest, abdomen and pelvis regions in a vehicle test and profile in result of simulating the door deformation by using two actuators in the ASIS. It measured at 10-msec. intervals from 0 to 60 msec. The vehicle test data indicate that door intrusion depth changes different in the chest, abdomen and pelvis regions. In order to simulate the door deformation by using two actuators for the chest and

pelvis regions, the position of division of the abdomen region was essential. It was determined by two factors. One factor is simulation of profile change in door deformation of the each region. The position was determined in Figure 6 to reduce the differences of profile between vehicle test and ASIS simulation most. Another factor is the relative position of the MDB to the door. The bumper and taper of the MDB is the strong relationship with the door deformation.

Figure 7 shows the ASIS impactor that was devised on the basis of the simulation results in Figure 5 and 6. The impactor was divided into three sections in order to simulate the different intrusion depth of the door by using three actuators corresponding to the chest, pelvis and knee regions. The impactor simulates the shapes of the door metal parts.

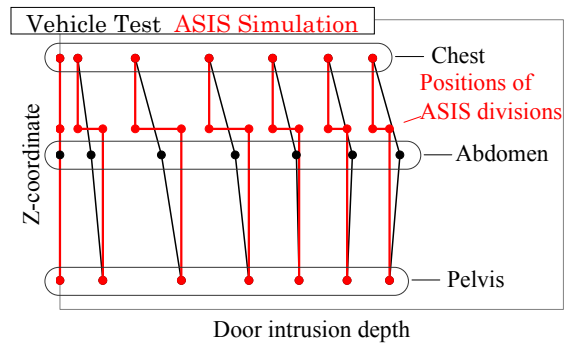


Figure 6. Comparison of profile of door deformation in the vehicle test and result of simulation in the ASIS.

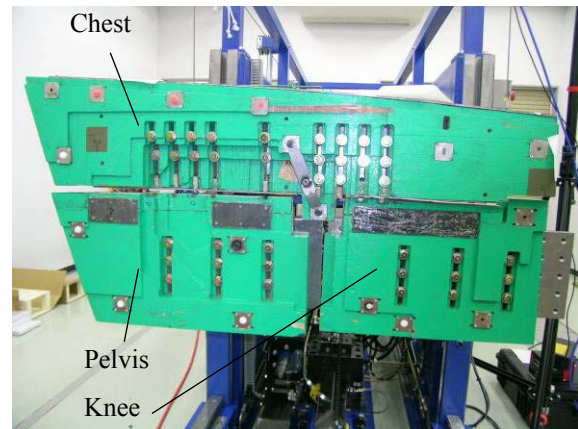


Figure 7. ASIS impactor.

2. Simulation of intrusion of rapidly accelerating door in the initial phase

Figure 8 shows the door and seat intrusion velocities recorded in a vehicle test and the input profiles of an ASIS test. As seen in Figure 9, there is a space between the door trim and the seat in the initial phase from 0 to 20 msec. The side airbag deploys in this initial phase. In order to simulate dummy responses, it is necessary to simulate the intrusion of the rapidly accelerating door, the deployment behavior of the

side airbag and the effect of the side airbag on reducing the force input to dummy.

To accomplish that, the high-output actuators were used. In addition, the actuators were reduced in size and mass because multiple actuators were used. These changes made it possible to simulate the intrusion of the rapidly accelerating door in initial phase, as shown in Figure 8. As a result, the simulated deployment behavior of the side airbag agreed with the vehicle test results, as seen in Figure 10. The deployment behavior higher than shoulder was different because the chest actuator was also used for the region higher than shoulder. But the deployment behavior of each dummy region agreed well.

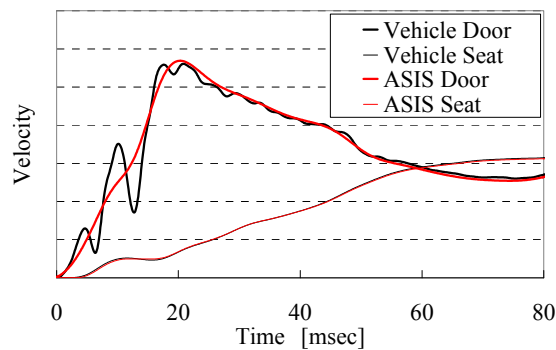


Figure 8. Velocity profiles door and seat.

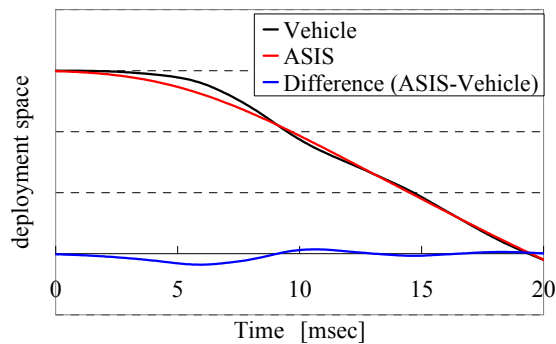


Figure 9. Deployment space of side airbag.

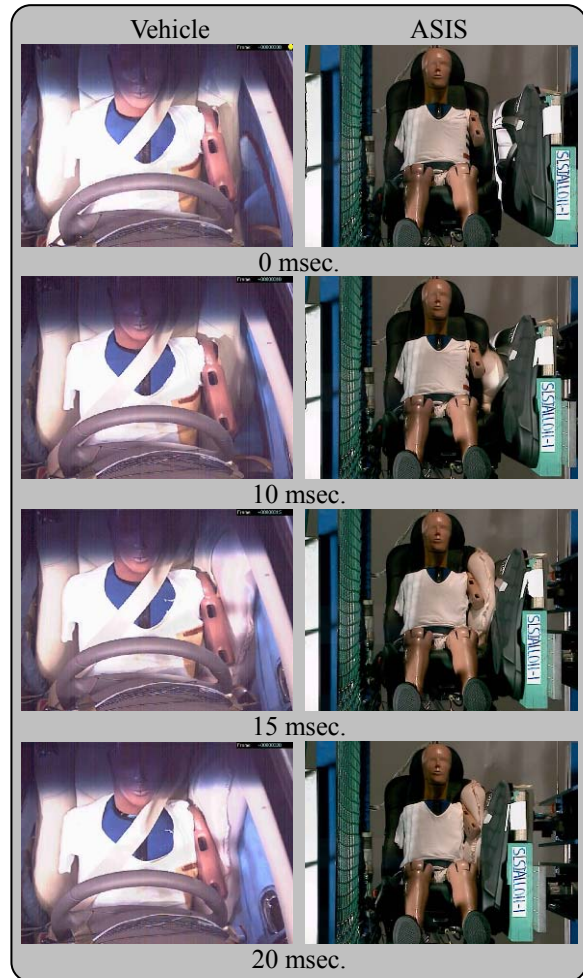


Figure 10. Side airbag deployment behavior.

3. Simulation of door and seat velocities by a feedback control function

A feedback control function was used to regulate the door and seat velocities of the actuators so that they would simulate the input velocity profile even if they were acted on by the reaction force of the dummy or other parts. Contact with the dummy or other parts causes the actuator velocities to decline substantially. A feedback control function was used for increasing the acceleration force of the actuators instantaneously so as to enable them to operate according to the input profiles. As a result, the door and seat velocities were simulated.

TEST SETUP

In the conventional methods, the velocity profiles, part shapes and layout, and other elements input for the purpose of predicting dummy responses have tended to differ from vehicle tests. One feature of this new method is that the input velocity profiles, part shapes and layout are all designed to agree with those of vehicle tests.

1. Design of door and seat input profiles

The input profiles were designed according to the acceleration data of previously conducted vehicle tests and computer simulations. A low-pass filter was used to remove the high acceleration components that could not be reproduced because of the limitations of the test equipment.

2. Design of impactor

The impactor simulates the shapes of the door metal parts. The impactor was divided into three sections. Two actuators for the chest and pelvis regions were used to apply to the chest, abdomen and pelvis of dummy. In addition, one actuator was used to apply force to the knee region, which contributes substantially to pelvis response. The position of division of the abdomen region was determined by two factors. One factor is simulation of profile change in door deformation. The position was determined in Figure 6 to reduce differences of shape between vehicle and ASIS most. Another factor is the relative position of the MDB to the door. The bumper and taper of the MDB is the strong relationship with the door deformation.

3. Design of part shapes and layout

Table 1 lists the parts needed to conduct a test. The part shapes and the layout were all designed to agree with those of vehicle. The asterisk (*) shows that the parts are not needed in the case with the vehicle targeted by the verification of this method.

Table 1. List of the parts

Parts	Needed or Not
Seat	Needed
Side Airbag	Needed
Door Trim	Needed
Seat Belt	Not Needed*
Curtain Airbag	Not Needed*
B-Pillar	Not Needed*

RESULTS AND DISCUSSION

1. Test configuration

ASIS tests were conducted in order to verify the results in comparison with vehicle test data. Table 2 lists the test configuration conducted.

Table 2. Test configuration

IIHS	EuroNCAP
MDB	MDB
50 km/h	55 km/h
Driver	Driver
SID-IIs Level D	ES-2

2. IIHS

The vehicle test data and the ASIS test results were compared with regard to the SID-IIs dummy responses under the IIHS configuration.

Figure 11 shows the door velocity profile in the vehicle test and the velocity profiles input into the ASIS actuators. Figure 12 compares the door deformation of the chest, abdomen and pelvis regions between the vehicle test and ASIS test.

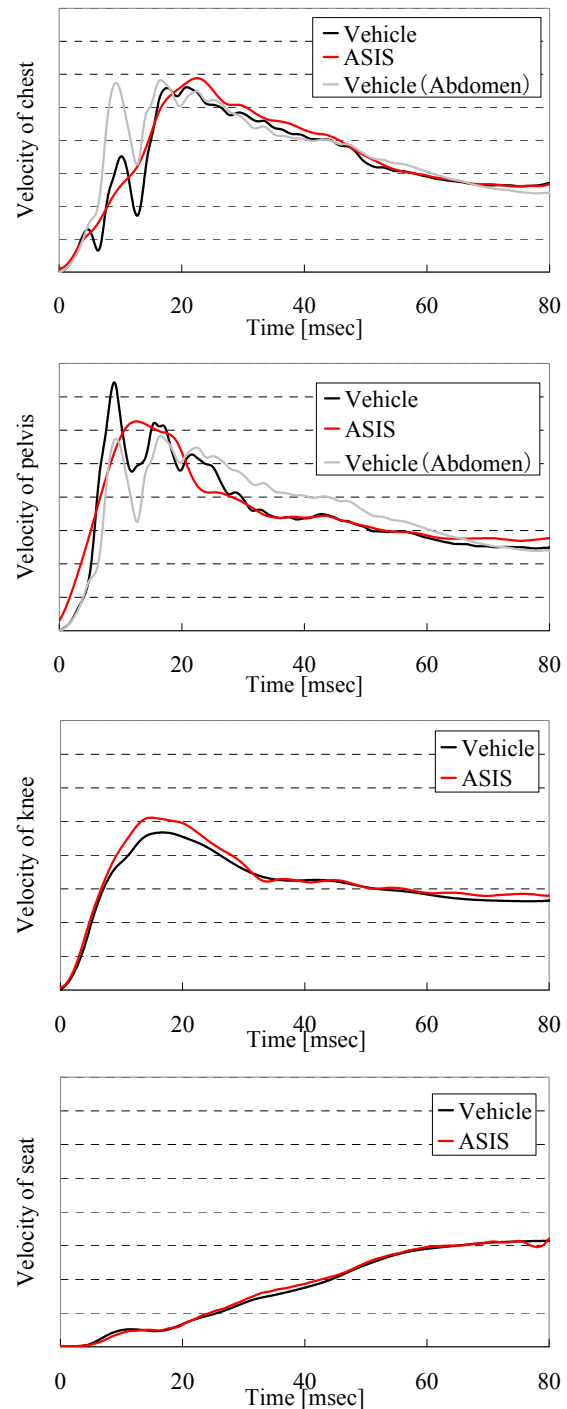


Figure 11. Velocity profiles of door and seat (IIHS).

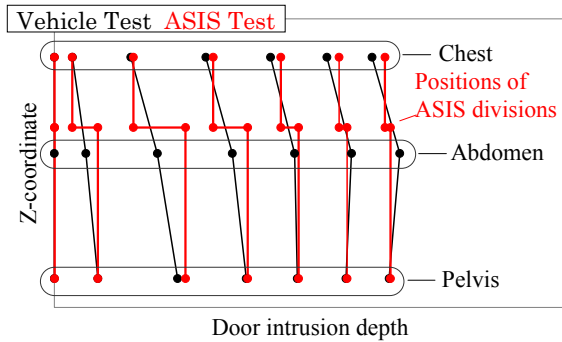


Figure 12. Door deformation in chest, abdomen and pelvis regions (IHS).

Figure 13 compares the dummy responses in the vehicle test and the ASIS test. The ASIS test data are shown as a percentage of the vehicle test data. The percentage of each rib deflection, acetabulum force, and distal femur moment are all within $\pm 5\%$ of the vehicle test data. The ASIS test data for the distal femur force and the iliac force are approximately 115% and 150% of the corresponding vehicle test data.

Figures 14-20 compare the dummy response profiles in the vehicle test and in the ASIS test. The dummy responses profiles of the ASIS for each rib deflection (Figures 14-15), force (Figure 16) agree well with the corresponding vehicle test profiles. This agreement is attributed to accurate simulation of the door deformation using the multiple actuators, the intrusion of the rapidly accelerating door using the high-output actuators and the input velocity profile using a feedback control function. It is also attributed to accurate simulation of the door deformation needed to reproduce dummy responses.

However, differences are seen for shoulder rib deflection, upper chest rib deflection, acetabulum force, viscous criterion (Figure 17-18) and deflection rate (Figure 19-20). Compared with the other dummy response regions, the ASIS test did not sufficiently reproduce the dummy responses. Two reasons for that can presumably be understood. One reason is number of actuator. Since only three actuators were used to simulate door deformation, just one actuator of chest was used for chest and shoulder regions. As a result, the force input from the door to the upper chest and shoulder rib regions could not be simulated. It was found that in order to reproduce the upper chest and shoulder rib responses, it is necessary to simulate the door deformation more accurately using more actuators. Accordingly, it is necessary to reduce the outer diameter of the actuator. Another reason is low-pass filtering of the input profiles. The difference in the input profiles presumably had a large effect on the viscous criterion and deflection rate. It was explained earlier with regard to the test setup of input profiles that low-pass filtering was done to remove high acceleration components. The filtering process was performed within a range that would not affect the simulation of dummy responses.

It was found that in order to reproduce the viscous criterion and deflection rate, it is necessary to simulate the high acceleration components that cannot be replicated due to the limitations of the ASIS equipment. Accordingly, it is necessary to increase the output of the actuators and reduce the mass of the impactor shown in Figure 7.

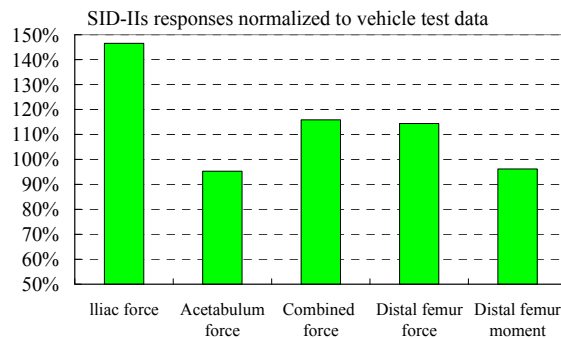
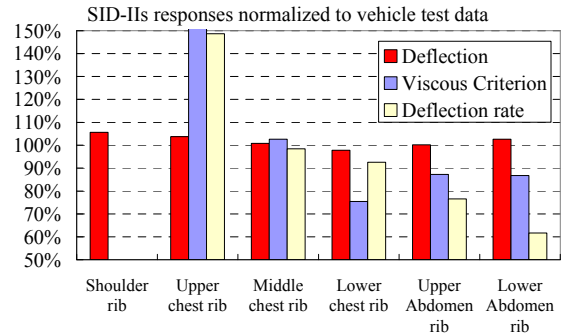


Figure 13. Dummy responses (IHS).

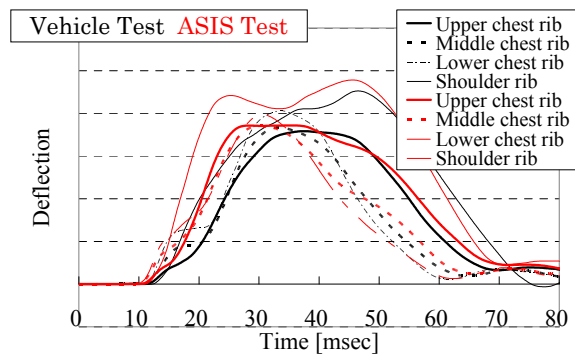


Figure 14. Shoulder and chest rib deflection (IHS).

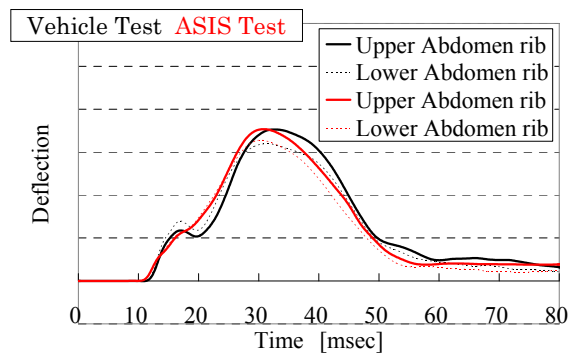


Figure 15. Abdomen rib deflection (IHS).

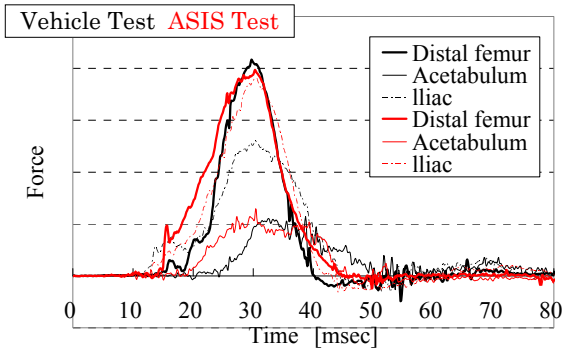


Figure 16. Pelvis force (IIHS).

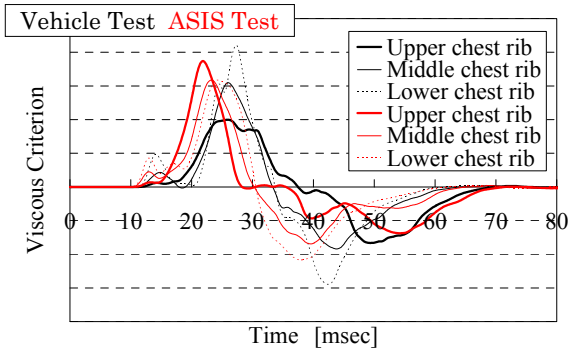


Figure 17. Chest rib viscous criterion (IIHS).

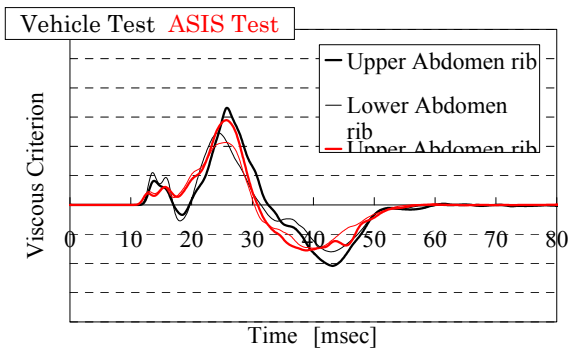


Figure 18. Abdomen rib viscous criterion (IIHS).

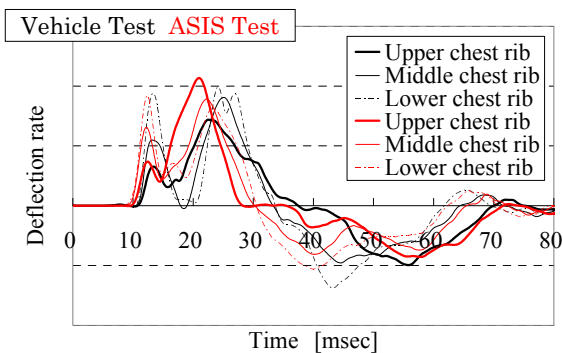


Figure 19. Chest rib deflection rate (IIHS).

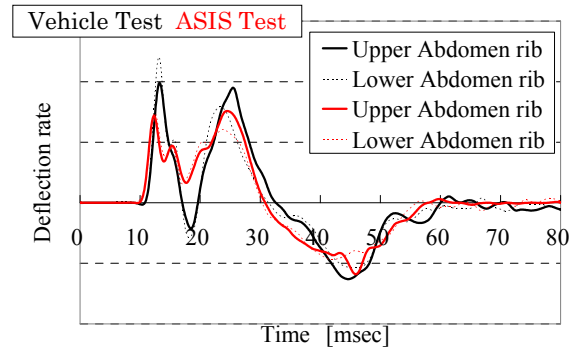
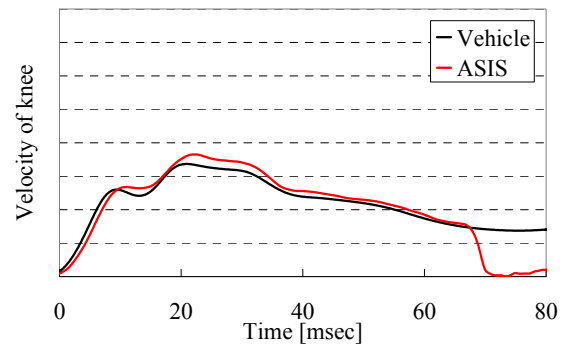
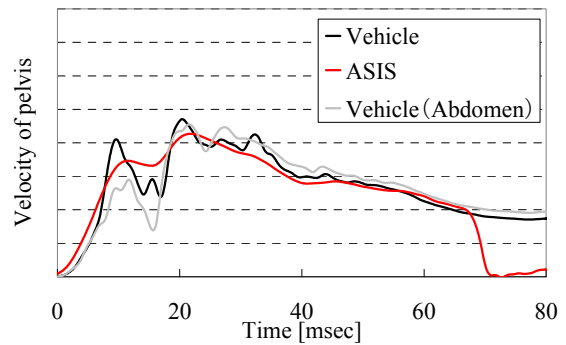
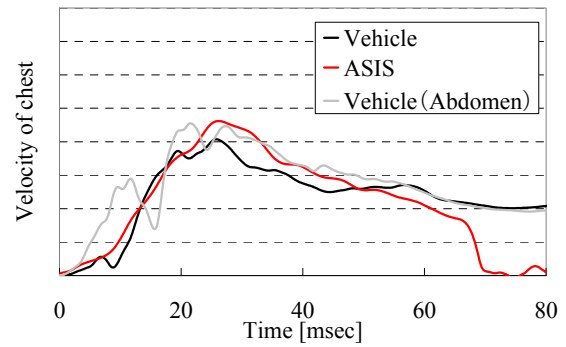


Figure 20. Abdomen rib deflection rate (IIHS).

3. EuroNCAP

The vehicle test data and the ASIS test results were then compared with regard to the ES-2 dummy responses under the EuroNCAP configuration.

Figure 21 shows the door velocity profile in the vehicle test and the velocity profiles input into the ASIS actuators. Figure 22 compares the door deformation of the chest, abdomen and pelvis regions between the vehicle test and ASIS test.



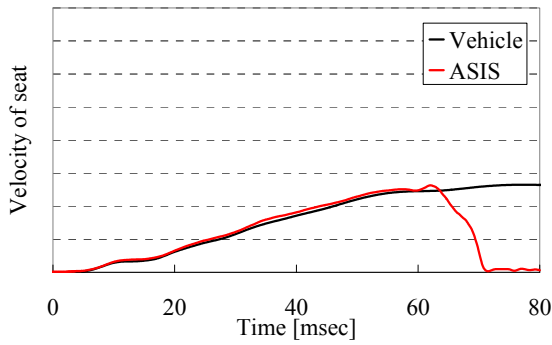


Figure 21. Velocity profiles of door and seat (EuroNCAP).

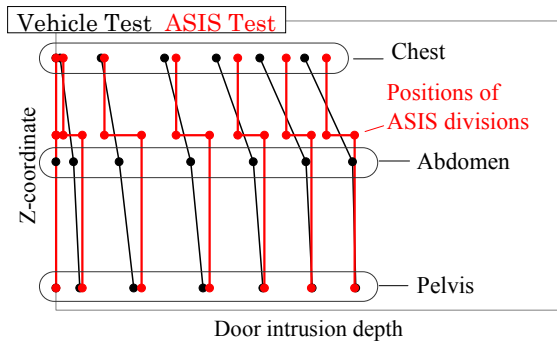


Figure 22. Door deformation in chest, abdomen and pelvis regions (EuroNCAP).

Figure 23 compares the dummy responses in the vehicle test and ASIS test. The ASIS test data are shown as a percentage of the vehicle test data. The ASIS test data of the lower rib viscous criterion is approximately 150% of the vehicle test data. The other dummy responses of ASIS are all within $\pm 10\%$ of the vehicle test data.

Figures 24-27 compare the dummy response profiles in the vehicle test and in the ASIS test. Similar to the results seen for the SID-II's dummy, the ASIS results for deflection (Figure 24) and force (Figures 26-27) reproduce the vehicle test data well. On the other hand, differences are seen in the viscous criterion profiles (Figure 25). The ASIS results do not reproduce the vehicle test data with sufficient accuracy. Similar to the case for the SID-II's dummy, two factors seem necessary. One is simulation of the door deformation more accurately using more actuators by reducing the outer diameter of the actuator. Another is less filtering of the input data by increasing the output of the actuators and reducing the mass of the impactor shown in Figure 7.

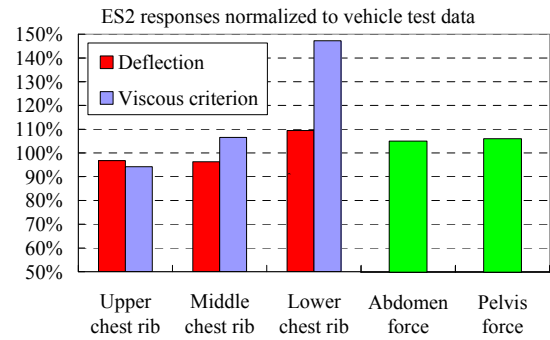


Figure 23. Dummy responses (EuroNCAP).

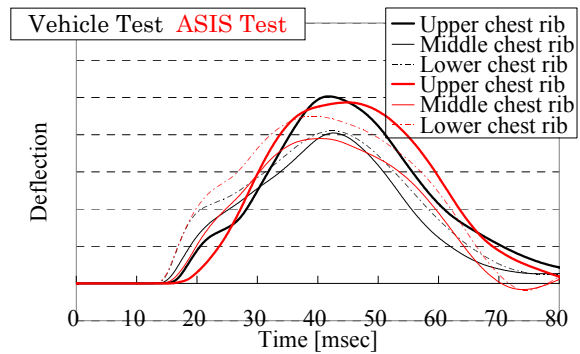


Figure 24. Chest deflection (EuroNCAP).

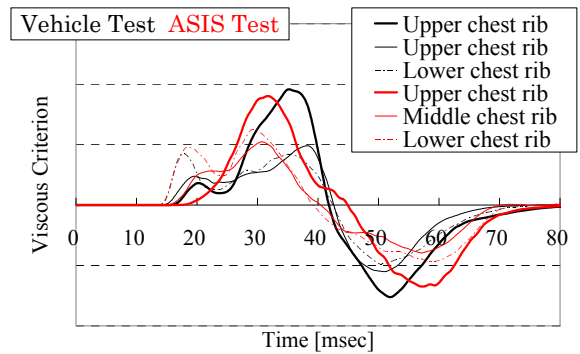


Figure 25. Viscous criterion (EuroNCAP).

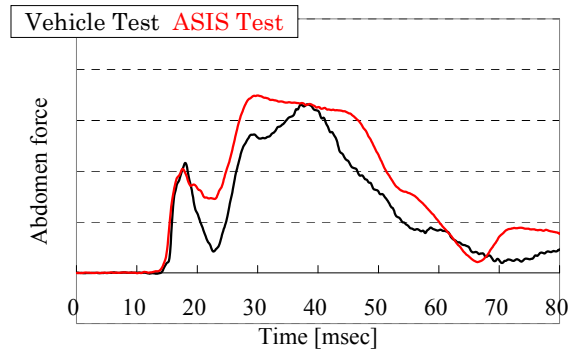


Figure 26. Abdomen force (EuroNCAP).

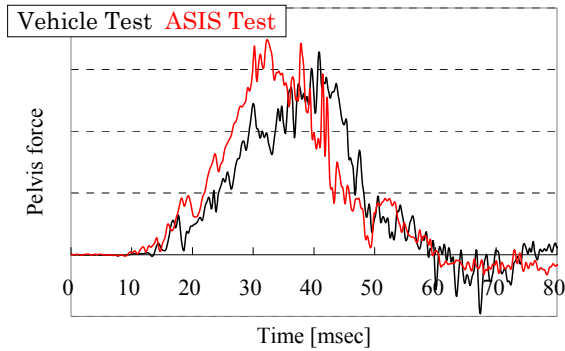


Figure 27. Pelvis force (EuroNCAP).

[3] H. Ikeno et al. "Side impact sled test method for investigation to reduce injury index", ESV18th Paper No. 266.

CONCLUSION

This paper describes a new test method for predicting each dummy response. This method, called the ASIS, has following features to simulate the door deformation behavior needed to predict each dummy response.

- Multiple actuators were used to simulate door deformation behavior.
- High-output actuators were used to simulate the intrusion of the rapidly accelerating door.
- A feedback control function was used to regulate the door and seat velocities of the actuators.

The position of door division is essential in using multiple actuators and was determined for two factors. One factor is door deformation at the positions of each dummy region. Another factor is relative position of the MDB to the door.

The ASIS test data obtained with the SID-II's dummy for each deflection, acetabulum force and the distal femur moment agreed well with the vehicle test data and were within $\pm 5\%$ of the latter. The ASIS test data obtained with the ES-2 dummy for chest deflection, abdomen force and pelvis force also agreed well with the vehicle test data and were within $\pm 10\%$ of the latter.

However, the viscous criterion and deflection rate have to be further improved. For this improvement, two factors seem necessary. One is simulation of the door deformation more accurately using more actuators by reducing the outer diameter of the actuator. Another is simulation of high door acceleration by increasing the output of the actuators and reducing the mass of the impactor.

REFERENCES

- [1] B. Sarri et al. "New Method of Side Impact Simulation for Better Waveform Reproduction and Door Interaction", SAE Paper No. 2004-01-0472.
- [2] K. Aekbote et al. "A Dynamic Sled-to-Sled Test Methodology for Simulating Dummy Responses in Side Impact", SAE Paper No. 2007-01-0710.

SIDE IMPACT SAFETY: ASSESSMENT OF HIGH SPEED ADVANCED EUROPEAN MOBILE DEFORMABLE BARRIER (AE-MDB) TEST AND WORLDSID WITH 'RIBEYE'

Mervyn Edwards, David Hynd, Jolyon Carroll and Alex Thompson

TRL (Transport Research Laboratory)

United Kingdom

Paper Number 11-0082

ABSTRACT

In 2009, 2,222 people were killed and 24,690 were seriously injured in road traffic accidents in Great Britain (GB). About half the people killed were car occupants and just over one third of these were killed in side impacts.

Over the past ten years, since the introduction of the side impact regulation in Europe, much research work has been performed internationally to develop new and modified test procedures to improve the level of occupant protection offered by vehicles in side impacts. In Europe, this research has been co-ordinated by the European Enhanced Vehicle safety Committee (EEVC) and focused on contributing to the development of WorldSID and three test procedures. These are an Advanced European Deformable Barrier (AE-MDB) test, a pole test and an interior headform test.

This paper describes work performed by TRL on behalf of the UK Department for Transport to inform UK policy regarding side impact protection and provide the UK contribution to EEVC activities. The work described consisted of two parts.

For the first part, three full-scale crash tests were performed with Euro NCAP 5 star rated cars to investigate the implications of an AE-MDB test at a higher test speed than the current 50 km/h, in particular how much the occupant protection level in a current vehicle would have to be improved to meet the requirements of such a test and how representative the AE MDB is of a car at these higher speeds. The tests performed indicated that the safety level of a current Euro NCAP 5 star rated car is close to being able to meet the current UNECE Regulation 95 requirements in a 60 km/h AE-MDB test, but would need substantial modifications for higher speeds. Also, several issues were highlighted which need to be considered further. These included (1) the suitability of the current barrier face, because it was very close to bottoming out in the test performed, and (2) the appropriateness of the ES-2 dummy, because of the particularly high T12 spine loads recorded, which indicated that it may not have behaved in a biofidelic manner in the test performed.

For the second part, component level pendulum tests were performed with a WorldSID to assess the RibEye system, in particular to compare the RibEye measured deflection with the deflections that would be obtained using a 1D or 2D IR-Tracc sensor and to gain information on the best position for the two off-axis LEDs used with RibEye. In addition, a 60 km/h AE-MDB test was performed with a WorldSID 50th percentile driver and 5th percentile rear passenger to compare the performance of the WorldSID with the ES-2 dummy and to provide a further assessment of the RibEye system. It was found that the RibEye system was integrated well into the WorldSID and, in general, worked well. However, a potential issue was identified with the shoulder rib deflection measurement. This and other findings are discussed further in the paper.

INTRODUCTION

Over the past ten years, since the introduction of the side impact regulation in Europe, much research work has been performed internationally to develop new and modified test procedures to improve the level of occupant protection offered by vehicles in side impacts. This has included the development of a new anthropometric dummy test tool, namely the WorldSID. This work has been co-ordinated in Europe by the European Enhanced Vehicle safety Committee (EEVC) and worldwide via *ad hoc* working groups set up by interested governments (e.g. the International Harmonization of Research Activities (IHRA) working groups, which were active until 2005) and groups formed by standard committees (e.g. ISO). In Europe the focus has been on the development of WorldSID and three test procedures. These are:

- An Advanced European Mobile Deformable Barrier (AE-MDB) test, the aim of which is to improve occupant protection in car-to-car impacts.
- A pole test, the aim of which is to improve occupant protection, especially for head injury, in car to 'narrow object' impacts. Examples of narrow objects are poles and trees. It should also help to improve head protection in other side impact configurations through the introduction of 'Head Protection Systems' such as side curtain airbags.
- An interior headform test, the aim of which is to improve head protection by improvement of the

padding on stiff vehicle interior structures that the head is likely to strike.

Much of the recent work in Europe to develop these test procedures and the WorldSID 5th percentile female dummy was performed by a large integrated European Commission 6th Framework project called APROSYS [1].

This paper describes work performed by TRL on behalf of the UK Department for Transport to inform UK policy regarding side impact protection and provide the UK contribution to EEVC activities. The work described consisted of two parts: the first an assessment of an AE-MDB test with a higher test speed and the second an assessment of WorldSID, in particular the ‘RibEye’ system for the measurement of rib deflection. This work is described in further detail below.

ASSESSMENT OF AE-MDB TEST WITH HIGHER TEST SPEED

In 2006 the EEVC WG13 (side impact) was tasked by the EEVC steering committee to perform a review of the need to change the side impact regulation (UNECE Regulation 95) and, if necessary, bring forward appropriate proposals. The first part of this review, an analysis of accident databases to determine the magnitude and nature of side impact accidents, was performed by WG21 (accident studies) [2]. This analysis identified the most significant injuries and their mechanisms and also provided information to help define appropriate test configurations, especially for the AE-MDB test. However, the issue of the test speed was not answered fully. The only accident data available to help set the test speed, the UK CCIS accident data, indicated that an AE-MDB test speed of around 65 km/h may be more appropriate than the current test speed of 50 km/h, assuming that the aim is to address a substantial (about 50%) proportion of MAIS 3+ injured casualties [Figure 1].

The two red lines on the graph show the delta-v expected in Regulation 95 (barrier mass 950 kg) and AE-MDB (barrier mass 1500 kg) tests with a car of mass 1250 kg and a test speed of 50 km/h. It is seen that to address 50% of MAIS 3+ casualties the AE-MDB test speed would have to be raised to give a delta-v of 35 km/h, which for a 1250 kg car would equate to a test speed of about 65 km/h.

The objective of the work performed was to determine the implications of an AE-MDB test with a higher test speed, in particular how much the occupant protection level in a current vehicle would have to be improved to meet the requirements of such a test and how

representative the AE-MDB is of a striking car at these higher speeds.

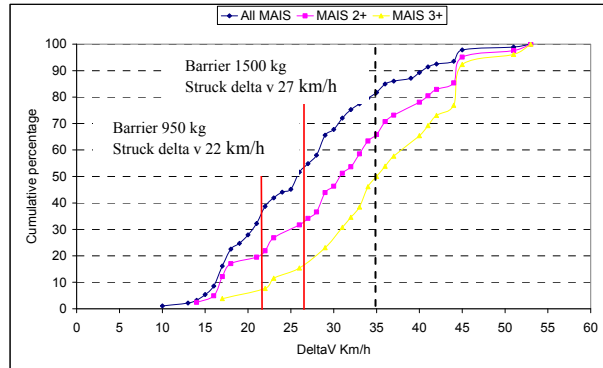


Figure 1. Cumulative percentage of delta-v for all MAIS, MAIS 2+ and MAIS 3+ from analysis of UK CCIS data.

Approach

Three full-scale crash tests (highlighted in Table 1) were performed to obtain the maximum amount of information from a limited number of tests and the test data already available from the APROSYS project, EEVC WG13 members and Euro NCAP.

Table 1.

Test matrix. Note: tests highlighted in green performed within this study. Other tests performed by APROSYS project, EEVC WG13 members and Euro NCAP.

No.	Target	Bullet	Speed (km/h)	Comment
1	Golf V	AE-MDB v3.10	50	Target car stationary; Impact centre 250 mm rear of R-point*
2	Golf V	AE-MDB v3.10	60	Impact centre 250 mm rear of R-point
3	Golf V	Golf V	48	Target car moving at 24 km/h; Impact centre R-point
4	Golf V	Golf V	65	Target car stationary; Impact centre 250 mm rear of R-point
5	Fiesta (MY 2009)	Golf V	65	Target car stationary; Impact centre 250 mm rear of R-point
6	Golf V	R95 MDB	50	Target car stationary; Impact centre R-point

*Note: Impact centre 250 mm rearwards of R-point is the standard AE-MDB test configuration to allow loading of rear seated dummy and reproduce conditions of car-to-car impact with both cars moving.

The VW Golf Mk V was chosen as the target car for all of the tests except one because it was representative of a Euro NCAP 5 star rated car and other test data were available for comparison purposes. A test with a Ford Fiesta was performed to check that the performance of the Golf V was typical of other Euro NCAP 5 star rated cars. The AE-MDB v3.10 was used because it was the latest version of the barrier and fell within the

AE-MDB force deflection performance corridors derived by EEVC WG13 for definition of the barrier stiffness [3]. Car-to-car tests were performed at 65 km/h rather than AE-MDB tests because in the 60 km/h AE-MDB test the barrier was close to ‘bottoming out’ and hence may not have been representative of a car in a 65 km/h impact.

Results

Figure 2 and Figure 3 illustrate the approximate alignment of the AE-MDB (coloured in green) and Golf bullet car lower rails and bumper crossbeam (coloured in brown) with Golf V and Fiesta target cars, respectively, to help understand the dummy injury criteria values. The amount the AE-MDB overlaps the rear wheel should be noted because in the 60 km/h AE-MDB to Golf V test the barrier nearly bottomed out on the wheel, so bottoming out may occur in tests at higher speeds and/or with cars with shorter wheel bases such as the Fiesta.

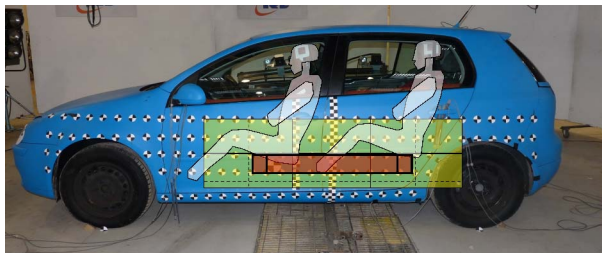


Figure 2. Approximate alignment of AE-MDB and bullet car lower rails with Golf V target car and ES-2 dummies.

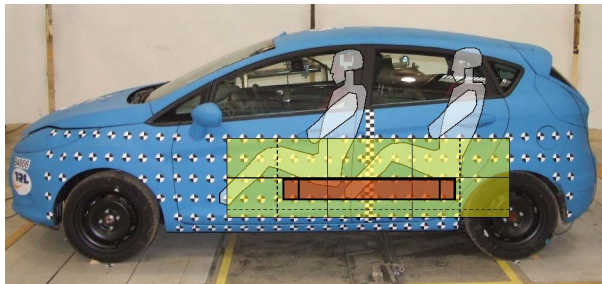


Figure 3. Approximate alignment of AE-MDB and bullet car lower rails with Fiesta target car and ES-2 dummies.

There were some issues noted for each of the tests but it is not thought that they affected the test results significantly. For example, in the AE-MDB vs Golf 60 km/h test there was an incorrect curtain airbag deployment. Specifically, interaction between the bag and the B-pillar and seat belt upper anchorage point prevented the bag unfolding and deploying correctly.

Also, the rear door fully unlatched and opened during the test.

The driver dummy injury criteria values and accelerations are compared in Figure 4 and Figure 5 respectively.

For the driver dummy it is seen that, for the Golf 60 km/h AE-MDB and 65 km/h car-to-car tests, all injury criteria values were less than about 80% of the legislative performance limits. This indicates that the Golf offered a good level of protection, even at the higher impact speeds. However, the spine T12 loads were high (greater than the Euro NCAP lower limit for a full modifier) in particular the Fy force, which indicates possible unloading of the thorax. This is an issue caused by the lack of biofidelity of the ES-2 dummy lumbar spine. It is much stiffer than a human lumbar spine and hence it can transmit greater loads than a human spine. The outcome of this is that when the ES 2 dummy pelvis is subjected to large loads the lumbar spine will transmit unrealistically large loads to the thorax. This can help displace the thorax sideways and hence reduce thorax loading via other load paths, such as through the ribs, and in turn reduce the associated injury criteria values. It is expected that this problem has been resolved with the WorldSID because it has a more flexible lumbar spine which should not transmit unrealistically large loads.

For the Fiesta 65 km/h car-to-car test the injury criteria values, in general, were higher than for the Golf, but still below the legislative limits with the exception of the pubic symphysis force. However, as for the Golf the spine T12 loads were high which again indicates possible unloading of the thorax.

Figure 5 shows that the driver dummy accelerations are substantially increased for the higher speed tests, in particular in the pelvis and lower spine areas. These are the areas of the dummy that are more closely aligned with the barrier and bullet car.

The rear passenger dummy injury criteria values and accelerations are compared in Figure 6 and Figure 7 respectively.

For the rear passenger dummy it is seen that for the Golf 60 km/h AE-MDB test the injury criteria were below the legislative limits. However, spine T12 loads and backplate forces were high indicating possible unloading of the thorax. For the Golf car-to-car test at 65 km/h the dummy injury criteria exceeded the legislative limits for the pubic symphysis. The high pelvis loading was exacerbated by the alignment of the main rail of the bullet Golf with the bottom of the dummy pelvis [Figure 2]. Again, spine T12 loads were

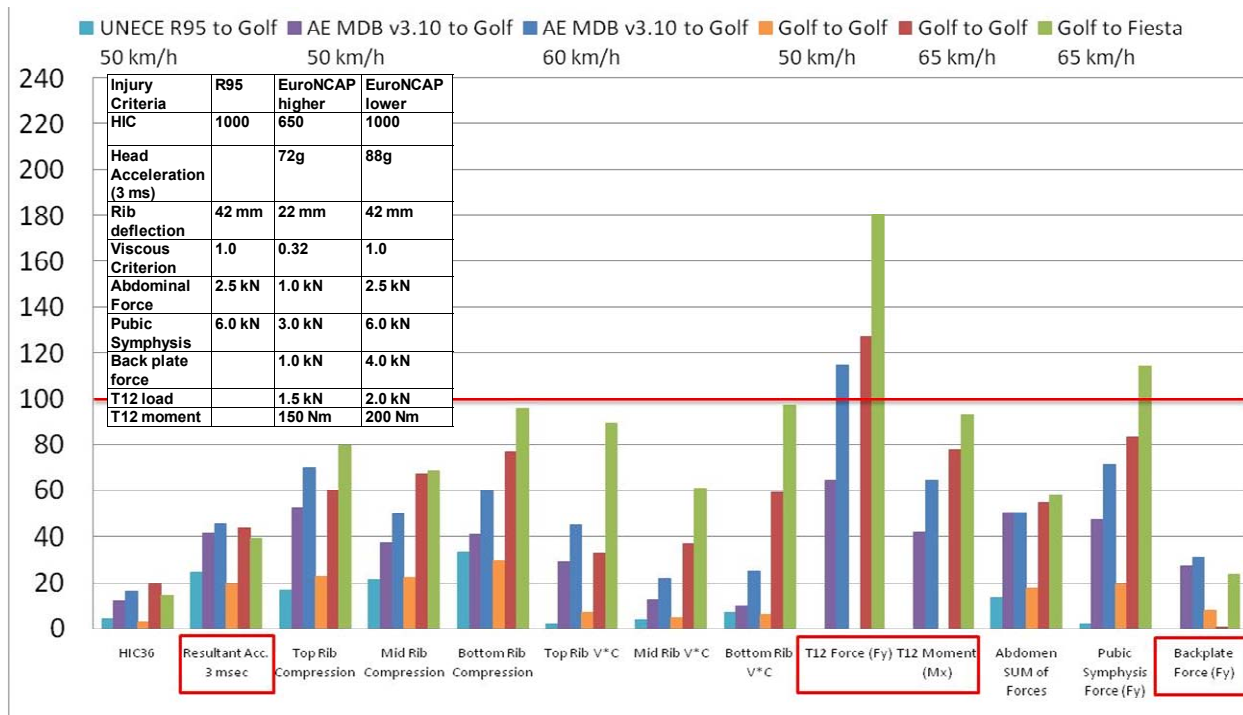


Figure 4. Driver injury performance as a percentage of legislative or Euro NCAP lower limits. Notes: Criteria not used in legislation are indicated with red boxes. In 50 km/h Golf vs Golf test target car was also moving at 24 km/h.

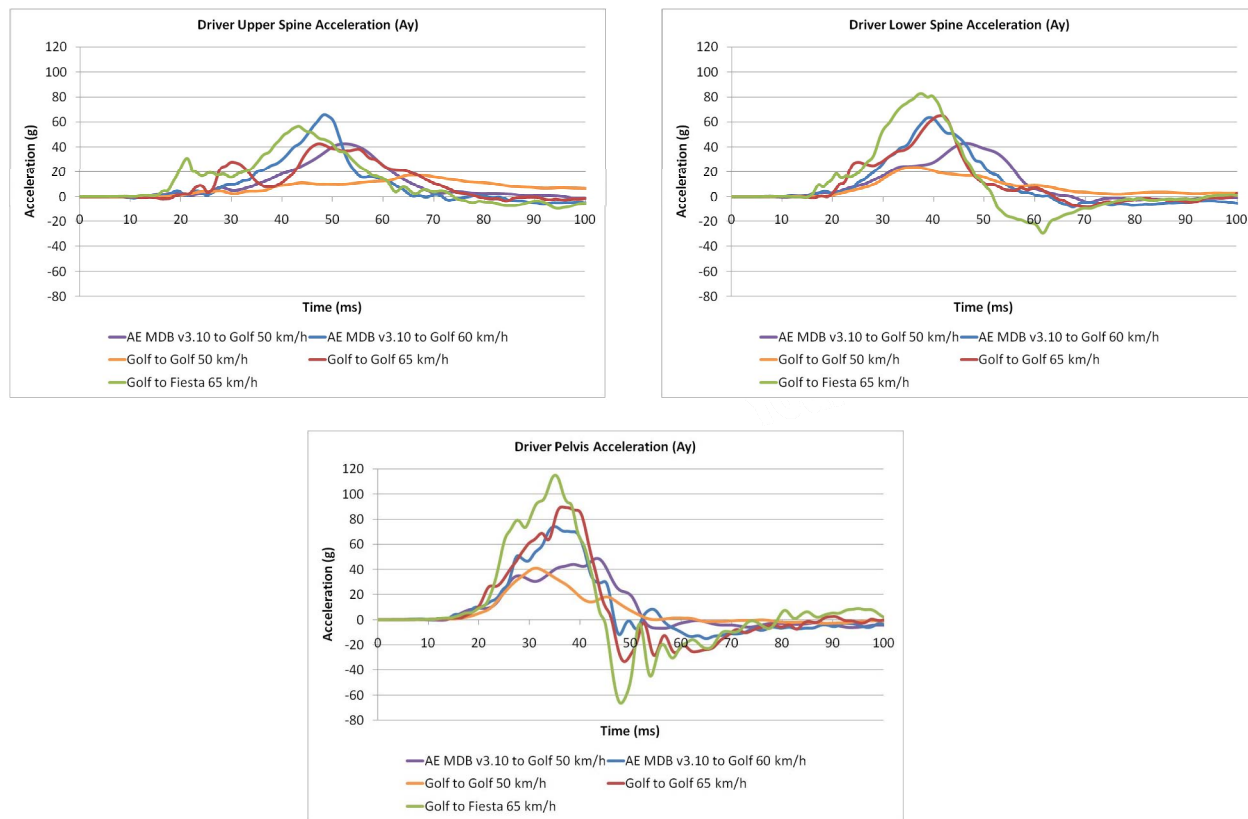


Figure 5. Driver upper spine, lower spine and pelvis accelerations. Note: R95 results not available.

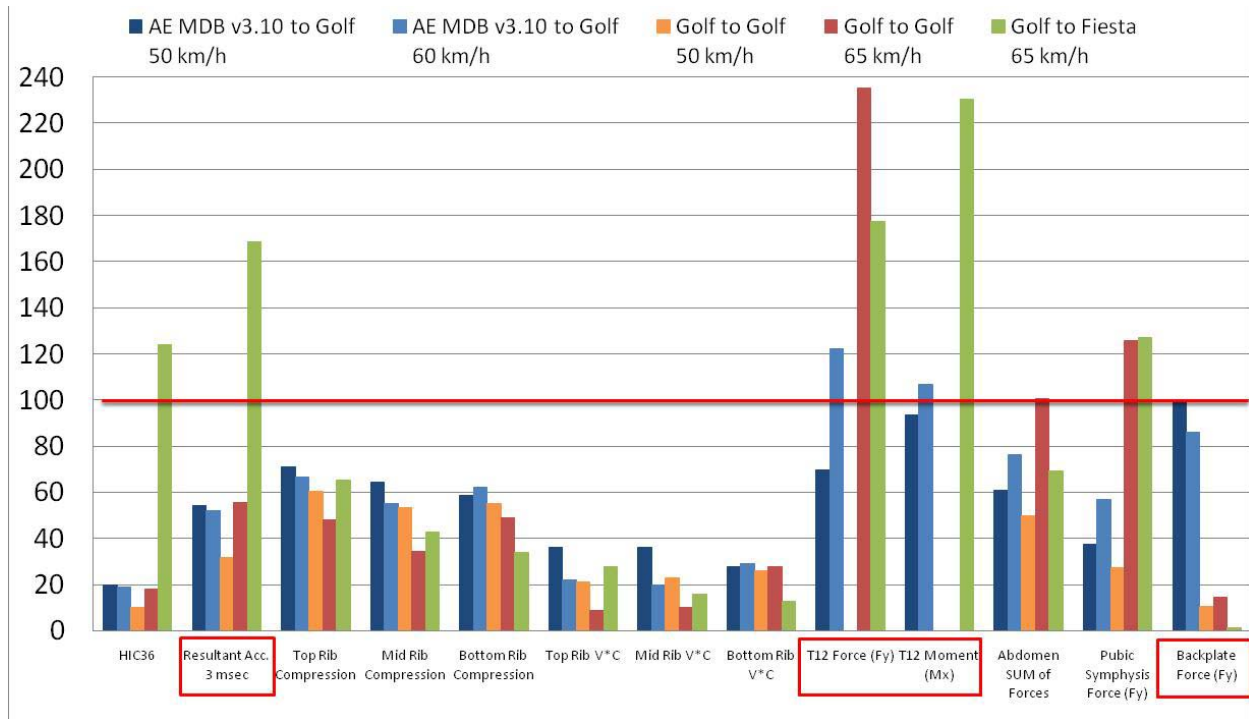


Figure 6. Rear seat passenger injury performance as a percentage of legislative or Euro NCAP lower limits.

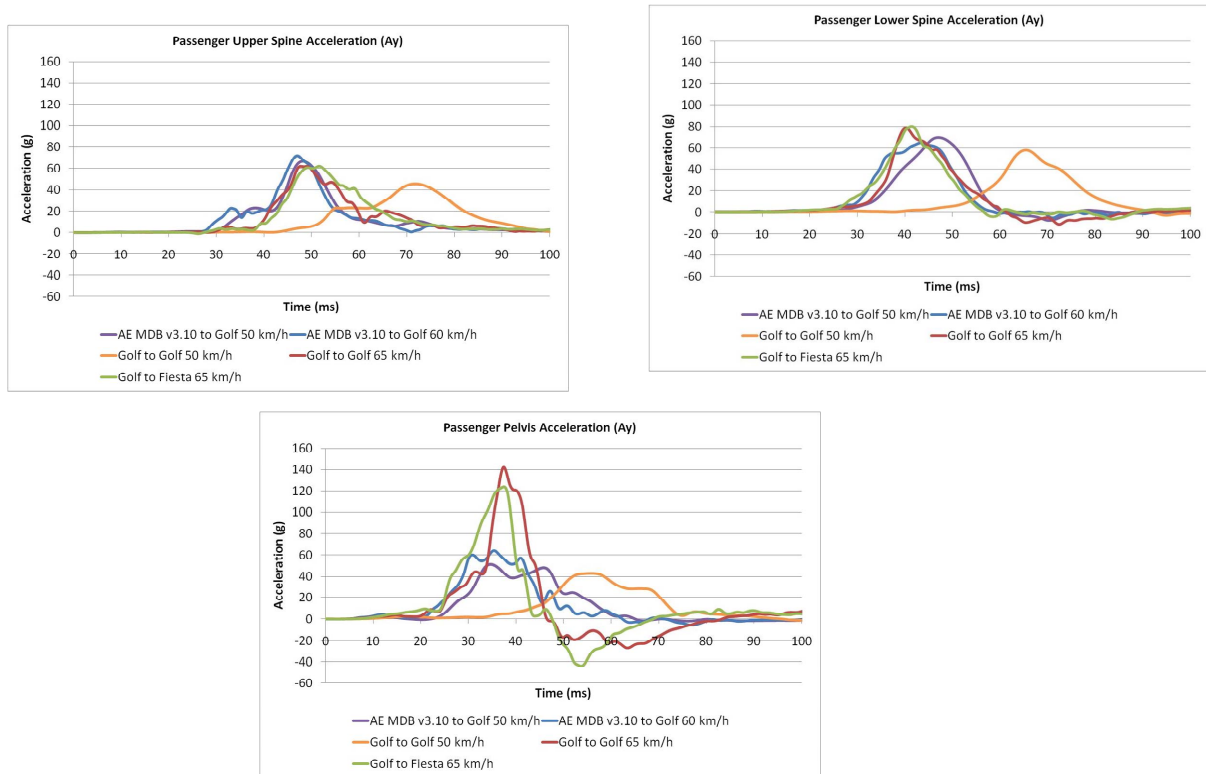


Figure 7. Rear seat passenger upper spine, lower spine and pelvis accelerations.

high indicating possible unloading of the thorax. For the Fiesta car-to-car test the dummy injury criteria exceeded the legislative limits for the pubic symphysis and the head. The high head injury criteria were a result of the head impacting the C-pillar. This vehicle was not fitted with a curtain airbag which probably would have prevented this. As for the Golf, spine T12 loads were high.

For the rear passenger dummy accelerations [Figure 7] two interesting observations were made. The first was the delay in the acceleration of the dummy in the Golf-to-Golf 50 km/h test compared to the other tests. This is a result of the different test configuration for this test, in particular that the target car was moving at 24 km/h and the barrier impact point on the car was 250 mm forward compared to the other tests. The result of this was that the barrier moved into alignment with the dummy later in the impact than in the other tests. The other observation is the much larger pelvis accelerations for the 65 km/h car-to-car tests. This was a result of the alignment of the main longitudinal member of the bullet car with the bottom of the dummy pelvis in these tests, which increased the dummy loading. It should be noted that the AE-MDB uses six areas which have different stiffnesses to represent the stiffness profile of a car.

Hence, it does not represent precisely the highly localised stiffness of a car's longitudinal member.

Figure 8 shows the measured deformations of the target cars. It is seen for the tests with the Golf car that the deformation was substantially larger in the higher speed tests at mid-door and waist rail levels and in particular for the Golf to Golf tests at 65 km/h. The deformation in the Golf to Fiesta 65 km/h test was larger than for the Golf to Golf test and also a different shape. In the Fiesta test the B-pillar was deformed more than in the Golf test with the result that the Fiesta had more of a C-shaped deformation profile compared to the Golf's M-shaped profile. It should be noted that there was little localised penetration of the target car in the car-to-car tests due to the good performance of the bumper crossbeam on the bullet Golf car.

Figure 9 shows the deformation of the barrier in the 60 km/h AE-MDB to Golf test. It is seen that the AE-MDB was close to 'bottoming out' near its bottom right hand corner due to interaction with the Golf's rear wheel and C-pillar. This indicates that bottoming out may occur in tests at higher speeds and/or with cars with shorter wheel bases such as the Fiesta.

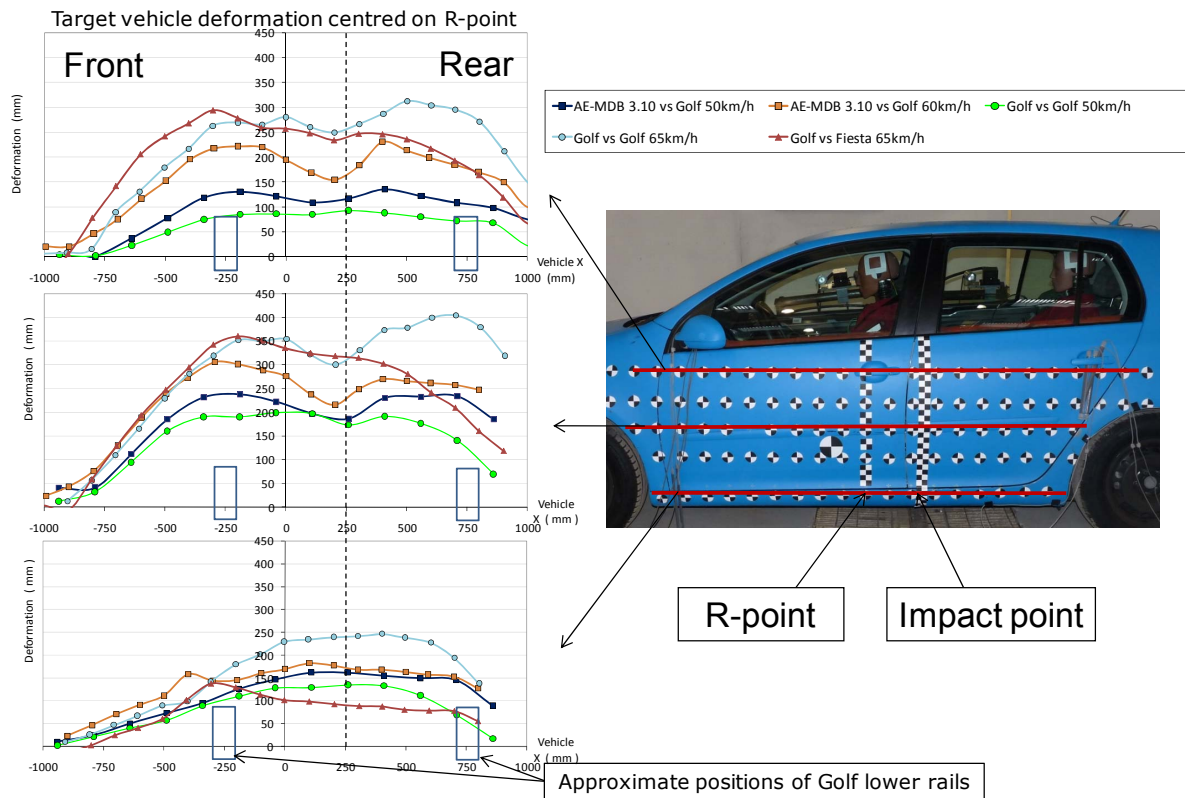


Figure 8. Vehicle deformation measurements at sill, mid-door and waist rail levels.



Figure 9. AE-MDB from 60 km/h Golf test showing that barrier was close to ‘bottoming out’.

Conclusions

- Both the driver and passenger dummy injury criteria values were less than 80 percent of the regulatory limits in the 60 km/h AE-MDB test with the Golf V. However, during the test the door unlatched which would have failed the legislative requirement that no door opens during the test. In addition, issues were noted with the deployment of the curtain airbag and that spine T12 loads were high, which is an indication of possible unloading of the thorax. Also, the barrier was close to bottoming out in the test.
- In the 65 km/h car-to-car tests, for at least one body region, either the driver or passenger dummy injury criteria values or both exceeded the legislative limits in both tests, although by less than about 25 percent. Furthermore, the spine T12 loads were particularly high in these tests, (up to 230 percent of the Euro NCAP lower limit for application of a modifier) which is an indication of possible unloading of the thorax.
- In summary, the tests performed indicated that the safety level of a current Euro NCAP 5 star rated car is close to being able to meet the requirements of a 60 km/h AE-MDB test but would need substantial modifications for higher speeds. In addition, issues regarding a higher speed test were highlighted, in particular the suitability of the current barrier because it was close to bottoming out and the suitability of the ES-2 dummy because of the particularly high T12 spine loads which indicate that the dummy may be behaving in a non-biofidelic manner. It is expected that the more flexible lumbar spine of the WorldSID would help to resolve this issue.

ASSESSMENT OF WORLDSID

The assessment of WorldSID consisted of two main parts. The first part was a series of component level pendulum tests to assess the new RibEye™ Multi-Point Deflection Measurement System (from here on referred to as ‘RibEye’) for measuring the deflection of the WorldSID shoulder, thorax and abdominal ribs. The main objective was to compare the output from the RibEye optical rib deflection measurement system with the more conventional measurements that would be obtained with a one dimensional (1D) or two dimensional (2D) IR-Tracc sensor.

The second part consisted of a 60 km/h AE-MDB full-scale crash test to compare the performance of the WorldSID dummy with the ES-2 dummy and to provide a further assessment of the RibEye system.

The ‘RibEye’ Deflection Measurement System

It is generally accepted that the WorldSID dummy is superior in thorax biofidelity to other side impact dummies [4]. Until the introduction of WorldSID, little consideration was given to the biofidelity of side impact dummies for oblique loading, because the older dummies were designed to be sensitive in the lateral axis only. A feature of the WorldSID is that oblique and off-axis chest deformations are possible. A consequence of this is that measurement of the chest deflection needs to take into account oblique and off-axis deformations.

When it was introduced, the WorldSID 50th percentile male dummy was instrumented with a 1D IR-Tracc sensor on each rib to measure the deflection. Unfortunately, these dummies displayed a reduced sensitivity of the rib deflection measurement system to oblique and offset impact as any rotation of the IR-Tracc was not taken into account. This limitation was shown in testing conducted at TRL [5] as part of the EC 5th Framework SIBER project and in various other studies.

Figure 10 illustrates this problem. Under lateral impact the forward component in rib displacement introduces extension of the rib deflection measurement system (indicated by the red dotted line). This reduces the compression output of the measurement system. Under rearward oblique impact [Figure 10(c)], there is more forward rib deformation. This leads to an even greater underestimate of the lateral rib compression and therefore of the risk of injury, if based on a single axis lateral deflection measure.

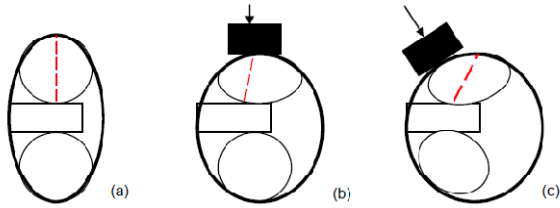


Figure 10. WorldSID rib schematic top view undeformed (a), deformation under lateral impact (b), and deformation under rearward oblique impact (c).

The APROSYS project [6] developed and tested two-dimensional (2D) IR-Traccs with potentiometers at their base to improve the sensitivity of the WorldSID thorax to oblique impact. The 2D IR-Traccs showed improved sensitivity to off-axis deformations, but some error in the measurements was still seen when compared with the true, peak deflection.

In parallel, but on a longer timeframe, an optical rib deflection measurement system was developed, the RibEye. The differences between the RibEye and 2D systems are that the RibEye measures vertical displacements as well as lateral and fore-aft, and the deflections are assessed at three different positions around the rib. This is achieved by using sensors mounted on the spine box which optically track three LEDs on each rib in three dimensions throughout the impact [Figure 11]. Using the data obtained from the forward, middle, and rearward LED positions, more complicated deformation patterns of the ribs can be measured than would be possible based on a single point measurement system.

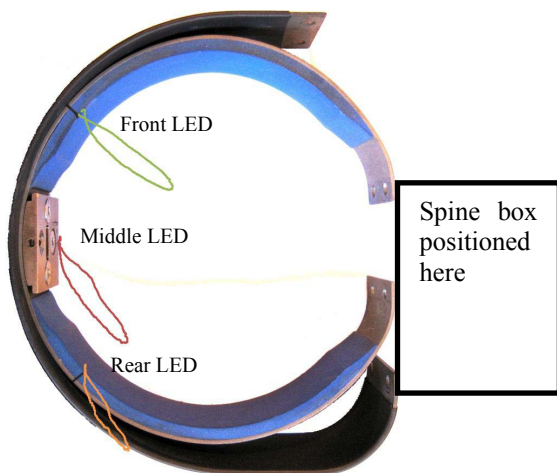


Figure 11. Example of RibEye resultant deflection measurements at the front, middle, and rear LED positions with forward oblique loading.

Assessment of WorldSID ‘RibEye’ using Pendulum Tests

Forty pendulum impactor tests were performed on a WorldSID 50th percentile male (50M) in broadly two regimes, namely oblique and offset [Figure 12], for two different postures of the WorldSID. These were either suspended in a seated position until the moment of impact (without any other support) or reclined on the WorldSID’s certification bench.

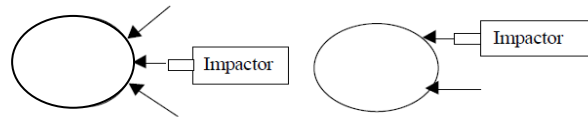


Figure 12. Oblique impact (left) and offset impact (right), schematic overhead views.

The tests were configured to evaluate the RibEye deflection measurement system with respect to the existing 1D and 2D IR-Tracc measurement systems. Equivalent 1D and 2D IR-Tracc measurements were calculated from the RibEye measurements. It should be noted that the tests were set up to minimise vertical rib displacements and hence were not suitable to evaluate the importance of the vertical measurement that RibEye offers.

For a 1D IR-Tracc measurement it was found that even for purely lateral impacts, there was a slight underestimate of the rib deflection. For the oblique and offset impacts this under-estimate increased substantially. Table 2 shows the measurements from the offset tests in which the WorldSID was suspended. It is seen that the 1D IR-Tracc deflection measurement under-estimates were greatest when the loading was most offset, only 61 percent of the 2D resultant deflection for 75 mm offset impact.

Table 2. Rib deflections for offset tests with WorldSID suspended (all values in mm)

Impact offset	1-D IR-Tracc equivalent	2-D calculated lateral disp.	2-D resultant deflection	RibEye middle LED resultant	RibEye front LED resultant
-75	23.0	26.7	37.5	37.5	36.1
-50	27.8	30.4	39.4	39.5	34.1
-25	28.4	29.2	31.8	31.8	27.8
0	24.3	24.4	24.8	24.8	25.2
25	22.3	22.4	23.0	23.1	23.0
50	18.3	18.7	20.7	21.0	23.9

This is because with offset impacts a greater component of the rib deformation comes from x-axis displacement than in lateral tests. This is evident from comparison of the difference between the 2-D lateral and resultant

measurements, which are closer for the tests with the smallest offset.

For RibEye measurement of lateral displacement it was found that the forward of lateral rib measurement LED position provided greater peak lateral displacement values than the middle LED. This indicates that the forward position could provide useful additional information, if assessing risk of injury based on lateral rib displacement. This should represent an advantage to considering the middle LED position alone, as in a 2D IR-Tracc system.

For measurement of resultant displacement it was found that the resultant deflection was rarely greater at the forward LED position than at the middle position. From this it can be inferred that the front position was not picking up a particularly greater aspect of the overall rib loading. Hence, if the resultant deflection was considered as the key criterion, it seems as though alternative rib deflection assessment positions would be useful only when there is localised loading. To assess this further it is recommended that the relative measurements from the LEDs be considered in loading expected to cause localised deflections of the rib cage. For instance, one might consider testing the thorax when tightly constrained by a seat-belt and when loaded with a non-flat impact surface.

Assessment of WorldSID in 60 km/h AE-MDB Test

A full-scale side impact crash test was performed between a Volkswagen Golf and an AE-MDB v3.10 at 60 km/h using a WorldSID 50M driver and a WorldSID 5F rear passenger. The WorldSID 50M was fitted with RibEye and hence equivalent measurements for 1D and 2D IR-Tracc systems could be calculated. The WorldSID 5F was fitted with a 2D IR-Tracc system. The main aim of the test was to compare the performance of the WorldSID dummies with the performance of ES-2 driver and rear passenger dummies which were tested as part of the investigation of increased test speed reported previously. A further aim of the test was to compare the different rib deflection measurement systems used in the WorldSID dummies, namely the 1D IR-Tracc, 2D IR-Tracc and RibEye in a full-scale test.

In order to undertake a comparison of the relative performance of the WorldSID and ES-2 dummies, it was necessary to check that the performance of the vehicles in both tests was similar. The vehicle accelerations and deformations in each of the tests were compared and judged to be similar enough to allow

comparison of the dummies. However, it should be noted that the head curtain airbag did not deploy correctly in either test. The central section of the airbag appeared to be caught on the top of the B-pillar trim or seatbelt anchorage which prevented the central section from fully deploying. In addition, in the WorldSID test the airbag did not fully unfurl next to the driver dummy's head. However, these issues did not have a detrimental effect on the dummy results and the driver's head was still protected by the airbag in both tests.

A comparison of the WorldSID and ES-2 dummy performances

is reported below for the driver and passenger dummies. The WorldSID and ES-2 dummies have significant differences in their anthropometries [Figure 13]. The top rib of the ES-2 dummy approximately aligns with the shoulder of the WorldSID dummy. Also the WorldSID and ES-2 dummies have different seating position procedures. As a result of these differences the initial positions of WorldSID 50M and ES-2 dummies in the tests were significantly different, e.g. the head to roof measurement was 74 mm for the ES-2 compared to 119 mm for WorldSID 50M.



	ES-2 (m m)	WorldSID (mm)
Shoulder width	485	480
Pelvis width	355	410
Sitting height (neck/torso interface)	660	600
Sitting height (erect)	920	870

Figure 13. Comparison of anthropometry of ES-2 and WorldSID.

The injury parameter outputs for the ES-2 and WorldSID dummies in the tests are shown in Table 3.

The main points of interest are the peak force levels recorded for the WorldSID 50M shoulder, which is significantly higher than the ES-2 driver, and the pubic symphysis, which is significantly lower than the ES-2.

Table 3.
ES-2 and WorldSID injury parameter outputs

	Parameter	ES-2 driver	ES-2 passenger	WorldSID 50M driver	WorldSID 5F passenger
	HIC ₃₆	163.47	188.22	137.7	201.3
Head	Peak resultant accel (g)	42.38	48.00	42.14	49.55
	3ms exceedence (g)	40.12	45.92	40.67	46.79
	Force y (kN)	0.65	1.87	3.21	_****
Shoulder	Deflection (mm)	-	-	> 40***	49.11
	Top rib deflection (mm)	29.36	28.07	18.39*	25.55**
Thorax	Middle rib deflection (mm)	21.01	23.11	22.31*	13.20**
	Bottom rib deflection (mm)	25.06	26.12	27.64*	18.85**
	Top rib V*C (m/s)	0.45	0.22	0.22*	0.40**
	Middle rib V*C (m/s)	0.22	0.20	0.27*	0.14**
	Bottom rib V*C (m/s)	0.25	0.29	0.27*	0.31**
	Abdomen Force summation (kN)	1.26	1.91	-	-
Abdomen	Abdomen Rib 1 deflection (mm)	-	-	32.01*	23.93**
	Abdomen Rib 2 deflection (mm)	-	-	35.44*	35.59**
	Abdomen Rib 1 V*C (m/s)	-	-	0.47*	0.49**
	Abdomen Rib 2 V*C (m/s)	-	-	0.51*	1.00**
	T12 acceleration Y (g)	63.75	64.50	54.41	101.32
	Pelvis	Pubic symphysis force (kN)	4.28	3.41	0.99
Pelvis accel Y (g)		74.32	64.28	80.22	74.35

*Based on equivalent 1D IR-TRACC measurement

**Based on equivalent calculated lateral component from 2D IR-TRACC

***Value taken prior to channel failures. Estimated peak value approximately 50-60 mm, based on curve fitting to equivalent 1D IR-TRACC measurements before and after channel measurement range exceeded.

****Shoulder load cell not fitted to dummy



Figure 14. Comparison of driver dummy kinematics (ES-2 left, WorldSID 50M right), showing ES-2 shoulder moving forward away from ribs (shrugging).

Considering the difference in shoulder loads, comparison of the driver dummy kinematics showed that the dummies' shoulders interacted with the door differently. The ES-2 dummy's shoulder was pushed forward and rotated away from the ribs during the impact, whilst the WorldSID 50M shoulder did not rotate and was directly loaded by the door structure [Figure 14]. Likely contributory factors to this were (1) the significant structural differences in the design of the shoulder between the two dummies and (2) the difference in alignment of dummies' shoulders with the door structure; the WorldSID 50M shoulder aligned directly with the door structure due to the dummy's lower initial position compared to the ES-2.

Considering the difference in pubic symphysis loading, both the driver dummies showed significant pelvis movement away from the door which was consistent with the high pelvis accelerations observed for both dummies (approximately 80 g). However, this did not explain the significant difference in pubic symphysis load, where the ES-2 experienced much higher loading than the WorldSID 50M. The differences in dummy design probably contributed to some of this difference. However, it is also possible that the WorldSID pelvis was loaded through a different load path, perhaps at the rear of the pelvis where the load would not have been picked up by the pubic symphysis load cell. The WorldSID 50M can have a sacrum load cell fitted at the rear of the pelvis which may have provided this information. However the dummy used in this test did not have this instrumentation fitted.

The WorldSID 5F rear passenger kinematics showed that the head curtain airbag did not protect the dummy's head during the impact. Despite initial contact with the lower part of the airbag, the dummy's head was not prevented from contacting the door [Figure 15].



Figure 15. WorldSID 5F rear passenger showing head contact with door - head not protected by airbag.

However, the values for HIC and 3ms exceedence recorded by the dummy indicated that this head contact was not significant in terms of injury risk. A similar phenomenon was seen for the WorldSID 5F in a test performed by APROSYS [7].

In the test with the ES-2, as reported previously, high levels of T12 loading were recorded possibly due to the poor biofidelity of the ES-2 spine in this area. This may have unloaded the ribs. The WorldSID is a more biofidelic dummy than the ES-2, and as such it was expected that loading through T12 would not be as high and hence any unloading of the ribs would not be as great. As such, higher rib deflections were expected to be observed for the WorldSID 50M than the ES-2. However, this was not the case. A possible reason for this result was the increased loading of the WorldSID 50M shoulder in the test which may have unloaded the ribs. It should be noted that the WorldSID is not fitted with a T12 load cell, and as such it was not possible to make any conclusions about whether the improved biofidelity of the WorldSID lumbar spine reduced the T12 loads.

In order to compare the performances of the WorldSID and ES-2 dummies, a calculation of the estimated injury risk for each dummy's body region was made using known injury risk functions. Injury risk functions were not available for the ES-2, so ES-1 risk curves were used. The injury risks for the WorldSID 50M dummy were calculated using the risk functions developed by Petitjean *et al.* [8]. The injury risks for the WorldSID 5F dummy were calculated using the risk functions developed within the APROSYS project [9]. It should be noted that the only injury risk functions available for the WorldSID 50M rib outputs were based on the 1D IR-Tracc measurements, whilst risk functions were available for the WorldSID 5F using 1D and 2D IR-Tracc outputs. Therefore, for the purposes of this comparison, the rib outputs for the WorldSID 50M were based on the equivalent 1D IR-Tracc measurements calculated from the RibEye outputs, whilst the rib outputs for the WorldSID 5F were based on the 2D IR-Tracc calculated lateral displacement measure.

The calculated injury risks are shown in Table 4. Comparison of the injury risks between the ES-2 and WorldSID dummies showed that the ES-2 driver predicted a significantly higher injury risk than the WorldSID 50M driver for the thorax and abdomen, with a similar injury risk for the pelvis based on acceleration. However, the WorldSID 50M had a very high risk of AIS2+ shoulder injury which cannot be compared to the ES-2 because no risk function was available.

Table 4.
Comparison of ES-2 and WorldSID injury risks

Injury risk comparison		ES-2 driver	ES-2 passenger	WS50M driver	WS5F passenger
Shoulder	Deflection	-	-	>2% AIS2+***	-
	Force	-	-	92% AIS2+	-
Thorax	Top Rib deflection	12% AIS3+	10% AIS3+	<1% AIS3+*	21% AIS3+**
	Top Rib V*C	26% AIS3+	10% AIS3+	[4% AIS3+*]	-
	Mid Rib deflection	4% AIS3+	5% AIS3+	<1% AIS3+*	7% AIS3+**
	Mid Rib V*C	10% AIS3+	9% AIS3+	[6% AIS3+*]	-
	Bot Rib deflection	6% AIS3+	7% AIS3+	<1% AIS3+*	13% AIS3+**
	Bot Rib V*C	11% AIS3+	13% AIS3+	[6% AIS3+*]	-
	Force	15% AIS3+	16% AIS3+	-	-
Abdomen	Abdomen Rib 1 deflection	-	-	<1% AIS3+*	7% AIS3+**
	Abdomen Rib 1 V*C	-	-	[<2% AIS3+*]	-
	Abdomen Rib 2 deflection	-	-	<1% AIS3+*	14% AIS3+**
	Abdomen Rib 2 V*C	-	-	[<2% AIS3+*]	-
	T12 Acceleration	46% AIS3+	47% AIS3+	<2% AIS3+	-
Pelvis	Force	20% AIS2+	13% AIS2+	<1% AIS2+	<2% AIS2+
	Acceleration	24% AIS2+	21% AIS2+	19% AIS2+	[~35% AIS2+]

*Based on equivalent 1D IR-TRACC measurement

**Based on calculated lateral component from 2D IR-TRACC

***Based on value recorded prior to channel failure at 32ms, likely to be much higher

It is likely that the high load on the shoulder reduced the loading on the ribs and therefore contributed to the low injury risk for the thorax. It should be noted that there are concerns regarding the injury risk calculated for rib viscous criterion in the WorldSID 50M, as it is calculated based on the equivalent 1D IR-Tracc rib compression which does not take into account the rotation of the rib and therefore does not necessarily relate to the lateral deflection of the rib. As such these values are shown in square brackets. Also, it should be noted that the shoulder rib front and middle LED measurements dropped out during the test, probably due to the high deflection of the shoulder rib in all three dimensions (lateral, fore/aft and vertical), which in turn probably led to the rib LEDs being positioned such that they could not be seen by the sensors.

The WorldSID 5F rear passenger injury parameters could not be directly compared to the ES-2 rear passenger dummy due to the differences in the sizes of the dummies. However, it could be seen that the WorldSID 5F had generally higher risk of AIS3+ chest injury than the ES-2.

A comparison of the rib deflection measurement systems

for the WorldSID 50M was made. Using the RibEye middle LED measurements equivalent measurements for 1D and 2D IR-Tracc systems were calculated [Table 5]. Comparison of the 1D IR-Tracc measurement with the 2D IR-Tracc lateral measurement (EY) shows that the 1D IR-Tracc consistently underestimated the lateral deflection of the ribs. This was due to the fact that it does not take the rib rotation, and therefore fore/aft movement of the rib, into account. The comparison of the 1D IR-Tracc

compression with the 2D IR-Tracc calculated resultant deflection (ER) showed an even larger difference. As no injury risk functions were available for the 2D IR-Tracc on the WorldSID 50M dummy, it was not possible to assess the impact that the underestimation of rib deflection by the 1D IR-Tracc would have had on the likelihood of occupant injury.

Table 5.
Comparison of 1D and 2D IR-TRACC equivalent measurements for WorldSID 50M driver

	1D IR-TRACC Equivalent	2D IR-TRACC (Equivalent from Ribeye Middle LED)		
		EX	EY	ER
Shoulder	32.31*	31.51*	50.59*	59.60*
Thorax 1	18.05	20.47	19.3	26.51
Thorax 2	22.05	19.34	22.83	28.26
Thorax 3	26.59	17.93	29.53	34.48
Abdomen 1	30.87	19.93	34.32	39.64
Abdomen 2	34.00	20.68	37.91	43.00

*Values recorded prior to channel measurement range being exceeded

Conclusions

Assessment of WorldSID ‘RibEye’ in pendulum tests:

- Even in the purely lateral impacts, there was a slight underestimate in the rib deflection arising from the 1-D IR-Tracc measurement. This increased to 61 % of the resultant, in the case of the 75 mm offset impact test.
- RibEye LED position.
 - The forward of lateral LED position often provided a larger lateral (y-axis) displacement measurement than the middle LED position.
 - Unless the loading is particularly oblique (> ~30 degrees) or offset (~ 50 mm) there is no additional benefit in using the resultant deflection data from the forward of lateral LED position.
 - Only with particularly concentrated loading would it be expected that the rearward of lateral LED position would measure greater rib deflection values than the forward of lateral and middle LED positions.

Assessment of WorldSID in 60 km/h AE-MDB test.

- Dummy kinematics.
 - The WorldSID 50M and ES-2 driver exhibited different behaviour, in particular for the interaction of the shoulder with the car door.
 - The WorldSID 5F head was not protected by head curtain airbag due to a low head position.

The head contacted the door at the base of the window. However, the values for HIC and 3ms exceedence indicated that this head contact was not significant in terms of injury risk.

- Injury criteria and risks
 - There was a significantly higher shoulder load for the WorldSID 50M compared to the ES-2. This most likely reduced the loading to the thorax. Likely contributory factors were the different alignment of the dummies with the cars’ structures and the different designs of the dummies’ shoulders. The different dummy alignment was a result of the difference in the anthropometry of the dummies and the different seating procedures.
 - There was a significantly lower pubic symphysis loading for WorldSID 50M compared to the ES-2 even though both dummies had similar pelvis accelerations. The differences in dummy design probably contributed to some of this difference. However, it is also possible that the WorldSID pelvis was loaded through a different load path, perhaps at the rear of the pelvis where the load would not have been picked up by the pubic symphysis load cell.
 - The injury risk predicted by the WorldSID 50M was generally lower than that predicted by the ES-2 apart from the shoulder. For the WorldSID 50M high shoulder loads and deflections were measured and a high risk of AIS2+ shoulder injury was predicted. For the ES-2 relatively low shoulder loads were measured but an injury risk could not be calculated because a shoulder injury risk function was not available for ES-2. It should be noted that injury risk curves for the WorldSID 50M were only available for 1D IR-Tracc measurements.
- Other
 - A potential issue was identified with WorldSID shoulder and RibEye system
 - The shoulder rib middle and forward LEDs deflected out of range of RibEye sensor causing signal dropout during the test.

ACKNOWLEDGEMENTS

The authors gratefully acknowledge the UK Department for Transport, Transport Canada, FTSS, Boxboro systems, APROSYS SP1 project members EEVC WG13 members and Euro NCAP for their support for this work.

This paper used accident data from the United Kingdom Co-operative Crash Injury Study (CCIS) collected during the period 2000-2009. CCIS was managed by TRL Limited, on behalf of the DfT (Transport Technology and Standards Division) who funded the project along with Autoliv, Ford Motor Company, Nissan Motor Company and Toyota Motor Europe. Previous sponsors of CCIS have included Daimler Chrysler, LAB, Rover Group Ltd, Visteon, Volvo Car Corporation, Daewoo Motor Company Ltd and Honda R&D Europe(UK) Ltd. Data was collected by teams from the Birmingham Automotive Safety Centre of the University of Birmingham; the Transport Safety Research Centre at Loughborough University; TRL Limited and the Vehicle & Operator Services Agency of the DfT.

Further information on CCIS can be found at <http://www.ukccis.org>

REFERENCES

1. Advanced Protection Systems (APROSYS) EC 6th Framework project FP6-PLT-506503. www.aprosys.com
2. Thomas P, Welsh R, Lenguerrand E, Vallet G, Otte D, and Standroth J (2009). 'Priorities for Enhanced Side Impact Protection in Regulation 95 Compliant Cars', 21st International Technical Conference on the Enhanced Safety of Vehicles (ESV), Stuttgart, Germany, June 15-18, 2009.
3. Ellway J (2005). 'The Development of an Advanced European Mobile Deformable Barrier (AE-MDB) face,' 19th International Technical Conference on the Enhanced Safety of Vehicles (ESV), Washington, USA, June 6-9, 2005.
4. EEVC (European Enhanced Vehicle-safety Committee) 2009. 'Status of WorldSID 50th Percentile Male Side Impact Dummy', EEVC Working Group 12 report, March 2009. Report published on the EEVC web site: www.eevc.org.
5. Hynd D, Carroll J, Been B and Payne A (2004). 'Evaluation of the shoulder, thorax and abdomen of the WorldSID pre-production side impact dummy'. IMechE Vehicle Safety Conference, Westminster, London, UK, 14-15 December, 2004. Institution of Mechanical Engineers.
6. Waagmeester K and Been B (2009). 'Single rib and 2D rib deflection sensor drop table impact tests; sensitivity to impact load and impact direction'. APROSYS SP5 Deliverable D5.2.8: AP-SP52-0058.
7. Versmissen T, Palacios E, Nombela M (2009). 'Evaluation of the use of the WorldSID dummy in

the AE-MDB test', APROSYS SP1.1, Deliverable D111C-Part2, AP-SP11-0147. www.aprosys.com

8. Petitjean A, Trosseille X, Petit P, Irwin A, Hassan J and Praxl N (2009). 'Injury risk curves for the WorldSID 50th Male Dummy', Stapp Car Crash Journal, Vol. 53, November 2009. pp. 443-476.
9. Carroll J, Eggers A, Martinez L and Been B (2009). 'WorldSID Small female Side Impact Injury Risk Functions for Thorax, Abdomen and Pelvis based on dummy biomechanical testing and existing injury data', APROSYS SP5, Deliverable D5.2.11, AP-SP52-0062B. www.aprosys.com

© Copyright TRL Limited 2011.

SIDE IMPACT AIR BAG EFFICACY, INJURY MITIGATION PERFORMANCE IN VEHICLE MODELS WITH AND WITHOUT SIDE IMPACT AIR BAGS AND INFLATABLE HEAD PROTECTION

Robert Lange
Nathan Soderborg
Harry Pearce
Karen Balavich
Su-Wei Huang

Exponent
United States
Paper Number 11-0115

ABSTRACT

New injury control technologies are continually emerging in the automotive marketplace. Insertion mechanisms and rates vary based on the complexity and stability of the technology, the cycle of new vehicle and platform introductions, and consumer acceptance. The injury control effectiveness of newly emerging technologies is assessed based upon changes recorded in collision related injury and fatality data from US Federal and State motor vehicle collision databases. This analysis provides an assessment of side impact air bag (SIAB) effectiveness based upon data from the Fatality Analysis Reporting System (FARS). The study considers vehicle models over the time period 1998 to 2008 that converted from having no side impact air bags available to having side impact air bags as standard equipment. Distinctions are made between two types of side impact air bags: torso (or thorax) side air bags and roof rail mounted head curtain air bags. Estimates of effectiveness are based on comparisons of fatality rates for the 2 years prior to insertion of the injury control technology and 2 years following insertion in each model pair.

SIDE IMPACT AIR BAG INSERTION HISTORY

Coincident with the near ubiquitous installation of driver frontal air bags and the increasing density of passenger front air bags into the light vehicle fleet during the late 1990s, motor vehicle manufacturers began to engineer and install air bag restraints for side impact. Initial side impact air bag applications were intended to provide supplemental energy absorption to driver and passenger torso exposure to near side (same side of the vehicle) impact insult. Some early side impact air bags were mounted in the outboard seat back bolster and some were mounted in the door above the arm rest. As the technology has matured, seat mounted torso air bags have become the predominant location.

Side impact air bag systems were developed in an extra-regulatory environment; that is the first, and several subsequent generation side impact air bag systems were developed and inserted into the stream of commerce without a governing regulation. Therefore motor vehicle manufacturers themselves were responsible to establish the performance parameters, deployment characteristics, and acceptance criteria that each individually developed and applied to side impact air bag systems. Air bag systems were thereby validated to each manufacturers' own test standards and criteria without the regulatory overlay requiring certification.

Nearly at the same time side impact air bags were being developed for production applications, the adverse unintended consequences of frontal air bag inflation induced injuries became evident. Many manufacturers were able to adopt side impact air bags and simultaneously generate internal standards and acceptance criteria for side impact air bag deployment characteristics so as to control the risk of injury to out of position occupants. Eventually, with the assistance of the Insurance Institute for Highway Safety (IIHS) and the Canadian Ministry of Transportation (MOT), manufacturers developed a voluntary industry standard to control side impact air bag inflation induced injury risk. The resultant test conditions and acceptance criteria for out of position occupant considerations and the sponsoring manufacturers' commitment to the procedures and criteria were documented in a transmittal letter from the IIHS, the "Alliance of Automobile Manufacturers", and the "Association of Import Automobile Manufacturers" to The Administrator of the National Highway Traffic Safety Administration (NHTSA) dated August 8, 2000 [1].

Since early side impact air bag systems were first introduced into the stream of commerce in the late 1990s, motor vehicle collision injury control has greatly advanced and the penetration of side impact air bags for torso protection deepened into the new

car and light duty truck fleet (herein after for simplicity, the “new car fleet”) and additional design features have been added to improve side impact restraint effectiveness in side collisions including the emergence of technologies to provide inflatable head protection in near side impacts.

This paper builds upon work performed by Exponent and described in “Installation Patterns for Emerging Injury Mitigation Technologies,” paper 11-0088 presented at the 2011 ESV Conference [2]. Exponent compiled data regarding the application of multiple safety technologies by manufacturer, vehicle make, vehicle model and vehicle model year. That data matrix was used to identify the paired models and model years in which a given vehicle model converted from not having a safety technology to having the safety technology installed as standard equipment in the model year immediately following.

By studying paired populations of like make/model vehicles without and with side impact air bags, we can calculate the side impact injury likelihood for each of the paired populations individually, and thereby also compare the likelihood of injury in near side impacted vehicles without side impact air bags and with side impact air bags. The reduction in injury likelihood compared to the original probability of injury in the paired models that are not equipped with side air bag technology is a measure of efficacy in side impact injury reduction.

Table 1 is a sample of the make/model/model year matrix for head curtain side air bags in model year 2003. A clear or white cell indicates that the base model of that vehicle make/model in 2003 had no head curtain air bag available. A yellow cell indicates that the make/model combination had the head curtain air bag available as an option in 2003. A green cell indicates that the make/model had the head curtain air bag installed as standard equipment for the 2003 model year.

The penetration growth of a new injury mitigation technology into the new car fleet can be tracked and illustrated by counting the number of unique make/models in a given model year with the technology of interest as standard or optional equipment and calculating the proportion of the entire new vehicle fleet (based upon an aggregate count of unique make/models). The resulting plot then provides a history of new technology penetration into the new vehicle fleet. Figure 1 illustrates the

insertion history for head curtain air bags. Figure 2 illustrates the same for torso air bags.

Examination of model year matrices as illustrated in Table 1 permit comparisons among one model year to the immediately following model year and were used to identify paired couplings of make/model/model year vehicle combinations wherein the first year of the pair did not have the technology and the second year of the pair did have the technology as standard equipment. To capture more injury data for the paired comparisons, the last two model years without the technology were compared to vehicles in the first and second model years in which the technology was applied as standard equipment.

METHODOLOGY

Injury data was obtained for each make/model pair from the FARS [4]. Because FARS reports fatal injuries for whole calendar years, injuries for a particular vehicle model were tallied through 2008 beginning with the calendar year equal to the model year “+1.” For example the injury count for a 1998 Buick LeSabre would be the sum of all fatal injuries in fatal crashes for which the main impact was a side impact for calendar years 1999 through 2008.

Injury rates were calculated using years of vehicle registration for denominator data. For example, vehicle registration years for a 1998 Buick LeSabre would be tallied by adding up the counts of U.S. registrations for 1999 to 2008 Buick LeSabres.

The resultant injury rates for a particular model were thus calculated as fatal injuries per registered vehicle year as shown in Equation 1.

$$injury\ rate = \frac{\text{driver right front passenger} \\ \text{fatal injuries in near side impacts}}{\text{registered vehicle counts for calendar} \\ \text{years corresponding to} \\ \text{injuries represented in the numerator}} \quad (1).$$

In making paired comparisons, the numerator and denominator in Equation 1 would include counts for two successive vehicle model years—the first rate in the pair accounting for the last two model years without the technology under consideration and the second rate in the pair accounting for the first and second years in which the technology was applied.

The measured improvement is an efficacy calculation:

$$efficacy = \frac{(\text{rate without SIAB}) - (\text{rate with SIAB})}{\text{rate without SIAB}} \times 100\% \quad (2).$$

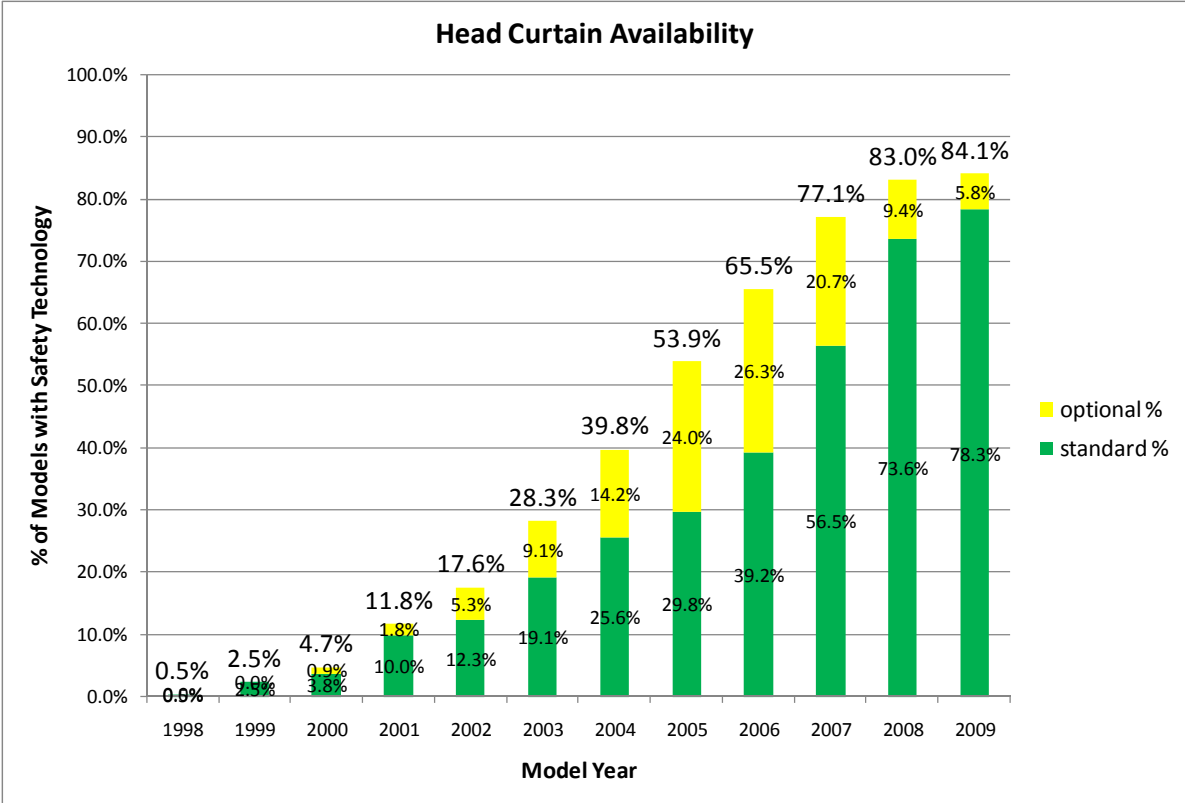


Figure 1. Head curtain air bag availability by model year [3].

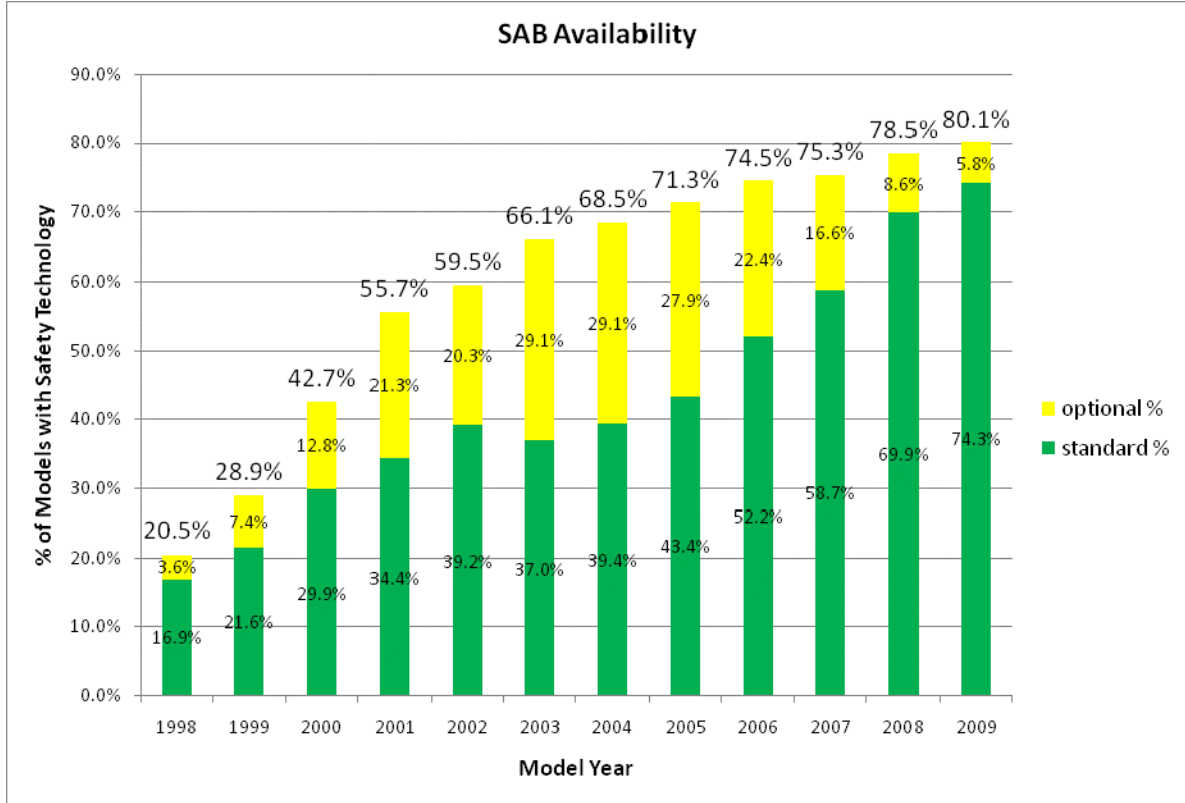


Figure 2. Seat or door deployed side air bag availability by model year [3].

SIDE IMPACT AIR BAG TECHNOLOGY MATCHED PAIRS

The matched pairs that fit these selection criteria are: (1) torso side air bag insertion from not available to standard equipment in immediately successive model years and (2) head curtain air bags insertion from not available to standard equipment in immediately successive model years. Table 2 lists the pair matches for torso side air bags. Group 1 in Table 2 are pair vehicles not equipped with torso side air bags and Group 2 are pair vehicles that have torso side air bags as standard equipment.

Table 3 lists the pair matches for head curtain air bags. Group 1 are pair vehicles that were not equipped with head curtain air bags; some models may have been equipped with torso side air bags as standard equipment. Group 2 are pair vehicles that have head curtain air bags as standard equipment; some models may also have torso side air bags as standard equipment. See the bottom of Table 3 for an exact definition of Group 1 and Group 2.

For each vehicle matched pair we assume as a null hypothesis that the fatal injury rate in vehicle models with the side air bag is not different than the fatal injury rate in vehicle models without side impact air bags. For each matched pair of vehicle models we calculated a p-value test statistic: the probability that the number of fatal injuries occurring in the model population with side impact air bags is less than or equal to the actual observed value. If the p-value is sufficiently small, commonly taken as 5%, the null hypothesis is rejected and we conclude that the reason the observed value of fatalities is smaller than expected when assuming the null hypothesis is that the fatality rate for the model population with side air bags is lower than that for the model population without side airbags.

For several vehicle models, even though the calculated efficacy measure is fairly high, the p-value is not low enough to provide statistical significance for an improvement. Larger vehicle sample sizes or longer time periods would be required to obtain more statistical certainty for individual models.

For the specific set of vehicle models under study, we also aggregated data over the two populations, those not having side air bags and those having side air bags. For the aggregated data, we totaled the number of fatal injuries for all of the vehicle model population with side air bags and totaled the number of fatal injuries for all of the population without side air bags; these aggregate values then become

numerator data for rate calculations. The aggregate vehicle registration-based rate calculation is exact in that the numerator and denominator data are straight counts of events and registrations for the set of vehicles under study.

In an attempt to characterize average efficacy in some way, we calculated the average z-score for comparisons between the population without side air bags and the population with side air bags for the aggregated sets. The z-score for a particular model is the difference between the observed value and the expected value expressed as a proportion of the standard deviation for that model. The observed values are taken for the vehicle model group equipped with side air bags. The expected values for comparison are calculated as the product of the exposure values for the population with side air bags and the fatality rate for the population equipped without side air bags.

$$z - score = \frac{(observed\ fatalities) - (expected\ fatalities)}{standard\ deviation} \quad (3).$$

The z-score is a standardized score indicating the difference from expected value in units of standard deviation; the standardization allows scores to be averaged across cases with different standard deviations. A negative value of the average z-score would indicate an improvement (reduction) in fatality rate has been realized for the population with side air bags as compared to the population without side air bags.

Finally, we also applied Fisher's combined probability test to the aggregated data. This method combines p-values from individual vehicle hypothesis tests into a single test statistic. The null hypothesis for this "meta-analysis" is that all of the separate null hypotheses are true (i.e., all fatality rates are the same before and after air bag implementation). This hypothesis is rejected when p is small (< 5-10%). The alternative hypothesis is that at least one of the separate alternative hypotheses is true (at least one of the model specific rates is different following implementation).

STUDY RESULTS

Figure 3 shows the proportional change (improvement or increase) for the torso air bag (SIAB) vehicle pairs. The rate calculations are for near side fatal injuries per registered vehicle year for the fleets equipped with torso side air bags and not so equipped. The chart plots data for all of the vehicle pairs for which there was at least one fatal injury over

**Table 2.
SIAB matched pairs**

Vehicle	Group 1	Group 2	Vehicle	Group 1	Group 2
Acura CL	1998-1999	vs. 2001-2002	Hyundai Sonata	1997-1998	vs. 1999-2000
Acura TL	1998-1999	vs. 2000-2001	Infiniti I30	1996-1997	vs. 1998-1999
Acura RL	1997-1998	vs. 1999-2000	Jaguar XJ-Series	1996-1997	vs. 1998-1999
Acura Integra/RSX	2000-2001	vs. 2002-2003	Land Rover Range Rover	1997-1998	vs. 2000-2001
Audi A4	1996-1997	vs. 1998-1999	Lexus ES	1996-1997	vs. 1998-1999
Audi A6	1996-1997	vs. 1998-1999	Lexus GS	1996-1997	vs. 1998-1999
Buick LeSabre	1998-1999	vs. 2000-2001	Lexus LS	1995-1996	vs. 1997-1998
Buick Park Avenue	1998-1999	vs. 2000-2001	Lexus SC	1999-2000	vs. 2002-2003
Cadillac Catera	1997-1998	vs. 2000-2001	Mitsubishi Montero	1999-2000	vs. 2001-2002
Cadillac DeVille	1995-1996	vs. 1997-1998	Oldsmobile Aurora	1998-1999	vs. 2001-2002
Cadillac Escalade	1999-2000	vs. 2002-2003	Oldsmobile Bravada	2000-2001	vs. 2002
Cadillac Seville	1996-1997	vs. 1998-1999	Oldsmobile Silhouette	1996-1997	vs. 1998-1999
Chevrolet Suburban	1998-1999	vs. 2000-2001	Pontiac Bonneville	1998-1999	vs. 2000-2001
Chevrolet Tahoe	1998-1999	vs. 2000-2001	Pontiac TransSport/Montana	1996-1997	vs. 1998-1999
Chevrolet Blazer/Trailblazer	2000-2001	vs. 2002	Porsche 911	1997-1998	vs. 1999
Chevrolet Venture	1997	vs. 1998-1999	Porsche Boxster	1997	vs. 1998-1999
GMC Jimmy/Envoy	2000-2001	vs. 2002	Suzuki Aerio	2003-2004	vs. 2005-2006
GMC Suburban/YukonXL	1998-1999	vs. 2000-2001	Toyota Avalon	1996-1997	vs. 1998-1999
GMC Yukon	1998-1999	vs. 2000-2001	VW Passat	1996-1997	vs. 1998-1999
Honda Odyssey	2000-2001	vs. 2002-2003	Volvo 850	1994-1995	vs. 1996-1997
Honda Pilot	2001-2002	vs. 2003-2004	Volvo 960	1994-1995	vs. 1996-1997

Group 1: No Airbags Available
Group 2: Airbag is Standard Equipment

**Table 3.
Head curtain matched pairs**

Vehicle	Group 1	Group 2	Vehicle	Group 1	Group 2
Acura MDX	2002-2003	vs. 2004-2005	Honda Pilot	2004-2005	vs. 2006-2007
Acura RL	2003-2004	vs. 2005-2006	Jaguar XJ-Series	2002-2003	vs. 2004-2005
Acura TL	2002-2003	vs. 2004-2005	Land Rover Range Rover	2001-2002	vs. 2003-2004
Audi A4	1998-1999	vs. 2001-2002	Lexus ES	2000-2001	vs. 2002-2003
Audi A6	1998-1999	vs. 2001-2002	Lexus GS	1999-2000	vs. 2001-2002
Audi A8	1998-1999	vs. 2000-2001	Lexus LS	1999-2000	vs. 2001-2002
Cadillac Catera/CTS	2000-2001	vs. 2003-2004	Lexus RX	2002-2003	vs. 2004-2005
Cadillac Deville/DTS	2004-2005	vs. 2006-2007	Mercedes G-Class	2003-2004	vs. 2005-2006
Cadillac Escalade	2005-2006	vs. 2007	Mitsubishi Endeavor	2005-2006	vs. 2007
Cadillac Escalade ESV	2005-2006	vs. 2007	Mitsubishi Outlander	2006	vs. 2007
Cadillac Escalade EXT	2005-2006	vs. 2007	Suzuki XL7	2005-2006	vs. 2007
Cadillac STS ¹	2003-2004	vs. 2005-2006	Toyota Avalon	2003-2004	vs. 2005-2006
Chevrolet Impala ¹	2004-2005	vs. 2006-2007	VW Passat	1999-2000	vs. 2001-2002
Honda Odyssey	2003-2004	vs. 2005-2006			

Includes vehicles with the following configurations:
Group 1: No bags available; Group 2: Standard Curtain
Group 1: Seat Torso Bag Standard; Group 2: Seat Torso and Curtain Airbag Standard
Group 1: Seat Torso Bag Standard; Group 2: Curtain only Standard

¹Analysis for passenger side only

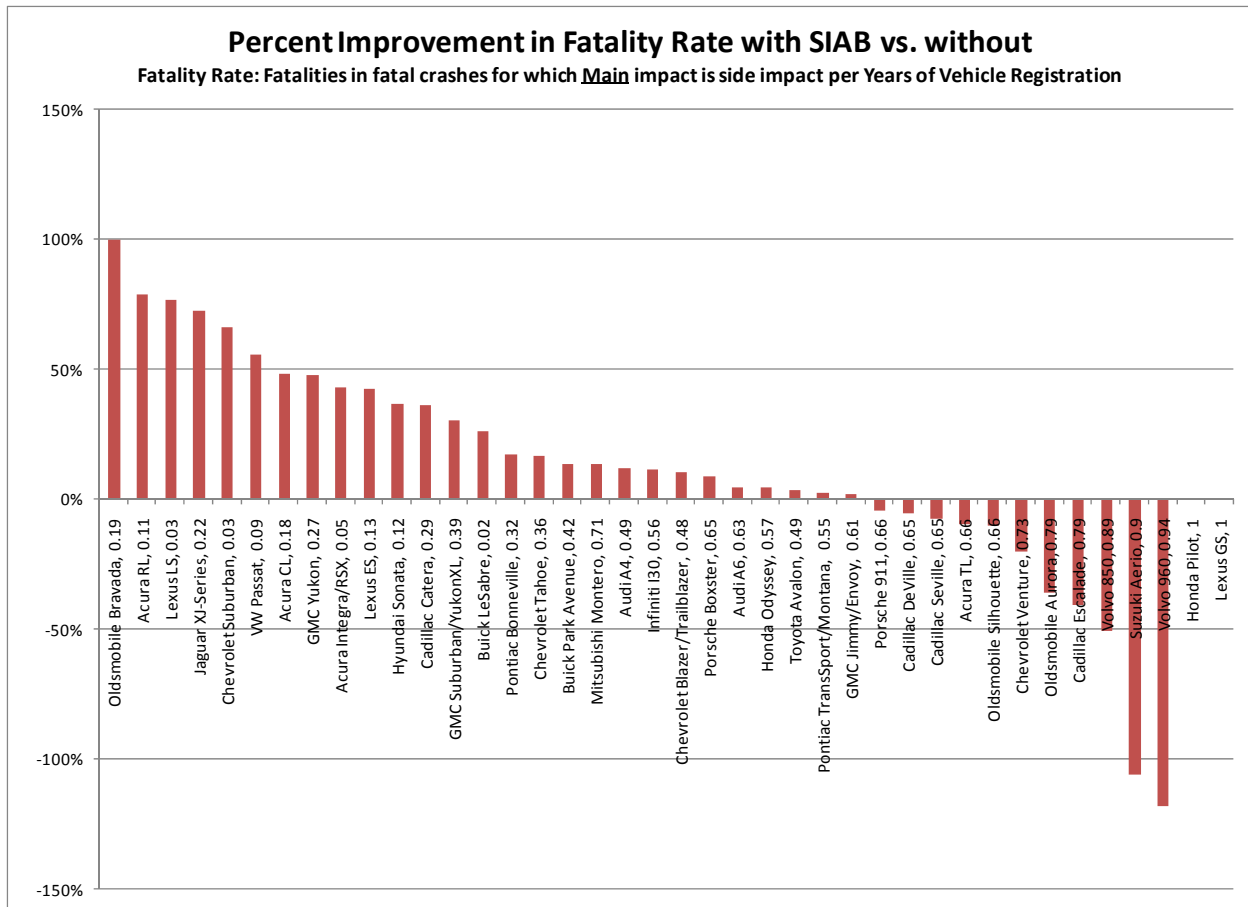


Figure 3. Fatal injury rate change for the torso side air bag matched fleet.

the period without torso side air bags and for which a p-value could be calculated. Aggregated data for the paired populations registered a fatality rate of 1.76 E-05 without torso side air bags and 1.47 E-05 with torso side air bags, a 16 % reduction in fatal injury rate for the population with torso side air bags as standard equipment. The average z-score is -0.39. The Fisher's p-value is 1.87 E-06. Each of these results support the conclusion that torso side air bags have a positive effect in reducing fatalities. It should be noted that in Figure 3, some vehicles show a reduction in efficacy. In general, sample sizes are quite small for those examples. For comparison, see Figure 4 which shows only vehicles in which there were 12 or more fatalities in the period without airbags. In this situation, with larger samples, all but one vehicle model showed an increase in efficacy.

Figure 5 shows the proportional change (improvement or increase) for the head curtain air bag vehicle pairs. The rate calculations are for near side fatal injuries per registered vehicle year for the fleets equipped with head curtain air bag and not so

equipped. The chart plots data for all of the vehicle pairs for which there were at least six fatal injuries and for which a p-value could be calculated.

Aggregated data for the paired populations registered a fatality rate of 9.23 E-06 without head curtain air bags and 6.19 E-06 with head curtain air bags, a 33 % reduction in fatal injury rate for the population with head curtain air bags as standard equipment. The average z-score is -0.41. The Fisher's p-value is 1.11 E-06. Each of these results supports the conclusion that head curtain side air bags have a positive effect in reducing fatalities.

SUMMARY

The technology insertion patterns for both torso side air bags and for head curtain air bags follow a common pattern for injury control technology insertion: small or modest penetration in early years of adoption, a monotonic increase in fleet insertion proportion, a mix of optional and standard equipment availability throughout the insertion period, and relatively high penetration levels in later years.

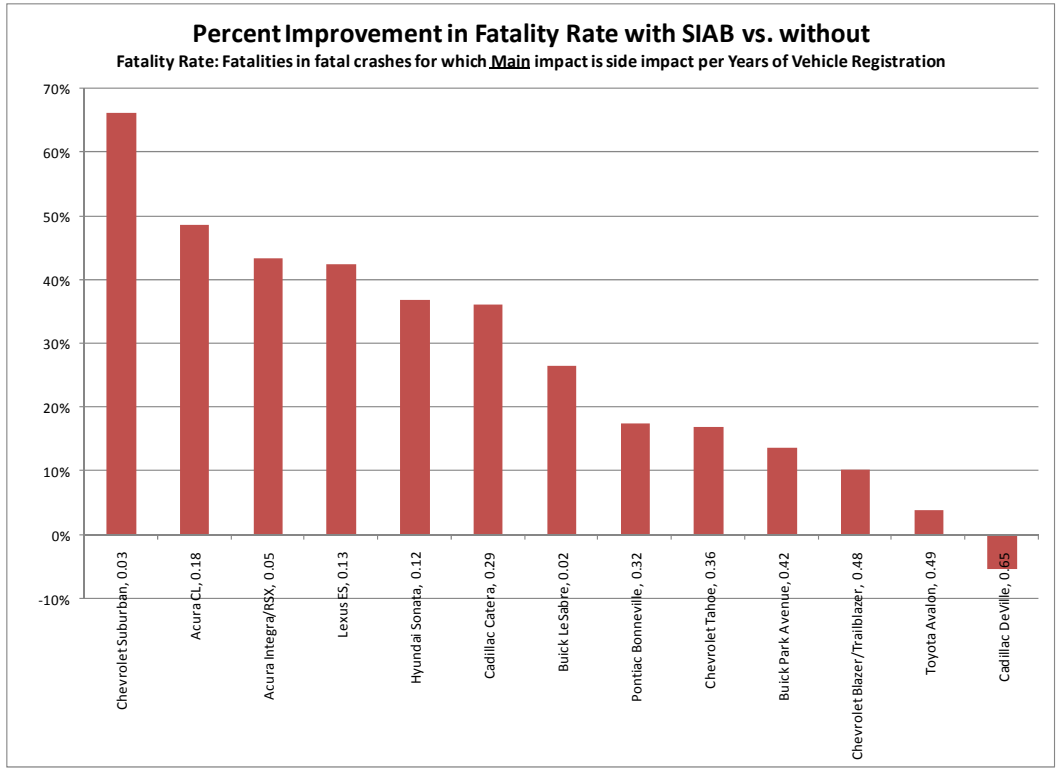


Figure 4. Fatal injury rate change for the torso side air bag matched fleet, cases with 12 or more fatalities during the period without torso side air bags.

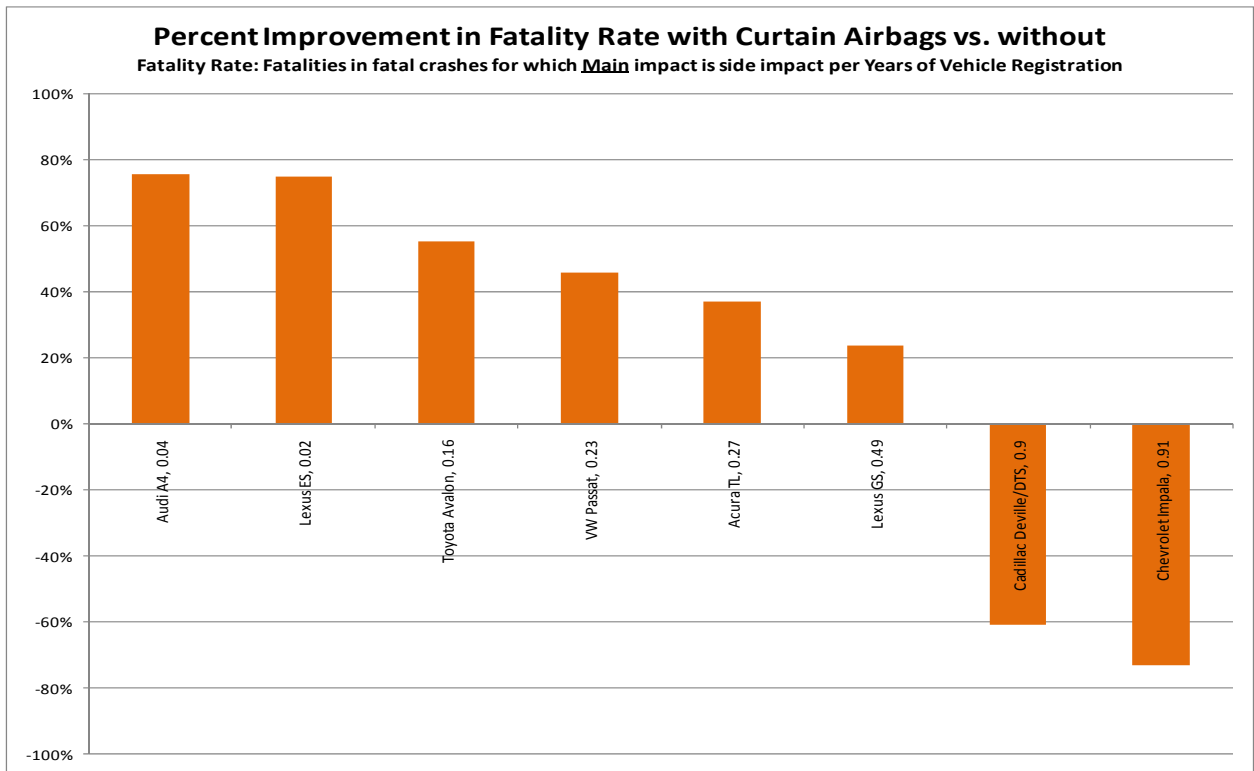


Figure 5. Fatal injury rate change for the head curtain air bag matched fleet.

Insertion of both of these technologies has been influenced somewhat by the industry voluntary agreement to improve vehicle to vehicle side impact compatibility [5] and both of these technologies will likely become ubiquitous consequent to Federal Motor Vehicle Safety Standard 214 finalized in September 2007 and now in the third year of its phase-in schedule.

With somewhat limited data for relative small vehicle fleets, an analysis was conducted of FARS data and national vehicle registration data from R.L. Polk. Only 42 vehicle model pairs were available for study of torso air bag effects and 27 pairs for study of head curtain air bags. Even so, the analysis registered a real occupant protection improvement in near side crashes for both technologies. In the vehicle population studied, torso side air bags were about 16% effective in reducing the probability of near side impact fatal injury and head curtain air bags were about 33% effective in reducing near side impact fatal injury.

A review of the technology improvements registered at the paired vehicle model level in Figures 3 and 5 show large variations. Variation at the vehicle model level would be expected as the values for fatal injury counts are all quite small; the chance inclusion or exclusion of an event will yield large rate variation. Additionally, individual comparisons among models would likely be affected by integrated vehicle design characteristics, base vehicle architectural changes (that often may enable installation of new technologies that present architectural challenges or unique architectural criteria), and the possible inclusion of other vehicle safety countermeasures. However, close examination shows that “sister” vehicles (those sharing common architectures and technology but sold under different make nameplates) exhibit variation over nearly the entire range of improvements. Compare, for example, the improvement for Oldsmobile Bravada to that for the Chevrolet Blazer/Trailblazer and the GMC Jimmy/Envoy or the Chevrolet Suburban to the Cadillac Escalade. This suggests perhaps the performance variations measured at the individual paired model level may be due to chance rather than performance variation among models identical save

for name plates. Additionally, at the individual paired model level, many of the comparisons are themselves not statistically significant.

As noted, some negative improvement rates for individually paired vehicle models were calculated. The uncertainty placed on individual fatality rate improvement calculations are affected by a small sample size in addition to compounding influences such as crash severity exposure and vintage of technology.

A future improvement to this work could be to use numbers of police reported or tow-away crashes as exposure (denominator) data in the rate calculations. This would improve the estimate of rates for efficacy of performance in a crash rather than efficacy per years of vehicle registration. Differences in crash rates between vehicle types could have a large affect on the rates calculated in this paper.

REFERENCES

- [1] IIHS, Alliance of Automobile Manufacturers, and Association of Import Automobile Manufacturers. 2004. “Side Airbag Test Procedure and Evaluation Protocol; Alliance Member Commitment.” NHTSA Docket 98-5098-32.
- [2] Lange, R., H. Pearce, E. Jacuzzi, N. Soderborg, K. Balavich, and Su-Wei Huang. 2011. “Installation Patterns for Emerging Injury Mitigation Technologies.” Proceedings of the 2011 ESV Conference, paper number 11-0088.
- [3] Pearce, H. and R. Lange. 2010. “Exponent Vehicle Database.”
- [4] NHTSA. 2010. Website <http://www.nhtsa.gov/FARS>.
- [5] Alliance of Automobile Manufacturers and Association of International Automobile Manufacturers. 2004. “Docket Letter and Report, Enhancing Vehicle-to-Vehicle Crash Compatibility, Commitment for Continued Progress by Leading Automakers.” NHTSA Docket 2003-14623-13.

AN ASSESSMENT OF WORLDSID 50TH PERCENTILE MALE INJURY RESPONSES TO OBLIQUE AND PERPENDICULAR POLE SIDE IMPACTS

Thomas Belcher, Mark Terrell

Australian Government Department of Infrastructure and Transport

Suzanne Tylko

Transport Canada

Paper No. 11-0133

ABSTRACT

Pole side impact crash tests are in use in regulatory and consumer programs around the world. There is some diversity in the test methods that are applied, including the suitability of available side impact dummies for use in these tests. For the WorldSID 50th percentile adult male dummy, much theoretical discussion has focussed on the likely rib response, including the direction of this response in oblique and perpendicular pole side impacts. With the advent of multi-dimensional rib deflection measurement systems, such as 2D-IRTRACC and “RibEye”, it is possible to investigate this question.

This paper reports on a series of six vehicle-to-pole side impact tests conducted using a WorldSID 50th percentile male dummy on the struck side of the vehicle fitted with the “RibEye” measuring system for the abdomen, thorax and shoulder. In addition, a WorldSID 50th percentile male fitted with the conventional IRTRACC system was installed on the non-struck side. Two large Australian made passenger sedans were tested using three different pole side impact methods. The test methods investigated were a perpendicular impact aimed at the head centre of gravity, a perpendicular impact aimed 100 mm forward of the head centre of gravity, and an FMVSS 214 based oblique impact. All tests were conducted with an impact velocity of 32 km/h. Theoretical IRTRACC deflections are calculated from the “RibEye” data.

The objective of this study was to evaluate the effect of pole impact angle and alignment on injury risk as predicted by struck and non-struck side WorldSID 50th percentile adult males. Important contributing factors to this response including the vehicle structural response, recorded airbag fire time, and airbag deployment characteristics are also analysed.

Both vehicle models selected were fitted with combination head and thorax side airbags, but with different impact sensing systems. The vehicles also represented different generations of structural and airbag development.

X and Y axis deflections are analysed in comparison with the calculated IRTRACC values.

These show a distinct difference between perpendicular and oblique test configurations, and differences resulting from impact location. An additional factor is airbag deployment, as in some cases airbag entrapment resulted in differences in thorax and head response.

Occupant-to-occupant interaction is also analysed, with this contact producing HIC36 results normally associated with a high probability of fatal head injury in five of the six tests conducted.

INTRODUCTION

The development of the WorldSID 50th percentile male (WorldSID 50th male) began in June 1997. A WorldSID Task Group comprised of government and industry representatives was formed under the ISO working group on Anthropomorphic Test Devices (TC22/SC12/WG5). Key objectives of this group included; the realisation of a world harmonized side impact dummy to eliminate the use of different dummies in different parts of the world, and development of a side impact dummy with superior biofidelity and anthropometry, suitable for use in side impacts $\pm 30^\circ$ from pure lateral (i.e. perpendicular $\pm 30^\circ$ impacts). The first production version of the WorldSID 50th male was released in 2004.

The ISO WorldSID Task Group has evaluated the biofidelity of the WorldSID 50th male using the ISO/TR9790 impact test methods and biofidelity rating scale [4]. Overall and individual body region ratings are reported on a scale between 0 (unacceptable) and 10 (excellent). Drop tests, pendulum impact tests and sled tests are used to determine individual biofidelity ratings for the head, neck, shoulder, thorax, abdomen and pelvis. Each individual rating is determined from a weighted comparison of dummy responses with defined (i.e. target) 50th percentile adult male corridor responses. The overall biofidelity rating is then calculated by weighting and summing the individual body region biofidelity ratings. The ISO/TR9790 biofidelity rating for the WorldSID 50th production dummy is 8.0 [9], which is considered “good”, and represents a significant improvement on the 5.7 of BioSID, 4.6 of ES-2, 4.2 of ES-2re and 2.3 of USDOT-SID.

The United States National Highway Traffic Safety Administration (NHTSA) has also completed an evaluation of the WorldSID 50th male [8] using an updated version of the NHTSA biofidelity ranking system first described in Rhule [7]. Internal and external biofidelity ratings were determined for the WorldSID 50th male and ES-2re dummies. External biofidelity provides a measure of how closely a given dummy simulates PMHS external loadings to the surrounding impact structures (as measured by pendulum and sled load plate force-time history responses). Internal biofidelity provides a measure of how closely the internal injury responses of a dummy simulate post mortem human subject (PMHS) internal injury responses (e.g. rib deflection). This NHTSA biofidelity evaluation also showed the WorldSID 50th male to have superior internal and external biofidelity to ES-2re.

In 2009, Petitjean et al [6] published injury risk curves for the WorldSID 50th male shoulder, thorax, abdomen and pelvis. It is important to note that these injury risk curves were derived from numerical correlation of PMHS Abbreviated Injury Scores (AIS) and WorldSID injury responses in matched lateral pendulum and sled impact tests. The WorldSID 50th male thorax and abdomen rib deflection responses, as measured by the conventional IRTRACC system, are therefore expected to have occurred in a lateral direction. This means the abdomen and thorax injury risk curves are likely to be most suitable for application in pole test conditions producing predominantly lateral rib deflections, but the injury risk from loadings producing any substantive deflection of the WorldSID 50th male ribs in the longitudinal and vertical directions is not known.

At the 151st session of the United Nations World Forum for Harmonization of Vehicle Regulations (WP.29), the United States of America submitted a proposal to establish a GRSP informal group to finalize the development of the WorldSID 50th percentile male and 5th percentile female dummies [14]. WP.29 agreed to the establishment of this group to be chaired and sponsored by the United States. The group aims to complete the technical tasks necessary for the WorldSID 50th percentile male and 5th percentile female dummies to be used in regulation. These tasks include; finalization of the dummy specifications, calibration procedures, and injury risk curves, as well as compilation and documentation of biofidelity, durability, repeatability and reproducibility.

Also at the 151st session of WP.29, Australia submitted a proposal to establish a GRSP informal group to develop a Global Technical Regulation (GTR) on Pole Side Impact [1]. It was agreed to

develop this GTR and establish an informal group. Australia is now technical sponsor and chair of this group. The Australian proposal envisaged this GTR would require the use of WorldSID dummies, given the superior biofidelity of these dummies.

There are currently two impact angles used in pole side impact tests applied in regulation and/or used by various consumer evaluation programs. A 29 km/h perpendicular pole side impact test is currently used in EuroNCAP, ANCAP, KNCAP and FMVSS 201. A 32 km/h oblique (75°) pole side impact test is currently being phased in, as a mandatory requirement of FMVSS 214 [13].

The WorldSID rib deflection response and the measurement of this response are expected to be an important consideration for both the WorldSID and pole side impact informal groups. There are currently three rib deflection measurement systems available for the WorldSID 50th male. These are the conventional IRTRACC system, the 2D-IRTRACC system, and “RibEye” multipoint sensing.

The conventional IRTRACC (Infra Red Telescoping Rod for the Assessment of Chest Compression) system is shown in Figure 1. Each IRTRACC has two pivot points; one at the accelerometer mounting block and one at the central spine box of the dummy. The IRTRACC can compress/expand along the measurement axis and rotate forward/back and up/down. The deflection recorded by the IRTRACC represents the change in length of the IRTRACC (relative to the undeformed / zero output condition), and is unequivalent to the change in distance between the two pivot points. However, WorldSID ribs are capable of moving in all three dimensions. The IRTRACC system is therefore not capable of measuring rib motion in all directions which the ribs could move during side impact testing. For this reason, much theoretical discussion has focussed on the likely rib response, including the direction of this response, in oblique and perpendicular pole side impacts.

The WorldSID 50th male “RibEye” system uses two sensor sets to measure the three dimensional location of a total of 18 light emitting diodes (LEDs) mounted on the shoulder, thorax and abdomen ribs. Both sensor sets are mounted near the spine box inside the inner ribs. The “RibEye” LEDs used in the “RibEye” multipoint rib deflection measurement system are shown in Figure 2. Each rib is fitted with three LEDs (front/middle/rear). The middle LED (see Figure 2) is fitted to the accelerometer mounting block at the same location as the IRTRACC pivot attachment point (see Figure 1). The front and rear LEDs of

the dummy used in this study were fitted using double sided tape and heat shrink tubing. This system can measure the three dimensional motion of three points on each rib, and is therefore capable of measuring rib motion in all directions the ribs may deflect during side impact.

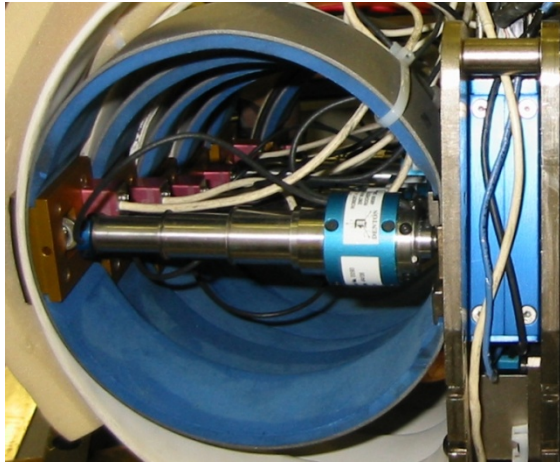


Figure 1. A WorldSID 50th lower abdomen rib fitted with an IRTRACC rib deflection measurement system (viewed from below).



Figure 2. A WorldSID 50th male rib fitted with three "RibEye" LEDs.

At the time of this study there was only one WorldSID 50th male with "RibEye" in the world. The tests reported in this study were conducted with the original WorldSID 50th male "RibEye" dummy. This "RibEye" system has since been improved / updated. More detailed information on the current (as of early 2011) "RibEye" rib deflection measurement system for the WorldSID 50th male is included in an updated user's manual [3].

METHOD

A series of six full scale vehicle-to-pole side impact tests were conducted with WorldSID 50th male

dummies in each of the two front row seating positions.

Two large Australian made, 5-door, right hand drive, passenger sedan models were used in this study (designated as Model A and Model B). Model A is a previous generation vehicle released in August 2004 and superseded in August 2006. Model B is a current (as of March 2011) generation vehicle released on the Australian market during 2008. Both these vehicle models had seat mounted OEM head/thorax combination (front row) side airbags. Deployed airbags are shown for each model in Figure 3. Model A was designed to detect side impacts using left and right lower b-pillar mounted acceleration type sensors (see Figure 4). For Model B, side impacts are detected by left and right side front row door cavity pressure sensors (see Figure 4) and left and right side c-pillar door striker mounted acceleration type sensors. Both vehicles were certified to UNECE R95 and Model B achieved a 5-star ANCAP rating, including the maximum two points for head protection in the ANCAP pole test.



Figure 3. Deployed head/thorax combination side airbags (left: Model A; right: Model B).

All vehicles were tested at a test mass approximately equal to; the sum of the unladen vehicle mass, a 136 kg cargo mass and the mass of one WorldSID 50th male. The second WorldSID 50th male and the onboard test equipment were counted as part of the cargo mass. Non structural components, including radiators, were removed from the front of each test vehicle to achieve a mass distribution between the front and rear axles, as representative as possible of the mass distribution of the vehicle when loaded to its unladen vehicle mass, plus the mass of one struck side WorldSID 50th male and a 136 kg cargo mass centred over the luggage carrying area.



Figure 4. Model A lower b-pillar acceleration type sensor (left) and Model B door cavity pressure sensor (right).

A WorldSID 50th fitted with the “RibEye” [3] multipoint sensing system was used in the struck side front row seating position. A WorldSID 50th fitted with the IRTACC rib deflection measurement system was used in the non-struck side front row seating position.

All vehicles were impacted on the left (passenger) side. The WorldSID 50th dummies were provided by Transport Canada and were delivered to Australia instrumented for left hand impact. Although it is relatively straight forward to transfer IRTACCs from the left ribs to the right ribs, this process is much more complicated and problematic for the “RibEye” multipoint sensing system. It was decided that the results obtained from left hand impact tests would be just as valid for the purposes of this study.

Multi-coloured paint markings were used to obtain a visual record of head, thorax and abdomen interactions between adjacent dummies as well as the vehicle interior, including the struck side armrest, centre console and side airbags.

Although the tests produced responses from interaction between the two dummies, these were clearly separable in time from the struck side dummy responses. For the struck side dummy separate head injury response maxima were therefore calculated for the interaction with the airbag / pole and any interaction with the adjacent front seat occupant. These separate local head injury criteria and acceleration maxima were calculated using the method shown in Newland et al. 2008 [5]. The presence of a non-struck side dummy does not affect the assessment of struck side injury risk.



Figure 5. An example of multi-colour paint markings used to leave evidence of dummy contact during a test.

Three pole side impact test methods were investigated in this study; a perpendicular test based on the EuroNCAP pole side impact protocol [2], an offset perpendicular test based on the test method recommended in APROSYS SP11-0086 ‘An

Evaluation of the Side Impact Pole Test Procedure’[15] and an oblique test based on the FMVSS 214 pole test [13].

The struck side dummy was positioned according to the WorldSID 50th percentile adult male seating procedure draft 5.2. For Model A, the seatback angle was set to achieve the nominated manikin torso angle (as measured by an SAE J826 H-Point machine) of 23° [11]. For Model B, the seatback angle was set to achieve a manufacturer recommended manikin torso angle of 25°. All front row seats were positioned at the first available seat track position at least 20 mm rearward of mid-track (two positions rearward of mid-track in both vehicles). The struck side (passenger) seat base heights were not adjustable. The non-struck side (driver) seat base heights were adjustable, and were set to match the struck side seat base heights as closely as possible (20 mm up from lowest position for both vehicle models). A FARO arm was used to measure the head centre of gravity and H-Point location of each dummy in each test. For each vehicle model, the struck side dummy head centre of gravity and H-Point locations were matched as closely as possible for all three test methods. In each test, the non-struck side dummy was positioned to match the struck side dummy X and Z position coordinates as closely as possible.

All tests were conducted at a target impact speed of 32 km/h to achieve a constant (i.e. control) impact energy for each test method. A carrier sled was used to impact the vehicles with a standard 254 ± 3 mm diameter (i.e. 10 inch) pole. The perpendicular and offset perpendicular tests were conducted with a 90° angle between the direction of travel of the carrier sled and the vehicle longitudinal centreline / axis. In the oblique tests, this angle was 75°. The pole was aimed directly at the head centre of gravity (C.O.G.) in the perpendicular and oblique tests, and 100 mm forward of the head centre of gravity in the offset perpendicular tests. The test methods investigated are summarized in Table 1.

**Table 1.
Summary of Test Methods**

Test Method	Target Impact Angle (Degrees)	Targeted Pole Impact Alignment	Target Impact Speed (km/h)
Perpendicular	90 ± 3	At head centre of gravity (± 38 mm)	32 ± 0.5
Offset Perpendicular	90 ± 3	100 mm forward of head centre of gravity (± 38 mm)	32 ± 0.5
Oblique	75 ± 3	At head centre of gravity (± 38 mm)	32 ± 0.5

As Model A was a previous generation vehicle for which there were no pole side impact tests known to have demonstrated reliable performance, it was anticipated that the vehicle might produce variable airbag firing times and/or unreliable airbag deployment. Inconsistent airbag deployment would have introduced another test variable which would have made comparison of results difficult. For this reason it was decided to remotely deploy the struck side airbags 7 ms after first contact of the vehicle with the pole. This 7 ms fire time was chosen to ensure the airbag deployed no later than would have otherwise been achieved in any test, and no earlier than could be realistically achieved through optimization of the vehicle sensors. The struck side airbag was disconnected from the airbag control module and replaced by a resistor. This resistor was used to simulate the resistance of the airbag to the airbag control module. The voltage across the resistor was measured and used to determine the time at which the airbag control module would have fired the airbag in each test.

It was anticipated that the airbags in Model B would fire consistently and reliably for each test method. For this vehicle model, the airbag control module was relied upon to fire the airbags, and a current clamp was used to measure airbag fire time.

Accelerometers were used in both vehicles to measure vehicle accelerations in several locations; including at the vehicle centre of gravity, the airbag control module, the a-pillar, the b-pillar, and the c-pillar. For Model B, a pressure sensor was also used to measure the struck door cavity pressure at a location recommended by the manufacturer, near the vehicle pressure sensor.

Figure 6, Figure 7 and Figure 8 show vehicle Model B mounted on the carrier sled (at t-zero) in the perpendicular, offset perpendicular and oblique impact modes.

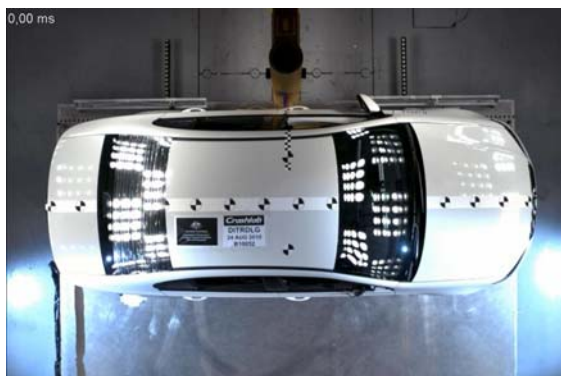


Figure 6. Overhead view of a perpendicular pole side impact test (Model B at time-zero).



Figure 7. Overhead view of an offset perpendicular pole side impact test (Model B at time-zero).



Figure 8. Overhead view of an oblique pole side impact test (Model B at time-zero).

All dummy and vehicle sensor data were collected at a 10 kHz sampling frequency. All data presented in this paper is in accordance with the filtering and sign conventions specified by SAE J211-1 (December 2003) [10].

This paper focuses on the injury response data from the struck side (left passenger) dummy. Occupant-to-occupant interaction and non-struck side dummy responses are reported wherever a significant injury risk was recorded.

RESULTS

Impact Detection and Airbag Firing

Table 2 shows the recorded airbag fire time for each pole side impact crash test conducted. The TTF times shown represent the time at which an airbag fire signal was detected from the airbag control module in each test vehicle. As previously mentioned, the struck side airbag in Model A was remotely fired 7 ms after first vehicle contact with the pole in all three tests. No airbag control module fire signal was able to be detected for the offset perpendicular pole test conducted on Model A. The reason for this has not been determined. For Model B, the struck side airbag was fired by the vehicle airbag control module signal.

Table 2.
Recorded Airbag Control Module Fire Time

Airbag Control Module (TTF from t-zero) (ms)		
Test	Model A	Model B
Perpendicular	8.0	11.9
Offset Perpendicular	-	12.3
Oblique	13.5	12.2

Note: Model A airbag fire times cannot be directly compared to Model B airbag fire times. Model A has a flush door handle design and first contact of the vehicle with the pole (t-zero) is made by the door panel. In contrast, first contact of the Model B door handle with the pole (t-zero – see Figure 6, Figure 7 and Figure 8) occurred up to 2.6 ms before first contact of the outer door panel with the pole.

For Model A, it is important to note that the airbag control module would have actually fired the airbag 5.5 (13.5 – 8.0) ms later in the oblique test, than the perpendicular test. For Model B, the combination head/thorax side airbag consistently fired around 12 ms after first contact with the pole in each test.

Figure 9 shows vehicle Model A y-axis acceleration at the lower b-pillar mounted airbag sensor, for each pole impact method. As indicated in this figure, the airbag control module fired the struck side airbag 2.1 ms and 2.4 ms after the peak y-axis acceleration in the perpendicular and oblique tests, respectively. In the offset perpendicular test, similar peak y-axis acceleration was recorded at approximately 10 ms, yet no fire signal was detected. The accelerometer data from the test vehicle suggests the airbag control module probably should have fired the airbag at around 12.5 ms (i.e. 2 to 2.5 ms after the peak sensor acceleration), as indicated by the dashed red line in Figure 9.

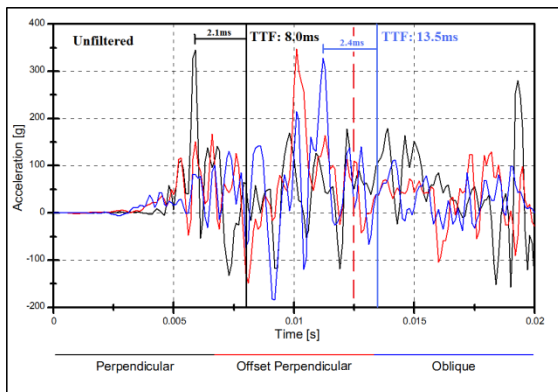


Figure 9. Model A lower b-pillar airbag sensor y-axis acceleration time history (unfiltered).

Figure 10 shows the vehicle Model B struck door cavity pressure response for each pole side impact test. The door cavity pressure time histories are quite similar for all three test methods, particularly during the first 10 ms.

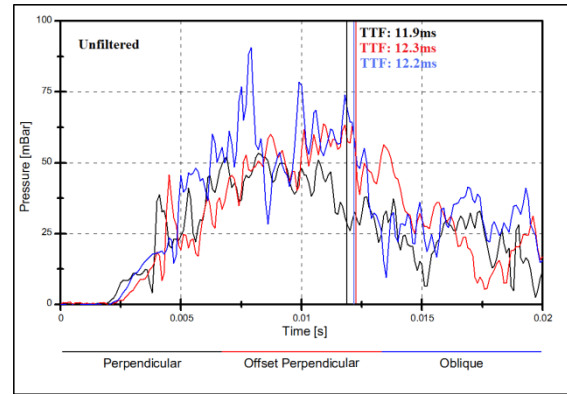


Figure 10. Model B front left door cavity pressure time history (unfiltered).

Airbag Deployment – Model A

Figure 11 shows the Model A head/thorax combination side airbag deploys from beside the lower thorax and abdomen of the WorldSID 50th male. This airbag was observed to be vulnerable to entrapment below the shoulder, between the thorax and the intruding interior door trim. To provide head protection, this airbag must successfully inflate up past the point of the dummy shoulder, before the available gap becomes too small or closes completely.



Figure 11. Model A airbag deployment near lower thorax and abdomen of WorldSID male.

The Model A head/thorax combination side airbag deployed fully in the oblique pole test, but was entrapped beneath the dummy shoulder, between the thorax and door trim, in the perpendicular and offset perpendicular pole tests.

Figure 12, Figure 13 and Figure 14 show the vehicle Model A airbag deployment 18 ms after first contact with the pole during the perpendicular, offset perpendicular and oblique pole side impact tests. Each figure is a still frame taken from the high speed video footage, to illustrate the most critical interactions between the airbag, dummy and the interior door trim in each test.



Figure 12. Model A airbag deployment 18 ms after first vehicle contact with the pole in the perpendicular test.

Figure 12 shows the intruding door trim, had by $t = 18$ ms, pushed the airbag underneath the upper arm and shoulder of the dummy. The airbag was entrapped and unable to deploy fully. A small hole, formed by pressure in excess of the capacity of the seam stitching, is visible at the lower front corner of the airbag. The high speed footage goes on to show the airbag gradually venting through this small hole.



Figure 13. Model A airbag deployment 18 ms after first vehicle contact with the pole in the offset perpendicular test.

The 18 ms still frame from the offset perpendicular impact (see Figure 13) shows a noticeably larger gap between the dummy shoulder and the Model A b-pillar than the perpendicular impact (see Figure 12). In the offset perpendicular impact the Model A airbag was very close to deploying through the gap, but caught the interior door trim, before bursting and venting rapidly along the entire length of the lower airbag seam. These differences in airbag bursting and venting may not be repeatable, and should be noted when comparing thorax results from the perpendicular and offset perpendicular tests of vehicle Model A.



Figure 14. Model A airbag deployment 18 ms after first vehicle contact with the pole in the oblique test.

When fired at 7 ms, the Model A airbag was able to pass between the point of the WorldSID 50th male shoulder and the interior door trim in the oblique test. The 18 ms still frame from the oblique impact (see Figure 14) shows the largest gap between the dummy shoulder and the Model A b-pillar. The Model A airbag was very close to catching on the interior door trim in the oblique test. Had the airbag control module been relied upon to fire the airbag, the airbag would have actually fired 6.5 ms later at $t = 13.5$ ms (see Table 2). If the airbag deployment shown in Figure 14 had been allowed to occur 6.5 ms later (i.e. at 13.5 ms instead of 7 ms), it is very likely, if not certain, the airbag would have caught on the interior door trim, been pushed beneath the shoulder and burst, as occurred in the perpendicular and offset perpendicular tests.

The propensity of the Model A airbag to become entrapped and rupture is therefore affected by both the time at which the airbag fires and the relative lateral velocity between the point of the dummy shoulder and the section of interior door trim immediately behind the airbag. Bringing the airbag firing time forward increases the time available for the airbag to inflate between the point of the shoulder and the door. The gap between the dummy shoulder and the door trim closes more rapidly as the relative lateral velocity between the point of the dummy shoulder and the interior door trim is increased.

There are therefore two factors most likely to have contributed to the observable differences in the gap between the dummy shoulder and the door trim in vehicle Model A. Firstly, the pole was most closely aligned with the point of the dummy shoulder in the perpendicular test and furthest from the point of the dummy shoulder in the oblique test. Secondly, the lateral component of impact velocity in the oblique test (V_y) is approximately 30.9 km/h (i.e. $V_y = 32\sin(75) = 30.9$), which is slightly lower than

the 32 km/h lateral impact component in the perpendicular and offset perpendicular tests.

The WorldSID 50th male dummy fitted with the “RibEye” multipoint measurement system was successfully able to detect the different airbag venting rates observed, following bursting of the Model A airbag in the perpendicular and offset perpendicular tests. For example, Figure 15 shows the theoretical IRTACC deflection vs. time response of thorax rib 3 in the perpendicular and offset perpendicular pole tests conducted using vehicle Model A.

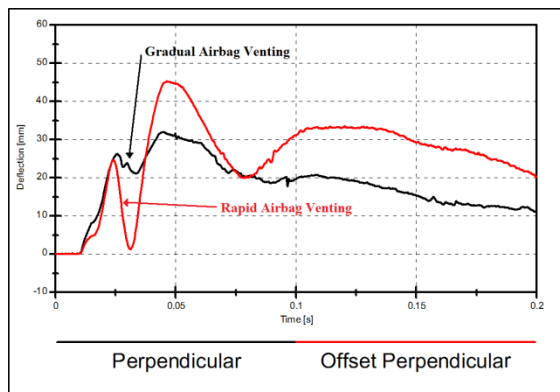


Figure 15. Thorax rib 3 theoretical IRTACC deflection vs. time (Model A).

Airbag Deployment – Model B

Figure 16 shows the vehicle Model B head/thorax combination side airbag deploys from beside the shoulder of the WorldSID 50th male. The high speed video footage goes on to show this airbag unfolds and inflates in both directions (up/down) from shoulder level. The Model B airbag successfully deployed to cover both the thorax and the head in all three tests.



Figure 16. Model B airbag deployment near shoulder of WorldSID male.

Struck Side Head Protection

Figure 17 shows the Model A airbag deployment 50 ms (around time of maximum head acceleration)

after first vehicle contact with the pole in the oblique pole test. This was the only test in which the Model A airbag was inflated in a position to prevent hard head contact with the pole.



Figure 17. Side view of Model A airbag deployment, 50 ms after first vehicle contact with the pole in the oblique pole test.

For comparison, Figure 18 shows the Model B airbag deployment 50 ms after first vehicle contact with the pole in the oblique pole test. This airbag was observed to provide similar coverage of the WorldSID 50th male head for each test method.



Figure 18. Side view of Model B airbag deployment, 50 ms after first vehicle contact with the pole in the oblique pole test.

Figure 19 and Figure 20 show the struck side WorldSID 50th male resultant head acceleration responses from interaction with the side airbag/pole in all six pole side impact tests conducted in this study.

For Model A, the perpendicular and offset perpendicular tests produced very similar resultant head acceleration responses. In both cases, the dummy head experienced hard contact with the pole, producing head accelerations and HIC36 results indicating a high probability of fatal head injury. Offsetting the pole, 100 mm forward of the head centre of gravity did not make any difference to the head injury risk predicted by the dummy. When offset 100 mm forward of the head centre of gravity, the 254 mm pole diameter is large enough

to ensure the dummy head is sufficiently overlapped by the pole (i.e. the 127 mm radius pole overlaps the head c.o.g. by 27 mm). High speed video footage from the offset perpendicular test conducted on vehicle Model A captured the forehead of the dummy impacting the pole. The head then rotated sufficiently, to directly interact with the pole through the head centre of gravity. For vehicle Model A, the oblique test produced a completely different resultant head acceleration response due to the previously discussed differences in the side airbag deployment.

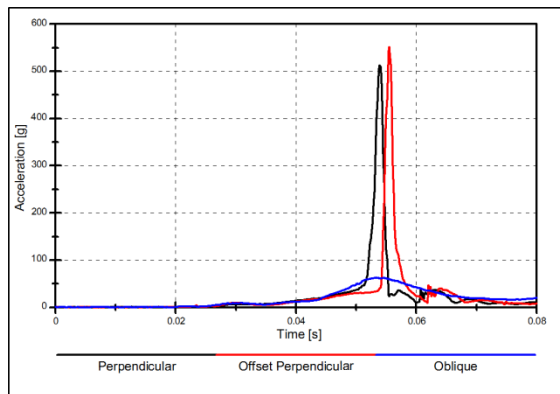


Figure 19. Struck side dummy, resultant head acceleration time history responses from each pole side impact test conducted on Model A.

For Model B, the offset perpendicular and oblique tests produced almost identical head acceleration responses. For this vehicle model, the head acceleration response in the perpendicular impact was phased slightly earlier than the offset perpendicular and oblique pole side impacts. The peak accelerations and HIC36 results indicate similar AIS 3+ head injury risk for each of the tests.

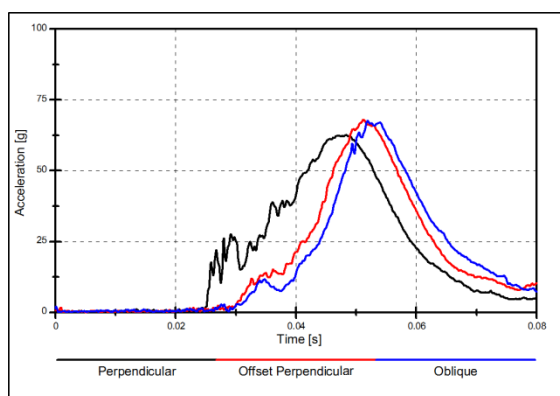


Figure 20. Struck side dummy, resultant head acceleration time history responses from each pole side impact test conducted on Model B.

Although both, the Model A and Model B head/thorax combination side airbags were relatively narrow (i.e. do not extend very much forward of the head) in width, they were both able to provide adequate (i.e. HIC36 << 1000) struck

side head protection from the pole in the 75° oblique pole side impact.

Multi-dimensional Analysis of RibEye Responses

The “RibEye” multipoint rib deflection measurement system provides a very large amount of data. Despite this, the results were able to be relatively easily analysed using computational methods. Filtered “RibEye” data was exported to a spreadsheet and a macro developed and used to plot the incremental position changes of the ribs. These plots were then exported as slide show images and then combined in a 1000 frame per second movie using a movie making software package. Each movie was then able to be conveniently synchronised, for analysis purposes, with the high speed video test footage.

For example, Figure 21, Figure 22 and Figure 23 show still frame images taken from the “RibEye” movies produced for the middle thorax rib in the oblique, perpendicular and offset perpendicular tests conducted using Model B. Each still plot shows the x-y plane position of the “RibEye” LEDs at maximum theoretical IRTRACC deflection. For left-hand impact, the coordinate system is oriented such that each rib is viewed from below (i.e. is in accordance with the sign conventions of SAE J211-1 [10]). The horizontal x-axis is therefore positive in the forward (to the right of page) direction. The position of the rear (left most), middle and front (right most) “RibEye” LEDs are indicated by the blue round dot markers. The position where the IRTRACC of an IRTRACC equipped dummy would have been located is indicated by the double blue line. Lines of constant theoretical IRTRACC deflection (purple and red lines) were used to gauge the magnitude of the deflection. A black polygon was plotted to represent the approximate location of the “RibEye” middle LED ± 1 mm accuracy measurement range for z-axis deflections less than 10 mm.

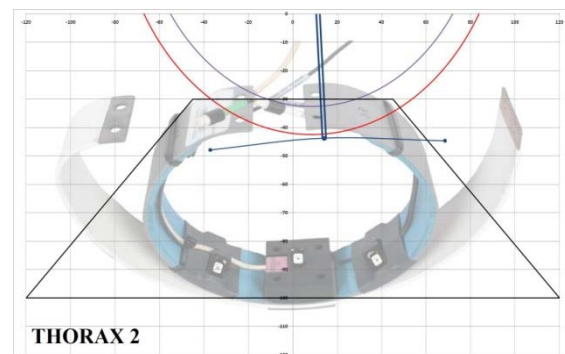


Figure 21. Still frame (at maximum theoretical IRTRACC deflection) from the “RibEye” movie used to analyse thorax rib 2 motion for the oblique pole test conducted on Model B.

Figure 21 indicates that a thorax rib 2 IRTRACC of an IRTRACC equipped dummy would have deflected in a predominantly lateral direction (i.e. the theoretical IRTRACC position is close to parallel with the y-axis). This is typical of the thorax and abdomen rib deflection responses produced in the oblique pole tests conducted in this study. In fact, both oblique pole tests (i.e. Model A and Model B) were observed to produce predominantly lateral peak rib deflection responses for all thorax and abdomen ribs.

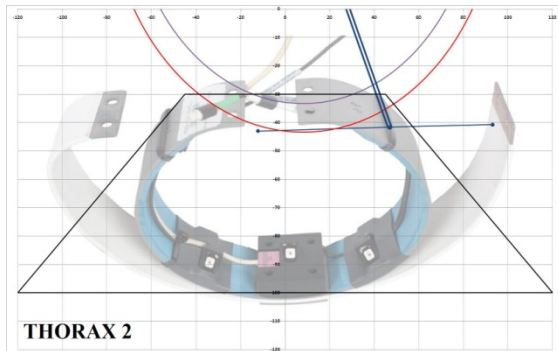


Figure 22. Still frame (at maximum theoretical IRTRACC deflection) from the “RibEye” movie used to analyse thorax rib 2 motion for the perpendicular pole test conducted on Model B.

In contrast, Figure 22 indicates that a thorax rib 2 IRTRACC of an IRTRACC equipped dummy would have been pushed forward (i.e. the theoretical IRTRACC is angled forward of the y-axis). This substantial forward x-axis movement of the rib is typical of the thorax and abdomen rib responses produced in both perpendicular pole tests conducted in this study.

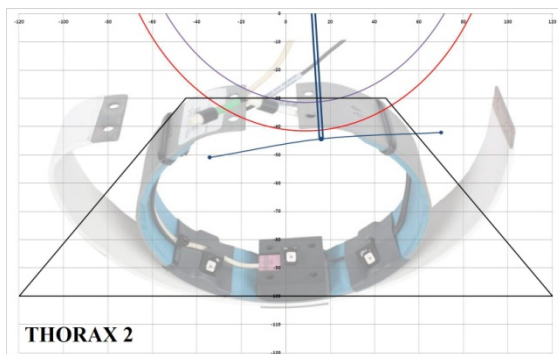


Figure 23. Still frame (at maximum theoretical IRTRACC deflection) from the “RibEye” movie used to analyse thorax rib 2 motion for the offset perpendicular pole test conducted on Model B.

The thorax rib 2 response from the offset perpendicular test shown in Figure 23 is very similar to the thorax rib 2 response from the oblique test shown in Figure 21. For vehicle Model B, the offset perpendicular test produced predominantly lateral peak rib deflection responses. For vehicle

Model A, the offset perpendicular test produced some forward x-axis movement of the ribs, however this forward movement was less than the forward movement recorded in the perpendicular test.

This movie analysis is an example of how the “RibEye” data was able to be used to understand the multi-dimensional rib response of the WorldSID 50th male in each pole side impact test. The availability of “RibEye” data removed the need to hypothesise about the multi-dimensional nature of the rib responses in oblique vs. perpendicular pole side impacts.

Theoretical IRTRACC Responses

As explained in the introduction, the middle “RibEye” LED is fitted to the accelerometer mounting block where the IRTRACC outer pivot attachment point would otherwise have been located. Theoretical IRTRACC deflections are therefore able to be calculated from the “RibEye” data, using the following equation [3]:

$$\text{IRTRACC Deflection} = P_y - \sqrt{[(P_y - |R_y|)^2 + R_x^2 + R_z^2]}$$

Where:

P_y = IRTRACC pivot-to-pivot dimension of an unloaded rib.

R_x = RibEye middle LED position change in the x direction.

R_y = RibEye middle LED position change in the y direction.

R_z = RibEye middle LED position change in the z direction.

The IRTRACC pivot-to-pivot point dimensions used for each rib were taken from the “RibEye” hardware user’s manual [3] and are based on the CAD design dimensions for the WorldSID 50th male dummy. Each theoretical IRTRACC deflection therefore represents the linear deflection of the IRTRACC outer pivot attachment point relative to the inner pivot attachment point, otherwise measured by an IRTRACC in an IRTRACC equipped dummy.

Figure 24 shows y-axis displacement of the middle “RibEye” LED and theoretical IRTRACC deflection, for the middle thorax rib in the oblique pole test conducted on Model B. For this rib, in this oblique pole test, the theoretical IRTRACC deflection is approximately equal to the y-axis displacement of the middle LED. This means the x-axis and z-axis movements of the middle LED were too small to significantly influence the theoretical IRTRACC response, and indicates the peak rib deflection occurred in a predominantly lateral direction. This was observed to be the case for all thorax and abdomen ribs in both oblique pole tests (i.e. for Model A and Model B).

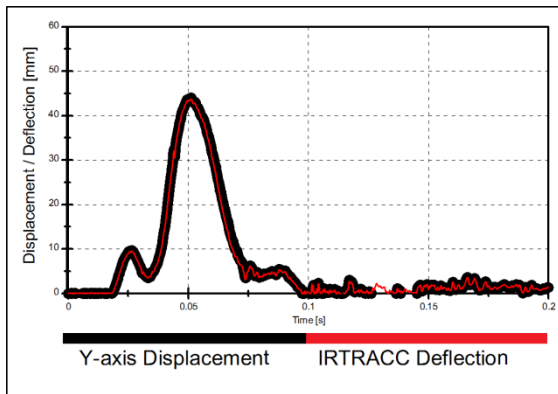


Figure 24. Y-axis displacement of the Thorax Rib 2 middle LED vs. theoretical IRTRACC deflection in the oblique pole test conducted on Model B.

In contrast, in the perpendicular test conducted on Model B, the thorax rib 2 peak theoretical IRTRACC deflection was substantially less than the y-axis displacement of the middle LED (see Figure 25). This is a result of the forward movement of the rib previously shown in Figure 22. For a given R_y and R_z , increasing R_x will reduce the IRTRACC deflection (see above equation for theoretical IRTRACC deflection). Similar differences in the y-axis displacement of the middle “RibEye” LED displacement and the theoretical IRTRACC deflection were observed for all thorax and abdomen ribs in both perpendicular pole tests conducted in this study.

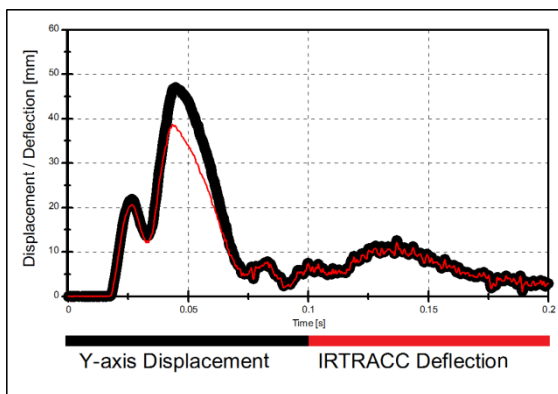


Figure 25. Y-axis displacement of the Thorax Rib 2 middle LED vs. theoretical IRTRACC deflection in the perpendicular pole test conducted on Model B.

As previously discussed, the Model A airbag deployed successfully in the oblique test, but became entrapped and burst in the perpendicular and offset perpendicular tests. Variable airbag bursting and venting characteristics were also observed for Model A. Different rib deflection responses were therefore produced for each test conducted on Model A. However, it is difficult to distinguish the affect of variable airbag deployment from the affect of variable structural loadings.

The Model B airbag deployed consistently and without entrapment or bursting in all three tests. For this vehicle model, the offset perpendicular and oblique pole tests produced larger peak theoretical IRTRACC deflections than the perpendicular test. In fact, the complete time history response (i.e. time phasing, magnitude, shape etc.) of each thorax and abdomen rib response was observed to be very similar for the offset perpendicular and oblique pole tests. Figures 26 to 30 show theoretical thorax and abdomen rib IRTRACC response time histories for the offset perpendicular and oblique pole tests conducted on Model B.

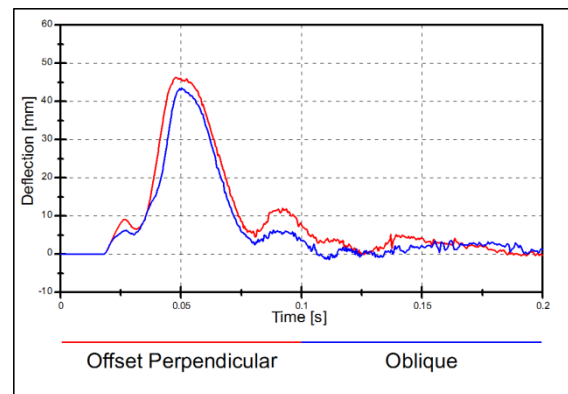


Figure 26. Thorax Rib 1 theoretical IRTRACC deflection vs. time (Model B).

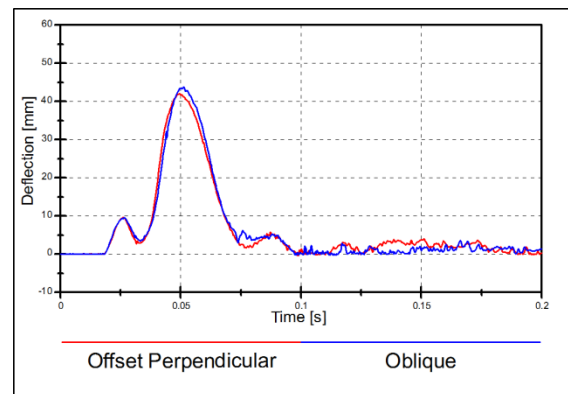


Figure 27. Thorax Rib 2 theoretical IRTRACC deflection vs. time (Model B).

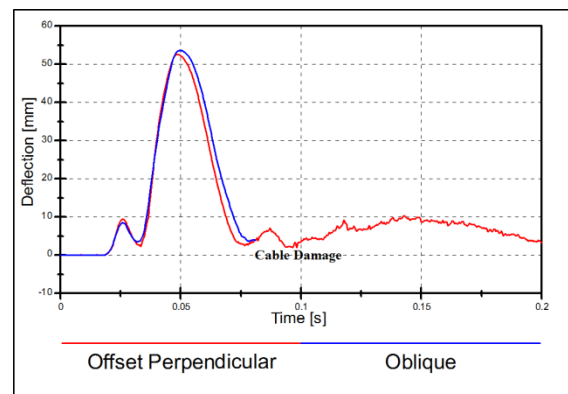


Figure 28. Thorax Rib 3 theoretical IRTRACC deflection vs. time (Model B).

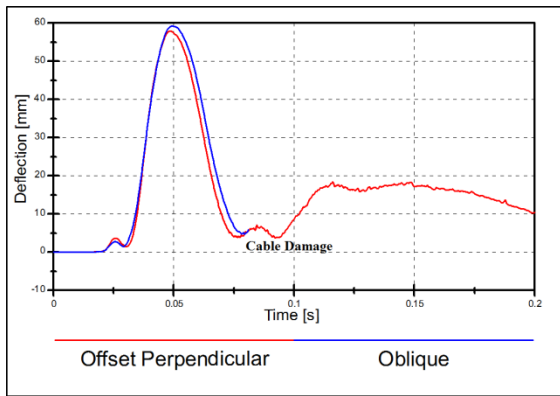


Figure 29. Abdomen Rib 1 theoretical IRTRACC deflection vs. time (Model B).

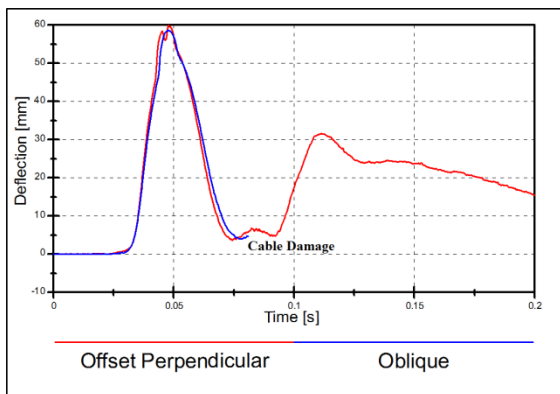


Figure 30. Abdomen Rib 2 theoretical IRTRACC deflection vs. time (Model B).

The cable damage indicated in Figure 28, Figure 29 and Figure 30 prevented lower thorax and abdomen rib data from being collected beyond $t = 82$ ms in the oblique pole test conducted on Model B. This was caused by the damage to the lower thorax and abdomen “RibEye” sensor cable connector shown in Figure 31. The upper and lower sensor cable connectors were connected at the base of the “RibEye” controller inside the right (non-struck side) lower abdomen rib of the dummy used in this study. This damage is believed to have been caused by interaction with the centre console. The sensor cable connections have since been redesigned and are now connected higher up inside the thorax on the side of the “RibEye” controller [3].



Figure 31. Damage to “RibEye” controller sensor cable connector in the oblique pole test conducted on Model B.

In each 32 km/h pole side impact test conducted in this study, the peak struck side dummy rib loadings were recorded around 50 ms after first vehicle contact with the pole. Notably, Figure 32 and Figure 33 show a similar structural deformation response and vehicle-to-pole alignment at $t = 50$ ms in the offset perpendicular and oblique pole tests conducted on vehicle Model B.



Figure 32. Overhead (plan) view of offset perpendicular impact of Model B, 50 ms after first vehicle contact with the pole.



Figure 33. Overhead (plan) view of oblique impact of Model B, 50 ms after first vehicle contact with the pole (note: image has been digitally rotated 15 degrees clockwise for comparison purposes).

Abdomen-to-Armrest Interaction

It was observed from the post crash dummy paint markings, that the head/thorax combination side airbags in both vehicle models did not extend down low enough to provide much coverage of the WorldSID 50th abdomen, especially the lower abdomen rib.

Figure 34 shows the paint markings left during the loading of the WorldSID 50th lower thorax and abdomen ribs in the oblique pole test conducted on vehicle Model A. In this case, the red paint mark represents the upper abdomen rib (1) and the blue paint mark represents the lower abdomen rib (2).



Figure 34. Struck side dummy thorax/abdomen rib to airbag and armrest interaction in the oblique pole test conducted on Model A.

Likewise, Figure 35 shows the paint markings left during the loading of the WorldSID 50th lower thorax and abdomen ribs in the oblique pole test conducted on vehicle Model B. In this test, the blue paint mark represents the upper abdomen rib (1) and the yellow paint mark represents the lower abdomen rib (2).



Figure 35. Struck side dummy thorax/abdomen rib to airbag and armrest interaction in the oblique pole test conducted on Model B.

The struck side WorldSID 50th male dummy fitted with the “RibEye” measurement system was also successfully able to detect differences in airbag loading from the upper thorax to the lower abdomen. Figure 36 shows the theoretical IRTACC deflection vs. time response of the upper thorax, lower thorax and lower abdomen ribs during the oblique pole test conducted using vehicle Model A. These rib response time-history traces are consistent with the evidence provided by the paint markings shown in Figure 34. Wherever a rib substantially interacts with the airbag, the rib deflection response is broadly characterized by an initial increase to a local maxima followed by a decrease to a local minima and a further increase to the overall maximum rib deflection (see generalised example inset top right corner of Figure 36). Thorax rib 1 illustrates this response characteristic most clearly. In contrast, there is little evidence of this type of initial rib response for abdomen rib 2. This is because thorax rib 1 interacted with the

airbag, while abdomen rib 2 directly impacted the armrest below the airbag (as shown by the blue paint mark in Figure 34). Similarly, the abdomen rib 2 deflection response for vehicle Model B (see Figure 30) shows no evidence of airbag interaction and the post test paint markings support this (see Figure 35).

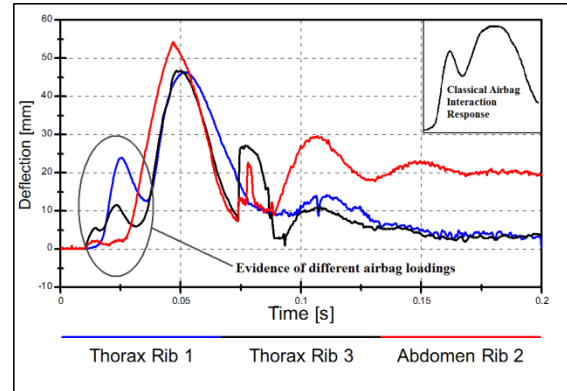


Figure 36. Theoretical IRTACC deflection vs. time responses from the oblique pole test conducted on Model A.

Summary of Results / Estimated Injury Risk

Table 3 and Table 4 summarize the struck side WorldSID 50th male responses and estimated AIS 3+ injury risk for each pole side impact test conducted on Model A and Model B respectively. In each of these tables, the struck side dummy head injury response and injury risk values are for the dummy head to airbag / pole interaction phase (i.e. $t \leq 80$ ms). The legend below defines the colour coding used in this paper to indicate the estimated injury risk, as well as the abbreviated WorldSID rib descriptions used in Table 3 and Table 4. The methods used to estimate each AIS 3+ injury risk are also noted.

Legend	
AIS 3+ Injury Probability	P ≤ 25%
	25% < P < 50%
	P ≥ 50%
Rib 1 = Shoulder Rib	
Rib 2 = Upper Thorax Rib = Thorax Rib 1	
Rib 3 = Middle Thorax Rib = Thorax Rib 2	
Rib 4 = Lower Thorax Rib = Thorax Rib 3	
Rib 5 = Upper Abdomen Rib = Abdomen Rib 1	
Rib 6 = Lower Abdomen Rib = Abdomen Rib 2	
Notes:	
HIC36 injury risks were determined using the Prasad/Mertz AIS 3+ skull fracture probability risk function [12].	
Thorax, abdomen and pelvis injury risks were determined from the survival method AIS 3+ injury risk curves published by Petitjean et al., 2009 [6].	

Table 3.
Summary of Struck Side Dummy Response
and AIS 3+ Injury Risk (Model A)

Model A		Test Method		
Body Region	Injury Criteria	Oblique	Perpendicular	Offset Perpendicular
Head	HIC36	275	5667	5944
	3ms Head Acceleration (g)	60.2	103.6	84.7
Thorax	Rib 2 Deflection (mm)	46.3	36.4	> 46
	Rib 2 Viscous Criterion (m/s)	0.74	0.40	-
	Rib 3 Deflection (mm)	43.4	35.5	50.9
	Rib 3 Viscous Criterion (m/s)	0.68	0.54	0.95
	Rib 4 Deflection (mm)	46.7	32.0	45.3
	Rib 4 Viscous Criterion (m/s)	0.89	0.32	0.62
	Rib 5*Deflection (mm)	56.0	28.7	53.4
	Rib 5*Viscous Criterion (m/s)	0.82	0.19	0.82
	Rib 6*Deflection (mm)	54.2	23.8	43.9
	Rib 6*Viscous Criterion (m/s)	0.83	0.43	0.65
Abdomen	Rib 5*Deflection (mm)	56.0	28.7	53.4
	Rib 5*Viscous Criterion (m/s)	0.82	0.19	0.82
	Rib 6*Deflection (mm)	54.2	23.8	43.9
	Rib 6*Viscous Criterion (m/s)	0.83	0.43	0.65
	3ms T12 Acceleration (g)	55.7	45.9	58.3
Pelvis	3ms Pelvis Acceleration (g)	67.0	44.3	70.1
	Pubic Symphysis Force (kN)	1.23	0.74	1.19

The rib deflections shown in Tables 3 and 4 are theoretical IRTRACC values and the viscous criterion values have been calculated from the theoretical IRTRACC responses.

For vehicle Model A, the struck side dummy head responses indicate a high probability of fatal head injury in the perpendicular and offset perpendicular pole tests, and a low probability of AIS 3+ skull fracture in the oblique pole test. This is a predictable consequence of the head/thorax combination side airbag failing to deploy fully and therefore failing to prevent hard head contact with the pole in the perpendicular and offset perpendicular tests.

According to the survival method injury risk curve values published by Petitjean et al. [6], none of the Model A tests produced more than 25% probability of AIS 3+ abdomen or pelvis injury. However, some of the viscous criterion values from the offset perpendicular and oblique tests exceeded the 50% probability of AIS 3+ thoracic skeletal injury threshold.

*Note: Petitjean et al., 2009 [6] expressed AIS 3+ thoracic skeletal injury risk in terms of both thorax and abdomen rib responses. This is based on the fact that humans have 12 thorax ribs (on each side) some of which cover a portion of the WorldSID 50th abdomen. The 50% AIS 3+ dummy response thresholds were lower for thoracic skeletal injury than for abdomen injury. In this table, abdomen rib responses have therefore been included in both the thorax and abdomen body region sections. For each section, the abdominal rib responses have been shaded to indicate either probability of AIS 3+ thoracic skeletal injury or AIS 3+ abdominal soft tissue injury, as applicable.

Table 4.
Summary of Struck Side Dummy Response
and AIS 3+ Injury Risk (Model B)

Model B		Test Method		
Body Region	Injury Criteria	Oblique	Perpendicular	Offset Perpendicular
Head	HIC36	343	377	355
	3ms Head Acceleration (g)	65.0	61.5	65.1
Thorax	Rib 2 Deflection (mm)	43.5	42.6	46.3
	Rib 2 Viscous Criterion (m/s)	0.82	0.42	0.80
	Rib 3 Deflection (mm)	43.8	38.7	42.1
	Rib 3 Viscous Criterion (m/s)	0.66	0.60	0.75
	Rib 4 Deflection (mm)	53.6	45.9	52.6
	Rib 4 Viscous Criterion (m/s)	0.83	0.89	0.89
	Rib 5*Deflection (mm)	59.2	50.6	57.9
	Rib 5*Viscous Criterion (m/s)	0.98	1.02	1.04
	Rib 6*Deflection (mm)	58.6	41.6	60.0
	Rib 6*Viscous Criterion (m/s)	1.77	0.71	2.22
Abdomen	Rib 5*Deflection (mm)	59.2	50.6	57.9
	Rib 5*Viscous Criterion (m/s)	0.98	1.02	1.04
	Rib 6*Deflection (mm)	58.6	41.6	60.0
	Rib 6*Viscous Criterion (m/s)	1.77	0.71	2.22
	3ms T12 Acceleration (g)	59.6	69.9	61.4
Pelvis	3ms Pelvis Acceleration (g)	66.4	70.2	74.2
	Pubic Symphysis Force (kN)	1.18	1.07	1.33

For vehicle Model B, each struck side dummy head-to-airbag interaction response indicates a low probability of AIS 3+ skull fracture. Notably, the peak theoretical IRTRACC deflections were higher in the oblique and offset perpendicular test than the perpendicular test.

According to the survival method injury risk curve values published by Petitjean et al. [6], the lower thorax and abdomen rib deflection and viscous criterion values recorded in the oblique and offset perpendicular tests indicate greater than 50% probability of AIS 3+ thoracic skeletal injury. The lower abdomen rib viscous criterion values from the oblique and offset perpendicular tests also indicate greater than 50% probability of AIS 3+ abdomen injury; however the lower abdomen rib deflection values suggest less than 25% probability of AIS 3+ abdomen injury. The risk of AIS 3+ pelvis injury was less than 25% in each test.

Dummy Occupant-to-Occupant Interaction

Dummy occupant-to-occupant head interactions produced HIC36 results normally associated with a high probability of fatal head injury in five of the six tests conducted. The oblique pole test conducted on vehicle Model A was the only test which did not produce a dummy occupant-to-occupant head interaction with a HIC36 greater than 1000. In this test, the 75° impact angle generated sufficient forward motion of the non-struck side dummy head relative to the struck side dummy head, to limit the head interaction to a glancing contact only. Table 5 summarizes the dummy occupant-to-occupant head interaction responses for each test conducted in this study.

Table 5.
Summary of Occupant-to-Occupant
Head Interaction Response and
AIS 3+ Head Injury Risk

Head Interactions		Test Method		
Body Region	Injury Criteria	Oblique	Perpendicular	Offset Perpendicular
Model A				
Struck Side	HIC36	108	6242	5767
	3ms Head Acceleration (g)	26.8	74.0	47.3
Non-Struck Side	HIC36	232	6803	6255
	3ms Head Acceleration (g)	44.7	85.0	92.1
Model B				
Struck Side	HIC36	2561	17979	4252
	3ms Head Acceleration (g)	50.7	75.2	39.1
Non-Struck Side	HIC36	2709	18089	4269
	3ms Head Acceleration (g)	56.0	76.8	58.5

Note: The occupant-to-occupant head interaction responses were calculated for $t > 80$ ms, as per method previously used in Newland et al. 2008 [5]. HIC36 injury risks were determined using the Prasad/Mertz AIS 3+ skull fracture probability risk function [12].

Significant non-struck side dummy lower thorax and abdomen rib responses were also recorded as a result of interaction with the centre console in vehicle Model B. For example, a 37 mm lower thorax rib IRTRACC deflection was recorded in the oblique test and a 36 mm upper abdomen rib IRTRACC deflection was recorded in the offset perpendicular test, of this vehicle model.

DISCUSSION

The “RibEye” multipoint measurement system proved a very useful analysis tool for the purposes of this study. Although this system provides a lot of data, computational methods can be developed and used to aid and expedite the data analysis. The availability of 3-dimensional rib response data eliminated the need for complicated theoretical assumptions and analyses to interpret the results. The “RibEye” system also provided important information about the multi-dimensional nature of the rib responses, not measured by the conventional IRTRACC system.

The peak thorax and abdomen rib deflections of the struck side dummy occurred predominantly in the lateral (y-axis) direction in both oblique pole tests (i.e. oblique tests for Model A and Model B). Although the vehicle impacts the pole at a 75° angle in the oblique pole test, results show the direction of the dummy rib deflections cannot simply be assumed to have occurred in the same oblique direction. This is because, unlike the vehicle, the dummy does not impact directly with the pole. The dummy instead impacts the airbag next to the interior door trim which is in the relatively complex process of dynamically deforming around the pole.

The offset perpendicular pole side impact test conducted using Model B also produced predominantly lateral peak thorax and abdomen rib deflection responses. There was some forward movement of the thorax and abdomen ribs in the offset perpendicular test conducted using Model A.

Both perpendicular pole tests (i.e. tests for Model A and Model B) produced substantial forward (x-axis) movement of the ribs. This could be due to the pole impacting behind the reclined dummy thorax and abdomen in the perpendicular test method.

In this series, the 15° rotation of the vehicle longitudinal axis in the oblique test method was small enough to ensure the impact was predominantly lateral in nature, but large enough to bring the impact point sufficiently forward on the vehicle to better engage the lower thorax and abdomen, and avoid substantial forward (x-axis) movement of the WorldSID 50th male ribs. Aligning the pole 100 mm forward of the head centre of gravity, as per the offset perpendicular test method, was observed to have a similar affect.

As previously discussed, the thorax and abdomen injury risk curves developed by Petitjean et al. 2009 [6], were derived from results of WorldSID 50th and PMHS purely lateral pendulum and sled impact tests. It was logically assumed that these simple lateral impact tests would have

produced predominantly lateral rib deflections, directly measured by the conventional IRTRACC system. This assumption seems entirely reasonable, logical and well founded given the simple lateral nature of the tests, but could be validated through analysis of some matched lateral pendulum and sled impact tests with a “RibEye” equipped dummy.

The currently available injury risk curves for the WorldSID 50th male were therefore concluded by Petitjean et al. to be applicable to lateral rib loadings only. Notably, in both perpendicular pole tests in this series, the y-axis displacement of the middle LED of each rib was somewhat larger than the corresponding theoretical IRTRACC deflection. This was a result of forward (x-axis) movement of each rib. The IRTRACC point-to-point deflection measurement, and hence the injury risks attributed to these IRTRACC deflections in Table 3 and Table 4 may therefore understate the actual injury risk produced in the perpendicular tests conducted in this study.

Given the predominantly lateral rib responses recorded by the “RibEye” system in both oblique pole tests conducted in this study, it is possible the current WorldSID 50th male injury risk curves might actually be more suitable for application in 75° oblique pole tests than perpendicular pole tests aimed at the head centre of gravity.

CONCLUSIONS

- The struck side dummy head injury responses were significantly affected by the airbag deployment in the tests conducted on vehicle Model A.
- The angle of impact and the alignment of the vehicle relative to the pole affected the timing of the Model A airbag control module fire signal.
- The “RibEye” multipoint measurement system provided important, useful and informative multi-dimensional rib response data.
- The WorldSID 50th “RibEye” responses reveal that oblique pole tests should not simply be assumed to produce oblique rib loadings and perpendicular pole tests should not simply be assumed to produce lateral rib loadings:
 - predominantly lateral peak rib deflection responses were recorded for each thorax and abdomen rib in both oblique pole tests; and
 - significant forward (x-axis) movement was recorded for each thorax and abdomen rib in both perpendicular pole tests.
- The WorldSID 50th male rib deflection responses were influenced by the initial impact alignment of the pole relative to the vehicle and dummy:
 - the offset perpendicular test method produced less forward (x-axis) movement of the WorldSID 50th male ribs than the perpendicular test method; and
 - the offset perpendicular and oblique tests produced almost identical thorax and abdomen rib responses for vehicle Model B.
- For each vehicle model, the peak theoretical thorax and abdomen rib IRTRACC deflections were higher for the oblique and offset perpendicular tests than the perpendicular test.

REFERENCES

- [1] Australian Department of Infrastructure and Transport, 2010, “Proposal to Develop a New Global Technical Regulation on Pole Side Impact”, 151st Session United Nations WP.29 (June 22-25 2010), <http://www.unece.org/trans/doc/2010/wp29/ECE-TRANS-WP29-2010-81e.pdf>.
- [2] European New Car Assessment Programme (EuroNCAP), 2009, “EuroNCAP Pole Side Impact Testing Protocol Version 5.0”, EuroNCAP, <http://www.euroncap.com/files/Euro-NCAP-Pole-Protocol-Version-5.0--0-67e37cf7-8e74-4fe5-a72a-db24061a8e91.pdf>.
- [3] Handman, D., 2011, “HARDWARE USER’S MANUAL: RibEye™ Multi-Point Deflection Measurement System 3-Axis Version for the WorldSID 50th ATD”, Boxboro Systems, http://www.boxborosystems.com/worldsidhwmanu_a122011_1.pdf.
- [4] International Standards Organization (ISO), 1999, “ISO/TR 9790:1999(E) — Road vehicles — Anthropomorphic side impact dummy — Lateral impact response requirements to assess the biofidelity of the dummy”, ISO, Geneva, Switzerland.
- [5] Newland, C., Belcher, T., Bostrom, O., Gabler, H.C., Cha, J.G., Wong, H.L., Tylko, S., Dal Nevo, R., “Occupant-to-Occupant Interaction and Impact Injury Risk in Side Impact Crashes”, Stapp Car Crash Journal Vol. 52 (November 2008), pp. 327-347, Society of Automotive Engineers, Warrendale, PA.
- [6] Petitjean, A., Trosseille, X., Petit, P., Irwin, A., Hassan, J., and Praxl, N., 2009, “Injury Risk Curves for the WorldSID 50th Male Dummy”, Stapp Car Crash Journal Vol. 53 (November 2009), pp. 443-476, Society of Automotive Engineers, Warrendale, PA.

[7] Rhule, H.H., Maltese, M.R., Donnelly, B.R., Eppinger, R.H., Brunner, J.K., and Bolte, J.H.IV. , 2002, "Development of a New Biofidelity Ranking System for Anthropomorphic Test Devices", Stapp Car Crash Journal Vol 46, pp. 477-512, Society of Automotive Engineers, Warrendale, PA.

[8] Rhule, H.H., Moorhouse, K., Donnelly, B.R., and Stricklin, J., "Comparison of WorldSID and ES-2re Biofidelity Using an Updated Biofidelity Ranking System", Paper No. 09-0563, <http://www-nrd.nhtsa.dot.gov/pdf/esv/esv21/09-0563.pdf> , Proceedings 21st ESV Conference, Stuttgart, Germany.

[9] Sherer, R., Bortenschlager, K., Akiyama, A., Tylko, S., Hartlieb, M., Harigae, T., "WorldSID Production Dummy Biomechanical Responses", Paper Number 09-0505, <http://www-nrd.nhtsa.dot.gov/pdf/esv/esv21/09-0505.pdf> , Proceedings 21st ESV Conference, Stuttgart, Germany.

[10] Society of Automotive Engineers (SAE), Safety Test Instrumentation Standards Committee, 2003, "SAE J211-1 Dec 2003: Instrumentation for Impact Test—Part 1—Electronic Instrumentation", SAE International, Warrendale, PA.

[11] Society of Automotive Engineers (SAE), Human Factors Engineering Committee, 1987, "SAE J826 May 1987: Devices for Use in Defining and Measuring Vehicle Seating Accommodation", SAE International, Warrendale, PA.

[12] US Department of Transportation, Office of Regulatory Analysis and Evaluation, "FMVSS No. 214 Amending Side Impact Dynamic Test Adding Oblique Pole Test", August 2007, <http://www.unece.org/trans/doc/2010/wp29grsp/RD-2e.pdf>.

[13] US Department of Transportation, National Highway Traffic Safety Administration (NHTSA), "FMVSS Standard No. 214; Side Impact Protection", Code of Federal Regulations, <http://frwebgate.access.gpo.gov/cgi-bin/get-cfr.cgi?TITLE=49&PART=571&SECTION=214&TYPE=PDF>.

[14] US Department of Transportation, National Highway Traffic Safety Administration (NHTSA), 2010, "Proposal to develop a new global technical regulation on side impact dummies (WorldSID Proposal)", 151st Session United Nations WP.29, <http://www.unece.org/trans/doc/2010/wp29/ECE-TRANS-WP29-2010-82e.pdf>.

[15] Versmissen, T., Edwards, M., Bosch, M., and Puppini, R., 2007, "An Evaluation of the Side Impact Pole Test Procedure: AP-SP11-0086", Advanced Protection Systems (APROSYS) SP1, www.aprosys.com/.../AP%20SP11%200086%20D112A%20-%20June%202007.pdf.

ACKNOWLEDGEMENTS

The authors would like to acknowledge the technical support provided by PMG technologies and the NSW RTA Crashlab.

The opinions expressed and the conclusions reached are solely the responsibility of the authors and do not necessarily represent the official policy of the Australian Government Department of Infrastructure and Transport, or Transport Canada.

A STUDY OF CURTAIN AIRBAG DESIGN FACTORS FOR ENHANCEMENT OF EJECTION MITIGATION PERFORMANCE

Eung-Seo, Kim

Dae-Young, Kwak

Hyeong-Ho, Choi

Han-II, Bae

HYUNDAI MOTOR COMPANY, Korea

Seung-Hui, Yang

Seung-Man, Kim

Dong-Jun, Lee

Autoliv Korea, Korea

Kwang-Soo, Cho

HYUNDAI MOBIS, Korea

Paper Number 11-0173

ABSTRACT

A curtain airbag (CAB) plays a significant role in not only protecting an occupant head from side impact crashes, but also preventing an occupant being partially or totally ejected during rollover accidents. As the seriousness of rollover accident has been statistically studied and reported, the latter function of CAB become more emphasized than before. At last, NHTSA released FMVSS226 final rule in January 2011 which limits the linear travel of impactor headform by 100mm.

This paper focuses on how to meet the requirement by enhancing CAB design and on establishing design guideline through its parametric study. For this, 9 design factors are selected which have major effect on ejection mitigation performance and the effectiveness of each factor is analyzed. They are cushion pressure, amount of coating, cushion shape, cushion depth, overlapping area between door trim and cushion, strength of cushion mounting tab and tether, location of front tether and lastly, distance between impact target point (A3) and cushion mounting.

From this study, the parametric guideline of CAB design factors for satisfying the required excursion limit of 100mm is found out and the test result with the CAB module applied these parameter level shows that the goal is successfully achieved within the excursion of 80mm in all target locations with the test speed of 24kph in accordance with NPRM. At last part, the future work to optimize this for smaller glazing is mentioned.

INTRODUCTION

Rollover crash is a kind of accident which causes relatively more severe fatalities. According to the statistical research of NASS-CDS, although the ratio of rollover crash in all kind of the types is about 2~4% in USA in every year, the fatality rate in the rollover situation has been over 30% (31% in 2003), 33% in 2004, 35% in 2007). Especially, Figure 1 shows that 58% of the 10,378 fatalities in 2003 is due to being partially or fully ejected by rollover accident. From this annual report, we can come to the conclusion that it can be an effective method to help reducing fatalities that mitigating the occupant ejection through side windows. NHTSA (National Highway Traffic Safety Administration) recognized this seriousness of rollover accident and organized IPT (Integrated Project Team) in 2002, which published a guidebook³⁾ in 2003 for safety-improving from the viewpoints of vehicle, roadway and behavioral strategies by conducting rollover and another kinds of tests. On the basis of this, rulemaking activity for mitigating the vehicle occupant ejection had been proceeded and NHTSA

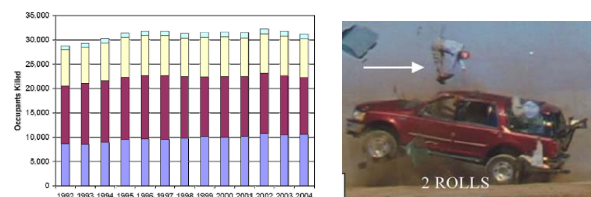


Figure 1. Statistical data of occupant fatalities and complete ejection in rollover crash accident.

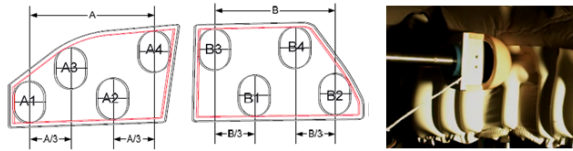


Figure 2. Target locations and test method.

released FMVSS 226 NPRM in December 2009, as well as its final rule in January 2011.

The NPRM limited the linear travel of the 18kg impactor headform by 100mm from the inside of the tested vehicle's glazing in all 4 or less locations when impacting it on curtain airbag with the speed of 24kph at 1.5 seconds after it deployed and 16kph at 6 seconds or on punched advanced glazing. But the final rule eased the regulation by reducing the impacting speed from 24kph to 20kph, and also tightened it rotating the headform and targets by 90 degrees to a horizontal orientation.

This paper proposes the curtain airbag design guideline for satisfying the FMVSS 226 by parametric study. For this, 9 design factors are selected which have major effect on ejection mitigation performance and then their effectiveness is independently analyzed assuming that they have no interactions with one another. They are cushion pressure, amount of coating, cushion shape, cushion depth, overlapping height between door trim and cushion, strength of cushion mounting tab and tether, location of front tether and distance between impact target point (A3) and cushion mounting. For some factors, ejection mitigation performance is evaluated by testing same kind of CAB modules which are made to have two or three parameter levels. And for the other factors, the effectiveness is analyzed using several CAB modules which are already developed and in production for their vehicles. Basically parametric values of guideline are drawn from the test speed of 24kph according to NPRM considering its severity of energy level and because of not enough test data under standards of final rule after it was released.

PRESSURE AND COATING

The performance of CAB's inner pressure can be evaluated by the capability to absorb the impact energy from side impact crash and to maintain high pressure as long as possible at 1.5 and 6.0 seconds after it is deployed when impactor headform hit the

cushion. These two characteristics conflict with each other, so it would be the order of priority firstly to find the appropriate cushion pressure for side impact crash (SINCAP MDB and Pole test mode), secondly to keep the maximum pressure as can as possible making gas leakage minimized and then to modify the other design factors for reducing the excursion of headform.

Evaluation of Pressure in Cushion according to Coating Amount

Test method Inner pressure of three OPW (One Piece Woven) cushions is measured which have the same shape and size, only different silicon coating amount of $35\text{g}/\text{mm}^2$, $75\text{g}/\text{mm}^2$ and $95\text{g}/\text{mm}^2$ respectively. Three locations for fixing pressure port are selected on front, mid and rear cushion chamber in longitudinal direction for pressure monitoring as shown in Figure 3. The tests are conducted three times for each cushion having a coating amount.

Test result The average pressures in three locations have almost same level. The locational pressure property of cushion is closely related with the chamber design and deployment performance in case of first impact (side impact crash within 50ms)⁸⁾, but comparatively it have nothing to do with ejection mitigation performance due to the enough time to fill the gas into entire cushion chamber.



Figure 3. The locations of pressure measuring port and its installation.

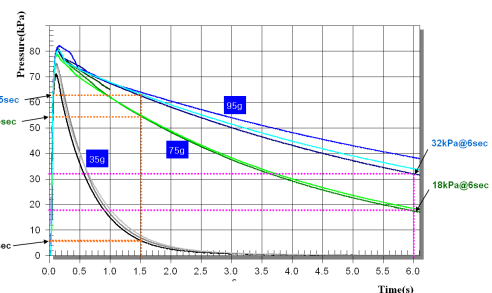


Figure 4. Inner pressure of cushion at 1.5s and 6s in different coating condition (35g, 75g, 95g).

Figure 4. shows that the average pressures are 63.3kPa(1.5s), 34.8kPa(6s) with the coating amount of 95g, and 55kPa(1.5s), 18kPa(6s) with that of 75g. The increase of coating amount by 20g(75g → 95g) results in the pressure increase of 15% at 1.5s and 93% at 6s. This means the coating factor become more important as times goes on.

Evaluation of Headform Travel According to Coating Amount

Test method The ejection mitigation tests are performed at 4 target locations(A1, A2, A3, A4) in 1st row using CABs with 75g, 95g coated. In this test, the cushions are filled with the gas in the same pressure as the lowest values of former pressure monitoring test using pressure controllable gas injection device instead of using inflator.

Test result The result shows that increase of coating amount is more effective when the impact time is at 6 seconds with the test speed of 16kph (See Table 1). This is due to that although the pressure loss at 6 seconds is more than at 1.5 seconds, the difference of gas leakage between the cushion having 75g and 95g coating also increases as time goes by. In the aspect of target location, coating factor is most effective at A4 where the inflated cushion depth is thickest in all the test conditions and there are 7% and 16% improvement at the weak point of A1 and A3 respectively with the increase of 20g coating. The maximum improvement is 91% at 6 seconds at the location of A4 where the inflated cushion depth is biggest. The decrease of excursions of all locations with the speed of 24kph(1.5s) or at A1 location with all test speed are around or under 10%, so cushion chamber shape or the other factors are to be modified to enhance the performance.

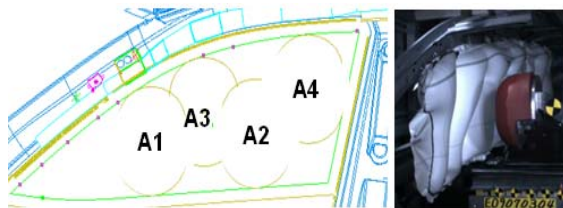


Figure 5. Target locations and tested cushion pressure.

Table 1.

Excursion and improvement according to coating amount.

Location	16kph, 6s			20kph, 1.5s			24kph, 1.5s		
	75g	95g	Excursion Difference (%)	75g	95g	Excursion Difference (%)	75g	95g	Excursion Difference (%)
A1	112.4	104.4	8 (7%)	125.5	123	2.5 (2%)	137.2	137.2	0
A2	55.9	26.5	29.4 (53%)	43.8	38.3	5.5 (13%)	79.3	71.9	7.4 (9%)
A3	107.8	91	16.8 (16%)	107.2	102.1	5.1 (5%)	137.2	132.4	4.8 (4%)
A4	35	3	32 (91%)	12.4	3	9.4 (76%)	35.7	40.1	4.4 (12%)

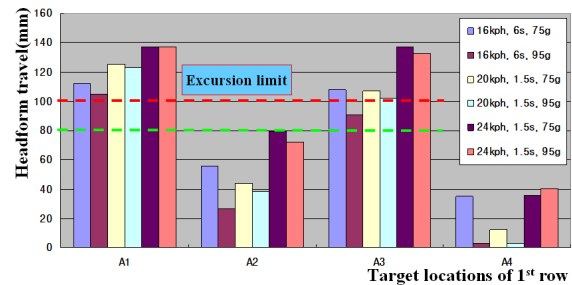


Figure 6. Headform travel according to target location and coating amount.

The Guideline of Cushion Pressure and Coating Amount of CAB

Generally, cushion pressure required for getting good head injury in side impact tests (SINCAP MDB and Pole test mode) ranges from 40kPa to 80kPa with varying vehicle segments and structural performances. But the CAB used in this test is SUV's and the guideline is that the cushion pressure needs over 65kPa at 1.5 seconds and 35kPa at 6 seconds with the impactor speed of 24kph and 16kph respectively and coating amount is 95g/mm² by OPW(One Piece Woven) fabric made of Nylon 66 material.

CUSHION CHAMBER SHAPE

Test Method

The excursions at A1 and B1 are compared each other according to active chamber, whose target point are comparatively far from the cushion mounting on body panel and are irrelevant to impact point of side crash test so that there usually have little inflated chamber. About A1 location, the test is carried out using two cushion designs as shown in

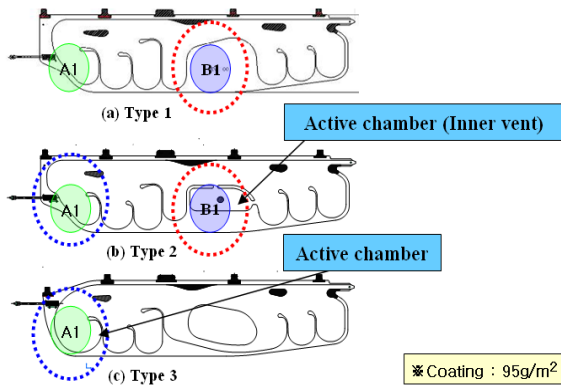


Figure 7. Cushion shape according to inflatable chamber at A1 and B1 target locations.

volume except different thickness at the point in conditions of 33kPa and 40kPa (24kph, 1.5s). About B1 location, the test is conducted using two cushion designs as shown in Figure 7 (a)Type 1 and (b)Type 2 which have same volume but only type 2 have active chamber at the point in conditions of 33kPa (24kph, 1.5s). All the CAB cushions have 95g/mm² coating.

Test Result

It is shown that there is improvement of 25~30mm between type 2 and type 3 at A1 location and that the higher the inner pressure is, the more effective the thicker cushion is (See table 2). Decrease of headform travel at B1 is 35mm from cushion type 1 to type 2. Especially, we applied inner vent to the chamber design on B1 location in type 2, which is also called delay chamber.

Table. 2
Headform travel according to inflatable chamber at A1 and B1.

		Speed	24kph(1.5s)	
		Location	A1	B1
TEST RESULT	Type #1	33kPa@1.5s(1.8 mol)	157	185
	Type #2	33kPa@1.5s (1.8 mol)	160	150
		40kPa@1.5s (2.0 mol)	152	
	Type #3	33kPa@1.5s (1.8 mol)	135	
		40kPa@1.5s (2.0 mol)	132	



Figure 8. Ejection mitigation test of type 2 at A1.

This chamber is filled with inflator gas near after 1 second later than first impact time span (i.e. side crash impact) by narrowing the entrance to the aimed chamber. This design helps improving ejection mitigation performance without increasing inflator capacity (cost). Another example is shown in Figure 9.

The Guideline of Cushion Shape Design

Inflated chamber is needed at A1 and B1 location. The inflated chambers at A1 and B1 are to be set up so that they can include impactor headform projected area at A1 and target point (headform center point) as shown in Figure9. A-pillar structure cannot support CAB cushion at A1 location so that chamber needed to cover all of the headform. On the other hand, it is permitted that inflated chamber covers only B1 target point because B-pillar structure helps supporting the CAB cushion. In some cases of small glazing, the inflated chamber at B1 cannot be needed if the chamber depth of B-pillar area is thick enough to support CAB cushion. At both of A1 and B1 locations, inner vent design is applicable.

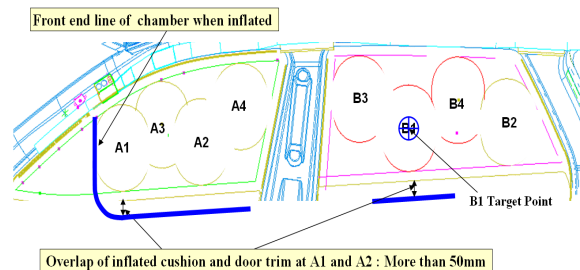


Figure 9. The area for inflated chamber

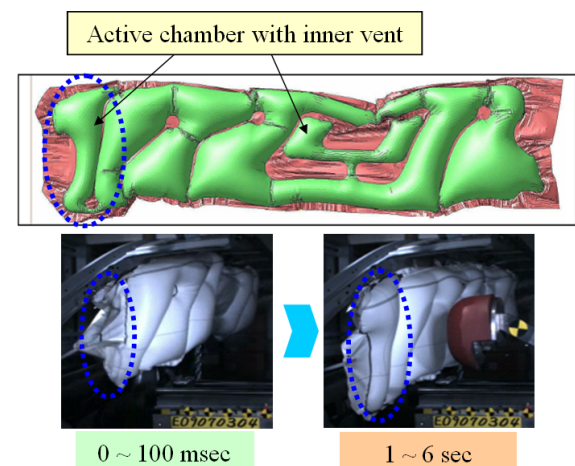


Figure 10. Inner vent (delay chamber) design.

DEPTH OF INFLATED CUSHION CHAMBER AT TARGET LOCATIONS

The depth of inflated cushion chamber is the design factor which directly affect to ejection mitigation performance so that the improvement is big when increasing its thickness in the state of high pressure level. But if it is increased without limit for only enhancing ejection mitigation performance, the inflator should be bigger and more expensive. In addition, the thickness is closely related with the development of rollover sensing system. The CAB firing time is determined predicting whether a vehicle is going to roll over or not considering roll-angle, roll-rate, lateral acceleration, occupant behavior, etc. In case of high speed roll-over situation like curb-trip mode, there cannot be enough time to determine TTF (Time to Fire) in order for CAB to be deployed stably before occupant head come to CAB cushion if its depth is too thick. Consequently, the guideline of cushion depth has only lower limit of 100mm without upper limit. The upper limit is depends on the behavioral characteristics of vehicle and occupant, and on CAB's deployment performance.

OVERLAPNG HEIGHT OF CUSHION AND DOOR TRIM

Test Method

The ejection mitigation performance according to overlapping height between door trim and cushion can be evaluated by using different CAB modules having different height in a vehicle. But if varying the cushion's height, it is very hard to make the CAB modules having same pressure property but only different height, and this result in interactions with another design factors. Thus, in this test, a CAB

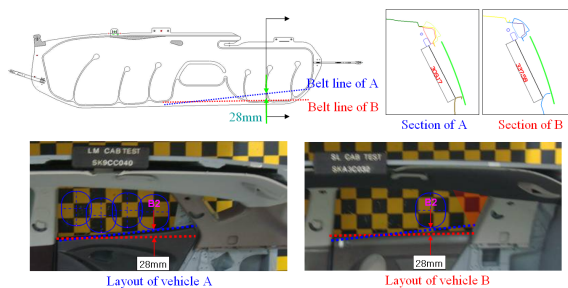


Figure 10. Two vehicles having same CAB module but different door trim height.

module is evaluated which is already developed and applied to two different vehicles which have same structural layout (CAB route and mounting position) but different height of door trim in second row. The target locations of second row are set to one vehicle and the coordinates are transferred to the other vehicle. And the overlap height is measured about the CAB module which satisfies the excursion limit of 100mm (20kph) in the inflated state.

Test Result

The improvement of excursion is 21 mm at B1 location from the overlap difference of 28mm comparing the test results conducted in vehicle A and B as shown in Figure 11. This test seems to be reliable considering that excursion deviations at another location except A1 between two vehicles are within 1mm. It is thought that the difference at A1 is due to the A-pillar layout. It is expected that the overlapping height between door trim and cushion is effective at A1, A2, B1 and B2 which are close to door trim.

Another test result of CAB module whose maximum excursion is 79mm (24kph) also shows that the excursion decrease rapidly at the location which has the overlap height of over 50mm in the inflated state.

Table 3. Test result according to overlap difference between two vehicles.

Vehicle	A				B			
	24kph				24kph			
Location	A1	A2	A3	A4	A1	A2	A3	A4
First row	96			39	79			38
Location	B1	B2	B3	B4	B1	B2	B3	B4
Second row		112	56			133	55	

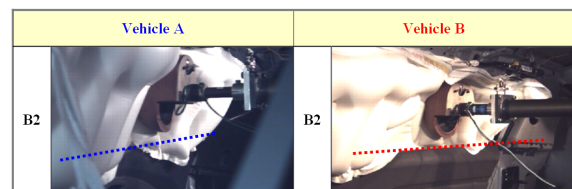


Figure 11. Ejection mitigation test at B2 location

Vehicle C	Speed	24kph	
	Location	A1	A'
1 st row		79	33.5
Location	B1	B2	
2 nd row		66	7

Figure 12. The cushion overlap with beltline and ejection mitigation test. (Part of car body test)

STRENGTH OF CUSHION MOUNTING TAB AND TETHER

When the 18kg impactor headform is impacted to CAB cushion with the speed of 24kph, the energy of 400J is applied to the cushion exerting tensile force to the mounting tab and tether around the target location. Thus, they are needed to be designed not to be broken and easily stretched. Actually it sometimes happened that tether bracket was broken or cushion mounting tab was torn in ejection mitigation test increasing headform excursion or not containing it within vehicle's inboard side of CAB cushion.

Test Method

The specimens of seven kinds of cushion mounting tab-bracket and ten kinds of tether-bracket assembly were cut from six kinds of CAB modules and they were examined by grab test using UTM device. Each kind of specimen is tested three times with the speed of 100mm/min. The specimen and test setup method are shown in Figure 13. In this test, breaking strength (maximum tensile force in this paper) and stretched length at that point are simply used instead of tensile strength and elongation because the specimen is composed of more than two materials and doesn't follow the specimen standard.

Test Result

The breaking strength variously ranges from 100kgf to 410kgf. The broken locations are also different in mounting tab, sewing line, tether bracket and tether itself. On the whole, cushion mounting has low breaking strength and short stretched length, while tether has the opposite properties. In ejection mitigation test of a vehicle, impactor headform stopped at almost same time when the mounting tab was broken, and this can tell us that 128kgf is the

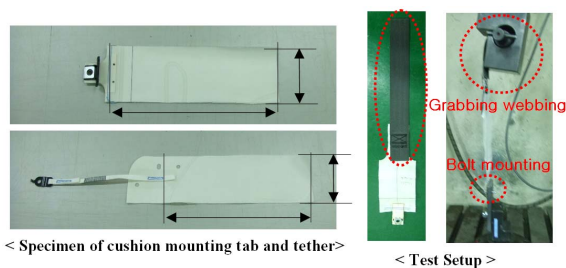
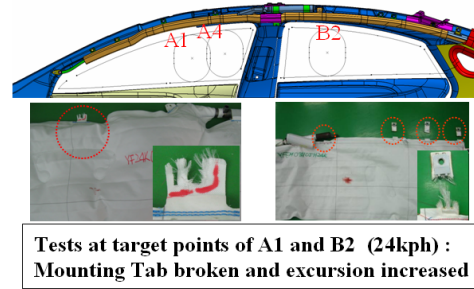


Figure 13. Test setup and specimen.

(a) Ejection Mitigation test



(b) Grab test : Breaking strength 128kgf with 36mm stretch

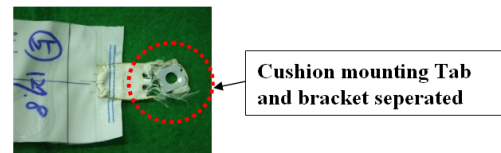


Figure 14. Breakage in ejection mitigation and grab test result.

minimum required strength level against impactor energy, which is the breaking strength of this mounting tab in grab test.

The Guideline of Cushion Mounting Tab and Tether strength.

High breaking strength prevents the mounting parts being disconnected and the shorter the stretched length is, the better the ejection mitigation performance is. Therefore, as the ratio of breaking strength to stretched length (kgf/mm) is increased, so the excursion of headform is decreased at the point when reaching to the breaking strength.

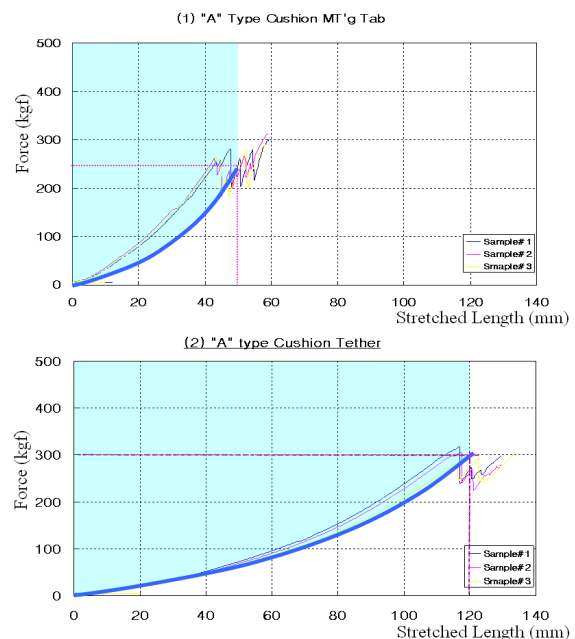


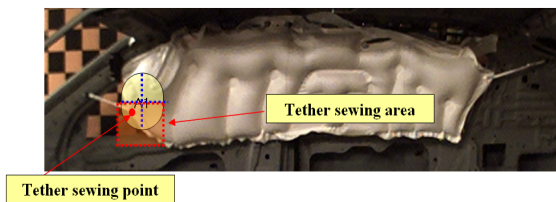
Figure 15. The result of grab test

The guideline for strength is determined so that mounting part can withstand the pulling force from impactor energy with the speed of 24kph and referring to the test result having high ratio of breaking strength to stretched length. The required parameter value for cushion mounting tab and tether is different. Mounting tab needs the breaking strength of over 250kgf and stretched length of below 50mm. Tether mounting needs the breaking strength of over 300kgf and stretched length of below 120mm. The ratios of cushion mounting tab and tether are 5kgf/mm, 2.5kgf/mm respectively as shown in Figure 15.

THE LOCATION OF FRONT TETHER MOUNTING

About the locations of A1 and A3, body structure of A-pillar cannot support CAB cushion because of the slanted feature of car body and the limit of cushion length in frontal direction. Therefore, tether is attached between A-pillar and front area of cushion in order to strongly grab the cushion against pushing force from headform to the outside of vehicle. In this case, the location of tether-cushion sewing and tether bracket mounting on A-pillar affect to ejection mitigation performance. As a result, their relative positions are determined so that the cushion can be constrained on body tightly as shown in Figure 16. Tether sewing is to be positioned below the A1 target point and location of tether bracket mounting, below the mid-height of cushion chamber when fully deployed.

a. Tether sewing location : Below the A1 target point when fully deployed.



b. Location of tether bracket mounting : Below the mid-height of cushion chamber when fully deployed.

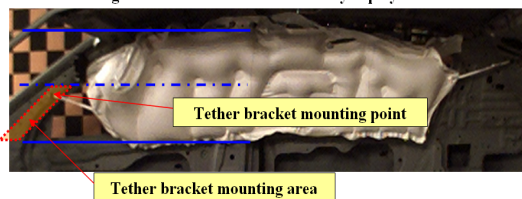


Figure 16. FRT The location of tether sewing and mounting.

THE DISTANCE BETWEEN A3 TARGET POINT AND ITS NEIGHBORING CUSHION MOUNTING

The relation between excursion and mounting distance from A3 target point is investigated for 5 vehicles. Mostly, the excursion limit of 100mm is satisfied except vehicle A at A3 and any clear correlation is not found (See Table 4.). It is thought that there are another design factors that affect more to ejection mitigation performance than this factor. Most of the distance ranges from 200mm to 300mm. It is recommended that the distance from A3 to its neighboring cushion mounting is below 300mm. It is expected that the closer the distance is, the smaller the excursion of impactor headform is.

CONCLUSIONS

Nine design factors are selected which have major effect on ejection mitigation performance and then their effectiveness is independently analyzed. With this, the curtain airbag design guideline is established for accomplishing the goal of 100mm limit of impactor headform's linear travel with the speed of 24kph (according to FMVSS226 NPRM). And the ejection mitigation test result for a CAB module of a SUV which this parameter level is applied to shows that the requirement of FMVSS226 NPRM is successfully achieved with the maximum excursion of 80mm as shown in Table 5.

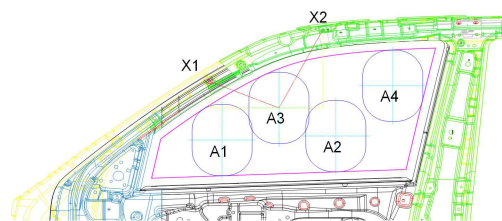
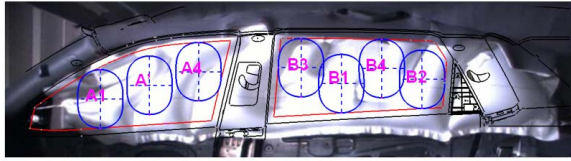


Figure 17. Distance between A3 target point and its neighboring cushion mounting.

Table. 4 Excursion according to mounting distance

Vehicle	A: A3-X1 (mm)	B: A3-X2 (mm)	A+B	Excursion(24kph)			
				A1	A2	A3	A4
A	221	281	501	138	27	106	29
B	413	286	699	85	35	53	-13
C	273	292	565	95	42	72	30
D	277	203 (346)	480 (623)	88	-45	57	-40
E	230	258	488	88	(13)	(88)	13

Table 5. Test result of the finally modified CAB.



█ : Eliminated target point
 * : Skip considering the result of 24kph test

Location		A1	A2	A3	A4	A'
First Row	16kph	29			*	*
	24kph	80			-6	56
Location		B1	B2	B3	B4	
Second Row	16kph	*	*	*	*	
	24kph	46	-58	-24	*	

※ Test condition : Full vehicle
 ※ Dynamic friction : less than 0.25
 ※ Target locations according to NPRM and Final rule are same.

Nevertheless, the proposed CAB design specification may be reinforced for accomplishing the objective of FMVSS226 NPRM about SUV, resulting in the rise of cost.

Hence, it would be future work to optimize the parameters suitable for the vehicle which have smaller size of window glazing (having maximum of 2 or 3 target points per a glass in a vehicle) and to develop more improved technologies to approach higher ejection mitigation performance with reduced cost for satisfying FMVSS226 final rule.

REFERENCES

[1] NHTSA Report. June 2003. "Initiatives to Address the Mitigation of Vehicle Rollover".

[2] "Motor Vehicle Traffic Crash Fatality Counts and Estimates of People Injured for 2007" National Center for Statistics and Analysis. National Highway Traffic Safety Administration. DOT-HS-811-034, Updated February 2009.

[3] "Initiatives to Address the Mitigation of Vehicle Rollover", National Highway Traffic Safety Administration, June 2003.

[4] Federal Register Proposed Rules, Vol. 74, No. 230, National Highway Traffic Safety Administration, December 2, 2009.

[5] L. Chang-Hyun, C. Jae-Soon, et. al. "A Study on

Curtain Airbag Component Test Methods for Evaluating Side Impact and Ejection Mitigation Performances using Numerical Simulations", JASE 150-20075279, 2007.

[6] J. Dix, K. Sagawa, L. Sahare, S. Hammoud, D. Fulk and A. Cardinali, "A Study of Occupant Ejection Mitigation During Rollovers for Front Row Occupants", SAE International 2010-01-0520, 2010.

[7] Wilke, Donald T., et. al. "Status of NHTSA's Ejection Mitigation Research Program", 18th International Technical Conference on the Enhanced Safety of Vehicles (ESV) paper 342, United States Department of Transportation, National Highway Traffic Safety Administration, 2003.

[8] Eung-Seo, Kim. "Development of Test Method for Evaluating Curtain Airbag Deployment Force" 22th International Technical Conference on the Enhanced Safety of Vehicles, Paper 09-0174, Stuttgart, Germany, June 15-18, 2009.

[9] NHTSA Advanced Glazing Research Team; "Ejection Mitigation Using Advanced Glazing: A Status Report," November 1995; DOT Docket NHTSA-1996-1782-3.

[10] R. Heuschmid, D. Bello, J. 2010. "Prospects for Fulfilment of Ejection Mitigation (FMVSS226)", Airbag 2010 Symposium, No. 15, Germany.

Update on Investigation of New Side Impact Test Procedures in Japan

Hideki Yonezawa
Naruyuki Hosokawa
Yoshinori Tanaka

Yasuhiro Matsui
National Traffic Safety and Environment Laboratory

Takeshi Korenori

Kiyohiko Hirakawa

Ministry of Land, Infrastructure and Transport

Koji Mizuno

Nagoya University

Japan

Paper Number 11-0200

ABSTRACT

The safety of cars in side impact accidents has been improved since regulations requiring improved performance in a side impact test (for example, ECE/R95 or FMVSS 214) have come into effect in many countries. However, many people continue to be injured in side impact accidents; and, as a consequence, further improvements in a car's performance in side impact crashes are desired. This paper has been written to provide an update on what future improvements may be required, and presents a study of recent side impact accident data collected in Japan and the effectiveness of the curtain side air bag in side impact crashes.

In evaluating the improvements of a car's safety performance in side impact accidents, the National Transportation Safety and Environment Laboratory (NTSEL) previously has conducted research and published papers about various full car side impact tests, for example, the regulatory ECE/R95 tests, moving deformable barrier (MDB) tests, and car-to-car tests. However, NTSEL considers that it is necessary to gain increased knowledge regarding the injured body regions of occupants involved in a side impact accident in order to evaluate the effectiveness of safety equipment in future side impact accidents.

In this study, we first investigated the recent side impact accident environment from accident data in Japan. In this review, we examined trends regarding collision partners, injured body regions, injury levels, and the curb mass of both the struck and striking vehicles. The results indicate the following two findings: Firstly, the head and chest are the main injured body regions in the fatal and serious injury side impact accidents. Secondly, the percentage of lighter vehicles is relatively large for the struck vehicles, and the percentage of heavier vehicles is relatively large for the striking vehicle in these fatal and serious injury side impact accidents.

Secondly, we investigated the occupants' seating postures in cars running on Japan's roads. The results show that 56% of the drivers' heads were in line or overlapped with the vehicles' B-pillars. A more detailed study about the seating postures of the driver also was conducted.

Thirdly, we conducted MDB-to-car side impact tests according to the Regulation ECE/R95 specification with the exception of the seating positioning of the dummy. The target vehicles were two same model K-cars, which are categorized in Japan as a very small size vehicle, and the seating positions were adjusted so that the dummy's head overlapped the B-pillar. One K-car had a Curtain Side Air Bag (CSA) and a Side Air Bag (SAB) installed; while, in the other K-car, the CSA and SAB were not installed. We compared these test data, previous test data collected for small vehicles, and the Japan New Car Assessment Program test data for the same model K-cars as well as other small cars. The compared data included the injury measures and kinematic behavior of the ES-2 dummies in the front seats of the struck vehicles. It was demonstrated that the CSA and SAB were effective for reducing the number of head and chest injuries in car-to-car crashes; however, it was also demonstrated that the degree of effectiveness was influenced by their design.

INTRODUCTION

Though the number of vehicle accidents has been decreasing recently in Japan, in 2010 it was greater than 720,000, and the number of injuries was greater than 890,000. Considering this traffic accident situation, regulations for occupant protection including the side impact protection [1] have been introduced in Japan. Additionally, The Japan New Car Assessment Program (JNCAP) conducts safety evaluation of new cars.

From the accident data analysis, it was shown that the contacts with the head and chest during side crashes are a major cause of serious injuries and death. In order to prevent the occupant's serious injuries during

side impact accident, manufacturers have installed curtain side air bags (CSAs) and thorax side air bags (SABs) as supplemental restraint systems. In general, the CSA protects the occupant from head, face, and neck injuries; and the SAB protects the occupant from thoracic and abdominal injuries.

There are many studies published about the effectiveness of the CSA and the SAB. For example, the Insurance Institute for Highway Safety (IIHS) estimated that the side air bags with head protection reduce driver deaths in cars struck on the near side by 37% [2]. Otte et al. conducted research to analyze side impact accident data to confirm the effectiveness of the SAB [3]. The National Agency for Automotive Safety and Victim's Aid (NASVA) conducted pole side impact tests on vehicles with and without CSAs and compared the resulting head injury measures.

But for the case of a side impact accident in which the striking object is a passenger vehicle, the effectiveness of the CSA has not been studied as extensively. This may be due to the fact that the dummy head injury measures are not so large for the tests based on the ECE/R95 test procedure and consequently the CSAs are not needed. For example, most of the head injury criteria (HIC) data measured in the Japan New Car Assessment Program (J-NCAP) have been less than 500.

In this study, building on the bases of our past studies [4-8], we hypothesized that the reason why the dummy head injury measures obtained from the ECE/R95 tests were not so large was due to the seating posture of the dummy. In almost all cases, the dummy head did not overlap the B-pillar under the ECE/R95 regulation. We conducted research on the side impact accidents in Japan and on the occupant seating postures in vehicles on the roads, and conducted full car side impact test series. Some of these results already have been published [8]. In this study, first we investigated the recent side impact accident data in Japan by injury levels and confirmed the macro trend. Next, we researched the occupant seating postures in vehicles on the roads and confirmed that 56% of drivers and 78% of passengers were seated such that their head overlapped the B-pillar (from a side view). And from our research sample study, we confirmed that the trend that, when the driver's height was large, the overlap of the head and B-pillar was large. We also found that the individual variability also had a large influence on the position as well as the height. Third, tests were conducted based on the specifications of Regulation ECE/R95 with the exception that the dummy was positioned so as the head would make contact with the B-pillar. To investigate the effectiveness of the CSA for head protection in car-to-car crashes, these tests were conducted for struck cars with and without a CSA for two types of vehicles. It was demonstrated that the CSA was effective for reducing the number of head injuries in car-to-car crashes.

STUDY ON SIDE IMPACT ACCIDENT IN JAPAN

In this study, the accident analyses in Japan were examined based on the Institute for Traffic Accident Research and Data Analysis (ITARDA) global accident data for 3 years (2005-2007). The side impact accident data were filtered to contain only belted occupants and crashes without multiple impacts. Figure 1 shows the percentage of striking vehicles and object types by the injured level (fatal, serious, and minor). The narrow objects (e.g., signals, telephone poles, and road signs) were defined as "poles." The injury level was defined by the days that the victim visited the hospital. The cases for which the visit to the hospital was over 30 days were defined as "serious" injuries, and the cases where the visits were under 30 days were defined as "minor" injuries. The cases that the occupants died within 24 hours of the accidents were defined as "fatal" accidents. In fatal accidents, 47% of the striking objects were a "passenger vehicle," 21% were "other object (without pole)," 19% were "pole," and 13% were "large vehicle, truck." In serious injury accidents, 81% of the striking objects were "passenger vehicle," 10% were "other object (without pole)," 5% were "large vehicle, truck," and 4% were "pole." In minor injury accidents, 97% of the striking objects were "passenger vehicle," 2% were "other object (without pole)," 1% were "large vehicle, truck," and 0.3% were "pole." The "passenger vehicle" was the largest source of striking objects for all the accidents though the percentage was relatively smaller in the fatal accidents and larger in the minor accidents. The "Large vehicle, truck," "pole," and "other object (without pole)" were large sources of striking objects in the fatal accidents, but very small in the minor injury accidents.

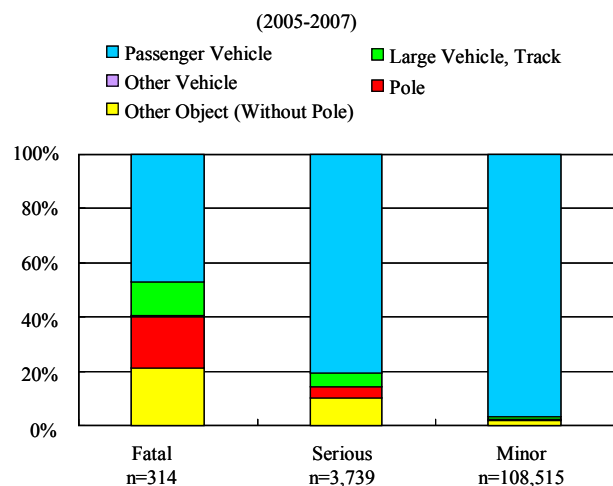


Figure 1 - Type of striking vehicle and object involved in side impact accidents (fatal, serious and minor injuries).

Figure 2 shows the injured body regions of the occupants by injured level. In the fatal accidents, 43%

of the injured body regions were the “head, face” and 28 % were the “thorax, back.” In the serious injury accidents, 32% of the injured body regions were the “thorax, back,” 21% were the “neck,” 19% were the “pelvis, lower extremities,” and 13% were the “head, face.” In minor injury accidents, 69% of the injured body regions were the “neck.” The “head, face” was the largest source in fatal accidents and not a small source in the serious injury accidents. The “thorax, back” was the next largest source in the fatal accidents and the largest source in the serious injury accidents. Thus, it has been determined that protecting the head and thorax of the occupant is important for reducing the fatal and serious side impact accidents.

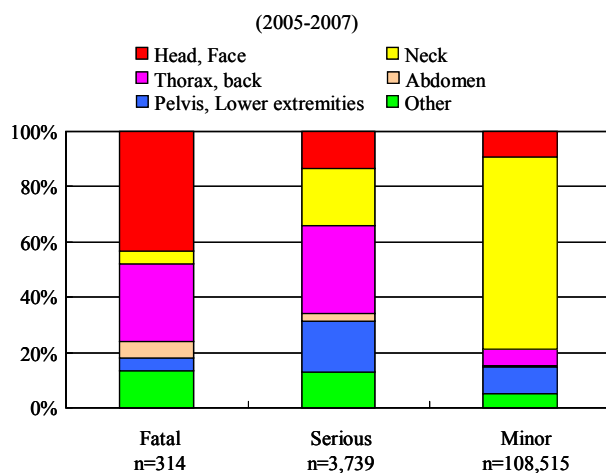


Figure 2 - Injured body regions in side impact accidents by injury level.

Figure 3 shows the injured body regions of the Figure 3, 4, and 5 show the injured body regions of the occupants by striking objects in the fatal, serious injury, and minor injury accidents. As for the fatal accidents, when struck by “passenger vehicles,” 36% of the injured body regions were the “thorax, back” and 34% were the “head, face.” When struck by “large vehicles, trucks,” 43% of the injured body regions were the “head, face” and 40% were the “thorax, back.” When struck by a “pole,” 60% of the injured body regions were the “head, face” and 13% were the “thorax, back.” When struck by “other object (without pole),” 50% of the injured body regions were the “head, face” and 15% were the “thorax, back.” In the side impact fatal accidents where the vehicle was struck by another vehicle, the number of occupants injured at the “head, face” and “thorax, back” was similar and larger than that for the other body regions. In the side impact fatal accidents where the vehicle was struck by “other object,” the number of the occupants injured at the “head, face” was larger than that for all of the other body regions.

As for the serious injury accidents, when struck by “passenger vehicles,” 33% of the injured body regions were the “thorax, back” and 24% were the “neck.” When struck by “large vehicle, truck,” 47% of the

injured body regions were the “thorax, back” and 24% were the “head, face.” When struck by “pole,” 27% of the injured body regions were “pelvis, lower extremities,” 25% were the “head, face,” and 22% were the “thorax, back.” When struck by “other object (without pole),” 27% of the injured body regions were the “pelvis, lower extremities” and 22% were the “thorax, back.” In the side impact serious accident of the vehicle struck by a “passenger vehicle,” the number of occupants that injured the “neck” was larger probably because the serious injury had been judged during the days that the victim visited the hospital. And in Japan, generally, the neck-injured occupants in a traffic accident visit the hospital for a longer time even though the injury may have had an AIS value of 1. In all cases, the percentage of occupants that injured the “thorax, back” was larger than 20%, especially for the case involving being struck by a “large vehicle, truck,” which was 47% and was larger than any other case. In the side impact fatal accidents involving a vehicle being struck by a “large vehicle, truck” and a “pole,” the percentage of occupants that injured the “head, face” was larger than 20% and was larger than that for the other cases. In the side impact fatal accidents involving vehicles being struck by objects, the percentage of occupant that injured the “pelvis, lower extremities” was 27% and was the largest body injured region for this case.

As for the minor injury accidents of a vehicle being struck by “passenger vehicles,” 70% of the injured body regions were the “neck.” As shown in Figure 1, 97% of the striking objects were “passenger vehicle” in minor injury accidents. That is, almost all of the injured body regions in minor accidents were the “neck.”

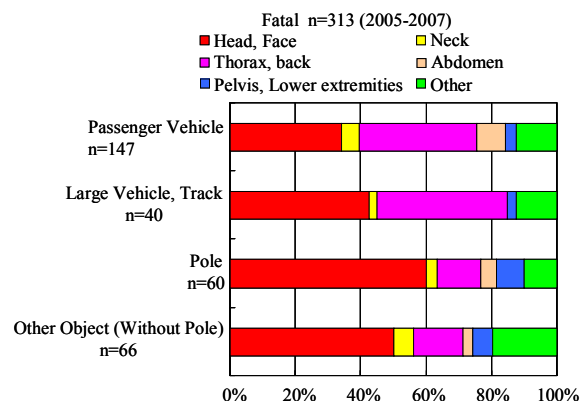


Figure 3 - Injured body regions for fatal side impact accidents by striking object.

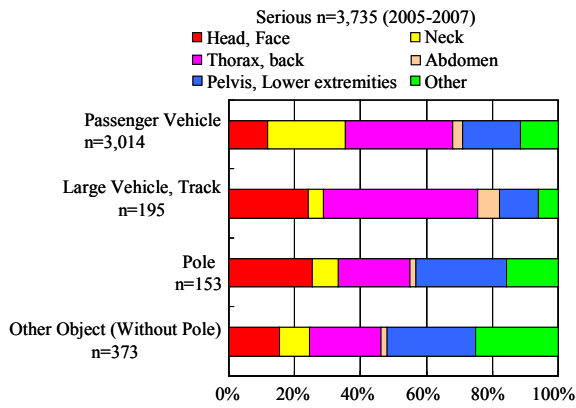


Figure 4 - Injured body regions for serious injuries in side impact accidents by striking object.

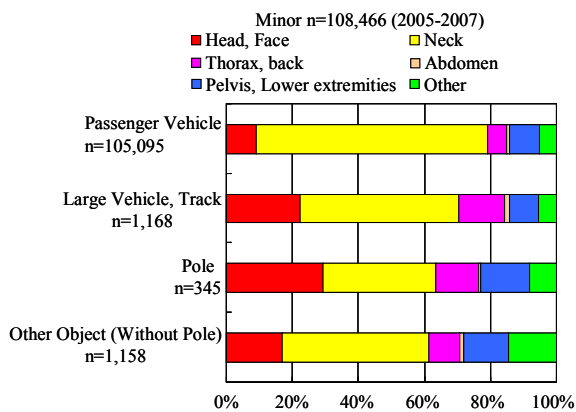


Figure 5 - Injured body regions for minor injuries in side impact accidents by striking object.

Figures 6, 7, and 8 show the curb mass of the striking vehicles and struck vehicles in the fatal accidents, serious accidents, and minor accidents, respectively. As for the fatal accidents, the percentage for which the curb mass of the striking vehicles was larger than 1500 kg was about 57%; while, in contrast, the percentage for which the curb mass of the struck vehicles was smaller than 1250 kg was about 76%. The percentage rate of the heavier vehicles was large for the striking vehicle, and the percentage rate of the lighter vehicles was large for the struck vehicle.

As for the serious accidents, the percentage of the striking vehicles that the curb mass was larger than 1500 kg was about 31%; while, the percentage of the struck vehicles that the curb mass was smaller than 1250 kg was about 76%. The percentage rate of lighter vehicles was relatively large for the struck vehicle. The percentage rate of heavier vehicles was relatively large for the striking vehicle in the serious accidents but smaller than that in the fatal accidents.

As for the minor accidents, the percentage rates of the curb mass of the striking vehicles and that of the struck vehicles were similar. In the serious injury and

fatal side impact accidents, the percentage rate of light weight vehicles was large for the struck vehicles.

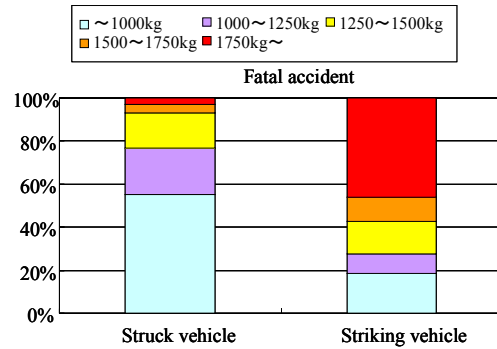


Figure 6 - Curb mass of the struck vehicles and striking vehicles for fatal in side impact accidents.

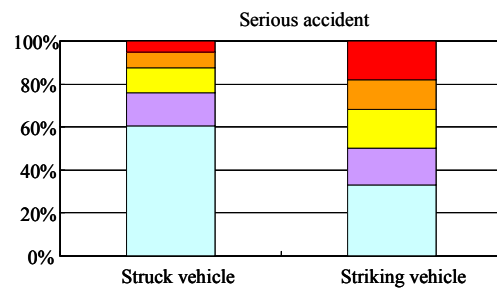


Figure 7 - Curb mass of the struck vehicles and striking vehicles for serious in side impact accidents.

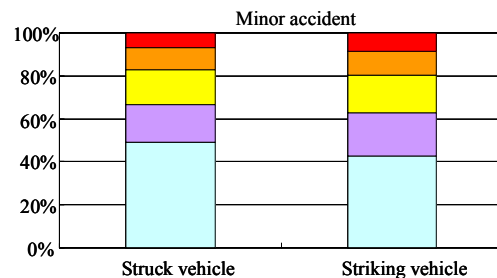


Figure 8 - Curb mass of the struck vehicles and striking vehicles for minor in side impact accidents.

INVESTIGATION OF RIDING POSTURE POSITION

VIDEO ANALYSIS

The seating postures of the driver and front passenger occupants in real-world driving conditions were surveyed in order to provide a basis for predicting injuries caused by the car interior in side impact accidents. The pictures of the position of a front seat occupant were recorded by a video camera from a side view of the vehicle, and the occupant's head position was observed. From the accident analyses, the head was determined to be a frequently injured body region in side impact accidents. Therefore, the percentage of

occupants whose head location overlapped with the vehicle's B-pillar was examined. By analyzing the results, the conditions for which occupant protection devices effectively work (i.e., the area to be covered by the occupant protection device) also could be estimated.

Side views of vehicles traveling in both directions on a road near an intersection were filmed with a video recorder. Using the side view of the filmed occupants, the percentage of the occupants whose head overlapped with the B-pillar was examined. The head positions of the drivers (right side) and the front passengers (left side) were surveyed. The surveyed vehicles were limited to the passenger cars (sedans, wagons, K-cars and IBOXs). That is, large vehicles (such as trucks and buses) and 2-door cars were excluded from the survey. In total, 565 cars were surveyed from the driver side, and 1,290 cars were surveyed from the front passenger side. However, note that only 165 front passengers were examined since the front passenger seating frequency was observed to be only 13%. Figure 9 shows the criterion used to evaluate whether the head overlapped the B-pillar. Note that, even if only a portion of the head overlapped with the B-pillar, it was defined as head/B-pillar overlap.

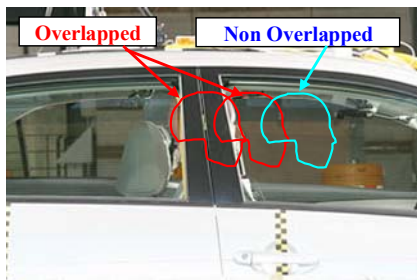


Figure 9 - The criterion of judgment for the head overlapping the B-pillar.

Figure 10 shows the percentage of vehicles that have passengers in the cars in this research. As already mentioned above, the number of vehicles that contained an occupant seated in the passenger seat was 165 during this research.

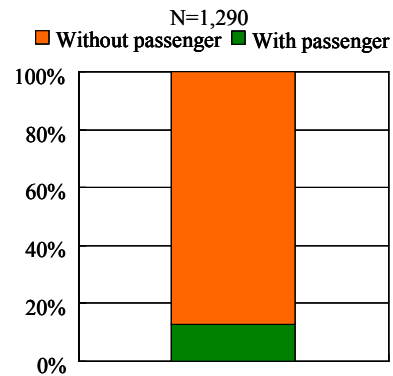


Figure 10 - The percentage of vehicles containing a front seat passenger occupant.

Figure 11 shows the percentages of head/B-pillar overlap for the driver and front passenger. Fifty-six percent of drivers and 78% of front passengers were determined to have head/B-pillar overlap. The percentage of front passengers was large probably because front passengers have the freedom to change their seat positions, whereas the driver must adjust the seat to accommodate reaching the steering wheel and floor pedals in order to drive the vehicle.

Based on the survey, it was found that 56% of the driver heads overlapped the B-pillar. Accordingly, it is predicted that the head is likely to contact the B-pillar during side crashes, and thereby lead to head injuries.

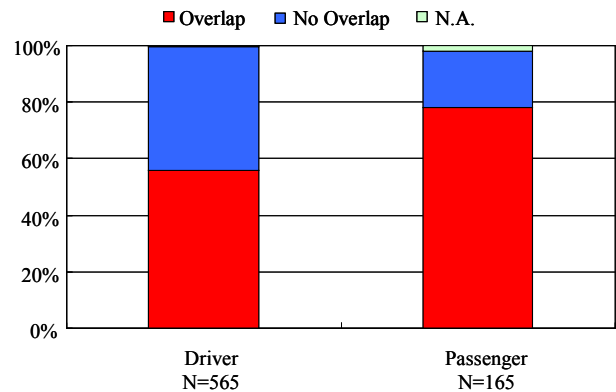


Figure 11 - Percentages with head and B-pillar overlap by front seat seating position.

SAMPLE ANALYSIS

A more detailed study about the seating postures of the driver was conducted. Pictures of the position of a front seat occupant were recorded with a vehicle that was the same as that tested. The examinees seated on the vehicle were members of the NTSEL staff. The pictures of the position of a driver were recorded by a camera from a side view of the vehicle. The distance from the B-pillar to the individual's head was measured. Also the height and sex of the examinees were recorded. The number of examinees was 38, with the number of males being 30 and the number of

females being 8. Figure 12 shows the vehicle and the camera position used in this study. Figure 13 shows an example case of this study. Figure 14 shows the measurements of the distance from the B-pillar to the head. The distance was measured from the center of the ear to the front edge of the B-pillar.

Figure 15 shows the heights of the examinees. The average height of the examinees was 169 cm, with that of the males being 172 cm and that of the female being 157 cm. In this study, the height of the 50th percentile Japanese male was 170 cm and that of the 50th percentile Japanese female was 158cm.

Figure 16 shows the different measurements made for locating the head position in this research. L is defined at the horizontal distance from the center of the ear hole to the front edge of the B-pillar. H is defined as the vertical distance from the Seat Reference Point (SRP) to the center of the ear hole. The zero point of L is defined to be the front edge of the B-pillar, and the positive direction is defined as the direction heading from the rear of the vehicle to the front of the vehicle. So when the parameter L measurement was large, the distance from the B-pillar to the head was large. And when the parameter L measurement was negative, the B-pillar and the ear hole were overlapped. The zero point of H is the SRP location, and the positive direction is in the direction from the seat bottom up to the roof of the vehicle.



Figure 12 - The vehicle and the camera position in this study.



Figure 13 - A sample picture in this study.



Figure 14 - The measurement of the distance from B-pillar to the head.

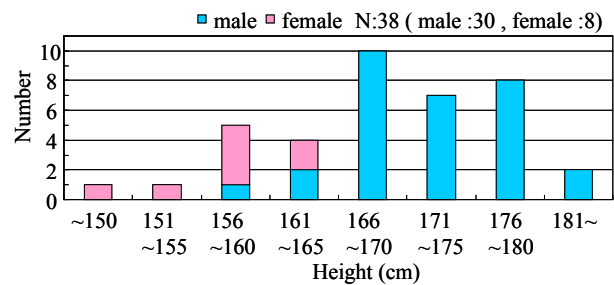


Figure 15 - The height of the examinees by the sex.

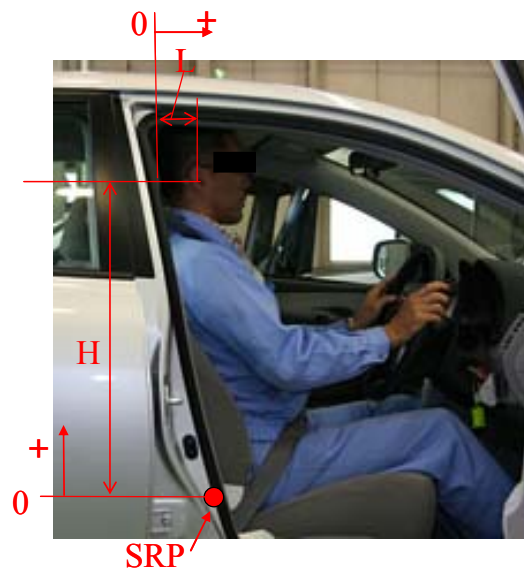


Figure 16 - The definition of the measurements.

Figure 17 shows the head positions of the examinees by the height in this research. The 50th percentile of the Japanese head length from the forehead to the rear of the head is about 180 mm. If the center of the ear hole is assumed to be the center of the head, an L measurement smaller than 90 mm indicates that the head and B-pillar were overlapped. The yellow area of Figure 17 depicts the measurements in which the L measurements were smaller than 90 mm. The number of measurements in the yellow area was 26 and

represented 68% of the examinees. From the pictures, the number that overlapped the head and B-pillar was 30 and near to the number from the judgment from Figure 17. It seemed to be a tendency that, when the height was large, the L was small and the distance from B-pillar to the center of the head was small. But, there were some cases that, even though the height was large, the L was large. For example, the maximum L of the height in the range “151~155” was larger than the minimum L of the height in the range of “171~175”. This was most likely due to that individual variability was larger than the influence of the height.

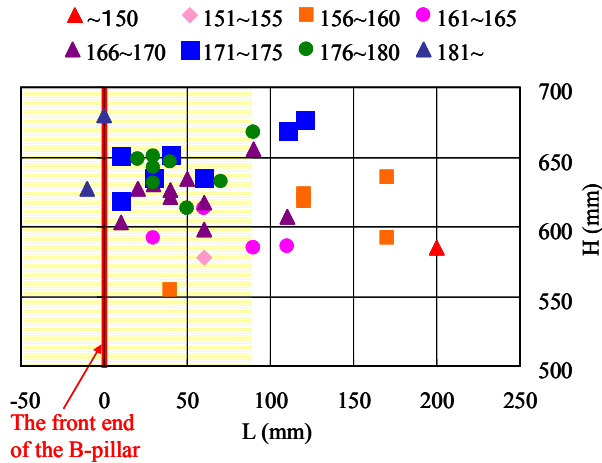


Figure 17 - The head positions of the research by the height.

FULL-SCALE SIDE IMPACT TEST

TEST METHOD

In order to understand the effectiveness of the CSA, a series of crash tests were carried out using two types of vehicles as a struck vehicle. Vehicle 1 was a sedan type small passenger vehicle that is popular in Japan. Vehicle 2 was a K-car that is categorized in Japan as a very small size vehicle. Vehicle 2 also is a popular K-car in Japan. Figure 18 shows Vehicle 1 and Figure 19 shows Vehicle 2. Table 1 presents the test vehicles’ specifications. The Vehicle 1 was 220 mm larger in width and 310 kg heavier in curb weight than Vehicle 2. Tests 1, 2, 4, and 5 were conducted based on the specifications of Regulation ECE/R95 other than the aspect for the positioning of the dummy as previously stated. The dummy position was defined such that the dummy head overlapped the B-pillar. Figure 20 shows the ECE/R95 mobile deformable barrier (MDB) used in this test series.

Figures 21 and 23 show the dummy seating postures in the Vehicle 1 and 2 before the tests 1, 2, 4 and 5. As shown, it is seen that the dummy head and B-pillar overlapped. Tests 3 and 6 were the JNCAP tests conducted of Vehicle 1 and Vehicle 2, from which data was used for reference, though the impact

velocity of the MDB was 55 km/h. Figures 22 and 24 show the dummy seating postures in the Vehicle 1 and 2 before the Tests 3 and 6 as the Regulation ECE/R95 dummy position.



Figure 18 - The photo of the Vehicle 1 that was the small passenger vehicle tested in this study.



Figure 19 - Photo of Vehicle 2 that was the K-car tested in this study.

Table 1 – Specifications of tested vehicles.

	unit	Vehicle 1	Vehicle 2
Length	mm	4410	3395
Width	mm	1695	1475
Height	mm	1460	1610
Curb mass	kg	1130	820
Engine displacement	cc	1496	658



Figure 20 - Photo of the ECE/R95 MDB used in this study.



Figure 21 - The photos of dummy seating position in Vehicle 1 before tests 1 and 2.



Figure 22 - Photo of dummy seating position in Vehicle 1 before test 3.



Figure 23 - Photos of dummy seating position in Vehicle 2 before tests 4 and 5.



Figure 24 - Photo of dummy seating position in Vehicle 2 before test 6.

Figure 25 and Table 2 show the test configuration and specifications of Vehicle 1. Figure 26 and Table 3 show the test configuration and specifications of Vehicle 2. For these tests, ES-2 dummies were seated in the front driver seats of the struck vehicle. In addition, a front facing child restraint system (CRS) was installed in the rear right seat (near side) and a Q3s dummy was placed in the CRS in Tests 1, 2, 4, and 5. Additionally, in Test 2, a rear facing CRS was installed in the rear left seat and a CRABI 6-month dummy was placed in the CRS. In this study, the injury measures and kinematic behavior of the ES-2 dummies in the front seats of the struck vehicles are compared.

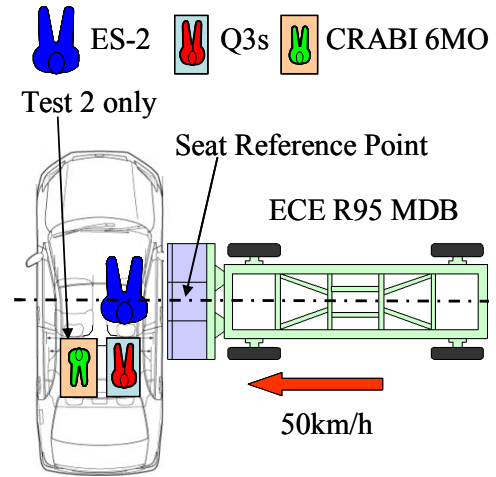


Figure 25 - Test configuration of Vehicle 1.

Table 2 – Test specifications of Vehicle 1.

Test No.		Test 1	Test 2	Test 3
Striking vehicle	Type	ECE/R95 MDB	ECE/R95 MDB	ECE/R95 MDB
	Mass	948 kg	948 kg	950 kg
	Velocity	50 km/h	50 km/h	55 km/h
Struck vehicle	Type	Vehicle 1	Vehicle 1	Vehicle 1
	Mass	1253 kg	1279 kg	1192 kg
	Front dummy	ES-2	ES-2	ES-2
	Rear dummy (near side)	Q3s with CRS	Q3s with CRS	-
	Rear dummy (far side)	-	CRABI 6MO with CRS	-
	Curtain side air bag	Without	With CSA	Without

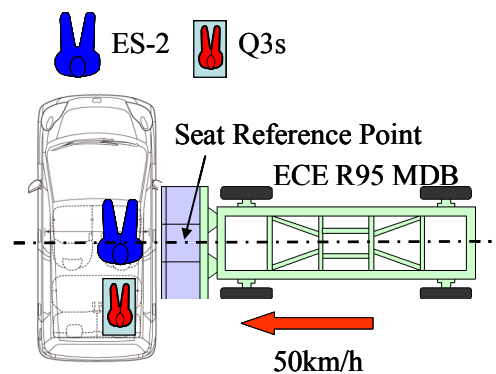


Figure 26 - Test configuration of Vehicle 2.

Table 3 – Test specifications of Vehicle 2.

Test No.		Test 4	Test 5	Test 6
Striking vehicle	Type	ECE/R95 MDB	ECE/R95 MDB	ECE/R95 MDB
	Mass	948 kg	948 kg	948 kg
	Velocity	50 km/h	50 km/h	50 km/h
Struck vehicle	Type	Vehicle 2	Vehicle 2	Vehicle 2
	Mass	958 kg	969 kg	894 kg
	Front dummy	ES-2	ES-2	ES-2
	Rear dummy (near side)	Q3s with CRS	Q3s with CRS	-
	Curtain side air bag	Without	With CSA	Without

Uni-axial accelerometers were attached to the B-pillar inner panel and to the opposite side sill at the center of the front door of the struck vehicles; and tri-axial accelerometers were attached to the center of gravity (C.G.) of both the striking MDB and struck vehicles. The locations where the accelerometers were attached are shown in Figures 27 and 28.

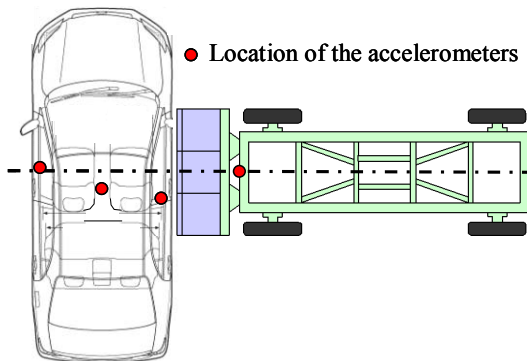


Figure 27 - Locations of accelerometers in Vehicle 1.

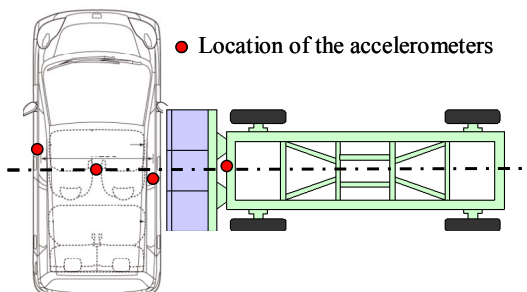


Figure 28 - Locations of accelerometers in Vehicle 2.

TEST RESULTS

Photographs of the vehicles taken after the Tests 1, 2, 4 and 5 were conducted are shown in Table 4. The deformations of Vehicle 1 for both tests and those of Vehicle 2 for both tests were very similar. Vehicle 2 in Test 4 rolled over a quarter turn during the impact test; but in Test 5, the vehicle did not roll over during the impact test.

Table 4 – The vehicles after crash test

Test 1	
Test 2	
Test 4	
Test 5	

Photographs of the vehicles interior conditions and dummy taken after Tests 1 and 2 were conducted are shown in Table 5, and those after Tests 4 and 5 were conducted are shown in Table 6. The contact points of the dummy head with the vehicle interior are marked with the red circles. As for the vehicle without a CSA (Tests 1 and 4), the contact points of the vehicle interior to the dummy head were the B-pillar. In Test 2, the paint mark of the dummy head was at the CSA inflated area. In Test 5, the paint mark from the head contact was at a section of the CSA where it did not inflate, but as can be seen in the photograph was very near to the inflated area.

Table 5 – The interior and dummy in Vehicle 1 after the crash test

Test 1	Vehicle interior	
	Dummy	
Test 2	Vehicle interior	
	Dummy	

Table 6 – The interior and dummy in Vehicle 2 after the crash test

Test 4	Vehicle interior	
	Dummy	
Test 5	Vehicle interior	
	Dummy	

The dummy kinematic behavior in Vehicle 1 as seen from a front view is shown in Table 7 and that from a side view is shown in Table 8. The dummy kinematic behavior in Vehicle 2 as seen from a front view is shown in Table 9 and that from a side view is shown in Table 10. The CSAs in Tests 2 and 5 started inflating between 10ms and 20ms. The time that the dummy head contacted the B-pillar in Tests 1 and 4 was between 40ms and 50ms. In Test 2, the center of the dummy head contacted the area of the CSA that was inflated. In Test 5, the center of the dummy head did not contact the area of the CSA that was inflated.

Table 7 – The dummy kinematic behavior in Vehicle 1 as seen from a front view

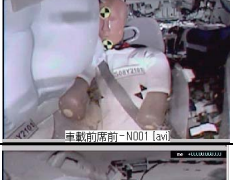
	Test 1 (without CSA)	Test 2 (with CSA)
0ms		
10ms		
20ms		
30ms		
40ms		
50ms		
60ms		
70ms		
80ms		

Table 8 – The dummy kinematic behavior in Vehicle 1 as seen from a side view

	Test 1 (without CSA)	Test 2 (with CSA)
0ms		
10ms		
20ms		
30ms		
40ms		
50ms		
60ms		
70ms		
80ms		

Table 9 – The dummy kinematic behavior in Vehicle 2 as seen from a front view

	Test 4 (without CSA)	Test 5 (with CSA)
0ms		
10ms		
20ms		
30ms		
40ms		
50ms		
60ms		
70ms		
80ms		

Table 10 – The dummy kinematic behavior in Vehicle 2 as seen from a side view

	Test 4 (without CSA)	Test 5 (with CSA)
0ms		
10ms		
20ms		
30ms		
40ms		
50ms		
60ms		
70ms		
80ms		

The exterior deformations of the struck vehicles at the belt line level and the Hip-point level after tests 1, 2, 4 and 5 are shown in Figure 29. At the belt line level of the SRP (i.e., at about -126 mm), the deformations of the struck vehicles measured in all tests were almost the same (about 140 mm). At the Hip-point level of the SRP, the deformations of the struck vehicles in all tests were almost the same (about 210 mm).

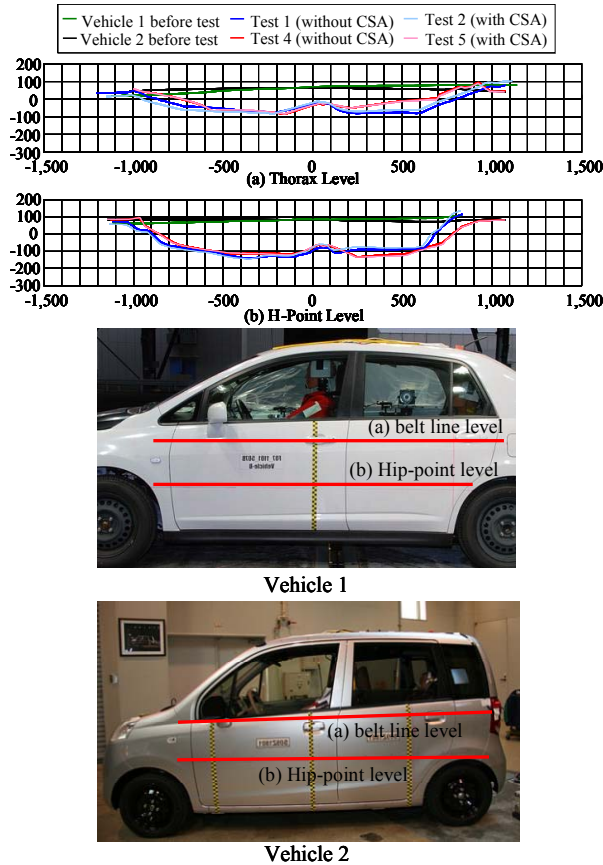


Figure 29 - Exterior deformation of struck vehicles.

of the dummies during these tests are shown in Figures 30 and 31. In all tests, the initial rise time of the head resultant acceleration occurred at about 20 ms. Sharp rises occurred at about 45 ms in Tests 1 and 3 and at about 50 ms in Tests 4 and 5. In Tests 2 and 6, a sharp rise did not occur. The reason why the sharp rise did not occur in Test 6 was that the head did not make contact to the vehicle interior during the test. As for the maximum resultant acceleration, Test 4 had the largest magnitude at 1207 m/s². The magnitude of the acceleration in Test 1 was the next largest at 996 m/s². The magnitude in Test 5 was next to Test 1 at 808 m/s². The magnitude in Test 6 was next to Test 5 at 556 m/s². The magnitude in Test 3 was next to Test 6 at 543 m/s². The magnitude in Test 2 was the smallest at 351 m/s².

Regarding a comparison between the same vehicle type, the dummy maximum head resultant acceleration in a vehicle with a CSA was smaller than that in a vehicle without a CSA. Also, the dummy maximum head resultant acceleration in a vehicle without a CSA when the dummy head was not overlapped with the B-

pillar was smaller than that when the dummy head was overlapped with the B-pillar (though the MDB impact speed was 5 km/h higher when the dummy head was not overlapped). As for the difference between the maximum head resultant accelerations of the dummies in a vehicle with and without a CSA, Vehicle 1 had a larger difference than Vehicle 2. The reason of the difference was probably due to the difference of the design of the inflated area of CSA, specifically the CSA equipped in Vehicle 1 restrained the dummy head before the dummy head made contact to B-pillar; whereas the CSA equipped in Vehicle 2 did not restrain the head before the contact occurred.

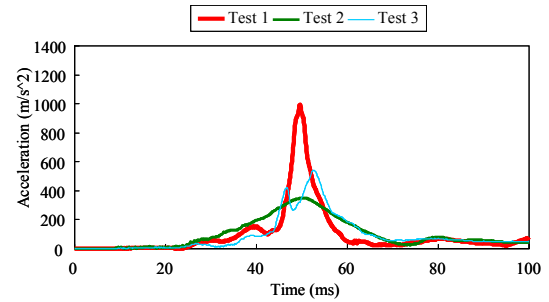


Figure 30 - Head resultant accelerations time histories in Vehicle 1.

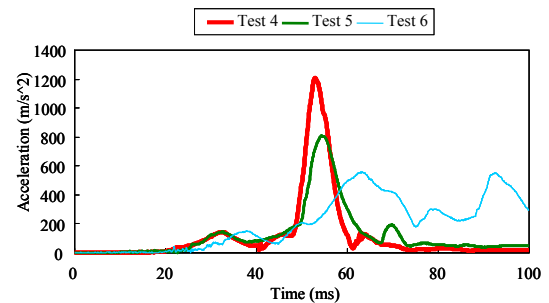


Figure 31 - Head resultant accelerations time histories in Vehicle 2.

The time histories of the thoracic rib deflections of the dummies are shown in Figures 32 and 33. As for the initial rise time of the thoracic rib deflection, the rise time in Test 2 occurred at about 15 ms and that in Test 5 occurred at about 16 ms. Both initial rise times occurred earlier in these tests than in the other tests. The initial rise time in Test 6 occurred at about 20 ms and was next in time after that for Tests 2 and 5. The initial rise time in Test 4 occurred at about 24 ms and was next in time after that for Test 6. The rise time in Test 1 occurred at about 29 ms and was next in time after that for Test 1. The rise time in Test 3 occurred at about 38 ms and was the latest in time of all of the tests. As seen in these figures, the initial rise times of the thoracic rib deflection in the vehicles with a CSA and SAB were earlier than those in the vehicles without a CSA and SAB.

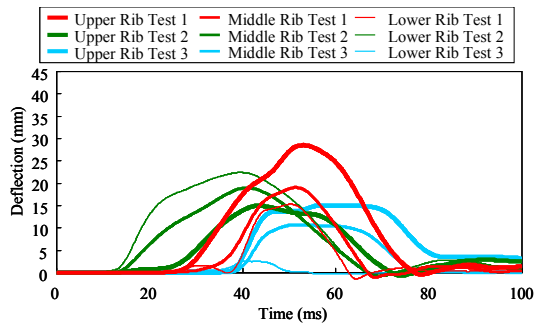


Figure 32- Thoracic rib deflections time histories in Vehicle 1.

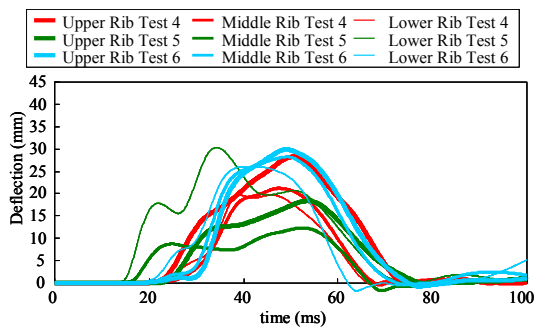


Figure 33- Thoracic rib deflections time histories in Vehicle 2.

The time histories of the abdominal forces of the dummies are shown in Figures 34 and 35. As for the initial rise time of the abdominal forces, the rise time in Test 5 occurred at about 16 ms and was the earliest occurring in all of the tests. The rise time in Test 2 occurred at about 20 ms and was the next earliest occurring. The rise time in Tests 3 and 6 occurred at about 22 ms and were next in time after Test 2. The rise time in Test 4 occurred at about 25 ms and was next in time after Tests 3 and 6. The rise time in Test 1 occurred at about 35 ms and was the latest occurring in all of the tests. Regarding the comparison between the same vehicle type, the initial rise times of the abdominal force in the vehicles with a CSA were the earliest and those in the vehicle of J-NCAP test conditions were the next earliest. Those in the vehicles without the SAB were the latest. This may be due to the fact that the SAB covered the abdominal area.

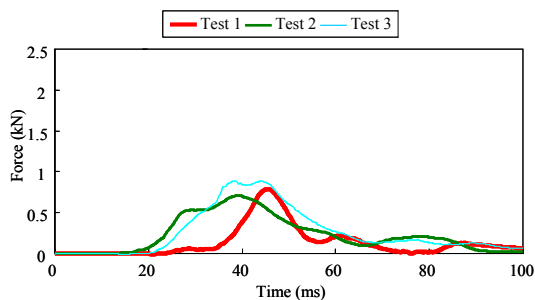


Figure 34- Abdominal force time histories in Vehicle 1.

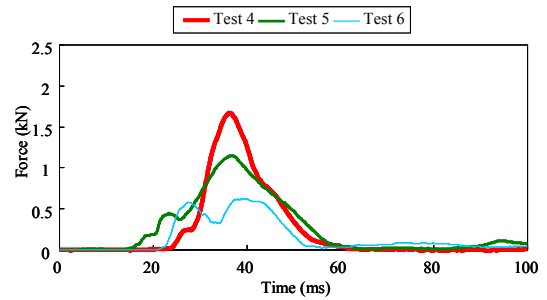


Figure 35- Abdominal force time histories in Vehicle 2.

The time histories of the pubic forces of the dummies are shown in Figures 36 and 37. The initial rise times of the pubic forces occurred at about 21 ms and were very similar in all tests. This may be due to the fact that the SAB did not cover the pelvic area.

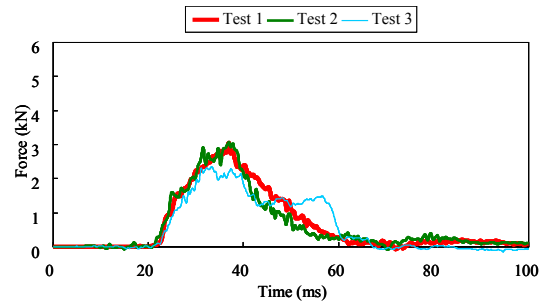


Figure 36 - Pubic force time histories in Vehicle 1.

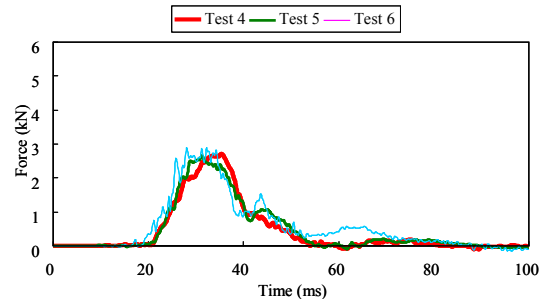


Figure 37 - Pubic force time histories in Vehicle 2.

The maximum injury measures of the ES-2 dummy and the corresponding IARVs for the dummy as specified by ECE R95 are shown in Tables 11 and 12. The ratios of the injury measures to the IARVs are shown in Figure 38. As can be observed, all of the injury measures were less than the corresponding IARVs.

As for the head performance criterion (HPC), more specifically the Head Injury Criterion (HIC), Test 4 was calculated to be 588 and was the largest of all the tests. Test 6 was calculated to be 411 and was the next largest, but the dummy head did not make contact to an object as seen from the video. (This is the reason why the shape of the head resultant acceleration time history of Test 6 was different from those of the other

tests as shown Figure 31). HPC is used for the case when the head makes contact to an object. So the HPC of Test 6 was the reference. Test 5 was calculated to be 274 and was the next to Test 6. Test 1 was calculated to be 255 and was next to Test 4; however, it was similar to that in Test 4. Test 3 was calculated to be 113 and was the next to Test 1. Test 2 was calculated to be 86 and was the smallest of all the tests.

As for the 3 ms maximum head resultant acceleration, Test 4 was 983 m/s² and was the largest of all the tests, Test 5 was 726 m/s² and was the next largest. Test 1 was 667 m/s² and was next to Test 5; however, it was similar to Test 5. Test 6 was 525 m/s² and was next to Test 1. Test 3 was 451 m/s² and was next to Test 6. Test 2 was 343 m/s² and was the smallest of all the tests.

Comparing the head injury measures with the same vehicle type, those for a vehicle with a CSA were smaller than those for a vehicle without a CSA. So, these may be due to the fact that the CSAs have a likely effectiveness in decreasing the head injuries. In making a comparison of the head injury measures between the Vehicle 1 and Vehicle 2, those for Vehicle 2 were larger than those for Vehicle 1. In making a comparison of the head injury measures between the difference of the dummy postures, those for the case when the dummy head was overlapped with the B-pillar were larger than those for the case when the dummy head was not overlapped with the B-pillar.

As for maximum thorax rib deflection, Test 5 was 30.7 mm and was the largest of all the tests, Test 6 was 29.9 mm and was the next largest; however, it was very similar to Test 5. Test 1 was 28.5 mm and was the next to Test 6. Test 3 was 28.3 mm and was next to Test 1; however, it was very similar to Test 1. Test 2 was 22.4 mm and was next to Test 3. Test 3 was 15.0 mm and was the smallest of all the tests.

As for the maximum thorax rib V*C, Test 5 was 0.51 m/s and was the largest of all the tests, while Test 6 was 0.39 m/s and was the next largest. That in Test 4 was 0.29 m/s and was next to Test 6. That in Test 1 was 0.24 m/s and was next to Test 4. That in Test 2 was 0.15 m/s and was next to Test 1. Test 3 was 0.14 and was the smallest of all the tests; however, it was very similar to Test 2.

Comparing the thoracic injury measures with that in the same vehicle type, those of the Vehicle 1 with a CSA and SAB were smaller than those of Vehicle 1 without a CSA and SAB; however, those of Vehicle 2 with a CSA and SAB were larger than those for Vehicle 2 without a CSA and SAB. This was most probably due to the judgment that the influence of an SAB on the thoracic injury measures is dependent on the designs of the SAB and vehicle, which have several parameters. For example, the SAB design parameters are the pressure, the size, the position, etcetera. The vehicle design parameters are the sensing

time, the position of the sensors, the space of the SAB deployed, etcetera. In making a comparison of the thoracic injury measures between the Vehicle 1 and Vehicle 2, those for Vehicle 2 were larger than those for Vehicle 1.

As for the abdominal force, Test 4 was 1.7 kN and was the largest of all the tests; Test 5 was 1.1 kN and was the next largest. Test 3 was 0.9 kN and was next to Test 5. Test 1 was 0.8 kN and was next to Test 3. Test 2 was 0.7 kN and was next to Test 1. Test 6 was 0.6 kN and was the smallest of all the tests. However, the maximum abdominal forces of Tests 1, 2, 3 and 6 were almost similar. The measured abdominal force of Vehicle 2 with a CSA and SAB was smaller than that of the Vehicle 2 without a CSA and SAB; however, that of Vehicle 1 with a CSA and SAB was very similar to that of Vehicle 1 without a CSA and SAB. Therefore, it was determined that the influence of SAB on the abdominal force was also dependent on the design of SAB and vehicle.

As for the pubic force, the pubic forces for Tests 1 and 2 were the same value at 3.1 kN and were the largest of all the tests. Test 6 was 2.9 kN and was the next largest. Test 4 was 2.7 kN and was next to Test 6. Test 5 was 2.6 kN and was next to Test 4. However, the maximum pubic forces of Tests 4, 5 and 6 were similar. Test 3 was 2.3 kN and was the smallest of all the tests. The force measures for the same vehicle type when the dummy seating postures were the same case were the same in each of the vehicles. Hence, the influence of a CSA and SAB on the pubic force was determined to be minimal in this study. The pubic force measures for the Vehicle 1 when the dummy seating postures were not the same case were different, though those for the Vehicle 2 when the dummy seating postures were not the same case were very similar. So this is most probably due to the judgment that the influence of dummy seating postures to the pubic force was dependent on the designs of vehicle.

Table 11 Maximum injury measures in Vehicle 1

	unit	Test 1	Test 2	Test 3	IARV
HPC		255	86	113	1000
Head resultant maximum acceleration (3ms)	m/s ²	667	343	451	-
Thorax upper rib deflection	mm	28.5	15.0	15.0	42.0
Thorax middle rib deflection	mm	19.1	18.9	10.6	42.0
Thorax Lower rib deflection	mm	15.3	22.4	2.6	42.0
Thorax upper rib V*C	m/s	0.24	0.07	0.14	1.0
Thorax middle rib V*C	m/s	0.16	0.08	0.07	1.0
Thorax Lower rib V*C	m/s	0.18	0.15	0.01	1.0
Abdominal force	kN	0.8	0.7	0.9	2.5
Pubic force	kN	3.1	3.1	2.3	6.0

Table 12 Maximum injury measures in Vehicle 2

	unit	Test 4	Test 5	Test 6	IARV
HPC		588	274	411	1000
Head resultant maximum acceleration (3ms)	m/s ²	983	726	525	-
Thorax upper rib deflection	mm	28.3	18.4	29.9	42.0
Thorax middle rib deflection	mm	21.2	12.3	28.2	42.0
Thorax Lower rib deflection	mm	19.7	30.4	25.9	42.0
Thorax upper rib V*C	m/s	0.23	0.11	0.38	1.0
Thorax middle rib V*C	m/s	0.21	0.06	0.39	1.0
Thorax Lower rib V*C	m/s	0.29	0.51	0.38	1.0
Abdominal force	kN	1.7	1.1	0.6	2.5
Pubic force	kN	2.7	2.6	2.9	6.0

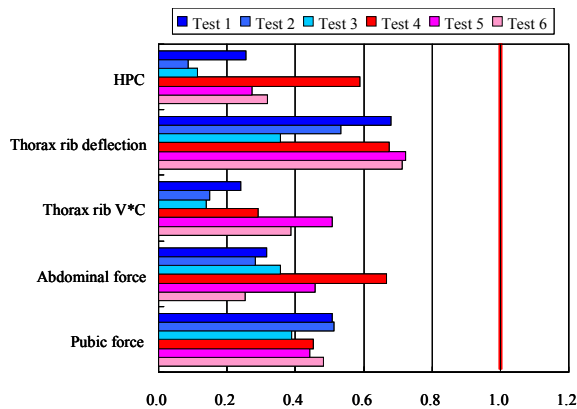


Figure 38 - Ratios of injury measures to IARVs.

DISCUSSION

In comparing the head injury measures within the same vehicle type, it was observed that those of the vehicle with a CSA were smaller than those for the vehicle without a CSA. As a result, it was determined that the CSA is effective in decreasing head injuries. However, the head injury measure ratio of Vehicle 1 with a CSA to that without a CSA was 0.33, and that of Vehicle 2 was 0.47; so the head injury measure

ratio for Vehicle 1 was smaller than that of Vehicle 2 (refer to Tables 11 and 12 and to Figure 38). This is probably because the center of the dummy’s head in Vehicle 2 did not make contact with the inflated area of the CSA (refer to Table 6). As a result, the center of the dummy’s head had a more severe contact with the B-pillar though the vehicle was equipped with a CSA; and the dummy’s head acceleration rose sharply and was the same as the dummy’s head acceleration in the vehicle without a CSA (refer to Figure 31). But the front area of the dummy head had contact with the CSA (refer to Table 10), so the HPC and head maximum resultant acceleration of the dummy in Vehicle 2 with a CSA were smaller than those in Vehicle 2 without a CSA. As for Vehicle 1, the center of the dummy head contacted the inflated area of the CSA (refer to Table 5), and the dummy head acceleration rose gently (refer to Figure 30). So this was most likely due to the judgment that the effectiveness of the CSA of Vehicle 2 would have been larger if the inflated area of the CSA of Vehicle 2 had been large enough to have had contact with the center of the dummy’s head.

In comparing the thoracic injury measures for the same vehicle, it was observed that those of Vehicle 1 with the CSA and SAB were smaller than those for Vehicle 1 without the CSA and SAB. However, the thoracic injury measures for Vehicle 2 with the CSA and SAB were larger than the measures for Vehicle 2 without the CSA and SAB. As can be observed from Tables 7 and 9, the SAB inflated between 10 ms and 20 ms. And as can be observed from the thorax deflection time histories (refer to Figures 32 and 33), the thoracic deflections of the dummies in the vehicle with the SAB rose earlier in time than those in the vehicle without the SAB, and the lower rib and middle rib deflections rose at about 15ms. From this observation, it is concluded that the SAB overlapped the dummy thorax middle rib and lower rib area in the vehicles used in this study. The maximum thoracic rib deflection of Vehicle 1 with the SAB was smaller than that without the SAB. However, the lower rib deflection of the dummy in Vehicle 2 with the SAB was the largest of all the rib deflections. It was determined a possibility that the pressure of the SAB of Vehicle 2 was high enough to induce the large rib deflection. This was most probably due to the judgment that the SAB could be effective in decreasing the maximum thorax rib deflection if the SAB had been designed for optimal performance.

Comparing the injury measures with the same vehicle but for the dummy seating postures were different, the cases when the dummy head was overlapped with the B-pillar were larger or very similar than the case when the dummy head was not overlapped with the B-pillar. Note that since the dummy head was not overlapped with the B-pillar under the ECE/R95 test condition, the ECE/R95 test condition probably was not the most severe condition.

The injury measures of the dummies in the Vehicle 2 were larger than those in the Vehicle 1 except for the thorax rib deflections and the pubic force. The thorax rib deflections of the dummies in Vehicles 1 and 2 without the CSA and SAB were very similar, and those in the Vehicle 1 with the CSA and SAB were smaller than those in the Vehicle 2 with the CSA and SAB. The pubic force of the dummy in Vehicle 2 was a little smaller than that in Vehicle 1. However, the difference was small. As stated previously, Vehicle 2 was a K-car, and so the weight of Vehicle 2 was about 300 kg lighter than of Vehicle 1. It is a possibility that the weight and width had a large influence on the injury measures.

SUMMARY/CONCLUSIONS

In order to discuss potential side impact test procedures for the future and to identify the issues in side collisions; accident analyses, a field survey of occupant posture, and crash tests were carried out. The results are summarized as follows:

1. In the recent side impact accident data collected in Japan, it was found that the number of accidents that a vehicle was struck by a “passenger vehicle” was the largest for all the accidents.
2. The cases that the occupant injured “head, face” and “thorax, back” were larger than for the other body regions were observed in the fatal accidents, and the cases that the occupant injured “thorax, back” was larger than for the other body regions were observed in the serious accidents. Thus, it is a possibility that improving the restraint system to protect occupants from head and thorax injuries would be effective for reducing the fatal and serious injury accidents.
3. In the fatal accidents, 57% of the striking vehicle’s curb mass were larger than 1500 kg; while, in contrast, 76% of the struck vehicle’s curb mass were smaller than 1250 kg. In the serious accidents, 50% of the striking vehicle’s curb mass were larger than 1250 kg; however, 76% of the struck vehicle’s curb mass were smaller than 1250 kg. So in the serious and fatal side impact accidents, the percentage rate of light weight vehicles was large for the struck vehicles and the percentage rate of heavy weight vehicles was large for the striking vehicles. This may be due to the fact that the light weight vehicles were less protective than the heavy vehicles.
4. From using video to the study of seating postures of the driver and front passenger in the real-world, it was observed that 56% of drivers and 78% of passengers had head/B-pillar overlap. As a result, it was determined to be possible that in side impact accidents head injuries would occur frequently due to contact with the B-pillar. From the more detailed study about the seating postures of the driver, the tendency was observed that, when the occupant’s height was large,

the distance from B-pillar to the center of the head was small. However, the individual variability was observed to be larger than the influence of the height.

5. The head injury measures of the dummies in the vehicles with curtain side air bags (CSAs) were smaller than those in vehicles without the CSAs. So, it was determined that the CSAs can be effective in decreasing the head injuries in the car-to-car side impact accidents. However, the effectiveness of the CSAs depends on their design, especially the relation of the CSA inflated area position and vehicle pillar position.

6. The thoracic injury measures of the dummy in Vehicle 1 with the side air bag (SABs) were smaller than those without the SAB. Also, the thoracic injury measures of the dummy in Vehicle 2 with the SAB were larger than those in Vehicle 2 without the SAB. The abdominal injury measure of the dummy in Vehicle 1 with the SAB was very similar to that without the SAB. The abdominal injury measure of the dummy in Vehicle 2 with the SAB was smaller than that without the SAB. So, the SABs would be effective in decreasing the thoracic and abdominal injury measures for the car-to-car side impact accidents; however, the effectiveness of the SABs depends on their designs.

ACKNOWLEDGMENTS

This study project was carried out under contract between the Japan Ministry of Land, Infrastructure, Transport, and Tourism (Japan MLIT) and the National Traffic Safety and Environment Laboratory (NTSEL). The side impact occupant protection working group was established and this study was conducted according to the opinions within the working group. The authors thank the members in the WG and researchers and engineers who cooperated in the experiments and for their support. These include members from the National Agency for Automotive Safety & Victim’s Aid, Japan Automobile Research Institute (JARI), and the Japan Automobile Transport Technology Association (JATA).

REFERENCES

1. ECE Regulation No.95, “Uniform provisions concerning the approval of vehicles with regard to the occupants in the event of a lateral collision” (1995)
2. Insurance Institute for Highway Safety (IIHS), Status Report, vol.41, No.8, October 7, 2006. on the web at www.iihs.org.
3. Dietmar, O., et al. “Effectiveness of Side-Airbag for Front Struckside Belted Car Occupants in Lateral Impact Conditions- An IN-Depth-Analysis by GIDAS”, SAE paper 2007-01-1157.

4. Yonezawa, H., et al. "Japanese Research Activity on Future Side Impact Test Procedures," 17th ESV, Paper Number 267 (2001).
5. Yonezawa, H., et al. "Investigation of New Side Impact Test Procedures in Japan," 18th ESV, Paper Number 328 (2003).
6. Yonezawa, Y., et al. "Investigation of New Side Impact Test Procedures in Japan" 19th ESV, Paper Number ,05-0188 (2005).
7. Matsui, Y., et al. "Investigation for New Side Impact Test Procedure in Japan", 20th ESV, Paper Number ,07-0059 (2007).
8. Yonezawa, Y., et al. "Investigation for New Side Impact Test Procedures in Japan" 21th ESV, Paper Number ,09-0369 (2009).

EFFECTIVENESS AND ESTIMATION OF THE LIKELY BENEFITS OF SIDE IMPACT AIRBAGS IN PASSENGER VEHICLES IN VICTORIA

Michael Fitzharris

Accident Research Centre, Monash Injury Research Institute, Monash University
National Trauma Research Institute, The Alfred (Alfred Health)
Melbourne, Australia

Samantha Cockfield

Jessica Truong

Michael Nieuwesteeg

John Thompson

Transport Accident Commission
Melbourne, Australia

Stuart Newstead

Accident Research Centre, Monash Injury Research Institute, Monash University
Melbourne, Australia

Paper Number 11-0245

ABSTRACT

The safety benefits of side impact airbag (SAB) systems have been demonstrated in a number of studies. Side airbags were first fitted as standard equipment in a locally manufactured passenger vehicle in Australia in the 2000 model year. By 2006, only 33% of new passenger vehicles (cars, sports utility vehicles and people movers) sold in the State of Victoria were fitted with front curtain airbags as standard equipment. The Transport Accident Commission - which functions as a statutory road crash compensation agency for the State, actively promoted the benefits of SAB systems to encourage purchasers of new vehicles to choose vehicles with SAB systems fitted. By the last quarter of 2010 the percentage of new passenger vehicles sold with front curtain airbags fitted had increased to 72%.

The aim of this paper was to estimate the future economic benefits of side impact airbags fitted into passenger vehicles in Victoria for the period 2011 to 2040 under a 'business-as-usual' scenario. In doing so, the benefits to the driver involved in a near (struck) side crash of SAB systems that protect the head and torso are compared to those afforded by torso only systems.

A range of inputs were used to calculate the economic benefits associated with side airbags including published estimates of their effectiveness in mitigating injury; the future number of passenger vehicles and an estimate of the future number of crashes. A 7% discount rate was used and benefit-cost ratio values were derived.

Under a business-as-usual scenario, it was assumed that side airbags would be fitted to all new passenger vehicles by 2014. Hence, by 2037 all registered passenger vehicles in the fleet would be fitted with SAB systems.

It was estimated that over the 30 year period (2011-2040), 738 lives would be saved and 17,361 drivers would avoid serious injury. Financial savings to the Victorian community were estimated to be \$A3.2 billion for an outlay of \$A1.6bn in today's terms. The resultant overall BCR was 2.07:1 assuming an installation cost of A\$600. The benefits were somewhat less when assuming torso-only SAB systems were fitted, although the BCR remained positive at 1.16:1.

The findings highlight the efficacy of SAB systems in mitigating individual and societal loss associated with side impact crashes. Moreover, the analysis lends weight to efforts by road safety stakeholders to increase the uptake of side airbag systems by consumers.

INTRODUCTION

In Australia some 21 000 people are admitted to hospital annually due to traffic crashes; for every 1 fatality another 13 are seriously injured and another 135 sustain minor injuries.[1] The annual cost of these crashes to the community has been estimated at \$A18 billion.[1] In the State of Victoria in 2006, 337 people were killed (21% of national total) and 8,225 were hospitalised due to their injuries, accounting for 21% and 26% of the national total respectively. In 2010, Victoria had the second lowest in fatality rate per capita at 5.2 deaths per 100,000 person, marginally higher than the Australian Capital Territory (cf. 5.0 per 100,000 persons).[2]

The high burden associated with crashes has been acknowledged by successive Federal and State Governments, who have recognised the need to be proactive in addressing the road toll. This has resulted in the development and implementation of road safety action plans supported by key government stakeholders.

The State of Victoria has an enviable road safety reputation and is widely viewed as being highly progressive. Victoria led the world with the introduction of mandatory seat belt laws and has implemented innovative road safety advertising campaigns, mass random alcohol and drug testing, and invested heavily into improved infrastructure and vehicle safety systems.[3-7] This application of the principles of the *safe systems approach* [8], inspired by the Haddon matrix[9], has delivered impressive reductions in the number of people killed in Victoria (Figure 1) as it has in other jurisdictions.[10] The articulation of the principles of the safe systems approach can be seen in Victoria's road safety strategy, *arrive alive* (<http://www.arrivealive.vic.gov.au/>).[11]

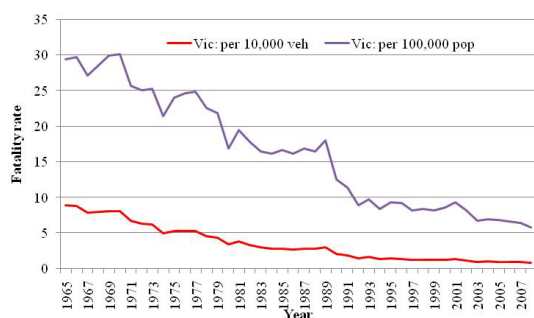


Figure 1. Victorian road toll (killed), per 100,000 person per 10,000 vehicles

Victoria has benefited from the introduction of Australian Design Rules (ADR) that sets the minimum safety performance of vehicle components and / or vehicle crashworthiness. The success of the ADR69 frontal crash protection performance-based standard –based on US FMVSS 208) - introduced in 1995 for new model year vehicles, well documented.[12, 13] More recent rulemaking by the Federal Government led to the introduction of a frontal offset protection standard (ADR73, introduced in 2000 for new model year vehicles; ECE R 94/01 equivalent)[14] and the side impact protection test (ADR72, introduced in 1999 for new model year vehicles; ECE95 equivalent).[15]

In recognition of the considerable harm associated with side impact crashes, there have been significant research programs that have defined the magnitude of the crash problem and devised effective countermeasures.[16, 17]

The side impact protection standard (ADR72) is a performance-based standard with manufacturers being free to meet this standard in any way they wish. Given the observed benefits afforded by frontal airbags, side impact airbags (SAB) were introduced as standard equipment in a locally manufactured (Australian) vehicle in the 2000 model year; this also included structural changes to

the side structures of the vehicle, including the B-pillar, the door and other vehicle components.

SAB are of two varieties: torso airbags designed to protect the thorax and abdomen, and combination airbags, or head/torso bags. The combination SAB systems have been shown to be most effective with Braver and Kyrychenko demonstrating a 45% reduction in risk of death due to combination SAB; but only 11% for the torso only SAB system.[18] The IIHS has shown a similar differential in SAB performance, noting a 37% reduction in fatality risk with the combination SAB in contrast to 26% for the torso only SAB system.[19]

In a study of injury severity, McGwin and colleagues estimated a 75% reduction in injury risk to the head (RR: 0.25, 0.08-0.79) and a 68% reduction in thoracic injuries (RR: 0.32, 0.11-0.91).[20]

In recognition of the benefits associated with SAB, the Transport Accident Commission (TAC), Victoria's compulsory no-fault insurer, has promoted the uptake of SAB by vehicle purchasers through active promotions on their website and through other means of targeted advertising; this has been described previously by Truong and colleagues.[21] The intent of the program was to accelerate the uptake of SAB systems in two ways: first, the creation of consumer pressure to fit SAB as standard equipment; and second, to fit SAB systems where available as an option. The content of these promotions may be viewed at <http://www.howsafeisyourcar.com.au> as well as and on the TAC 'youtube channel' (<http://www.youtube.com/user/TACVictoria>) which features a number of its television campaigns (see Figure 2 and Figure 3 for screen grabs).

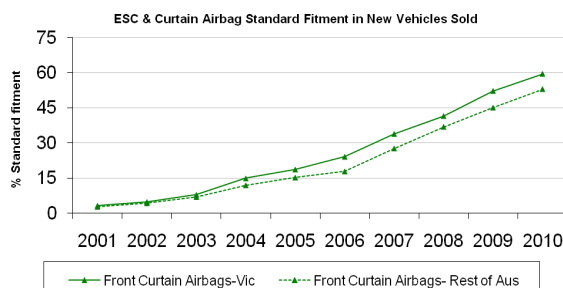
This approach has had positive outcomes, with the fitment of SAB into the vehicle fleet as standard equipment in Victoria outstripping fitment in the all other Australian jurisdictions (Figure 4). With respect to passenger vehicles (cars, SUVs, people movers), only 33% of passenger vehicles sold in Victoria in 2006 were available with front curtain airbags as standard equipment. This had increased to 72% by the last quarter of 2010.



Figure 2. ‘Screen-grab’ of TAC SAB television promotion (courtesy of the TAC)



Figure 3. ‘Screen-grab’ of TAC SAB television promotion (courtesy of the TAC)



Source: Transport Accident Commission, VicRoads Safety Initiative Reports.

Figure 4. Standard fitment rates for curtain airbags in new vehicles sold in Victoria and Australia.

The SAB educational program follows significant financial investment by the TAC in earlier road safety campaigns that were designed to shape the perceptions of road users with respect to road safety. There has also been recognition that side impact crashes are costly – both to the individual and their family as well as in community costs - and that SAB systems have the potential to play a role in mitigating injury in side impact crashes.

This study therefore aims to examine the likely benefits associated with the fitment of SAB under a business-as-usual approach, and in doing so, estimates savings in terms of injury reductions and in financial terms. In doing so, the study determines the introduction costs of SAB systems into new passenger vehicles sold in Victoria, permitting benefit-cost ratio values to be derived.

METHOD

The key parameter to estimate is the number of future crashes amenable to SAB systems, and then applying the injury reduction values attributable to SAB to determine the benefits on estimated injury numbers.

Using 2008 as the base year, the number of driver fatalities and the number seriously injured per registered passenger vehicle for drivers aged 15 years and older is derived. This data was obtained from Police Reported Casualty Crashes where fatalities were defined as death within 30 days of the crash and a ‘serious injury’ was an individual who had been admitted to hospital to at least 24 hours.

A number of successive steps were undertaken, these being:

- Step A: the number of drivers in near side impacts (damage on the right side) was determined;
- Step B: the rate of drivers involved in near side impact crashes per registered passenger vehicle was determined, by injury severity (Step B);
- Step C: Using the number of passenger vehicle registrations[22] and the Victorian population 15 years and older[23], the per capita vehicle penetration (*i.e.*, ‘vehicle-population ratio’) was calculated;
- Step D: Using the ABS population projection by year, the future number of registered passenger vehicles (for each year to 2040, 30 years) given the derived ‘vehicle-population ratio’ is calculated (from Step C); this assumes no change in the vehicle penetration rate into the future;
- Step E: Using the crash rate per registered passenger vehicle (Step B) and the future number of registered passenger vehicles every year from 2011 to 2040 (Step D), the number of driver fatalities and those seriously injured for near side impacts is calculated; note that this assumes no other changes in the injury rate into the future with 2008 as the ‘base’ year.

The result of Step E returns the number of driver fatalities and those seriously injured for drivers involved in near-side impacts. These crashes are in the *field of influence of SAB systems*.

The results of Step A and Step B are presented in Table 1, while Table 2 shows the estimated future number of registered passenger vehicles given the known vehicle-population ratio. The estimated number of fatalities and serious injuries obtained

by applying the known injury ratio (Step B; Table 1) is also presented (Column C, D)

Table 1. Estimation of current driver fatality and serious injury rates per registered passenger vehicles

Parameter	Value
Fatalities: number	57 (46.3% drivers killed involved in collisions / rollovers)
Serious injury: number	730 (24.8% drivers involved in collisions / rollovers and seriously injured)
Number of registered passenger vehicle[22]	3,249,418
Fatalities per registered passenger vehicle	0.00001754
Serious injuries per registered passenger vehicle	0.000224656
Population ≥ 15 years	4,437,151
Passenger vehicle per person ratio	0.732

Table 2. Estimated number of near side driver fatalities and serious injuries, 2011 to 2040

Year	Future pop. Estimate (Col. A)	Est. num. passenger vehicles† (Col. B)	Fatalities (Col. C)‡	Serious injury (Col. D)‡
2011	4,506,713	3,300,360	58	741
2012	4,577,236	3,352,005	59	753
2013	4,647,000	3,403,095	60	765
2014	4,717,375	3,454,632	61	776
2015	4,787,792	3,506,200	62	788
2016	4,857,898	3,557,540	62	799
2017	4,927,693	3,608,652	63	811
2018	4,997,766	3,659,968	64	822
2019	5,068,720	3,711,929	65	834
2020	5,140,106	3,764,207	66	846
2021	5,213,825	3,818,193	67	858
2022	5,289,029	3,873,266	68	870
2023	5,366,645	3,930,106	69	883
2024	5,445,063	3,987,533	70	896
2025	5,524,205	4,045,490	71	909
2026	5,604,031	4,103,949	72	922
2027	5,684,745	4,163,057	73	935
2028	5,766,342	4,222,812	74	949
2029	5,848,795	4,283,194	75	962
2030	5,932,073	4,344,180	76	976
2031	6,016,117	4,405,728	77	990
2032	6,100,881	4,467,802	78	1004
2033	6,186,298	4,530,355	79	1018
2034	6,272,274	4,593,317	81	1032
2035	6,358,742	4,656,639	82	1046
2036	6,445,605	4,720,251	83	1060
2037	6,532,653	4,783,998	84	1075
2038	6,619,674	4,847,725	85	1089
2039	6,706,591	4,911,376	86	1103
2040	6,793,369	4,974,925	87	1118
TOTAL			2157	27,630

† Predicted number of passenger vehicles = future ABS population* passenger vehicles per person ratio

‡ Estimates number future passenger vehicles*fatality rate (per registered passenger vehicles) (& *serious injury rate per registered passenger vehicle)

Accounting for SAB fitment and penetration into the fleet

While Step E returns the estimated number of driver near-side fatalities as shown in Table 2, we must then account for the number of SAB- fitted passenger vehicles and the increasing penetration into the fleet through time. This is the *SAB crash relevance factor*.

The number of passenger vehicles fitted in 2010 with SAB systems then becomes the 'base fitment level'. This approximates the level of fitment of SAB in the fleet and defines their influence in terms of crash numbers.

Using the SAB fitment growth rate of 14.8% over the period 2006 to 2010, we can project upwards to 100% fitment using 2010 as the base year; this is shown in Table 3. We observe that 100% fitment, based on past fitment trends will be achieved by 2013.

Table 3. Current and future estimated SAB fitment as standard equipment in new passenger vehicles sold in Victoria

Year	% new passenger vehicles sold with SAB
2006	33.1
2007	43.01
2008	52.04
2009	63.28
2010 (<i>base year</i>)	72.10
<i>Average. growth</i>	<i>14.8%</i>
2011	82.8
2012	95.0
2013	100
...	100
2040	100

†relevant until all new passenger vehicles fitted

As SAB systems will be fitted to new passenger vehicles in accordance with the introduction schedule noted above, we must then account for the penetration of passenger vehicles into the fleet, given their crash involvement by vehicle age.

The Australian Used Car Safety Rating Database (UCSRD) held by Monash University contains details of drivers of passenger vehicles manufactured since 1964 that have been involved in crashes since 1982. As at the end of 2010, the UCSRD contains records of 185,514 drivers injured in Victoria. The UCSRD was used to establish the age of passenger vehicles at the time of its crash as this permits the estimation of the penetration of new technologies into the fleet whilst accounting for natural de-registration and vehicle write-offs following crashes.

Of interest is the cumulative percent of crash involved passenger vehicles by vehicle age (Table 4, Column A). The interpretation of this is that 76.4% of injury crashes in Victoria involved passenger vehicles up to 15 years of age; alternatively, 23.6% of drivers injured were in passenger vehicles greater than 15 years of age.

The age-based passenger vehicle crash distribution is critical to understand how new technology moves through the fleet. By way of practical example, if for instance a safety technology was introduced in all new passenger vehicles in year X (0, its first year of life – or newly registered), that technology will only be applicable to 2.1% of passenger vehicle injury crashes, and we can then estimate that it would take 10 years for this technology to potentially influence half (52%) of all injury passenger vehicle crashes.

With respect to the above logic, this is shown in Column B of Table 4, where we multiply the percent of passenger vehicles fitted with SAB (Table 3), assuming 2010 is year 11 (given that SAB first appeared in 2000 model year passenger vehicles), by the vehicles involved in crashes (Column A, Table 4); the product of these two parameters is known as the ‘*technology – vehicle penetration multiplier*’.

Having derived the ‘technology-vehicle penetration multiplier’ specific to SAB systems in Victoria, we then derive the total number of fatalities and serious injuries that the device will likely influence. We use the estimated number of fatalities and serious injuries presented in Table 2 and the above ‘multiplier’ (Column B) to determine the number of killed and seriously injured drivers where SAB will have an influence. This in effect states that 47.3% of passenger vehicles involved in crashes will have a side airbag in year 1 of this analysis, which is 2011.

Table 4. Current and future estimated SAB fitment into passenger vehicles

Vehicle age at time of crash (given SAB fitted in 2000 MY vehicles)	Age of vehicles involved in injury crashes (cumulative % (Column A))	Year	Technology – vehicle penetration multiplier (Column B)
11.00†	0.57	2011	0.473
12.00	0.62	2012	0.589
13.00	0.67	2013	0.670
14.00	0.72	2014	0.717
15.00	0.76	2015	0.764
16.00	0.80	2016	0.805
17.00	0.84	2017	0.843
18.00	0.88	2018	0.875
19.00	0.90	2019	0.903
20.00	0.93	2020	0.925
21.00	0.94	2021	0.943
22.00	0.96	2022	0.957
23.00	0.97	2023	0.967
24.00	0.98	2024	0.975
25.00	0.98	2025	0.981
26.00	0.99	2026	0.985
27.00	0.99	2027	0.989
28.00	0.99	2028	0.991
29.00	0.99	2029	0.993
30.00	1.00	2030	0.995
31.00	1.00	2031	0.996
32.00	1.00	2032	0.997
33.00	1.00	2033	0.998
34.00	1.00	2034	0.999
35.00	1.00	2035	0.999
36.00	1.00	2036	0.999
37.00	1.00	2037	1.000
38.00	1.00	2038	1.000
39.00	1.00	2039	1.000
40.00	1.00	2040	1.000

† accounts for SAB being fitted in 2000MY vehicles (year 0, first year of life), so this commences at year 11.

Table 5 than presents the number of driver fatalities and those seriously injured that are amenable to the influence of SAB for each year 2011 to 2040, a 30-year period.

Table 5. Likely number of driver fatalities and serious injuries where SAB systems present

Year	Fatalities† (Column A)	Serious injury‡ (Column B)
2011	27	351
2012	35	444
2013	40	512
2014	43	557
2015	47	602
2016	50	643
2017	53	683
2018	56	720
2019	59	753
2020	61	783
2021	63	809
2022	65	833
2023	67	854
2024	68	874
2025	70	892
2026	71	909
2027	72	925
2028	73	940
2029	75	956
2030	76	971
2031	77	986
2032	78	1001
2033	79	1016
2034	80	1031
2035	82	1045
2036	83	1060
2037	84	1074
2038	85	1089
2039	86	1103
2040	87	1118
TOTAL	1992	25,534

†Note: product of Table 2-Column C* Table 4-Column B

‡Note: product of Table 2-Column D* Table 4-Column B

Derivation of ‘savings’

Having established the number of driver fatalities and serious injuries amenable to SAB, we are then in a position to overlay the known injury reduction benefits associated with combination SAB systems; i.e., those that offer both head and thorax/abdomen protection. As noted in the Introduction, a number of studies have demonstrated the benefits of SAB with respect to reductions in fatalities and serious injuries.

The SAB head-torso (‘combination’) system benefit values used here are:

- 37% reduction for fatalities[19], and
- 68% reduction for serious injuries (relevant for thorax, but higher for head injury reduction)[20].

An analysis was also conducted of the benefits and associated costs of torso only SAB systems given that a number of manufacturers install these

systems. The derived savings values therefore represent an absolute lower band of benefits. Based on the published literature, the following benefit values were used:

- 26% reduction for fatalities[19], and
- 34% reduction for serious injuries, which is half that for combination SAB systems[20].

Application of the SAB effectiveness estimate to the number of driver fatalities and serious injuries presented in Table 5 returns the estimated injury reduction savings for each year and severity (see Table 6). This becomes the basis for the estimation of the financial benefits associated with SAB.

RESULTS

Application of the process described above results in the estimation of driver fatality and serious injury savings associated with SAB system fitment.

Table 6 provides the injury savings for each year. These savings account for the projected number of crashes, SAB fitment and penetration into the fleet, and device effectiveness. Over the 30 year period, the installation of SAB head-torso systems would be expected to result in 738 lives being saved and 17,361 serious injuries being mitigated, assuming no other changes occur in crash rates and risk.

Reference to Table 2 shows that 17.2% (10 of 58) of fatalities would be expected to be avoided while 32% of driver near side serious injuries would avoided (i.e., 238/741) in 2011.

It is important to note that we do not account for a shift in injury severity in the above calculations, although it is reasonable to assume that those involved in side impact crashes would remain injured; the exact severity shift is however unknown. It would be reasonable to assume that those ‘previously killed’ and ‘previously seriously injured’ would sustain ‘minor injuries’. This is an important point as it recognises that SAB systems do not necessarily prevent all injuries sustained. This is accounted for by using the injury ‘cost’ value for minor injuries; the result of this is that the overall cost savings associated with SAB systems are somewhat less than if it was assumed these drivers would escape injury entirely. In the calculation of financial benefits, we thus assume that all drivers previously killed would sustain minor injuries, while those previously sustaining serious injuries would shift to the minor injury category with respect to financial values.

Table 6. Driver fatalities and serious injury reductions due to the influence of SAB for each year 2011 to 2040, accounting for fitment and penetration through the fleet

Year	Fatalities†	Serious injury‡
2011	10	238
2012	13	302
2013	15	348
2014	16	379
2015	17	409
2016	19	437
2017	20	465
2018	21	489
2019	22	512
2020	23	532
2021	23	550
2022	24	566
2023	25	581
2024	25	594
2025	26	606
2026	26	618
2027	27	629
2028	27	639
2029	28	650
2030	28	660
2031	28	671
2032	29	681
2033	29	691
2034	30	701
2035	30	711
2036	31	721
2037	31	731
2038	31	740
2039	32	750
2040	32	760
TOTAL	738	17,361

†Note: product of Table 5-Column A* SAB effectiveness (37%)

‡Note: product of Table 5-Column A* SAB effectiveness (68%)

Translation of benefits into financial savings

The translation of these injury reductions in terms of people killed and seriously injured into financial terms provides the basis for a BCR analysis.

Derivation of the present day value of crashes

-To derive the economic benefit associated with these predicted savings presented in Table 6, the Australian Government *Best Practice Regulation Guidance Note: Value of statistical life* was used as the basis of financial savings estimates. This guidance note stipulates an economic cost of \$A3.5 million per fatality on average expressed in 2007 dollars.[24] This value was inflated by a factor of 1.1049 to bring this value to 2010 dollar values (ABS, Consumer Price Index, CPI values).[25] It is necessary to derive the cost of serious injury, minor injury and property damage only (PDO) crashes by using the ratio of the BITRE costs shown in Table 7 and applying this to the current and known cost of a fatality.[1]

The ratio of fatal to other injury severities was established using the cost of crashes estimated by the BITRE, which were based on 2006 crashes and associated costs.

Table 7. Financial value of injuries, by severity (2010 values, \$AUD)

Injury Severity	BITRE injury cost ratio	CPI	\$A2007, Dept of Finance (Fatal: \$A3.5m, 2007 as index value)
Fatal	1	1.1049	\$3,867,346.94
Serious	0.099625	1.1049	\$385,284.44
Minor	0.005506	1.1049	\$21,293.61

Calculation of financial benefits associated with the reductions due to SAB - The number of fatalities prevented and serious injuries mitigated (Table 6) provides the basis for the calculation of the bottom line cost savings associated given the installation of SAB under a 'business-as-usual scenario', assuming a 37% fatality reduction benefit and a 68% serious injury reduction benefit due to the deployment of the SAB.

To obtain the financial savings we simply multiply the reductions in fatalities and serious injuries by the crash costs, and we subtract the cost associated with these same drivers sustaining minor injuries.

The total benefit savings by injury severity and the aggregate financial benefit are expressed in 2011 dollar values, however it is important to *discount* the benefit values per the practice as articulated by the Office of Best Practice Regulation [24]. A 7% discount factor was used and calculated for each year so that the total benefit in each of the 30 years can be determined. The discount rate is calculated by the following: $[1/(1.07)^{\text{number of years}}]$.

After applying the 7% discount factor for each successive year, the total cost saving associated with the installation of SAB to passenger vehicles for drivers under the business-as-usual scenario was estimated to be \$A3.2 billion over the 30 year period.

Table 8. Financial savings (\$A) associated with SAB installation from 2010 – 2040 under a business-as-usual scenario

Severity	Person-based reduction	Financial benefits
Fatal	738	\$1,014,107,336
Serious	17,361	\$2,259,025,240
TOTAL	-	\$3,273,132,576

Derivation of Benefit – Cost ratio for ESC (BCR)

Having obtained the aggregate financial benefits associated with SAB, the determination of costs follows which in turn permits the calculation of BCR for SAB.

Estimation of new passenger vehicles –

For each year in the period, 2011–2040 inclusive, the number of new passenger vehicles entering the fleet must be estimated. Simple linear regression was used to construct a prediction model to calculate the number of new passenger vehicles registered for the first time. The predictive model was constructed by using the historical relationship between new passenger vehicles and the population of Victoria 15 years and older in the period 2006-2010.[26, 27]

The basic linear regression model is shown in Equation 1.

$$Y [\text{passenger vehicle sales}] = \alpha + \beta x_i + \zeta_i \quad [1]$$

where:

α is an unknown parameter (model constant)

β_i is an unknown parameter, estimated using values of x

ζ_i is the *error term*

Equation 2 shows the derived relationship between new passenger vehicle sales and the Victorian population with a weak linear trend being evident. This model, while relatively poorly specified, serves as the basis for future estimates of the number of new passenger vehicles entering the fleet. By substitution of future population

projection values, the number of new passenger car sales into the future can be estimated.

$$Y [\text{passenger vehicle sales}] = -56268.75 + 0.051997 * x_i \quad [2]$$

where:

α is the model constant

β_i is the estimated population coefficient

x_i represents the (future) population values for Victoria as shown in Table 2.

These projection results rely on a number of assumptions, these being:

1. observed economic growth will continue, on an average basis, into the future, over the life of the projections
2. there is no change in the factors associated with the purchase of passenger vehicles for individual buyers, that is, demand side factors remain constant
3. there is no change in the factors relating to the production of passenger vehicles, that is, supply side factors remain constant
4. that the vehicle technology as of today remains constant with respect to the influence such technology has on vehicle purchasing choice
5. the impact of any future regulatory change on purchasing choices cannot be accounted for, and
6. that the projected population estimates derived by the Australian Bureau of Statistics (ABS) are i. accurate within their stated assumptions and limitations, and ii. the analysis here does not account for the possibility of future re-estimation by the ABS.

Given these assumptions, the number of new passenger vehicles entering the fleet over the next 30 years is presented in Table 9.

Accounting for SAB fitment rates into new passenger vehicles, and associated cost - As the benefits are derived on the basis of standard SAB fitment, the number of new passenger vehicles entering the fleet fitted with SAB for each year must be used rather than the overall total. We therefore use the product of the estimated number of new passenger vehicles by the SAB fitment rate for each year as shown in Table 3.

Following the derivation of the number of passenger vehicles fitted with SAB by calendar

year, and using the fitment value of \$A600 per passenger vehicle due to the need to fit both driver and passenger airbags and with a 7% discount factor applied for each year, the yearly and hence total cost over the 30 year period of SAB fitment is derived (Table 9).

There are two observations to be made:

1. the yearly cost increases, and is highest at 2013 – which coincides with all new passenger vehicles being fitted with SAB as standard equipment, and
2. from 2014 the total cost of installation falls per year, despite the increasing number of passenger vehicles sold, a feature that is in accord with the 7% discounting of the device cost.

As shown in Table 9, across the entire 30 year period the estimated total cost of SAB fitment assuming a device cost of \$AUD600 into the fleet in today's terms (i.e., 2011 dollars) was estimated to be A\$1.582 billion.

Table 9. Total number of new passenger vehicles entering the market and cost of SAB installation (base price, \$600, 7% discount rate)

Year	Num new. pass vehicles	New pass vehicles with SAB†	Cost at 7% disc. rate†	Install cost (\$A)
2011	178070	147442	\$561	\$82,677,716
2012	181737	172650	\$524	\$90,479,594
2013	185365	185365	\$490	\$90,787,619
2014	189024	189024	\$458	\$86,523,257
2015	192685	192685	\$428	\$82,429,226
2016	196331	196331	\$400	\$78,494,090
2017	199960	199960	\$374	\$74,715,005
2018	203604	203604	\$349	\$71,099,485
2019	207293	207293	\$326	\$67,652,205
2020	211005	211005	\$305	\$64,358,527
2021	214838	214838	\$285	\$61,240,837
2022	218749	218749	\$266	\$58,276,195
2023	222784	222784	\$249	\$55,468,575
2024	226862	226862	\$233	\$52,788,598
2025	230977	230977	\$217	\$50,230,061
2026	235128	235128	\$203	\$47,787,588
2027	239325	239325	\$190	\$45,458,483
2028	243568	243568	\$178	\$43,237,749
2029	247855	247855	\$166	\$41,120,407
2030	252185	252185	\$155	\$39,101,700
2031	256555	256555	\$145	\$37,176,906
2032	260963	260963	\$135	\$35,341,675
2033	265405	265405	\$127	\$33,591,753
2034	269875	269875	\$118	\$31,922,975
2035	274371	274371	\$111	\$30,331,602
2036	278888	278888	\$103	\$28,813,942
2037	283414	283414	\$97	\$27,365,969
2038	287939	287939	\$90	\$25,984,004
2039	292459	292459	\$84	\$24,665,279
2040	296971	296971	\$79	\$23,407,320
Total	178070	147442		\$1,582,528,340

†Obtained by multiplying the SAB fitment values from Table 3

Using these fitment cost values and the financial savings, the BCR values for each year and across the entire period can be calculated (Table 10).

The calculated BCR using a \$A600 SAB fitment cost across the entire period (in 2011 dollar values), assuming the business-as-usual fitment scenario and a 7% discount rate was 2.07:1

Table 10. Per annum BCRs with the aggregate BCR for SAB fitment over the 30 year period

Year	BCR
2011	1.42
2012	1.54
2013	1.65
2014	1.76
2015	1.87
2016	1.96
2017	2.04
2018	2.11
2019	2.17
2020	2.22
2021	2.25
2022	2.27
2023	2.29
2024	2.30
2025	2.31
2026	2.31
2027	2.31
2028	2.31
2029	2.31
2030	2.30
2031	2.30
2032	2.29
2033	2.29
2034	2.28
2035	2.28
2036	2.27
2037	2.27
2038	2.26
2039	2.25
2040	2.25
<i>Overall</i>	<i>2.07</i>

Summary of findings

A summary of the findings are presented in Table 11. The values rely on a number of inputs and these are:

- the ratio of injuries to registered passenger vehicles;
- the passenger vehicle penetration rate into the population; *note:* any potential future changes that might occur in this ratio due to an ageing population and a trend toward increasing urbanisation is not considered;

- the fitment rate of SAB systems into new passenger vehicles;
- the number of new passenger vehicle sales, and the progressive penetration of the fitted SAB into the fleet;
- The effectiveness estimate of the SAB system itself in mitigating fatalities and serious injuries, and the related assumption that these drivers would sustain minor injuries for financial cost purposes, and
- A discount rate of 7% over the 30 years.

It is important to note that while these inputs were based on historical trends, and were derived using the best available inputs at the time of analysis, it remains the case that any variation in any of these inputs would influence the number of drivers affected, and hence the overall BCR obtained.

In short and as can be observed from Table 11, the findings reported here are highly favourable and suggest significant savings will be made in the reduction of injuries sustained by drivers involved in near side impacts due to SAB systems.

Table 11. Overall view of person-based injury reductions, financial savings and benefits, and the overall BCR for combination SAB fitment

Benefit	Estimates
<i>Reductions in injuries (people)</i>	
Fatality savings @37% effectiveness	738
Serious injury savings @68% effectiveness	17,361
<i>Financial savings (@ 7% discount rate)</i>	
Fatality savings	\$A1,014,107,336
Serious injury savings	\$A2,259,025,240
<i>Total savings</i>	<i>\$A3,273,132,576</i>
<i>Total cost</i>	<i>\$A1,582,528,340</i>
<i>BCR (saving & device cost of \$A600 @ 7% discount rate)</i>	
<i>BCR</i>	<i>2.07:1</i>

Estimation of torso SAB effects

In the above calculation it is assumed that 100% of the SAB systems fitted would be combination SAB systems. It is the case however that a number of manufacturers choose to install torso only systems and this may be accompanied by substantial changes to the side structures of the vehicle. It is thus important to estimate the savings and costs associated with torso SAB systems. For this purpose, the fitment cost is as per the combination SAB system. For brevity, the only the results of the calculations are presented in Table 12 and Figure 5. This allows a direct comparison with the benefits and costs associated with the assumed 100% fitment of combination SAB systems.

Table 12. Overall view of person-based injury reductions, financial savings and benefits, and the overall BCR for torso only SAB fitment

Benefit	Estimates
<i>Reductions in injuries (people)</i>	
Fatality savings @26% effectiveness	518
Serious injury savings @ 34% effectiveness	8680
<i>Financial savings (@ 7% discount rate)</i>	
Fatality savings	\$A712,615,966
Serious injury savings	\$A1,129,512,620
<i>Total savings</i>	\$A1,842,128,586
<i>Total cost</i>	\$A1,582,528,340
<i>BCR (saving & device cost of \$A600 @ 7% discount rate)</i>	
<i>BCR</i>	1.16:1

Figure 5 shows the BCR's calculated for both SAB system configurations across an installation cost range of \$A400 to \$A1250. The break-even cost for the combination SAB system was \$A1325 and \$A700 for the torso only SAB system.

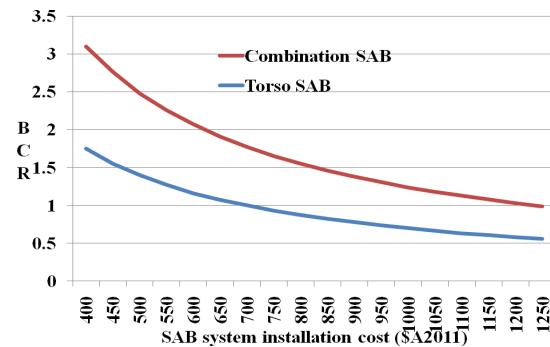


Figure 5. BCR value given SAB system fitment cost and benefits for combination and torso systems

DISCUSSION

The findings of this analysis estimate that the fitment of SAB systems fitted into new passenger vehicles sold in Victoria would be associated with 738 fewer deaths and 17,361 fewer serious injuries to drivers involved in near side impact crashes from 2011-2040. The financial savings are in the order of \$A3.273 billion with an expect outlay of \$A1.582 billion given SAB installation cost of \$A600 in today's dollar terms and the overall BCR was found to be 2.07:1.

The alternative analysis where the benefits of torso only SAB are used – and assumed to be fitted to all existing and new passenger vehicles are logically lower than those for described for combination SAB systems. In short, it could be expected that there would be 518 fewer deaths and 8680 fewer serious injuries to drivers involved in near side impact crashes over a 30-year period. The financial savings are in the order of \$A1.8 billion with an expect outlay of \$A1.582 billion given SAB installation cost of \$A600 in today's dollar terms. The overall BCR was found to be 1.16:1 over the next thirty years.

Consumer safety programs, such as NCAP and www.howsafeisyourcar.com.au have a significant role to play in creating consumer demand for improved passive and active safety features such as SAB, but also Electronic Stability Control, Brake Assist and an array of emerging life-saving technologies. The considerable savings – and the positive benefit-cost ratio, reported here, provide the basis for programs that encourage buyers of purchase passenger vehicles with SAB systems fitted, or alternatively, to elect to fit SAB where available as an optional extra.

The present paper has a number of limitations. First, we report only a single effectiveness value for fatal and serious injuries for each SAB configuration; ideally we would conduct a sensitivity analysis using a lower and upper range of benefits, and this is planned for the future work program. Second, we ideally require estimates of SAB effectiveness from the Australian fleet. Third, it is important to model the head injury benefits of side airbag systems, particularly given the significant life-time costs for those with severe traumatic brain injury; the mitigation of these types of injuries would result in larger financial savings, let alone the vastly different quality of life of those injured. Fourth, the analysis would benefit from more robust estimates of the future number of crashes and a differentiation of standard or optional SAB system fitment as well as the type of SAB system fitted into passenger vehicles in Victoria.

While the above points may be considered limitations, they also point a way forward to providing the basis for more robust estimators as well as the inputs required to assess the effect any changes in the fitment rate – either accelerated or slower, than the current business-as-usual model.

CONCLUSIONS

In summary, this analysis points to significant benefits to the Victorian community of the continued uptake of SAB into passenger vehicles through a significant reduction in the number of drivers killed and seriously injured in near-side impact crashes. These benefits were found to be greater for combination airbags which offer both head and torso protection as compared to torso only SAB. The benefits reported here are likely to be conservative given that only the driver in near side impacts was examined. It is important to note that the inclusion of drivers involved in far-side impacts and the inclusion of the front passenger would result in higher savings due to the dual deployment in the case of side impact crashes, with no additional fitment cost.

It is thus imperative that consumers are educated as to the benefits of choosing the safest car they can afford at the time of purchase. Consumer safety programs such as those initiated and supported by the TAC have a significant role to play in creating consumer demand for safer passenger vehicles and promoting the installation of new technologies. With this continued and sustained investment, the lives of a significant number of Victorians will benefit well into the future.

REFERENCES

1. Bureau of Infrastructure Transport and Regional Economics, Cost of road crashes in Australia 2006, Report 118. 2010, Department of Infrastructure, Transport, Regional Development and Local Government: Canberra.
2. Bureau of Infrastructure Transport and Regional Economics, Road Deaths Australia - February 2011. 2011, Australian Government: Department of Infrastructure and Transport: Canberra.
3. Legislative Council of Victoria of the State Government of Victoria, Investigation into the desirability of the compulsory fitting and the compulsory wearing of seatbelts, together with Minutes of Evidence and Appendices. 1969, A. C. Brooks, Government Printer: Melbourne.
4. Cameron, M., A. Canallo, and A. Gilbert, Crash-based evaluation of the speed camera program in Victoria 1990-1991. Phase 1: General effects. Phase 2: Effects of program mechanisms. 1992, Monash University Accident Research Centre: Melbourne. p. 131.
5. Cameron, M. and S. Newstead. Mass media publicity supporting police enforcement and its economic value. in Symposium on Mass Media Campaigns in Road Safety. 1996. Scarborough Beach, Western Australia.
6. Corben, B., C. Ambrose, and F. C, Evaluation of Accident Black Spot Treatments (Report 11). 1990, Monash University Accident Research Centre - Clayton.
7. Cameron, M., et al., The interaction between speed camera enforcement and speed-related mass media publicity in Victoria (Report 201) 2003, Monash University Accident Research Centre: Clayton.
8. OECD, Towards Zero: Ambitious Road Safety Targets and the Safe System Approach. 2008, OECD: Paris.
9. Haddon Jr., W., The changing approach to the epidemiology, prevention, and amelioration of trauma: the transition to approaches etiologically rather than descriptively. *American Journal of Public Health*, 1968. 58: p. 1431-1438.
10. Peden, M., et al., World report on road traffic injury prevention. 2004, World Health Organisation: Geneva.

11. State Government of Victoria, Victoria's Road Safety Strategy: Arrive Alive 2008-2017. 2008, State Government of Victoria, Melbourne.
12. Fitzharris, M., et al., Crash-based evaluation of ADR69: Past success and future directions, in Australian Transport Safety Bureau. 2006: Canberra.
13. Commonwealth of Australia, Vehicle Standard Australian Design Rule 69/00 – Full Frontal Impact Occupant Protection, Amendment 1. <http://www.comlaw.gov.au/Details/F2007C00772>, 2006.
14. Commonwealth of Australia, Australian Design Rule 73/00 - Offset Frontal Impact Occupant Protection. <http://www.comlaw.gov.au/Series/F2005L03990>. 2005.
15. Commonwealth of Australia, Vehicle Standard Australian Design Rule 72/00 - Dynamic Side Impact Occupant Protection, <http://www.comlaw.gov.au/Series/F2005L03992>. 2005.
16. Fildes, B. and K. Digges, eds. Occupant protection in far-side crashes. Monash University Accident Research Centre. Vol. 1. 2010, Monash University: Clayton.
17. Gibson, T., et al., Improved side impact protection: A review of injury patterns, injury tolerance and dummy measurement capabilities, Report 147. 2001, Monash University Accident Research Centre: Clayton.
18. Braver, E. and S.Y. Kyrychenko, Efficacy of Side Air Bags in Reducing Driver Deaths in Driver-Side Collisions. American Journal of Epidemiology, 2004. 159: p. 556–564.
19. Insurance Institute for Highway Safety, Surviving Side Crashes Status Report, 2006. 41(8).
20. McGwin, G.J., J. Metzger, and L. Rue, The Influence of Side Airbags on the Risk of Head and Thoracic Injury after Motor Vehicle Collisions. J Trauma, 2004. 56(3): p. 469-725.
21. Truong, J., et al. Case study - Penetration of electronic stability control and curtain airbags in the Victorian market. in Australasian Road Safety Research, Policing and Education Conference. 2010. Canberra, ACT.
22. Australian Bureau of Statistics, Motor Vehicle Census by make, model, postcode, vehicle body and State, At 31 March 2010 (Cat. 9309.0). 2011, Commonwealth of Australia: Canberra.
23. Australian Bureau of Statistics, 3222.0 - Population Projections, Australia, 2006 to 2101 2008, Commonwealth of Australia: Canberra.
24. Department of Finance and Deregulation, Best Practice Regulation Guidance Note: Value of statistical life. 2008, Office of Best Practice Regulation, Australian Government: Canberra.
25. Australian Bureau of Statistics, 6401.0 Consumer Price Index, Australia: TABLES 1 and 2. CPI: All Groups, Index Numbers and Percentage Changes. 2010, Australian Bureau of Statistics: Canberra.
26. Dupont, W.D., Statistical Modelling for Biomedical Researchers. 2002, Cambridge: Cambridge University Press.
27. Australian Bureau of Statistics, 3101.0 Australian Demographic Statistics, TABLE 4. Estimated Resident Population, States and Territories (Number). 2010, Australian Bureau of Statistics: Canberra.

VEHICLE GREENHOUSE SHAPE ANALYSIS FOR DESIGN OF A PARAMETRIC TEST BUCK FOR DYNAMIC ROLLOVER TESTING

Patrick Foltz

Taewung Kim

Jason R. Kerrigan

Jeff R. Crandall

Center for Applied Biomechanics, University of Virginia

United States

Paper Number 11-0271

ABSTRACT

The goal of this study was to define a set of vehicle greenhouse geometries that are representative of the current vehicle fleet for use on a parametric rollover test buck. Greenhouse geometry data for 60 vehicles were taken from New Car Assessment Program (NCAP) test reports and compiled in a database for analysis. The database was then used to determine XYZ coordinates for landmark points that characterized the greenhouse geometries for those 60 vehicles. These landmark-based greenhouse representations were then analyzed and grouped into one of three groups using an Optimization technique. The mean shape was found for each group, and this was used as a representation of the group. These three representative shapes were found to have a maximum variation of 15 degrees in the windshield angle, 120 mm in roof rail height, 119 mm in greenhouse roofline width, and 258 mm in B- to C-pillar length.

INTRODUCTION

While only accounting for 3% of crashes, more than one-third of vehicle occupant fatalities occur in crashes that involve rollover (NHTSA 2010). Epidemiological, computational, and experimental studies have implicated a variety of vehicle, crash, and occupant parameters affecting occupant fatality and injury risk (c.f. Gloeckner et al. 2006, Hu 2007, and Orłowski et al. 1985). Prioritization of these parameters for effective vehicle design, injury countermeasure development, or dynamic crashworthiness test procedure development, requires

a means to assess the effects of adjusting a single parameter independently of the other factors. Computational modeling provides for a means to perform such independent evaluations, but uncertainties regarding the validity of vehicle models in dynamic rollover simulations (Parent et al. 2010) suggest that simulation results should be used only to guide and not define parameter prioritization. While experimental analyses have the benefit of utilizing physical structures, which eliminates concerns regarding validity, parametric analysis of rollover crashes using experimental testing is complicated by variations in multiple parameters between vehicles. For instance, in general, while vehicle A may differ from vehicle B in roof strength, they also may vary in roof shape, roll moment of inertia, mass and a variety of other factors. Thus, any differences in vehicle response cannot be attributed to variations in roof strength any more than they can be attributed to variations in shape, moment of inertia or mass. However, a vehicle-like buck structure that could be configured to match a variety of vehicle geometric, inertial, and strength parameters, while allowing for independent adjustment of individual characteristics, would permit parametric evaluations of vehicle characteristics affecting occupant injury risk in rollover crashes. Use of the parametric rollover buck with a rollover crash test fixture designed for parametric variation of crash characteristics (Kerrigan et al. 2011) and with various occupant surrogates in various positions with various restraints full parametric analyses could be conducted. This study presents methodology and results of a part of a

larger research effort aimed at the development of a parametric rollover test buck for use in examining the effect individual vehicle parameters have on vehicle crashworthiness and occupant injury risk.

To ensure that parametric rollover testing yields applicable results, the buck should be representative of the current model vehicle fleet. Thus, the test buck was designed to mimic the current vehicle fleet in four separate categories: exterior geometry, interior (occupant space) geometry, inertial properties, and roof strength. For each of the individual parameters within each group, a range of values representative of the current fleet needs to be identified, and a design methodology that permits adjustment of the buck to achieve values within the range needs to be developed. For the inertial properties (including mass, moment of inertia, location of the center of gravity), identification of the parameter ranges for the current fleet can be determined from the literature (Heydinger et al. 1999, Bixel et al. 2010), and buck adjustment can be achieved by designing provisions to add and remove ballast weights from different locations on the vehicle. Similarly, interior geometry (e.g. occupant vertical, lateral and longitudinal headroom, lateral space from occupant to the door structure) can be determined from United States Department of Transportation (USDOT) frontal impact (FI) and side impact (SI) New Car Assessment Program (NCAP) reports, and buck adjustment can be obtained by adjusting the location of the occupant's seat relative to the vehicle's interior structures (door, roof rail, roof, B-pillar, instrument panel, etc). Regarding external (greenhouse) geometry and roof strength, adjustment of the buck to achieve particular values is a more complex problem. Since the buck's greenhouse (pillars and roof) should sustain plastic deformation as a result of a rollover test, parts of the greenhouse, or possibly the entire structure, will need to be replaced between tests. Thus, as an initial effort at identifying the sensitivity of occupant injury risk to changes in roof strength and exterior vehicle shapes, greenhouse structure designs exhibiting three different shapes and three different strengths will be developed. Once the baseline sensitivities are elucidated, an extensive computational modeling effort will be undertaken to complement

experimental results, and additional roof structures may be developed.

However, the problem of identification of the ranges of parameters exhibited by the vehicle fleet for strength and shape still exists. Roof strength can be conveniently represented on a linear scale using the strength-to-weight ratio (SWR) determined from a platen test like the Federal Motor Vehicle Safety Standard (FMVSS) No. 216 test. Since this test can be simulated computationally, once greenhouse geometries are identified, specific structural components of the greenhouses can be modified until the structures exhibit the targeted SWR. Thus, the last issue is how to identify three greenhouse geometries that are representative of the current vehicle fleet.

Since greenhouse geometries vary widely between vehicles, and more than three parameters are required (at a minimum) to characterize the geometries, identification of three specific geometries that are representative of the fleet is a challenging problem. It is hypothesized that specific geometries that are at or near the boundaries of vehicle-to-vehicle variation will be required to show significant effects on injury risk when the sensitivity of geometry is examined. The current study combines Generalized Procrustes Analysis (GPA) and a novel optimization technique to group greenhouse geometries from 43 vehicles, spanning 14 different classifications, into three separate groups based on geometric differences and identifies "average" geometries from each group. While it is clear that there are some relationships between greenhouse shape and size that result from the vehicle design process, the procedures presented here normalize vehicle geometries by their size to group vehicles by differences in their shape alone.

METHODOLOGY

Greenhouse geometry and landmarks

First, an initial study of original equipment manufacturer (OEM) vehicle classifications was conducted. Vehicle registration data [R.L. Polk & Co] was referenced to determine a ranking of OEMs by number of vehicles registered in the United States in 2008 and 2009. Over 70% of the vehicle fleet was

accounted for by the 14 different vehicle makes considered in this study. It was determined that the vehicle classifications used by the manufacturers of these 14 vehicle makes were one of 15 categories: Subcompact, Compact, Midsize Sedan/Coupe, Fullsize Sedan/Coupe, Sports Car, Compact SUV, Compact Crossover, Midsize SUV, Midsize Crossover, Midsize Pickup, Fullsize SUV, Fullsize Pickup, SUT (Pickup-SUV Hybrid), Minivan, and Fullsize Van. Once these 15 categories were determined, at least three vehicles from each category were selected to populate a database. Greenhouse geometry for each of the vehicles was specified using measurements collected from FI and SI NCAP test reports. However, NCAP reports for Fullsize Vans were unavailable, so this group was omitted. Also, in the case of the SUT class, only three vehicles fit into this class (Chevrolet Avalanche, Honda Ridgeline, Explorer Sport Trac), but FI and SI NCAP reports were not available for the Explorer Sport Trac, so only two vehicles were used for this category. In total, 60 vehicles were found encompassing the 14 remaining categories (Table 1, and Table A1).

Table 1. Number of Vehicles Included In Each Classification

Vehicle	Number
Subcompact	3
Compact Car	4
Midsize Sedan/Coupe	5
Fullsize Sedan/Coupe	4
Sports Car	3
Midsize Pickup	5
Fullsize Pickup	5
Compact SUV	3
Compact Crossover SUV	4
Midsize SUV	9
Midsize Crossover SUV	5
Fullsize SUV	5
Minivan	3
Pickup/SUV Hybrid	2
Total Vehicles	60

Eight geometric parameters for each of the 60 vehicles obtained from the FI and SI NCAP reports were added to the database (Figure 1): windshield angle, A- to B-pillar base length measured midline to midline, B- to C-pillar base length measured midline to midline, greenhouse base width from A-pillar edge to A-pillar edge, greenhouse roofline width from A-

pillar edge to edge beltline height, roof rail height, and overall roof height (US DOT FI/SI NCAP). From these parameters, the overall greenhouse height was calculated by subtracting the roof height from the beltline height, and the greenhouse rail height was calculated by subtracting the roof rail height from the beltline height (Figure 1). Histograms for each of the greenhouse geometric properties were created to examine differences across the vehicle fleet (Appendix Figure A1).

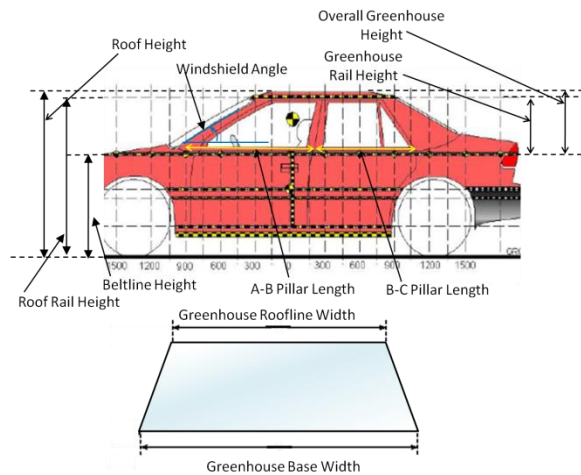


Figure 1. Vehicle geometric parameters used to characterize greenhouse geometry (US DOT FI/SI NCAP).

To more easily compare the differences in geometry between vehicles and facilitate grouping optimization (see *Grouping Using Optimization*) data, parameters were expressed as X-, Y-, and Z-coordinates of 18 landmarks on the vehicle (Figure 2). The origin of the coordinate system was located at the center base of the windshield (L_{16}), with the X-direction aligned with the longitudinal axis of the vehicle, the Y-direction aligned with the lateral axis of the vehicle, and the Z-direction aligned with the vertical axis of the vehicle. D-pillar geometry was not considered, even though SUVs and some other vehicles have a D-pillar, since front row occupants involved in lateral (barrel) rolls were the primary focus of the buck development. X-, Y-, and Z-coordinates for each of the 18 points on each vehicle were added to the database (Figure 2). Due to the way each of the landmarks were defined, all of the landmark coordinates could be determined from the coordinates

of a reduced set of landmarks (L_1 , L_4 , L_5 , L_6 , and L_7) referred to as the critical landmarks.

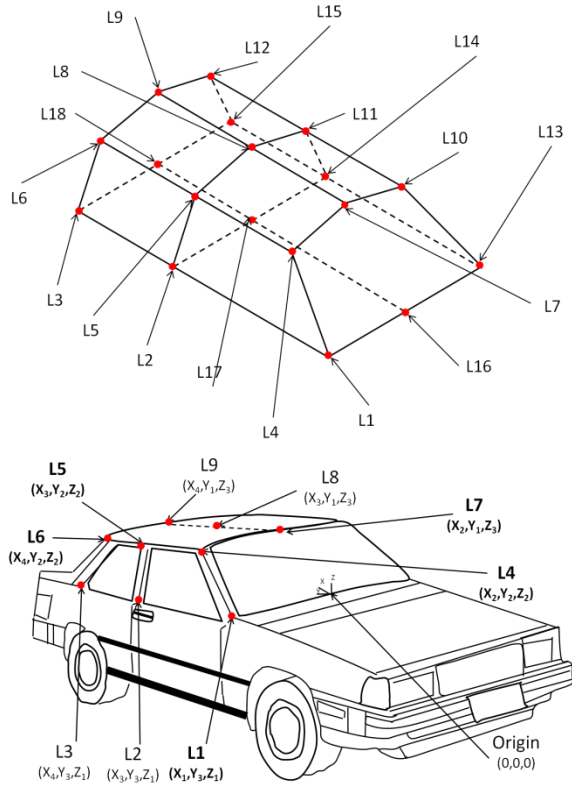


Figure 2. Top: 18 landmarks used to characterize greenhouse geometry. Bottom: Five particular landmarks (in bold) representing the reduced set of “critical” landmarks.

While some of the coordinates could be derived directly from the geometric parameters taken from the NCAP reports (Figure 1), some of the landmark coordinates had to be derived. The height of the roof rail (Z_2 from point L_4 in Figure 2) was calculated by subtracting the beltline height from the roof rail height, the overall greenhouse height (Z_3 from point L_7 in Figure 2) was derived by subtracting the beltline height from the overall roof height. Finally, the X-coordinate of the point at the top of the A-pillar X_2 was calculated using

$$X_2 = \frac{h_{\text{greenhouse}}}{\tan(\theta_{\text{windshield}})} \quad (1).$$

where h is the height of the roof rail, and θ is the windshield angle.

From the original 60 vehicles, complete data (all of the measurements from Figure 1) were only found for 52 vehicles. For the vehicles with complete data, not all measurements were included due to inconsistencies in the reported measurements (i.e. the value X_2 suggested the top of the A-pillar was between the B- and C-pillars) or because some vehicles lacked a C-pillar. The final set consisted of 43 vehicles, with less than three vehicles in the Subcompact, Compact, Fullsize Sedan and Sports Car categories. However Midsize Sedans, Trucks and SUVs were well represented (Table 2 and Appendix Table A1).

Table 2. Vehicles for Greenhouse Structure Shape Analysis

Vehicle	Number
Subcompact	1
Compact Car	2
Midsize Sedan/Coupe	4
Fullsize Sedan/Coupe	1
Sports Car	2
Midsize Pickup	4
Fullsize Pickup	3
Compact SUV	3
Compact Crossover SUV	3
Midsize SUV	8
Midsize Crossover SUV	5
Fullsize SUV	3
Minivan	2
Pickup/SUV Hybrid	2
Total with full data	43

Generalized Procrustes Analysis

Once the vehicle data were organized, Generalized Procrustes Analysis was used to translate and scale each of the greenhouse shapes to prepare the data for grouping optimization by shape (Dryden and Mardia, 1998). Translation of the shapes, and their landmark coordinates, resulted in a set of centered landmarks L_c , obtained by

$$L_{c,ni} = L_{ni} - \frac{1}{K} \sum_{j=1}^K L_{nj} \quad (2).$$

where L is a vector containing the coordinates of each landmark, n represents the vehicle number from 1 to 43, K is the total number of landmarks (18), and i represents the index of the landmarks from 1 to 18.

This step serves to express each landmark's vector relative to the centroid of points composed using all 18 landmarks for the particular vehicle. While all 18 landmarks were used to compute the centroid, only the five critical landmarks are needed to define the greenhouse geometry (Figure 3).

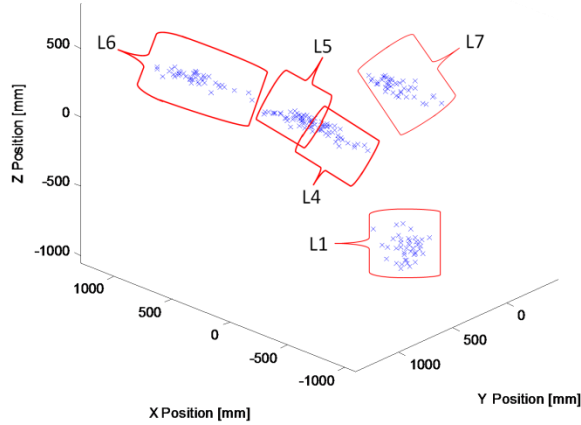


Figure 3. Centered critical landmark distributions for each of the 43 vehicles.

Then, each of the centered landmarks were scaled, or normalized, by the size variable r_n (Dryden and Mardia, 1998)

$$r_n = \left(\frac{1}{K} \sum_{j=1}^K L_{c,nj}^T L_{c,nj} \right)^{0.5} \quad (3a).$$

$$Q_{ni} = L_{c,ni} / r_n \quad (3b).$$

where r_n was the mean square root error of distances each landmark was from its centroid, and Q were the normalized vectors.

Grouping using Optimization

Once the landmarks were scaled and aligned with the same origin, three groups of greenhouse geometries were determined by optimization (Equation 4). The optimization relied upon the use of a weighting vector p_{mn} , which is similar to the probability that the n^{th} vehicle was included in m^{th} group, which was used as the design variable in this problem. Q_{nk} denoted the position of k^{th} landmark of n^{th} vehicle (the aligned and normalized landmark coordinates) and \bar{Q}_{mk} , which was the output of the optimization algorithm, represented mean location of the k^{th} landmarks of the m^{th} group.

Minimize

$$\sum_{m=1}^M \sum_{k=1}^K \sum_{n=1}^N p_{mn} (Q_{nk} - \bar{Q}_{mk})^T (Q_{nk} - \bar{Q}_{mk}) \quad (4a).$$

where

$$\bar{Q}_{mk} = \sum_{n=1}^N p_{mn} Q_{nk} / \sum_{n=1}^N p_{mn} \quad (4b).$$

Subject to

$$\sum_{m=1}^M p_{mn} = 1 \quad (\text{for } n = 1, \dots, 43) \quad (4c).$$

$$p_{mn} \geq 0 \quad (4d).$$

It should be noted that if the weights are uniformly distributed (equal) the objective function is maximized and the optimization cannot progress. Therefore, the weights were seeded randomly, and the optimization was performed 50 times with different seed values for the weights. The MATLABTM function *fmincon* was used to minimize the objective function each time. From the 50 results, the result with the lowest final value for the objective function was used. Then these steps were conducted nine more times to verify that the group weights p_{mn} resulted in the same distribution of groups, which verified the repeatability and robustness of the result.

The resulting weights showed that each vehicle was effectively put into one of the three groups: one value was close to 1, and the other two values were close to 0. Then mean shapes for each group were obtained by a simple average of the normalized coordinates for all of the vehicles in each group. Since the GPA process effectively removed size information from the data, the three mean greenhouses were then scaled back to real coordinates. The landmarks, \bar{Q}_{mk} , that are expressed in normalized coordinate system were scaled back to landmarks of the original coordinate system, \bar{L}_{mk} , by multiplying the mean size of the 43 vehicles.

$$\bar{L}_{mk} = \bar{Q}_{mk} \cdot \frac{1}{N} \sum_{n=1}^N r_n \quad (5).$$

RESULTS

Three separate greenhouse shapes were determined (Figure 4). 27, 9, and 7 vehicles were in group 1, group 2, and group 3, respectively (Table A1). All of the greenhouse coordinates were translated so that the

X- and Z-coordinates of L_{13} were aligned at 0 and 0, respectively and so that L_{16} had a Y value of 0 (Figure 5 and Table 3). The resulting coordinates of the mean group shapes were compared with those in the fleet (Figure A1). The geometric parameters defining greenhouse geometry were computed to compare with the fleet (Table 4 and Figure A2). To examine the relationship between size and shape of the greenhouses, the distribution of the size variables for each vehicle (Equation 3a) were compared with the distributions from each group (Figure 6).

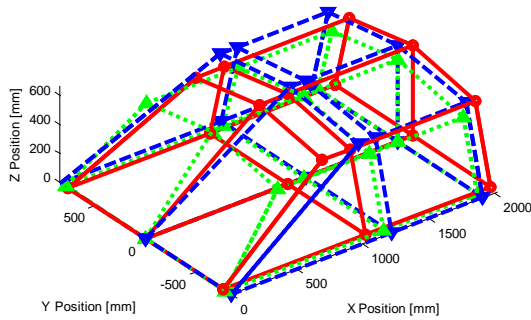


Figure 4. 3-D view of the 18 landmarks for each of the three average greenhouses.

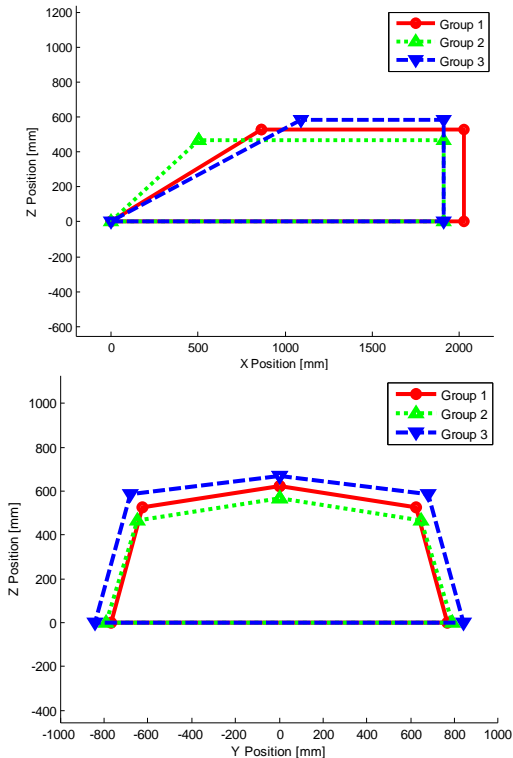


Figure 5. Front (top) and side (bottom) views of the group average greenhouses.

Table 3. Coordinates for the Critical Landmarks [mm]

Group 1 (n=27)					
	L ₁	L ₄	L ₅	L ₆	L ₇
X	0	863	1075	2027	863
Y	767	623	623	623	0
Z	0	528	528	528	624
Group 2 (n=9)					
	L ₁	L ₄	L ₅	L ₆	L ₇
X	0	503	1197	1913	503
Y	791	648	648	648	0
Z	0	466	466	466	570
Group 3 (n=7)					
	L ₁	L ₄	L ₅	L ₆	L ₇
X	0	1090	1217	1910	1090
Y	843	682	682	682	0
Z	0	586	586	586	669

Table 4. Geometric parameters for the three averaged greenhouses

	Group 1	Group 2	Group 3
Roof rail height (mm)	528	466	586
Overall roof height (mm)	624	570	669
AB pillar length (mm)	212	694	127
BC pillar length (mm)	951	716	693
Greenhouse roofline width (mm)	1246	1296	1365
Greenhouse base width (mm)	1535	1581	1686
Windshield angle (deg)	31	43	28

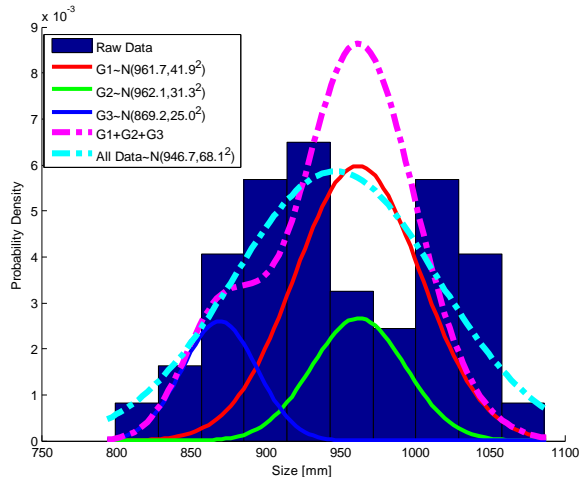


Figure 6. Distribution of the size variables for each group compared to all vehicles.

DISCUSSION

While the optimization problem defined in this study was not designed specifically to obtain unity for one of the elements of the weight vector for each vehicle, the resulting weight vectors showed that each vehicle was completely secluded to one of the three groups. This suggested that the optimization technique succeeded in effectively grouping the greenhouse shapes. After multiplying the mean greenhouse shapes by the same scale factor, it could be seen that group 3 had the tallest roof and greenhouse, but the shortest distance on the roof rail from the A-pillar to the C-pillar (AB Pillar Length + BC Pillar length) and the lowest windshield angle. Whereas group 2 had the lowest greenhouse and roof height, but the longest A-pillar to C-pillar length and highest windshield angle.

Despite the appearance of greater height in group 3, which is an indication only of its shape, the average size variable for the vehicles in group 3 was lower than that of the vehicles in groups 1 and 2 (Figure 6). While the vehicles in group 3 (only one Midsize Sedan, a Fullsize Pickup, a Midsize Pickup, a Midsize SUV, and three Midsize Crossovers (see Table A1) are typically referred to as larger vehicles, their average greenhouse size variable (Figure 6) was actually smaller because much of the size variable is based on the greenhouse length in the X-direction, which is typically larger in sedans than in trucks and SUVs. While group 1 and group 2 showed

differences in shape, their average size variables were nearly identical (with a higher variance in group 1) suggesting that for vehicles in these groups, relationships between size and shape could not be determined from the current study. In other words, the current study did not show that there were relationships between size and shape for the vehicles in groups 1 and 2. However, since the size of group 3 vehicles was actually smaller than that of the other groups, it appears that the shape characteristics of group 3 are not independent of size.

This study identified the distributions (Figures A1 and A2) of the greenhouse shapes of a variety of vehicles in the fleet. It successfully separated the geometric characteristics of size and shape to group vehicles based on their shape. To create a series of greenhouses for a rollover test buck, shape characteristics (or the mean shapes of each group) could be paired with certain vehicle sizes (using the data from Figure 6) to develop a series of roofs that span differences in the fleet in terms of vehicle shape and size. However, since data for shape and size have been separated, if three values of shape are paired with three values of size, nine roof geometries would need to be developed for each level of strength chosen. This will result in a cumbersome number of roof variations for a parametric analysis of the effects of roof strength and geometry on occupant injury risk. Additionally, it seems that this approach could result in unrealistic greenhouse geometries since a large size could be paired with a shape to create a greenhouse that is not available in the fleet. It is hypothesized that the effects greenhouse geometry has on occupant injury risk can only be seen by examining geometries that are at the boundaries of the distribution. Thus, it may make more sense to use the data from this study to determine the specific vehicle geometries that are at the boundaries of greenhouse geometry distributions for parametric examinations. As a next step, computational simulations could be used to examine how to determine which factors of greenhouse geometry are most important for rollover analyses.

CONCLUSION

This study aimed to identify three different greenhouse shapes that are representative of the

current vehicle fleet. The fleet was surveyed, and a novel optimization algorithm was used to determine three different geometries by minimizing the sum of the weighted distances between individual vehicle landmarks and the three group averaged geometries. The process separated the effect of greenhouse size from greenhouse shape to group geometries by shape only and permitted separate quantification of the distribution of greenhouse size. The result yielded three different mean greenhouses that are representative of the fleet in terms of differences shape. Additionally, the distribution of a variety of greenhouse geometric parameters for 43 vehicles in the fleet is presented. The next step in this work is to examine how these average shapes, coupled with appropriate sizes, compare to real vehicles in the fleet, and to determine how differences in greenhouse geometry affect occupant injury risk through experimental testing and computational analysis.

ACKNOWLEDGMENTS

This study was supported by the National Highway Traffic Safety Administration (NHTSA) under Cooperative Agreement No. DTNH22-09-H-00247. Views or opinions expressed or implied are those of the authors and are not necessarily representative of the views or opinions of the NHTSA.

REFERENCES

Arora J. (2004) Introduction to Optimum Design. Academic Press; 2nd edition (May 19, 2004).

Bixel RA, Heydinger GJ, Guenther DA. (2010) Measured vehicle center-of-gravity locations – including NHTSA’s data through 2008 NCAP. Society of Automotive Engineers (SAE). Paper Number 2010-01-0086. Warrendale, PA.

Dryden, IL, Mardia, KV. (1998) Statistical Shape Analysis. Chichester, New York

Gloeckner DC, Moore TLA, Steffey D, Bare C, Corrigan CF. (2006) Implications of vehicle roll direction on occupant ejection and injury risk. 50th Annual Proceedings of the Association for the Advancement of Automotive Medicine.

Heydinger GJ, Bixel RA, Garrott WR, Pyne M, Howe JG, Guenther DA. (1999) Measured vehicle inertial parameters – NHTSA’s data through November 1998. Society of Automotive Engineers (SAE). Paper Number 1999-01-1336. Warrendale, PA.

Hu J. (2007) Neck injury mechanism in rollover crashes – a systematic approach for improving rollover neck protection. PhD. Dissertation. Wayne State University. Detroit, MI.

Kerrigan JR, Jordan A, Parent D, Zhang Q, Funk J, Dennis NJ, Overby B, Bolton J, Crandall J. (2011) Design of a dynamic rollover test system. Society of Automotive Engineers (SAE). Paper Number 2011-01-1116. Warrendale, PA.

National Highway Traffic Safety Administration (NHTSA). (2010) Traffic Safety Facts 2008—A compilation of motor vehicle crash data from the fatality analysis reporting system and the general estimate system. Early Edition. DOT HS 811 170. <http://www-nrd.nhtsa.dot.gov/Pubs/811170.PDF>

Orlowski KF, Bundorf RT, Moffat EA. (1985) Rollover crash tests-the influence of roof strength on injury mechanics. Proceedings of the 29th Stapp Car Crash Conference. SAE Paper 851734. Society of Automotive Engineers, Warrendale, PA.

Parent DP, Kerrigan JR, Crandall JR. (2010) Comprehensive computational rollover sensitivity study part 1: influence of vehicle pre-crash parameters on crash kinematics and roof crush. Proceedings of the International Crashworthiness Conference, Paper 2010-010. Washington DC, USA.

US Department of Transportation. (2004-2010). “New Car Assessment Program (NCAP) Frontal Barrier Impact Test”. Retrieved from www.regulations.gov

US Department of Transportation. (2004-2010). “New Car Assessment Program (NCAP) Side Barrier Impact Test.” Retrieved from www.regulations.gov

APPENDIX

Table A1.

Vehicles examined, with report numbers for the FI and SI NCAP. Vehicles marked “excluded” could not be included in the analysis due to a lack of sufficient information.

Vehicle: Make/Model/ Year	FI NCAP Report Docket Number [1]	SI NCAP Report Docket Number [2]	Type	Group
Acura/RL/2005	NHTSA-1999-4962-0281	NHTSA-1998-3835-0247	Fullsize Sedan/Coupe	Excluded
BMW/5Series/2008	NHTSA-1999-4962-0439	NHTSA-1998-3835-0395	Fullsize Sedan/Coupe	1
BMW/Z4/2003	NHTSA-1999-4962-0223	NHTSA-1998-3835-0207	Sports Car	Excluded
Cadillac/CTS/2008	NHTSA-1999-4962-0469	NHTSA-1998-3835-0410	Midsize Sedan/Coupe	3
Cadillac/SRX/2010	NHTSA-1999-4962-0530	NHTSA-1998-3835-0497	Midsize Crossover	3
Chevrolet/Avalanche/2007	NHTSA-1999-4962-0389	NHTSA-1998-3835-0384	Fullsize SUV	1
Chevrolet/Aveo/2004	NHTSA-1999-4962-0370	NHTSA-1998-3835-0232	Compact	Excluded
Chevrolet/Camaro/2010	NHTSA-1999-4962-0512	NHTSA-1998-3835-0471	Sports Car	2
Chevrolet/Colorado/2006	NHTSA-1999-4962-0345	NHTSA-1998-3835-0262	Midsize Pickup	2
Chevrolet/Equinox/2005	NHTSA-1999-4962-0264	NHTSA-1998-3835-0227	Midsize SUV	1
Chevrolet/Malibu/2008	NHTSA-1999-4962-0467	NHTSA-1998-3835-0429	Fullsize Sedan/Coupe	Excluded
Chevrolet/Silverado/2007	NHTSA-1999-4962-0406	NHTSA-1998-3835-0386	Fullsize Pickup	2
Chevrolet/Suburban/2007	NHTSA-1999-4962-0362	NHTSA-1998-3835-0379	Fullsize SUV	1
Chevrolet/Tahoe/2007	NHTSA-1999-4962-0349	NHTSA-1998-3835-0382	Fullsize SUV	1
Dodge/Caliber/2007	NHTSA-1999-4962-0361	NHTSA-1998-3835-0323	Compact Crossover	1
Dodge/Dakota/2005	NHTSA-1999-4962-0298	NHTSA-1998-3835-0263	Midsize Pickup	2
Dodge/Grand Caravan/2008	NHTSA-1999-4962-0445	NHTSA-1998-3835-0415	Minivan	1
Dodge/Journey/2009	NHTSA-1999-4962-0457	NHTSA-1998-3835-0421	Compact SUV	1
Dodge/Nitro/2007	NHTSA-1999-4962-0392	NHTSA-1998-3835-0345	Compact Crossover	1
Dodge/Ram1500/2009	NHTSA-1999-4962-0492	N/A	Fullsize Pickup	Excluded
Ford/Escape/2008	NHTSA-1999-4962-0424	NHTSA-1998-3835-0364	Compact SUV	1
Ford/Expedition/2006	NHTSA-1999-4962-0226	NHTSA-1998-3835-0016	Fullsize SUV	1
Ford/Explorer/2002	NHTSA-1999-4962-0147	NHTSA-1998-3835-0185	Midsize SUV	Excluded
Ford/F-150/2009	NHTSA-1999-4962-0496	NHTSA-1998-3835-0459	Fullsize Pickup	3
Ford/Flex/2009	NHTSA-1999-4962-0471	NHTSA-1998-3835-0435	Midsize Crossover	1
Ford/Fusion/2008	NHTSA-1999-4962-0434	NHTSA-1998-3835-0297	Midsize Sedan/Coupe	1
Ford/Mustang/2010	NHTSA-1999-4962-0501	NHTSA-1998-3835-0477	Sports Car	2
Ford/Ranger/2007	NHTSA-1999-4962-0383	NHTSA-1998-3835-0020	Midsize Pickup	Excluded
Honda/Element/2007	NHTSA-1999-4962-0216	NHTSA-1998-3835-0346	Compact SUV	2
Honda/Fit/2009	NHTSA-1999-4962-0488	NHTSA-1998-3835-0457	Subcompact	Excluded
Honda/Odyssey/2005	NHTSA-1999-4962-0292	NHTSA-1998-3835-0257	Minivan	Excluded
Honda/Pilot/2008	NHTSA-1999-4962-0476	NHTSA-1998-3835-0440	Midsize SUV	1
Honda/Ridgeline/2006	NHTSA-1999-4962-0312	NHTSA-1998-3835-0328	Fullsize SUT	2
Kia/Borrego/2009	NHTSA-1999-4962-0484	NHTSA-1998-3835-0449	Midsize Crossover	1
Kia/Forte/2010	NHTSA-1999-4962-0519	NHTSA-1998-3835-0476	Midsize Sedan/Coupe	Excluded
Kia/Optima/2006	NHTSA-1999-4962-0393	NHTSA-1998-3835-0339	Fullsize Sedan/Coupe	Excluded
Kia/Rio/2006	NHTSA-1999-4962-0324	NHTSA-1998-3835-0327	Compact	1
Kia/Rondo/2007	NHTSA-1999-4962-0409	NHTSA-1998-3835-0358	Midsize Crossover	3
Kia/Sedona/2006	NHTSA-1999-4962-0344	NHTSA-1998-3835-0314	Minivan	1
Kia/Soul/2010	NHTSA-1999-4962-0502	NHTSA-1998-3835-0463	Compact Crossover	1
Kia/Sportage/2007	NHTSA-1999-4962-0403	NHTSA-1998-3835-0348	Midsize SUV	1
Lincoln/MKS/2009	NHTSA-1999-4962-0491	NHTSA-1998-3835-0444	Fullsize Sedan/Coupe	1

Vehicle: Make/Model/ Year	FI NCAP Report Docket Number [1]	SI NCAP Report Docket Number [2]	Type	Group
Mazda/3/2010	NHTSA-1999-4962-0537	NHTSA-1998-3835-0465	Compact	1
Mitsubishi/Lancer/2008	NHTSA-1999-4962-0416	NHTSA-1998-3835-0373	Compact	Excluded
Nissan/Armada/2006	NHTSA-1999-4962-0325	N/A	Fullsize SUV	Excluded
Nissan/Cube/2009	NHTSA-1999-4962-0511	NHTSA-1998-3835-0470	Compact Crossover	Excluded
Nissan/Frontier/2006	NHTSA-1999-4962-0355	NHTSA-1998-3835-0308	Midsize Pickup	3
Nissan/Murano/2009	NHTSA-1999-4962-0461	NHTSA-1998-3835-0422	Midsize Crossover	3
Nissan/Pathfinder/2005	NHTSA-1999-4962-0300	NHTSA-1998-3835-0251	Midsize SUV	3
Nissan/Titan/2006	NHTSA-1999-4962-0343	N/A	Fullsize Pickup	Excluded
Nissan/Xterra/2005	NHTSA-1999-4962-0313	NHTSA-1998-3835-0276	Midsize SUV	1
Smart/ForTwo/2008	NHTSA-1999-4962-0455	NHTSA-1998-3835-0420	Subcompact	Excluded
Toyota/4Runner/2010	NHTSA-1999-4962-0533	NHTSA-1998-3835-0500	Midsize SUV	1
Toyota/FJ/2007	NHTSA-1999-4962-0358	NHTSA-1998-3835-0311	Midsize SUV	2
Toyota/Highlander/2008	NHTSA-1999-4962-0442	NHTSA-1998-3835-0402	Midsize SUV	1
Toyota/Sequoia/2008	NHTSA-1999-4962-0464	N/A	Fullsize SUV	Excluded
Toyota/Tacoma/2006	NHTSA-1999-4962-0353	NHTSA-1998-3835-0304	Midsize Pickup	1
Toyota/Tundra/2006	NHTSA-1999-4962-0278	NHTSA-1998-3835-0150	Fullsize Pickup	2
Toyota/Venza/2009	NHTSA-1999-4962-0498	NHTSA-1998-3835-0467	Midsize Crossover	1
Toyota/Yaris/2008	NHTSA-1999-4962-0438	NHTSA-1998-3835-0456	Subcompact	1

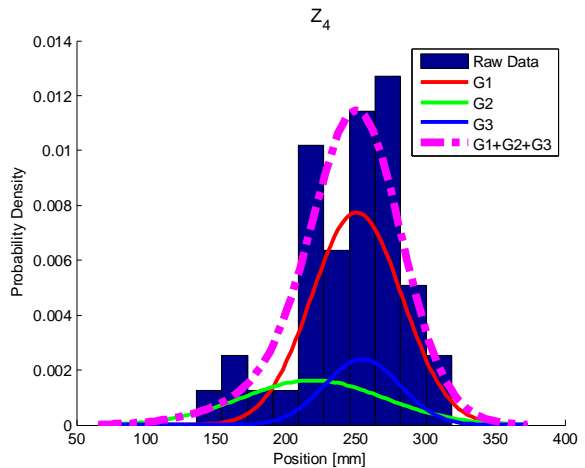
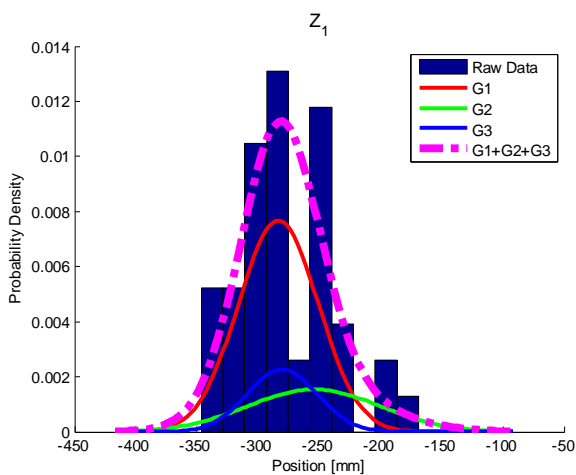
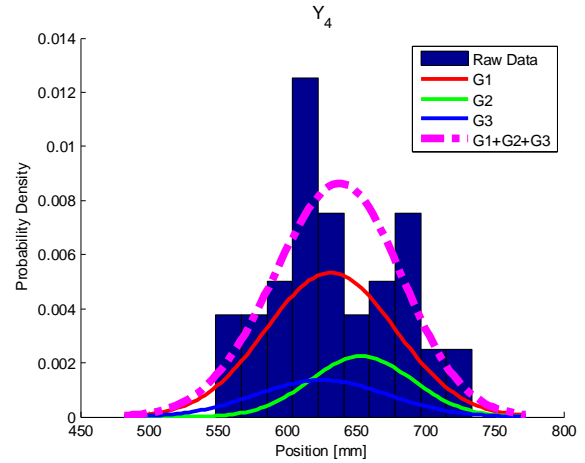
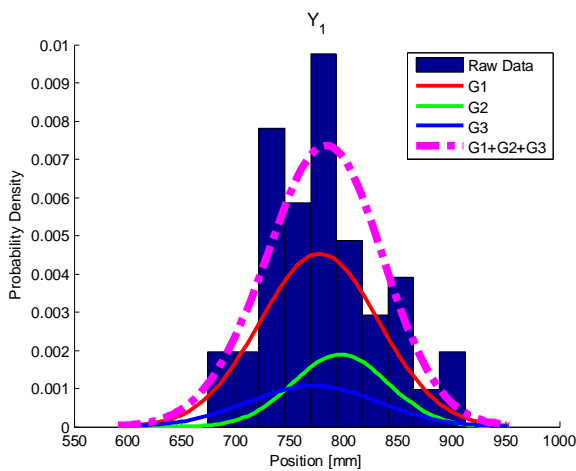
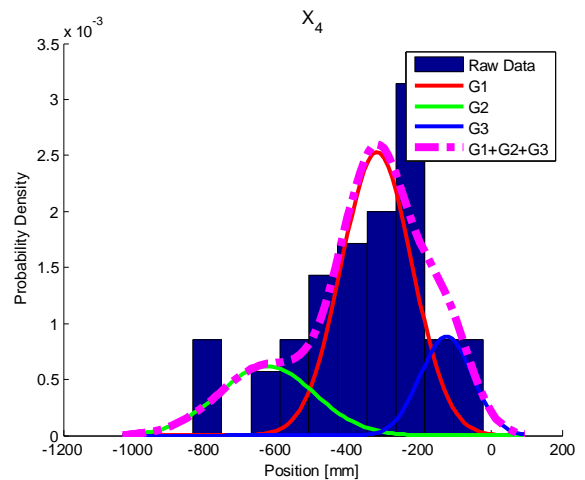
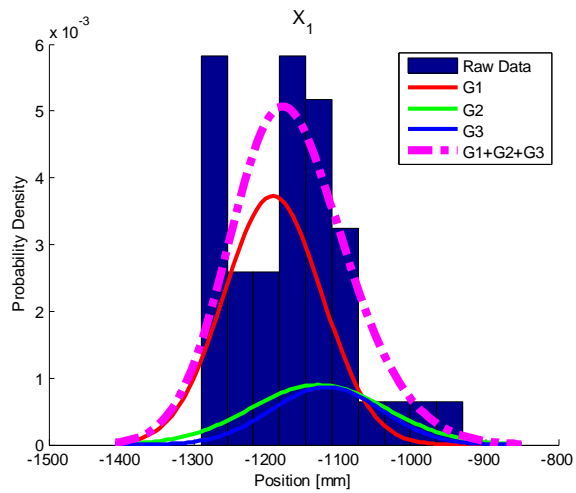


Figure A1. Distributions of each of the vehicle greenhouse critical landmarks for the 43 vehicles included in the optimization study (Cont'd).

Figure A1. Distributions of each of the vehicle greenhouse critical landmarks for the 43 vehicles included in the optimization study (Cont'd).

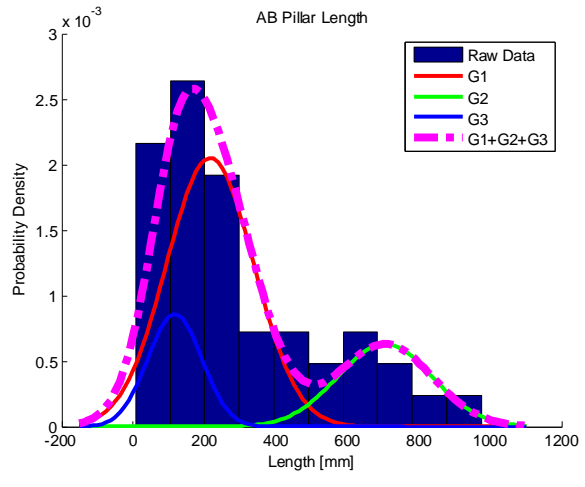
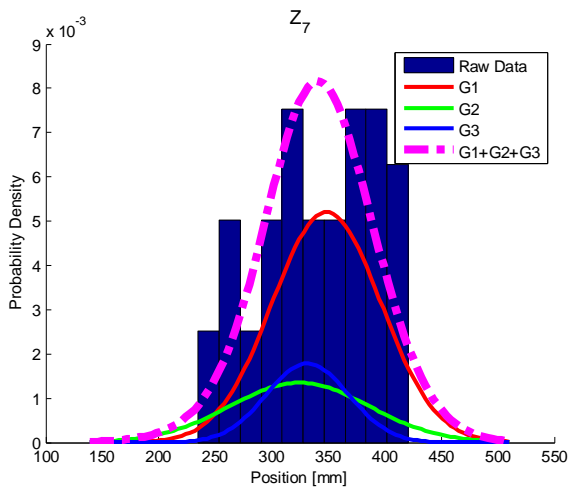
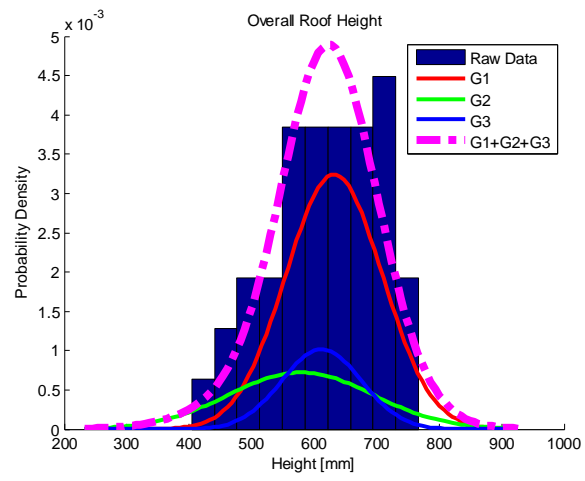
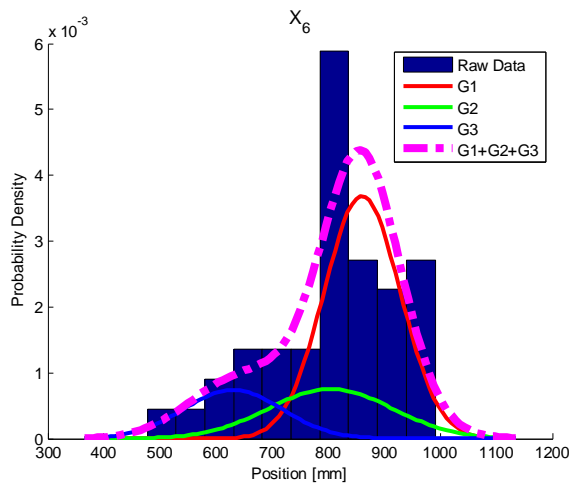
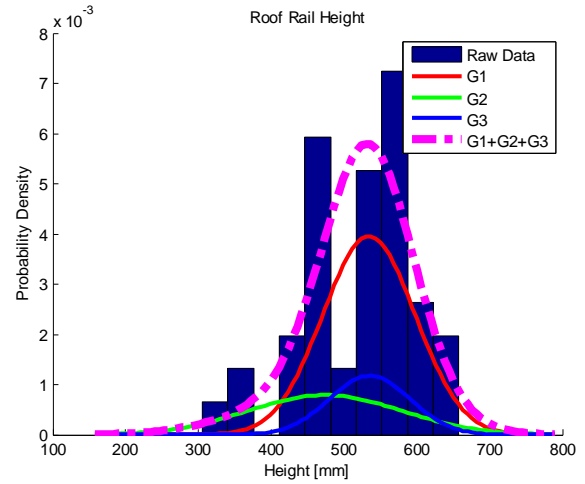
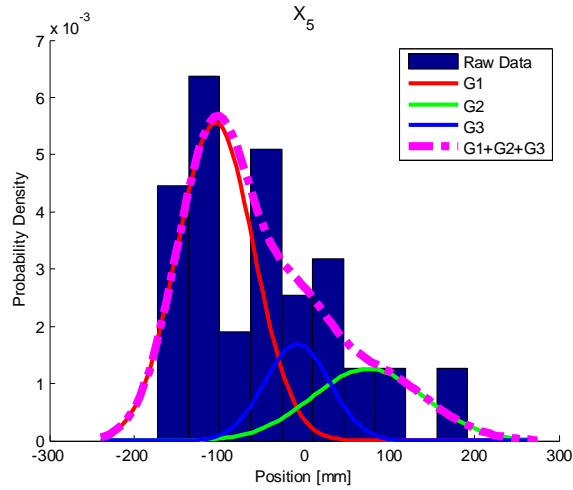


Figure A1. Distributions of each of the vehicle greenhouse critical landmarks for the 43 vehicles included in the optimization study.

Figure A2. Distributions of each of the vehicle greenhouse geometric parameters for the 43 vehicles included in the optimization study (Cont'd).

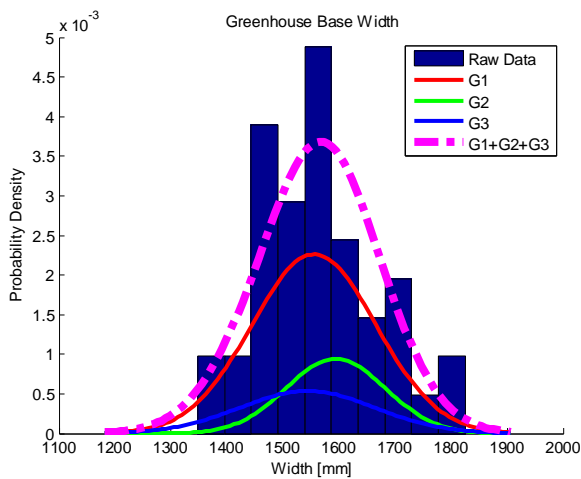
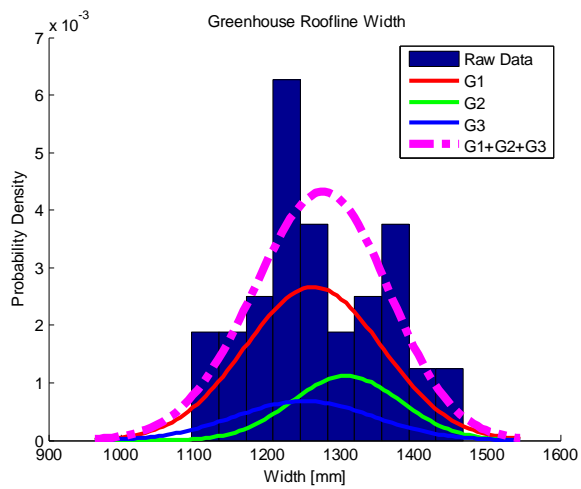
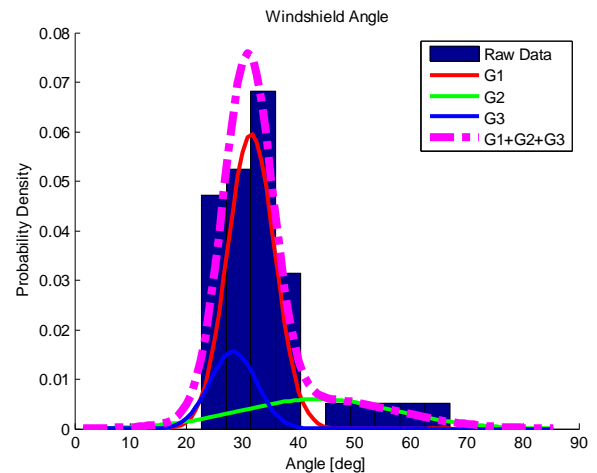
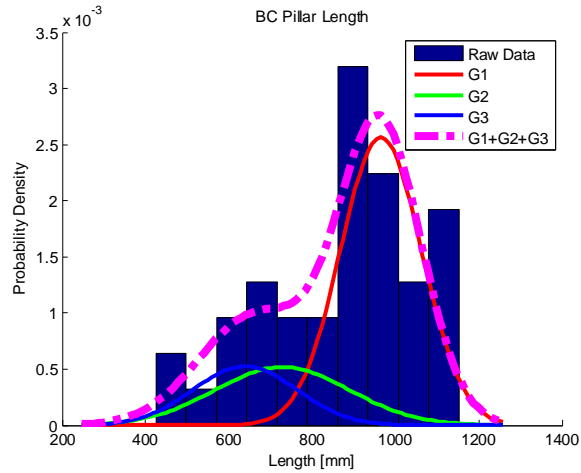


Figure A2. Distributions of each of the vehicle greenhouse geometric parameters for the 43 vehicles included in the optimization study.

Figure A2. Distributions of each of the vehicle greenhouse geometric parameters for the 43 vehicles included in the optimization study (Cont'd).

UPDATE OF NHTSA'S 2007 ANALYSIS OF ESC EFFECTIVENESS

Robert Sivinski

United States Department of Transportation
National Highway Traffic Safety Administration
United States
ESV Paper No. 11-0304

ABSTRACT

Objective - The primary goals of this analysis are to expand on and clarify the findings of the 2007 NHTSA analysis by using a greater variety of vehicles and several additional years of crash data. This analysis will also evaluate electronic stability control (ESC) effectiveness in all police-reported crashes.

The principal evaluation questions are:

- What is the effect of ESC on all police-reported crashes?
- What is the effect of ESC on fatal crashes?
- What are the effects of ESC on specific types of crashes?
- How does the effectiveness of ESC differ across passenger cars and light trucks/vans (LTVs)?
- What is the effect, if any, of ESC on collisions with pedestrians, bicyclists or animals?

Methods - Percent effectiveness of ESC was estimated by comparing the types of crashes that vehicle models experienced immediately before and immediately after the introduction of ESC. Because optional ESC generally cannot be identified from the VIN, only models that transitioned from no ESC system to a standard ESC system were included in this analysis. Effectiveness estimates were computed for different crash types relative to a control group of low-speed and similar crashes that are unlikely to be affected by ESC. The estimates should be interpreted as the reduction in the likelihood of a vehicle being involved in a specific type of crash as a result of ESC being added to that vehicle.

Results - When a vehicle is equipped with ESC, it has a smaller likelihood of being involved in a crash than a similar vehicle without ESC. Overall, ESC

was associated with a six percent decrease in the likelihood that a vehicle would be involved in any police reported crash and an 18 percent reduction in the probability that a vehicle would be involved in a fatal crash. For passenger cars, the reductions are 5 percent and 23 percent, respectively; for LTVs, 7 percent and 20 percent. Each of these reductions is statistically significant except for the 5 percent overall effect in cars. More specific crash types were also analyzed and these results are presented in the body of the paper.

Discussion - Estimates of effectiveness were especially large for crash types involving loss of vehicle control. Passenger cars and LTV's do not show large differences in effectiveness and show more similar results here than in previous analyses. The effect of ESC on collisions with pedestrians, bicyclists and animals, if any, is still unclear and will be monitored as more data becomes available.

INTRODUCTION

About ESC - Electronic stability control (ESC) is a computerized system that continuously monitors speed, steering wheel position, brake force at each wheel, yaw rate and lateral acceleration. This input allows the system to detect loss of directional stability at the rear wheels (spin out) or directional control at the front wheels (plow out). When loss of control is detected, the system acts by applying braking force to one or several wheels or by reducing engine torque output in order to slow the vehicle or correct its path. For example, if clockwise yaw due to oversteer is detected the system may apply brake force to the front left wheel in order to counteract the vehicle's rotation. This action takes place so quickly

that the system is essentially predictive, preventing loss of control before it occurs.

Through model year 2005, ESC was installed on less than 20 percent of the vehicles sold in the U.S. Due to mounting evidence of the effectiveness of ESC and ensuing legislation, from 2006 on there was a sharp rise in the number of vehicles sold with ESC installed. Although ESC is mandated on all new vehicles of model year 2012 or later, it will take several years for ESC equipped vehicles to saturate the on-road fleet.

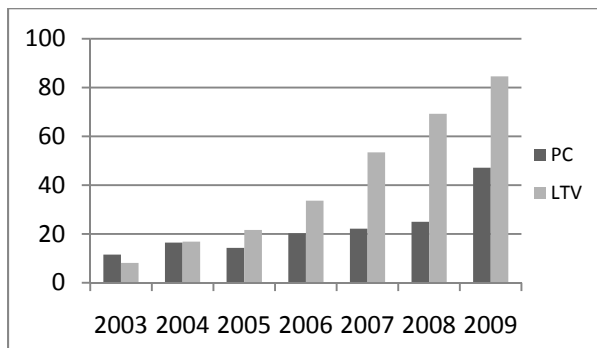


Figure 1. Percent of new vehicles sold in the US with standard ESC.

In 2008, the National Highway Traffic Safety Administration (NHTSA) issued Federal Motor Vehicle Safety Standard (FMVSS) No. 126 which required that passenger cars, multipurpose passenger vehicles (MPVs), trucks and buses with a gross vehicle weight rating (GVWR) of 10,000 pounds or less be equipped with an ESC system that meets the definition and performance requirements of the standard. The standard specified the following phase-in schedule:

Table 1. Mandatory phase-in schedule for ESC

Model Year	Production Beginning Date	Requirement
2009	September 1, 2008	55% with carryover credit
2010	September 1, 2009	75% with carryover credit
2011	September 1, 2010	95% with carryover credit
2012	September 1, 2011	Fully effective

Past Research -There have been several analyses of the effectiveness of ESC conducted by NHTSA, IIHS, and others in the past, all of which have found statistically significant reductions in crashes attributable to ESC. In 2007, NHTSA published its most comprehensive effectiveness analysis to date.^[1] It expanded on previous NHTSA evaluations with additional years of FARS (1997-2004) and State data (1997-2003). This analysis was able to investigate specific types of crashes, and found, among other large reductions, a 70 percent reduction in fatal rollover crashes in passenger cars and an 88 percent reduction in fatal rollover crashes in LTVs. In general, LTVs showed larger crash reductions due to ESC than passenger cars, with a 28 percent overall reduction in fatalities for LTVs and a 14 percent overall reduction in fatalities for passenger cars. A small non-significant increase in collisions with pedestrians, bicyclists or animals was found. This analysis also compared two and four-channel ESC systems, and found a significantly larger reduction in police-reported crashes for the four-channel systems.

Goals of the Evaluation - The primary goals of this analysis are to expand on and clarify the findings of the 2007 NHTSA analysis by using a greater variety of vehicles and several additional years of crash data. Previous research suggests that ESC has a large effect on fatality reduction and overall crash prevention. It is important to understand as clearly as possible the changes to the crash environment that will occur as a larger portion of the passenger vehicle fleet is equipped with ESC. This analysis will be better able to generalize the benefits of ESC due to the use of the National Automotive Sampling System – General Estimates System (NASS GES) to estimate the effects of ESC on all fatal and non-fatal crashes. This data is a nationally representative stratified sample of all police-reported crashes in the U.S. The use of FARS data, a complete census of fatal crashes in the U.S., will allow an in-depth analysis of the effects on all fatal crashes in the U.S.

The principal evaluation questions are:

- What is the effect of ESC on all police-reported crashes?
- What is the effect of ESC on fatal crashes?
- What are the effects of ESC on specific types of crashes?
- How does the effectiveness of ESC differ across passenger cars and LTVs?
- What is the effect, if any, of ESC on collisions with pedestrians, bicyclists or animals?

METHODS

Risk Ratio - The methodology for this evaluation is similar to that of the 2007 NHTSA evaluation. By examining the types of crashes that vehicle models are involved in immediately prior to and subsequent to the introduction of ESC, one can estimate the effectiveness of ESC by using contingency tables to compute associated risk ratios.^[2]

For example, if ESC has no effect on rollovers, then the ratio of vehicle rollovers to control-group collisions unlikely to be affected by ESC (such as being struck in the rear while parked) should remain the same before and after the introduction of ESC.

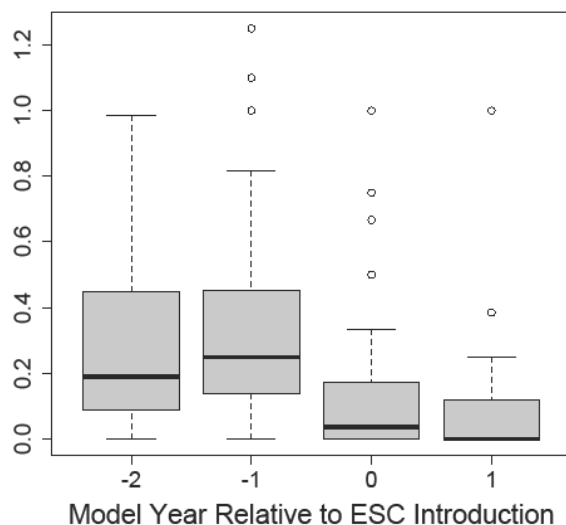


Figure 2. Ratio of rollover crashes to control crashes.

In Figure 2 each vehicle model in the analysis contributes four data points, one each for two years before, one year before, the year of and the year after ESC introduction on that model. The large drop observed in the ratio of rollovers to control crashes between the years before (-2,-1) and the years after (0,1) ESC introduction is evidence of ESC's effectiveness in reducing rollover crashes in relation to control crashes.

This report uses this concept to quantify ESC effectiveness in preventing different types of crashes. As an example, consider the Jeep Liberty, which received standard ESC in 2006. Simply comparing the number of rollovers in the two years before and two years after the introduction of ESC will not account for possible changes in the volume of sales, vehicle miles travelled, etc. That is why control group crashes are needed to give a baseline for comparison.

The following equation estimates ESC effectiveness on fatal rollover prevention in the Jeep Liberty by using data from the two model years before and after introduction of ESC (2004-2005 for the before ESC crashes and 2006-2007 for the after ESC crashes) from the Fatal Accident Reporting System (FARS) database. Any crashes taking place from 2004-2009 involving Cherokee model years 2004-2007 were eligible for inclusion. If ESC has no effect on the incidence of rollover crashes, then the ratio of rollover to control crashes should be similar in the time period before ESC and the time period after ESC, resulting in a risk ratio close to 1.000.

$$\left(\frac{\# \text{ rollovers after ESC}}{\# \text{ control crashes after ESC}} \right) / \left(\frac{\# \text{ rollovers before ESC}}{\# \text{ control crashes before ESC}} \right)$$

$$= \left(\frac{5}{38} \right) / \left(\frac{19}{87} \right)$$

$$\text{risk ratio} = 0.602$$

$$\text{percent effectiveness} = (1 - 0.602) * 100 = 40\%$$

The resulting risk ratio measures the effectiveness of ESC at reducing rollover fatalities. A risk ratio less than one implies a reduction in fatalities following introduction of ESC. When the risk ratio is subtracted from one, the result is the percent

effectiveness of ESC. In this example, the effectiveness of ESC is estimated to be 40 percent. In other words, adding ESC to a Jeep Liberty without ESC is estimated to result in a 40 percent reduction in the probability that that vehicle will be involved in a fatal rollover crash.

Control and Treatment Crash Groups - The method of analysis described above requires that vehicles are classified as belonging to either the control or a treatment group based on the type of crash involvement. An ideal control group vehicle would be a stationary vehicle that is struck by another motorist since the presence or absence of ESC in this vehicle would have no effect on the probability of crash involvement (this is not true for the striking vehicle, which is why this determination is made at the vehicle level rather than the crash level). However, there are not enough 'ideal' control vehicle cases to compose an adequate control group, so vehicles are assigned to the control group if their accident involvement is deemed unlikely to have been affected by the presence of ESC. The following list describes the circumstances under which a vehicle is assigned to the control group:

- Hit while parked/stopped
- Backing/parking/low-speed (1-10 MPH)
- Struck in rear
- Non-culpable involvement in a multi-vehicle crash on a dry road

Non-culpable involvements on dry roads make up a large portion of the control group, and this category relies heavily on the accuracy and completeness of the accident description included in the data files. To test if this group of crashes is introducing any bias, the NASS GES estimates were recomputed without the non-culpable involvements on dry roads in the control group. Reassuringly, the resulting weighted estimates were almost identical to those computed when they were included.

All vehicles that are not classified as control group vehicles are eligible to be included in a treatment crash group. The treatment groups are defined using available data gathered from sources such as the police accident report (PAR), which specifies the

circumstances of the crash and the role of each vehicle involved.

The treatment groups include:

All non-control group vehicles: This group includes all of the vehicles in the data files that do not meet the criteria for the control group. There will be a large variety of crashes in this group, and it is not expected to show as large of an effect of ESC as some of the other treatment groups that are specifically chosen because they are likely to be affected by vehicle control and stability.

All single-vehicle crashes (except collisions with pedestrians/bicyclists/animals): This group includes all single vehicle crashes in the data files, except for those involving pedestrians, bicyclists or animals, which are analyzed separately. Past research has shown that ESC is particularly effective in preventing single-vehicle types of crashes, which are very likely to be the result of loss of vehicle control.

First-event rollovers: This group is a subset of the single-vehicle crashes and is defined by examining the first harmful event in the crash sequence recorded in the data files. Subsequent-event rollovers, such as vehicles that strike a fixed object and roll as a result, are not included in this group.

All impacts with fixed objects: This group is a subset of single-vehicle crashes and includes all single-vehicle run-off-road crashes except first-event rollovers, collisions with pedestrians, bicyclists, animals or other movable objects such as trains, and non-collisions such as immersion in water or falling off a moving vehicle.

Side impacts with fixed objects: This group is a subset of all impacts with fixed objects. These vehicles are analyzed separately because side impacts are particularly characteristic of loss of vehicle control.

Culpable vehicles in multi-vehicle crashes: This group consists of vehicles that have been identified as the culpable party in a multi-vehicle crash. This group may contain vehicles that experienced loss of

control, but may also contain vehicles that were involved in crashes that would not have been affected by ESC. In past analyses these vehicles have shown a smaller benefit from ESC than those involved in single-vehicle crashes.

Collisions with pedestrians/bicyclists/animals:

This group is singled out for analysis because the 2007 NHTSA analysis showed a small non-significant increase in crash risk for vehicles with ESC. One way ESC functions is by attenuating driver steering and/or braking input that may result in loss of control, and it is possible that this could contribute to a reduction in the ability to make emergency evasive maneuvers.

All Crashes: This estimate is derived using results from the all non-control group crashes (it must be derived because the control group includes members of this crash group). Because an assumption of the analysis is that ESC will have no effect on the control group crashes we can estimate effectiveness in all crashes with the following formula:

$$effectiveness = \theta_t * x_t / (x_t + y_c)$$

Where:

θ_t = the estimated effectiveness for non-control group crashes

x_t = the number of non-control group crashes before ESC

y_c = the number of control group crashes before ESC

Because all crashes in the data are either contained in the control or non-control group, this will give an estimate of effectiveness in all crashes. The confidence interval for this estimate can be derived by replacing θ_t with the upper and lower bound estimates for the 95 percent confidence interval of the estimated effectiveness for all non-control group crashes.

All Multi-Vehicle Crashes: This estimate can be derived from the results of the culpable vehicles in multi-vehicle crashes group using the same logic and formula as the ‘All Crashes’ group above, with

x_t = the number of culpable vehicles in multi-vehicle crashes

θ_t = the estimated effectiveness for culpable vehicles in multi-vehicle crashes

Because all of the control group crashes are multi-vehicle crashes, and because all multi-vehicle crashes in the data files are contained in either the control group or in the culpable vehicles in multi-vehicle crashes group, this will give an estimate of effectiveness in all multi-vehicle crashes.

Included Vehicles - ESC is often offered as an optional feature whose presence is impossible to determine from the vehicle identification number (VIN). Accordingly, only vehicle models that transitioned from no ESC to standard ESC could be included in the analysis. Eligible vehicles were identified using previous NHTSA analyses, www.safercar.gov, and information provided by vehicle manufacturers. The two model years before and the two model years after the introduction of ESC were included when possible. In cases where a major vehicle redesign took place during this period, the included model years were truncated to ensure that only similar vehicles were compared. In some of the more recent models, rollover sensors were introduced and present a potential confound for analyses of rollover crashes. For these vehicles, model years were truncated in analyses including rollover crashes so that the presence of rollover sensors was consistent across all included model years. Some vehicle models are included that had a period of time that ESC was offered as an option; these optional model years are removed.

RESULTS

All Police-Reported Crashes - NASS GES data files from 1997-2009 were used to estimate the effectiveness of preventing vehicle involvement in treatment group crashes of any severity. This data is compiled annually from a nationally representative probability sample of every police reported crash in the U.S. Although many crashes are not reported to police, unreported crashes are unlikely to involve significant personal injury or major property damage.

There are 8040 total NASS GES cases included in this analysis taken from thirteen years of crash data

files. NASS GES data is available at three different levels, the crash level, the vehicle level, and the

occupant level. Crash types were assigned to each vehicle case in the vehicle level data using variables at the crash and vehicle levels. Analysis was conducted using SAS PROC SURVEYLOGISTIC to properly specify the survey design.

The results for each analyzed crash category are given in Table 2 below. The reported statistics are: unweighted and weighted risk ratios (see section 2.1 for an explanation of how risk ratios are computed from the crash data), 95 percent confidence intervals

100]. Any estimate with a 95 percent confidence interval whose upper and lower bounds are both less than 1.000 is statistically significant at the $p < .05$ level and is marked with an asterisk.

The unweighted risk ratio estimates are not nationally representative, but are reported because they can lend insight into the reliability of the weighted estimates.

for the weighted risk ratios, and percent effectiveness derived from the weighted risk ratio $[(1 - \text{risk ratio})^*]$

Crash Type	Risk Ratio (Unweighted)	Risk Ratio (Weighted)	95% CI (Wald)	Weighted % Effectiveness
Table 2.				
ESC Effectiveness in All Police-Reported Crashes (NASS GES)				
All Vehicles				
All crashes				
All non-convicted				
All single vehicle				
ped/bikes				
1 st event rollovers	.295	.332	(.223, .494)	67%*
All impacts w/ fixed obj.	.513	.424	(.342, .525)	58%*
Side impacts w/ fixed obj.	.372	.29	(.187, .449)	71%*
All multi-vehicle †	.979	1.003	(.974, 1.035)	0%
Culpable multi-vehicle	.924	1.011	(.901, 1.134)	-1%
Peds/Bikes/Animals	1.057	.955	(.681, 1.340)	4%
* = statistically significant at $p < .05$				
† = derived estimate, see METHODS, All Crashes				

Large differences between estimates based on the unweighted and weighted

data are often a symptom of insufficient sample size. This does not appear to be a problem with this data, as weighted and unweighted estimates do not differ substantially.

All of the single-vehicle crash categories showed large significant decreases in crash risk for ESC equipped vehicles. These decreases were particularly large for the crash types hypothesized to be affected most by vehicle control and stability: first- event rollovers (67% reduction) and side impacts with fixed objects (71% reduction). The results for multi-vehicle crashes and for collisions with pedestrians, bicyclists or animals are less clear. These estimates are close to zero effect and have large confidence intervals.

All Police-Reported Crashes (Passenger Cars) - When passenger cars were analyzed separately, there were too few cases to obtain significant estimates for most of the crash types. The only significant results were a 60 percent reduction in side impacts with fixed objects and a 72 percent reduction in first-event rollovers. Because small sample sizes lead to large confidence intervals, only very large estimates will be statistically significant. The point estimates for other crash types, while not significant, are similar to the combined results.

Table 3.
ESC Effectiveness in All Police-Reported Crashes (Passenger Cars Only)

Crash Type (PC Only)	Risk Ratio (Unweighted)	Risk Ratio (Weighted)	95% CI (Wald)	Weighted % Effectiveness
All crashes †	.92	.952	(.865, 1.067)	5%
All non-control group	.825	.881	(.666, 1.166)	12%
All single vehicle (except ped/bikes/animals)	.652	.677	(.452, 1.013)	32%
1 st event rollovers	.347	.278	(.090, .857)	72%*
All impacts w/ fixed obj.	.683	.696	(.451, 1.074)	30%
Side impacts w/ fixed obj.	.467	.397	(.192, .818)	60%*
All multi-vehicle †	.966	1.008	(.936, 1.104)	-1%
Culpable multi-vehicle	.884	1.028	(.750, 1.407)	-3%
Peds/Bikes/Animals	.990	.767	(.456, 1.291)	23%
* = statistically significant at p < .05				
† = derived estimate, see section 2.2				

The only non-

All Police-Reported Crashes (LTVs) - LTVs have a larger sample size and when analyzed separately from passenger cars the estimated reductions in loss-of-control crashes were all large and significant.

significant crash types were collisions with pedestrians, bicyclists or animals and multi-vehicle crashes.

Table 4.
ESC Effectiveness in All Police-Reported Crashes (NASS GES) Light Trucks and Vans Only

Crash Type (LTV Only)	Risk Ratio (Unweighted)	Risk Ratio (Weighted)	95% CI (Wald)	Weighted % Effectiveness
------------------------------	--------------------------------	------------------------------	----------------------	---------------------------------

All crashes †	.912	.933	(.898, .972)	7%*
All non-control group	.800	.836	(.750, .932)	16%*
All single vehicle (except ped/bikes/animals)	.455	.432	(.364, .512)	57%*
1 st event rollovers	.309	.359	(.239, .541)	64%*
All impacts w/ fixed obj.	.436	.332	(.263, .418)	67%*
Side impacts w/ fixed obj.	.332	.268	(.162, .445)	73%*
All multi-vehicle †	.979	1.003	(.972, 1.037)	0%
Culpable multi-vehicle	.923	1.011	(.894, 1.143)	-1%
Peds/Bikes/Animals	1.075	1.013	(.709, 1.013)	-1%
* = statistically significant at p < .05				
† = derived estimate, see section 2.2				

There are a couple of interesting observations to be made about the results for PCs and LTVs. In the 2007 NHTSA analysis, LTV's showed much larger effectiveness estimates than passenger cars. In this analysis the results seem much more similar across vehicle type. There could be a variety of reasons for this, such as improved stability in later models of

LTV's, inclusion of more compact utility vehicles (CUV's) in the LTV group, inclusion of more non-luxury models of passenger cars, and others. More detailed analysis did not reveal any one specific cause for the increased similarity of effectiveness across cars and LTV's.

Fatal Crashes - The effect of ESC on fatal crashes was estimated using data in 1997-2009 Fatal Analysis Reporting System (FARS). The same vehicle models that were used in the NASS GES analysis were used

here as well. This analysis included 6,172 vehicle cases from the FARS database.

Table 5.
ESC Effectiveness in All Fatal Crashes
All Vehicles

Table 5 presents the counts of vehicle cases, risk ratios, 95 percent confidence intervals for the risk ratios, and percent effectiveness estimates for each crash category. The confidence intervals were computed with SAS PROC FREQ, which uses the Cochran-Mantel-Haenszel (CMH) method of interval construction.

Crash Type	Vehicles w/o ESC	Vehicles w/ ESC	Risk Ratio	95% CI (CMH)	% Effectiveness
<i>Count of control crashes</i>	1477	787			
All crashes †	4296	1876	.82	(.77, .875)	18%*
All non-control group	2819	1089	.725	(.649, .81)	27%*
All single vehicle (except ped/bikes/animal)	1294	348	.505	(.436, .584)	49%*
1 st event rollovers	502	76	.284	(.22, .367)	72%*
All impacts w/ fixed obj.	648	212	.614	(.514, .733)	39%*
Side impacts w/ fixed obj.	152	34	.42	(.287, .615)	58%*
All multi-vehicle †	2384	1192	.939	(.895, .988)	6%*
Culpable multi-vehicle	907	405	.84	(.725, .969)	16%*
Peds/Bikes/Animals	415	242	1.094	(.914, 1.311)	-9%
* = statistically significant at p < .05					
† = derived estimate, see section 2.2					

Estimates of ESC effectiveness at preventing fatal single-vehicle crashes (excluding collisions with animals, bicycles, or pedestrians) are very similar to the results of the analysis of all police-reported crashes. This is not a surprising result, since single-vehicle crashes are likely to be loss-of-control crashes that occur at high speeds, regardless of whether they are fatal or not. In other words, one would expect

fatal single-vehicle crashes to be fairly representative of single-vehicle crashes in general.

For the single-vehicle crashes the results are clear; ESC is highly effective at preventing fatalities from these types of crashes. These estimates also show narrow confidence intervals, indicating small variance and low volatility. The reduction for all non-control crashes (27%) is also impressively large considering the variety of crashes included in this category.

These results are very similar to the effectiveness estimates for the same crash types reported in the 2007 NHTSA evaluation using FARS data from 1997-2004, however a detailed comparison will not

be given because statistical concerns make direct contrasts inappropriate.

Although there are some noticeable differences in the NASS GES and FARS estimates of the effects on collisions with pedestrians, bicyclists or animals and the culpable involvements in multi-vehicle crashes, these estimates are not statistically significant

Crash Type (PCs)	Vehicles w/o ESC	Vehicles w/ ESC	Risk Ratio	95% CI (CMH)	% Effectiveness
<i>Count of control crashes</i>	177	174			
All crashes [†]	656	495	.768	(.657, .911)	23%*
All non-control group	479	321	.682	(.53, .878)	32%*
All single vehicle (except ped/bikes/animal)	253	125	.503	(.373, .678)	50%*

regardless of data source and interpretation of ESC effectiveness in

these types of crashes will be deferred until sufficient data is available.

Fatal Crashes (Passenger Cars) - The results for passenger cars are very similar to the overall results. Although the reduction in culpable vehicles in multi-vehicle accidents is slightly larger, the sample size is smaller and the reduction is still non-significant. Despite the reduced sample size, the single vehicle

crash categories and group give statistical reduction.

Table 6.
ESC Effectiveness in All Fatal Crashes
Passenger Cars Only

1 st event rollovers	49	21	.436	(.251, .757)	56%*
All impacts w/ fixed obj.	170	89	.533	(.387, .742)	47%*
Side impacts w/ fixed obj.	49	17	.353	(.196, .637)	65%*
All multi-vehicle [†]	333	299	.916	(.81, 1.055)	8%
Culpable multi-vehicle	156	125	.815	(.595, 1.117)	18%
Peds/Bikes/Animals	45	48	1.085	(.687, 1.714)	-9%
<i>Total number of cases</i>	656	495			
* = statistically significant at p < .05					
† = derived estimate, see section 2.2					

The analysis of passenger car involvements by crash type shows large reductions across crash types, consistent with previous effectiveness analyses. The 23 percent effectiveness estimate for all crashes suggests that nearly a quarter of all fatal crashes in passenger cars may be prevented by adding ESC.

Fatal Crashes (LTV's) - LTV's also show large significant reductions in fatalities. This is the only analysis that showed a significant reduction in culpable multi-vehicle crashes. The only crash category that did not show a significant reduction was collisions with pedestrians, bicyclists or animals, which showed an 11 percent non-significant increase.

Crash Type (LTVs)	Vehicles w/o ESC	Vehicles w/ ESC	Risk Ratio	95% CI (CMH)	% Effectiveness
<i>Count of control crashes</i>	1300	613			
All crashes [†]	3640	1381	.805	(.752, .865)	20%*

Table 7.
ESC Effectiveness in All Fatal Crashes (FARS)
Light Trucks and Vans Only

All non-control group	2340	768	.696	(.614, .79)	30%*
All single vehicle (except ped/bikes/animal)	1041	223	.454	(.382, .54)	55%*
1 st event rollovers	453	55	.258	(.192, .346)	74%*
All impacts w/ fixed obj.	478	123	.546	(.438, .68)	45%*
Side impacts w/ fixed obj.	103	17	.35	(.208, .59)	65%*
All multi-vehicle [†]	2051	893	.923	(.888, .976)	8%*
Culpable multi-vehicle	751	280	.791	(.669, .935)	21%*
Peds/Bikes/Animals	370	194	1.112	(.912, 1.356)	-11%
<i>Total number of cases</i>	3640	1381			
* = statistically significant at p < .05					
† = derived estimate, see section 2.2					

FARS data is the most comprehensive and accurate fatal-crash data available, and this evaluation and others have shown that this data supports the assertion that ESC has a major impact on vehicle safety. The estimates derived from this data suggest that the inclusion of ESC on all new vehicles in the United States by MY 2012 will save thousands of lives every year due to prevention of fatal loss of control crashes.

In general the results for fatal crashes do not seem to differ greatly from the results for all police-reported crashes. Because ESC is designed to prevent high-speed loss-of-control crashes, which are likely to be fatal, this is not a surprising result.

DISCUSSION

In many ways, ESC is an ideal crash avoidance technology. Because it acts so quickly and without driver input it can prevent a crash without the driver of the vehicle being aware that the system has intervened. Most importantly, it has been shown by this analysis and several others, using a variety of methods, to be highly effective at preventing loss-of-control crashes.

By using NASS GES data this evaluation was able to compute nationally representative estimates of ESC effectiveness on crash involvements. This will be a valuable tool in attempts to predict the broad economic and safety related effects that ESC will have in the future.

Although the results of this analysis and others are very encouraging, it is important to consider any possible disbenefits associated with ESC. There have been no statistically significant increases in any crash type associated with the introduction of ESC. However, small, non-significant increases in the incidence of collisions with pedestrians, bicyclists and animals were observed in this study (FARS only, not GES) and in the 2007 NHTSA evaluation. Because these effects seem to be very small, if they do indeed exist, there is not yet enough data for statistically meaningful results. While this report draws no conclusions about pedestrian crashes, NHTSA plans to keep this category on the “watch” list and repeat the analyses when more data are available. It may also be useful to examine individual cases more closely in order to explore the effects, if any, of ESC on these types of crashes.

REFERENCES

[1]Dang, J. (2007) *Statistical Analysis of the Effectiveness of Electronic Stability Control (ESC)*

Systems – Final Report, NHTSA Technical Report
No. DOT HS 810 794, Washington, D.C.

[2] Evans, L. (1986). Double Pair Comparison - A
New Method to Determine How Occupant
Characteristics Affect Fatality Risk in Traffic
Crashes, *Accident Analysis and Prevention*, Vol. 18,
pp. 217-227.

EFFECT OF SIDE IMPACT PROTECTION IN REDUCING INJURIES

Helena Stigson (1)

Anders Kullgren (1, 2)

1) Folksam Research, Stockholm, Sweden

2) Department of Applied Mechanics, Vehicle Safety Division, Chalmers University of Technology, Göteborg, Sweden.

Paper Number 11-0319

ABSTRACT

The aim of this study was to identify risk factors in side impact. In particular risk factors such as kerb weight of striking/struck passenger car, age, gender, the presence of a front-seat occupant and side airbags influence the injury outcome. The Swedish database STRADA was used to analyze and identify risk factors in side impact crashes. All near-side front seat occupants in car-to-car side impacts reported by the police from year 2003 to 2009 were included (n=3360). The severity classification made by the police was used to compare the injury risk. Pair comparison technique was used to study the relative risk between the driver in the striking car and the near-side occupant in the struck car. The higher kerb weight of the striking passenger car, the higher risk of being severely injured in the struck passenger car. The opposite relation was found regarding the kerb weight of struck passenger car. Being senior or having a passenger beside in a side impact means a higher risk of sustaining serious injuries. Current side airbag systems, such as torso bags with or without head curtains, reduce the injury risk in side impact for near-side occupants.

INTRODUCTION

Side impact crashes stand for higher risk for the occupants than front and rear collisions. A driver involved in a side impact has twice as high fatality risk as driver involved in frontal impacts (Farmer et al., 1997). A typical side impact crash occurs at relatively low speed. However, the sides of a passenger car have a limited ability to absorb energy in crashes and therefore side impact crashes are already critical at relatively low change of velocity (ΔV). The fatality risk rapidly increases at ΔV 40 km/h and above (Sunnevang et al., 2009). There are many factors that affect the risk of sustaining injuries in a side impact crash. As in all crash situations it is a balance between crash severity, vehicle factors as well as human injury tolerance. Farmer et al (1997) have pointed out that it is favorable to be an occupant of a heavier vehicle than a occupant in a light weighted vehicle in a side impact. No influence of the striking vehicle's kerb weight was found. Furthermore, occupants in passenger cars are more likely to sustain severe injuries when the striking vehicle is a pickup truck

or sport utility vehicle (SUV) than in a car-to-car crash.

Near-side occupants are at higher risk than far-side occupants and account for more than 70 percent of all side impact injuries (Laberge-Nadeau et al., 2009). The risk of severe or fatal injuries is more than twice as high for a near-side occupant than for a far-side. Recently, occupant-to-occupant interaction has been identified as a risk factor. Newland et al (2008) have shown that a driver with a front seat passenger present has a higher risk than a driver without a passenger. It is known from previous studies that both age and gender influence the risk of being fatally injured in a car crash (Bedard et al., 2002). In particular, age and fatality risk are strongly correlated with each other (Braver and Trempe, 2004, Augenstein et al., 2005). In side impact crashes senior drivers are more than three times as likely as non-senior to be severely injured. Sunnevang et al (2009) have shown that senior drivers are killed at lower crash severity than non-senior in side impact. Furthermore, it is well-known that senior driver are overrepresented in intersection crashes (Braver and Trempe, 2004).

Since sides of passenger car have a limited ability to absorb energy in crashes, car manufacturers have worked hard to introduce different side impact protection systems. It has been both enforced structures in the doors and B-pillars, but also involving the mid section of the car, such as the Volvo SIPS (Jakobsson et al., 2010). But to date most cars are fitted with side airbags of different kinds. Side airbags were introduced on the market around 1994 and today they are more or less standard among new cars. The side airbag's performance has improved from just protecting the torso to also provide head protection. The benefits of the systems have been proved in crash tests as well as analysis of real-life data. In general cars have been safer during the last 20 years (Kullgren et al., 2009, Farmer and Lund, 2006). However, the improvements in vehicle design differ depending on crash type. A study made by IIHS shows that between 1980 and 2000, the overall car driver death rate in cars 1-3 years old decreased by almost 50% in the United States (Laberge-Nadeau et al., 2009). The improvement for frontal crashes was higher than for side impact crashes (52% compared to 24%). However, Volvo has proved that

improvement of the side impact protection has resulted in an overall injury reduction of more than 70 percent (Jakobsson et al., 2010). This is an effect of both structural changes as well as introduction of new systems as torso airbags and head protection curtains. The structural changes have not been studied separately. Recent studies in the USA have also shown that side airbags, protecting head and chest, are saving lives in side impacts. Side airbags reduce the risk of fatal injury by up to 37 percent (McCartt and Kyrychenko, 2007). However, Teoh and Lund (2011) recently show that fatality within the group of cars fitted with side airbag differ. A significant lower fatality rate was found for drivers of cars that performed good in IIHS side impact crash test than for drivers of cars that performed poorly.

The present paper aims to analyze different risk factors in side impact crashes. In particular risk factors such as kerb weight of striking/struck passenger car, age, gender, the presence of a front-seat occupant and of side airbags influence the injury outcome.

METHOD AND MATERIAL

The Swedish database STRADA (Swedish Traffic Accident Data Acquisition) include police-reported crashes was used to study the different risk factors in side impacts. All near-side front seat occupants in side impacts reported by the police from year 2003 to 2009 were included, in total 3360 crashes. Only car-to-car crashes with front-seat occupants 18 years old and above were selected as well as car manufactured in 1997 or later. The side impacts were selected by using the deformation classification made by the police (for driver vehicular damage on the left aspect of the car and for passenger vehicular damage on the right aspect of the car). Multiple event crashes were excluded. Furthermore, the identification number that Swedish Transport Administration assigns each car model was used to identify if the included cars were fitted with side airbag protection or not.

The dataset was divided into different groups to study effectiveness of side impact protection, influence of age, presence of another front-seat occupant, posted speed limit and kerb weight of the

striking and struck passenger car. To study the influence of age the dataset was divided into two subgroups; senior drivers (age 60 years and above, $n=655$) and non-senior drivers ($n=2711$). In 760 cases a front seat passenger accompanied the driver. The injury rate in these cases was compared with the rest of the crashes to study if the presence of a front-seat occupant influences the risk of being injured. Furthermore, the dataset was divided into two groups; crashes on roads with a posted speed limit under 70km/h and roads with a posted speed limit of 70km/h or above. The severity classification made by the police (non-injured, minor, serious, and fatal) was used to compare the injury outcome between the different subgroups. Fisher's exact test was used to analyze whether there was a difference in proportions of injuries between the categories (age, presence of a front-seat occupant, posted speed limit). In all analyses 95 percent confidence intervals (CIs) were used, and p-values from Fisher's exact tests were calculated using PASW 18.0 (<http://www.spss.com>).

To study effectiveness of side impact protection and influence of kerb weight on injury risk car-to-car crashes with known injury severity in both the striking and struck passenger car was selected, in total 1767 crashes. Pair comparison technique was used to study the relative risk between the driver in the striking passenger car and the near-side occupant in the struck passenger car (Hägg et al., 1992, Evans, 1991). Using a pair comparison makes it possible to control for crash severity. According to Evans (1986), the relative injury risk was calculated with paired comparisons. The relation of injuries for struck car and striking car is given in table 1. To study effectiveness of side airbags the data was divided into two groups; cars with ($n=1263$) and cars without ($n=435$) side airbags, table 2. Both torso bags with or without head curtains were included in the group with side airbags. Car models with optional status of side airbag were included in the group without side airbag. Seventy-nine cases were excluded since it was not possible to identify if car was fitted with airbag or not. In 1909 crashes data about kerb weight as well as the injury outcome in both the striking and struck passenger car were known.

Table 1. Categorization of crashes to be used in the paired comparisons

		<i>Drivers in the striking car</i>		Total
		drivers injured	drivers not injured	
<i>Near-side occupant in the struck car</i>	Near-side occupant injured	x_1	x_2	$x_1 + x_2$
	Near-side occupant not injured	x_3	x_4	
Total		$x_1 + x_3$		

x_1 = number of crashes with injured drivers/occupants in both cars

x_2 = number of crashes with injured drivers/occupants in the struck car and not in the striking car

x_3 = number of crashes with injured drivers in the striking car and not in the struck car

x_4 = number of crashes with no injured drivers/occupants in both cars

The risk ratio was calculated according to Eq. 1.

$$R = p_1 / p_2 = (x_1 + x_2) / (x_1 + x_3) \quad (1)$$

p_1 = injury risk in struck cars, p_2 = injury risk in striking cars

Risk ratio was calculated for the two groups; cars with and cars without side airbags. Confidence intervals were calculated using the Eq. 2.

$$V(R) = (p_1^* / p_2^*)^2 \left(\frac{1 - p_1^*}{x_1 + x_2} + \frac{1 - p_2^*}{x_1 + x_3} \right) \quad (2)$$

where p_1^* / p_2^* is estimated by R, while p_1^* and p_2^* must be chosen arbitrarily (Hägg et al., 1992). In this study p_2^* was chosen as 0.7 and $p_1^* = R * p_2^*$.

Table 2. Distribution of age, mean kerb weight for striking and struck passenger car

Mean	Without side airbag (n=435)	With side airbag (n=1263)
Age	45	46
kerb weight, struck car (kg)	1370	1490
kerb weight, striking car (kg)	1290	1390
mass ratio (μ)	1,06	1,07

Influence of car mass difference on injury outcome

The relation between the number of crashes with injured drivers/occupants in both passenger cars and the number of crashes with injured near-side occupant in the studied passenger car is a measure of the injury risk in the other passenger cars. The injury risk in car 2, p_2 , can therefore be estimated as the relation $x_1 / (x_1 + x_2)$. Assuming that for every car 1 studied, its colliding partners, car 2, would be of equal design, mass and structure, p_2 would be identical in every case. Similarly the injury risk in car 1, p_1 , can be estimated by the relation $x_1 / (x_1 + x_3)$.

The difference in the estimated p_2 and p_1 will differ depending on the influence of three factors; mass, aggressivity related to the structure and crash severity. By selecting passenger cars of different mass categories and where the structural aggressivity and crash severity could be regarded as equal it is possible to calculate the mass factor.

The cars were categorized in 200 kg intervals and the estimates of p_2 and p_1 were calculated for each comparison of mass categories. Both the kerb weight for the striking and the struck passenger car was divided in to the following categories: <1250,

≥ 1250 to < 1450 , ≥ 1450 to < 1650 and ≥ 1650 kg, table 3. The correlation between mass ratio and the estimates of p_2 and p_1 was used to study the influence of mass on injury risk in both striking and struck passenger cars. Mass factors were calculated to be used to adjust for the influence on mass on injury risk in the striking passenger car in the comparison between categories. The adjustment has to be made in order to compare the car groups studied to striking cars with identical average masses. The adjustment was made by applying a power function curve fit and reduce the power with a factor relating to half of the total influence of mass on relative injury risk, equal to the influence on the striking car group.

Table 3. Kurb weight distribution for striking and struck passenger car

Kurb weight (kg)	Struck car (n)	Striking car (n)
<1250	363	517
1250 - <1450	473	525
1450 - <1650	565	456
>1650	366	269
Total	1767	1767

RESULTS

The influence of mass differences on injury risk in striking and struck car groups seems to be of similar order, Fig 1. The reduction in risk for the struck car, p_1 , at increased mass ratio is similar as the increase in risk for the striking car, p_2 .

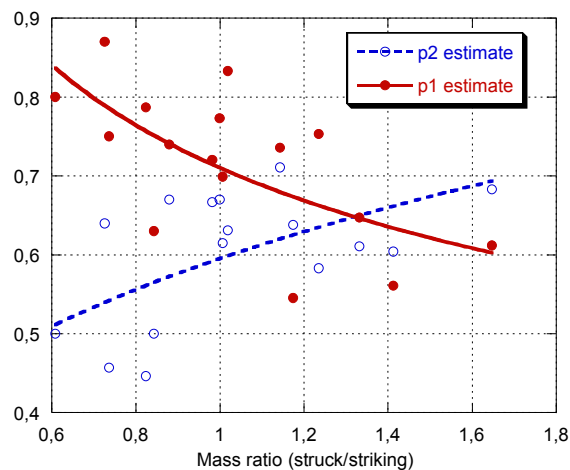


Figure 1. Relation between estimates of injury risk in the struck, p_1 , and striking cars, p_2 , at various mass ratios.

Higher kerb weight of the striking passenger car increased the relative risk of being seriously injured in the struck passenger car. The opposite relation was found with increasing kerb weight of the struck passenger car. Furthermore, a higher the mass ratio

(μ) was favorable for the struck passenger car. Figure 2 and 3 shows the relation between mass ratio and relative risk of all injury and serious injury and fatal respectively for the mass ratios studied. The figure also shows the calculated mass factors for the two injury categories studied. According to the equations found the measured relative risk should be reduced at low mass ratios and increased at high mass ratios. For all injuries the mass factor is $1.163 \mu^{-0.3355}$, and for fatal and serious it is $1.013 \mu^{-1.314}$.

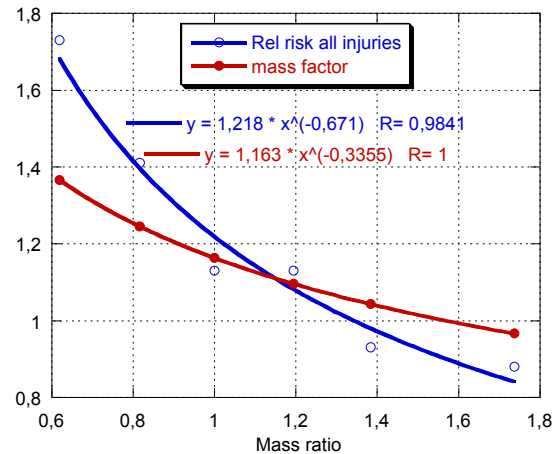


Figure 2. Correlation between relative risk for all injuries and mass ratio between struck and striking car, and calculated mass factor to be used for adjustment of measured injury risk.

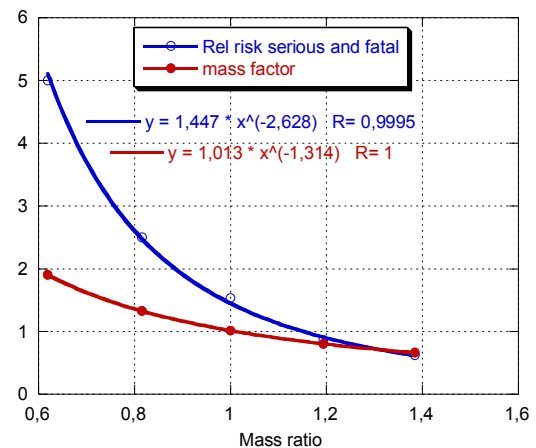


Figure 3. Correlation between relative risk for fatal and serious injuries and mass ratio between struck and striking car, and calculated mass factor to be used for adjustment of measured injury risk.

The risk of sustaining injury in a side impact was lower in a passenger car fitted with side airbags (Risk ratio 1.13, CI 1.078-1.182, Appendix table 1 and 3), protecting head and chest, than in a car without these systems (Risk ratio 1.28, CI 1.194-1.366, Appendix table 2 and 4). The relative injury

risk in car-to-car crashes, calculated with paired comparisons, indicates a risk reduction of almost 30 percent between the two groups: passenger car fitted with side airbags, protecting head and chest, and car without these systems. Also far-side occupants were found to have a positive effect of the side airbags.

The age influences the injury risk. Senior car occupants (age 60 years and above) had a significantly higher risk of sustaining serious injuries (26% higher risk in a car-to-car crash). Furthermore, the presence of a front-seat occupant influences the risk of being seriously injured irrespective of side protection system. An occupant besides you in a side impact means up to 45 percent higher risk of being injured. A significantly higher proportion of serious injuries occurred on roads with a speed limit of 70 km/h or above. The exposure for gender was similar except from that female occupants were more likely to sustain minor injuries.

DISCUSSION

The risk of being injured in a side impact is influenced by so many risk factors that it is impossible to identify the importance of just a single one. The present study shows that the absence of side airbags, the occupant's age, the presence of a front-seat occupant and kerb weight of both the striking and struck passenger car all influence the risk of being injured in a side impact crashes. Simultaneously as car manufacturers installed side airbag they also introduced structural innovations that in general improved the side impact protection. These improvements also influenced the kerb weight of the passenger cars. The mean weight of passenger cars with side airbags was 120 kg more than a passenger car without side impact protection. The result from the present study shows that it is favorable in a car-to-car crash if the struck passenger car was heavier than the striking. Furthermore, the fact that the far-side occupant have a positive effect of the side airbags indicate that passenger cars fitted with side airbags in general have a higher safety level.

Near-side occupants are at higher risk than far-side occupants and account for more than 70 percent of all side impact injuries. It is therefore natural that the car manufactures have had focus on side protection systems for the near-side occupant. Result from the present study shows that an occupant beside in a side impact means up to 45 percent higher risk of being injured. Newland et al (2008) have shown from both real-life data and crash tests that occupant-to-occupant interaction in side impact crashes can cause injuries. They found that the relative risk for sustaining severe injuries

(MAIS3+) was 8% higher for the near-side occupant in cases where a belted far-side was present than without a far-side occupant. An even higher risk (30%) was found in cases with an unbelted far-side occupant beside the driver. These results together point out that there is a need to develop some type of protection system that minimize the occupant-to-occupant interaction.

Senior drivers have particularly higher risk than non-senior drivers. These findings represent both crashes with and without airbag. Furthermore, it was expected that senior drivers would have a higher injury risk than non-seniors. Previous studies have shown that senior drivers are more likely to be severely injured (Sunnevång et al., 2009, Braver and Trempel, 2004, Farmer et al., 1997). However, little have been done to invent side impact protections that comply with different needs for non-senior and senior occupants.

It is known from previously studies that the effectiveness of side airbag is high in fatal crashes (Braver and Kyrychenko, 2004, McCart and Kyrychenko, 2007). This study indicates that the side airbag also reduce the number of injured occupants in car-to-car crashes. However, it was not possible to see any reduction of severe injures. The Swedish national database included very few seriously injured occupants in side-impact crashes during the 2003-2009 and therefore it was not possible to estimate the true effectiveness of the side airbag. Side airbag became widely available in car models manufactured after 1998 and in recent years there has been a growing trend among car manufactures to offer side airbag protection as standard. It is therefore a higher proportion of cars fitted with side airbags as standard included in the present study (74% of the total number). Data from USA shows that 79% of 2006 passenger car models had side airbag as standard (45%) or optional (34%) equipment (McCart and Kyrychenko, 2007). The Swedish national database included very few numbers of crashes involved cars manufactured in 1997 or later without side airbags. One possible method to increase the number would have been to extend the model year for the included cases. However, the authors did not change the inclusion criteria. The reason for this is that car safety have improved a lot during the last 20 years (Kullgren et al., 2009, Farmer and Lund, 2006). By including cars manufactured before 1997 would rather reflect other differences.

Teoh and Lund (2011) recently showed that fatality risk within the group of cars fitted with side airbag differ. A significant lower fatality rate was found for drivers of cars that performed good in IIHS side impact crash test than for drivers of cars that performed poorly. The result in this study might

have been influenced of the fact that different airbag design effect the fatality risk differently in side impact crashes. It is likely to believe that cars performing well in IIHS side impact crash test would have had a lower injury risk than the total injury reduction for side airbag system. In the present study different types of airbag systems including torso-only, torso-head (combination bag), torso-curtain or, inflatable tubular curtain were all included in the same group. Out of 1263 crashes where the car was fitted with side airbag, a majority were torso-curtain side airbags (69%). Due to the low number of crashes with serious injuries it was not possible to study the side airbag effectiveness for torso bags and head curtains separately.

Assuming a positive correlation between posted speed limit and impact speed it is natural that a higher proportion of serious injuries occurred on roads with a speed limit of 70km/h or above. Studies have shown that the posted speed limit strongly influences the impact speed and increases the risk of injury (Ydenius, 2009, Stigson, 2009). To minimize the injury outcome in side impact crashes it is therefore recommended to limit the posted speed limit and even better redesign the infrastructure. Road design solutions such as roundabouts have been shown to dramatically reduce the number of crashes resulting in injuries (by up to 80%) at intersections compared with traditional intersection designs (Persaud et al., 2001, De Brabander and Vereeck, 2007).

Limitations

There is a strong correlation between change of velocity and risk of injury (Kullgren, 1998, Gabauer and Gabler, 2006, Gabauer and Gabler, 2008). Using a pair comparison makes it possible to control for crash severity. It is therefore not necessary to have the impact severity in terms of change of velocity (ΔV) or compartment intrusion in each case. To evaluate the effect of a side airbag the injury risk for the driver in the striking car was compared with the risk of serious injuries in the struck car. This comparison was used since it is likely that the driver of the striking passenger car got a lower risk to sustaining severe injuries than the occupant in the struck car.

The study is based on police reported data. The study was therefore limited to analyses based on only injury severity classified by the police. It is known that the severity of crashes assigned by the police at the accident scene, i.e. whether those involved are considered seriously or slightly injured, is mainly based on whether the injured person is expected to be admitted to hospital or not. The classification of injury severity only gives a rough picture of the true severity of the injury (Farmer, 2003). Furthermore, it is a weakness that it

is unknown which type of injury the occupant got. The highest risk of serious injury is to the torso and the head and the side airbags are mainly design to reduce thorax and head injuries. It would therefore be more accurate to focus only on injuries to these two body region.

Previous studies have point out that driver of cars with side airbags probably are of higher socio-economic status because these cars are more costly. Travel patterns and driver behaviors such as speeding, influence of alcohol and seat belt vary systematically by socioeconomic status (Braver, 2003). Thereby drivers of cars with side airbags could have a lower likelihood of being in a serious crash. McCartt A. and Kyrychenko have adjusted for these potentially confounding factors by using frontal and rear end crashes. This has not been taken into consideration in the present study.

CONCLUSION

- The higher kerb weight of the striking passenger car, the higher risk of being seriously or fatally injured in the struck passenger car. The opposite relation was found regarding the kerb weight of struck passenger car.
- Being senior or having an occupant besides you in a side impact means a higher risk of sustaining serious or fatal injuries.
- Current side airbag systems, such as torso bags with or without head curtains, reduce the injury risk in side impact for near-side occupants.

ACKNOWLEDGEMENTS

The study was a part of a side impact project conducted during 2009 and 2010. The project was financially supported by the VINOVA (FFI program Ref: 2009-00507).

REFERENCES

- AUGENSTEIN, J., DIGGES, K., BAHOUTH, G., DALMOTAS, D., PERDECK, E. and STRATTON, J. 2005. Investigation of the Performance of Safety Systems for Protection of the Elderly. *49th Annual Proceedings of the Association for the Advancement of Automotive Medicine*. Barrington, IL.
- BEDARD, M., GUYATT, G. H., STONES, M. J. and HIRDES, J. P. 2002. The independent contribution of driver, crash, and vehicle characteristics to driver fatalities. *Accid Anal Prev*, 34, 717-27.

- BRAVER, E. R. 2003. Race, Hispanic origin, and socioeconomic status in relation to motor vehicle occupant death rates and risk factors among adults. *Accid Anal Prev*, 35, 295-309.
- BRAVER, E. R. and KYRYCHENKO, S. Y. 2004. Efficacy of side air bags in reducing driver deaths in driver-side collisions. *American Journal of Epidemiology*, 159, 556-64.
- BRAVER, E. R. and TREMPPEL, R. E. 2004. Are older drivers actually at higher risk of involvement in collisions resulting in deaths or non-fatal injuries among their passengers and other road users? *Inj Prev*, 10, 27-32.
- DE BRABANDER, B. and VEREECK, L. 2007. Safety effects of roundabouts in Flanders: signal type, speed limits and vulnerable road users. *Accid Anal Prev*, 39, 591-9.
- EVANS, L. 1986. Double pair comparison – a new method to determine how occupant characteristics affect fatality risk in traffic crashes. *Accid. Anal. and Prev.*, Vol. 18, pp 217-227.
- EVANS, L. 1991. *Traffic Safety and the Driver* New York, Van Nostrand Reinhold.
- FARMER, C. M. 2003. Reliability of police-reported information for determining crash and injury severity. *Traffic Inj Prev*, 4, 38-44.
- FARMER, C. M., BRAVER, E. R. and MITTER, E. L. 1997. Two-vehicle side impact crashes: the relationship of vehicle and crash characteristics to injury severity. *Accid Anal Prev*, 29, 399-406.
- FARMER, C. M. and LUND, A. K. 2006. Trends over time in the risk of driver death: what if vehicle designs had not improved? *Traffic Inj Prev*, 7, 335-42.
- GABAUER, D. J. and GABLER, H. C. 2006. Comparison of delta-v and occupant impact velocity crash severity metrics using event data recorders. *Annu Proc Assoc Adv Automot Med*, 50, 57-71.
- GABAUER, D. J. and GABLER, H. C. 2008. Comparison of roadside crash injury metrics using event data recorders. *Accid Anal Prev*, 40, 548-58.
- HÄGG, A., KAMRÉN, B., V KOCH, M., KULLGREN, A., LIE, A., MALMSTEDT, B., NYGREN, A. and TINGVALL, C. 1992. *Folksam Car Model Safety Rating 1991-92*, Stockholm, Folksam, 106 60 Stockholm, Sweden, ISBN 91-7044-132-4.
- JAKOBSSON, L., LINDMAN, M., SVANBERG, B. and CARLSSON, H. 2010. Real World Data Driven Evolution of Volvo Cars' Side Impact Protection Systems and their Effectiveness. *Ann Adv Automot Med*, 54, 127-36.
- KULLGREN, A. 1998. *Validity and Reliability of Vehicle Collision Data: Crash Pulse Recorders for Impact Severity and Injury Risk Assessments in Real-Life Frontal Impacts*. Ph.d Thesis for doctoral degree (PhD), Karolinska Institutet, Folksam Research.
- KULLGREN, A., LIE, A. and TINGVALL, C. 2009. Översiktlig beräkning av trafiksäkerhetsnyttan av utskrotning av äldre bilar. Stockholm: Folksam, S23 106 60.
- LABERGE-NADEAU, C., BELLAVANCE, F., MESSIER, S., VEZINA, L. and PICHETTE, F. 2009. Occupant injury severity from lateral collisions: a literature review. *J Safety Res*, 40, 427-35.
- MCCARTT, A. T. and KYRYCHENKO, S. Y. 2007. Efficacy of side airbags in reducing driver deaths in driver-side car and SUV collisions. *Traffic Inj Prev*, 8, 162-70.
- NEWLAND, C., BELCHER, T., BOSTROM, O., GABLER, H. C., CHA, J. G., WONG, H. L., TYLKO, S. and DAL NEVO, R. 2008. Occupant-to-occupant interaction and impact injury risk in side impact crashes. *Stapp Car Crash J*, 52, 327-47.
- PERSAUD, B., RETTING, R., GARDNER, P. and D., L. 2001. Safety Effects of Roundabout Conversions in the United States: Empirical Bayes Observational Before-After Study. *Transport. Res. Rec.*, 1751, 1-8.
- STIGSON, H. 2009. Evaluation of safety ratings of roads based on frontal crashes with known crash pulse and injury outcome. *Traffic Inj Prev*, 10, 273-8.
- SUNNEVÅNG, C., ROSÉN, E. and BOSTROM, O. 2009. Real-life fatal outcome in car-to-car near-side impacts--implications for improved protection considering age and crash severity. *Traffic Inj Prev*, 10, 194-203.
- TEOH, E. and LUND, A. 2011. IIHS Side Crash Test Ratings and Occupant Death Risk in Real-World Crashes. Arlington: IIHS.
- YDENIUS, A. 2009. Frontal crash severity in different road environments measured in real-world crashes. *International Journal of Crashworthiness*, 14, 525-532.

APPENDIX

Table 1. Risk of sustaining injury in a side impact in a passenger car without side airbag

Without side airbag		Driver in striking car		Total
		injured	not injured	
Occupant in struck car	injured	192	135	327
	not injured	63	35	
Total		255		

Table 2. Risk of sustaining injury in a side impact in a passenger car fitted with side airbags, protecting head and chest

With side airbag		Driver in striking car		Total
		injured	not injured	
Occupant in struck car	injured	556	336	892
	not injured	233	138	
Total		789		

Table 3. Risk of sustaining serious injury in a side impact in a passenger car without side airbag (Serious injuries in the struck car)

Without side airbag		Driver in striking car		Total
		injured	not injured	
Occupant in struck car	Sever injured	29	13	42
	not sever injured	226	157	
Total		255		

Table 4. Risk of sustaining serious injury in a side impact in a passenger car fitted with side airbags, protecting head and chest (Serious injuries in the struck car)

With side airbag		Driver in striking car		Total
		injured	not injured	
Occupant in struck car	Sever injured	72	27	99
	not sever injured	717	447	
Total		789		

PROTECTING OCCUPANTS IN ROLLOVER CRASHES: CASE EXAMPLES AND LATEST TECHNOLOGIES

by Byron Bloch, Auto Safety Expert
Potomac, Maryland, USA

www.AutoSafetyExpert.com

22ND ESV Conference 2011 - Paper 11-0344
Washington, D.C.

ABSTRACT

NHTSA has documented that rollover accidents account for about 3-percent of all vehicle accident in the United States, yet are responsible for about 30-percent of the deaths, plus thousands of quadriplegics (tetraplegics). The principal mechanisms of injury causation are due to roof crush and occupant ejection.

Therefore, stronger roof design is needed to prevent the buckling and crushing down of the roof into the occupants' "survival space". And improved side window glazing, such as using laminated glass instead of tempered glass, will help prevent occupant ejection during rollovers, as well as in other impact modes.

Using rollover accident case examples and exemplar vehicles, detailed inspections and analysis show how and why the roof structures failed to adequately maintain the passenger compartment "survival space" and how the consequences often caused quadriplegic injuries. The history and technology of roof design shows safer alternative designs that would have made a safety difference.

It is clear that Federal Motor Vehicle Safety Standard 216 (FMVSS 216) on Roof Crush Resistance, which is a *minimum* requirement, has not ensured a reasonably safe roof in rollover accidents. Upgrades are needed to ensure stronger roofs, with dynamic rollover testing to evaluate the total system of roof structural integrity, side window glazing, seatbelt restraints, side curtain airbags, and other measures that will help attain the Vision Zero compassionate goal of preventing needless deaths and injuries.

AFFIRMED: IN ROLLOVERS, ROOF CRUSH CAUSES QUADRIPLÉGIA

In a rollover accident, it is imperative to maintain the occupants' "survival space". It is a well-established principle in vehicle safety and crashworthiness that a vehicle should be designed so as to prevent or minimize intrusion or penetration into the passenger

compartment "survival space" in all types of foreseeable collisions... including front impact, side impact, rear impact, rollover. Automakers and vehicle safety specialists often refer to the critical need to provide a strong "roll cage" vehicle construction to protect the passengers.

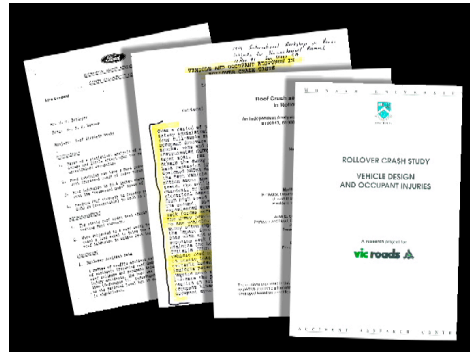


Figure 1. The mechanism of vehicle roof crush causing cervical-spinal injuries has been well-documented in the literature.

1968: Back in 1968, Ford Motor Company issued "the Weaver memo", an intra-company safety evaluation formally entitled "Roof Strength Study." With the advent of shoulder belts becoming mandatory in the late-1960's, Ford was concerned about the relationship between roof crush and lap-and-shoulder belted occupants who would be seated upright as the vehicle rolled over. As Ford noted:

"Roof intrusion may have a more pronounced effect on occupant injuries with increased usage of upper torso restraints. People are injured by roof collapse. The total number of nationwide deaths and injuries cannot be estimated but it is a significant number."

In other words, Ford was concerned that the collapse of the roof onto the passengers would cause deaths and injuries to those seat belted occupants. Ford then put it all into perspective:

"It seems unjust to penalize people wearing effective restraint systems by exposing them to more severe rollover injuries than they might expect with no restraints."

1973-74: The National Highway Traffic Safety Administration, or NHTSA, issued Federal Safety Standard 216 (FMVSS 216) as the *minimal* requirement for Roof Crush Resistance. In its rulemaking notices, NHTSA stated:

“... serious injuries are more frequent when the roof collapses.”

“It has been determined, therefore, that improved roof strength will increase occupant protection in rollover accidents.”

“After August 15, 1977, Standard 216 will no longer be a substitute for the Standard 208 rollover test. It is expected that as of that date Standard 216 will be revoked, at least with its application to passenger cars.”

FMVSS 216 also expressed concern about the integrity of side windows relative to occupant ejection, but no test requirement was included to ensure that side windows would not shatter out. But the anticipated rollover test was never mandated.

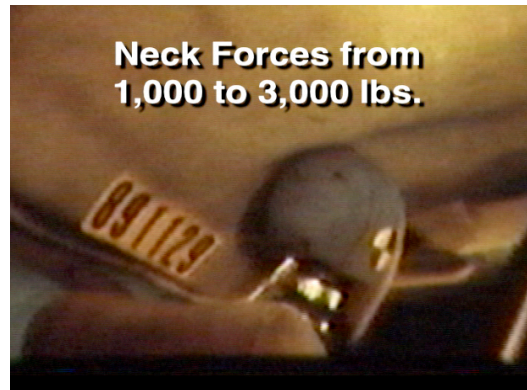
1982: In 1982, NHTSA issued a report on “Light Vehicle Occupant Protection – Top and Rear Structures and Interiors”. (SAE Report 820244.) This comprehensive NHTSA analysis pointed out a significant correlation:

“...accident statistics show that the degree of roof intrusion is highly associated with occupant injury severity and rate.”

1992: In 1992, the major report “Vehicle and Occupant Response in Rollover Crash Tests” was issued as a coordinated effort by NHTSA and by the Armstrong Laboratory, of the Department of the Air Force. It reported on the findings from a series of 24 rollover crash tests that NHTSA had sponsored to study vehicle and occupant dynamics. Roof crush varied from about 4 to 20 or more inches. The test dummies were instrumented to measure head and neck forces. Among the report’s conclusions:

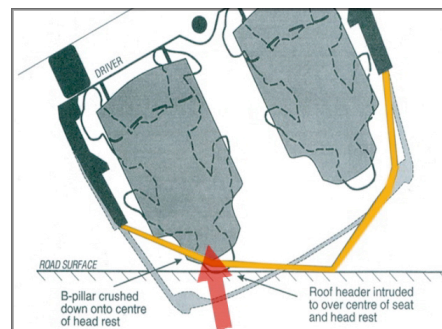
“Most of the tests resulted in significant roof crush. Often the body was trapped by the roof crush. In these cases, the head/neck system was vulnerable to large loads from the roof.”

In many of the rollover tests, the dummies received major compressive loads to their necks and cervical spine, with many in the 1,000 to 3,000 pounds range, sufficient to cause cervical fractures, spinal cord damage, and quadriplegia.



1994: In “Rollover Crash Study on Vehicle Design and Occupant Injuries” researchers at Monash University of Australia analyzed many actual vehicle rollover accidents, and correlated the extent of roof crush with the causation of cervical spinal injuries. Among their findings was this correlation:

“In mass data and other crash collections, the weight of evidence is in agreement with a relationship between roof crush and occupant injury. There is a convincing relationship between rollover and spinal cord injury. Finally, there is strong evidence of a connection between local roof crush and spinal cord injury.”



2005: In 2005, a study by Bidez, Cochran, and King evaluated “Roof Crush as a Source of Injury in Rollover Crashes.” The authors evaluated the data from instrumented dummies in a series of rollover tests of Ford Explorer SUVs, as conducted by Autoliv. Their conclusions included the following:

“Roof crush into the survival space of restrained dummies was the direct cause of neck loads, which were predictive of catastrophic neck injury in rollover crashes.”

“In the absence of significant roof crush into the occupant survival space, no dummy neck loads predictive of catastrophic injury were observed in this test series.”

2005: In 2005, at the urging of the US Congress, the National Highway Traffic Safety Administration (NHTSA) was required to amend FMVSS 216, which had been essentially the same since the mid-1970's, to increase the requirement for stronger roofs that would offer greater protection in rollover accidents. In its Notice of Proposed Rulemaking, NHTSA noted that:

“In sum, the agency believes that there is a relationship between the amount of roof intrusion and the risk of injury to belted occupants in rollover events.”

2009: Researchers at the Insurance Institute for Highway Safety (IIHS) correlated roof strength with injury risk in actual rollover accidents. Eleven midsize SUV roof designs were crushed using the slow-push test protocol of FMVSS 216. Applied forces were measured and the amounts needed to achieve crush of 2, 5, and 10 inches were recorded, and compared with the fatal or incapacitating injuries to drivers in single-vehicle rollover accidents. The analysis showed that *“Increased vehicle roof strength reduces the risk of fatal or incapacitating injury in single-vehicle rollover crashes.”*

The strongest roof of the studied SUVs had a strength-to-weight ratio up to 3.16, with roof excursions from 3.2 to 7.3 inches before the roof contacted the test dummy's head. Thus, vehicles with stronger roofs and different headroom clearances could have an even more profound effect. For example, for a taller driver in a car with 2 inches of headroom, a roof would need a greater SWR of perhaps 4.0 to 5.0 or greater to reduce the roof crush risk of fatal or quadriplegic injuries. There would be thus be safety advantages to a stronger roof, whatever the headroom clearances and sizes of the drivers and passengers.

These many authoritative studies cited above, and others, all point out and affirm the causal relationship between roof crush and spinal cord injuries. And they clearly contradict the proponents of the so-called *“diving theory”* who claim that roof crush does not cause cervical spinal injuries, but that such injuries are caused when the driver dives headfirst into the roof as the roof touches the ground. If one were to accept such a diving theory, then where are any efforts by the proponents to make safer seatbelts that will tighten up at the beginning of rollovers so as to prevent seat-belted occupants from any such unsafe diving? Of note, many of the diving theorists show up as defense experts in court cases to explain why

the allegedly-weak roof that buckled and crushed downward so excessively wasn't really the cause of the quadriplegic injuries after all.

THE HISTORY AND TECHNOLOGY OF ROOF STRUCTURE IN ROLLOVERS... and FMVSS 216

A vehicle roof is supposed to stay upright and safely maintain the occupant's *“survival space”*. The roof structure is generally described as an interconnected network of essential elements:

The windshield pillars, also called A-pillars.

The mid-body pillars, also called B-pillars.

The rear window pillars, also called C-pillars.

The windshield header, which extends laterally across the top of the windshield.

Roof siderails, along the outer sides of the roof.

Roof cross-members, laterally across the roof, in varying locations, including B-pillar to B-pillar.

Corner gussets, to interconnect the junctions where the various roof members meet each other.

All together, it is the strength of these elements and how they are reinforced and connected, that determines the overall strength of the roof.

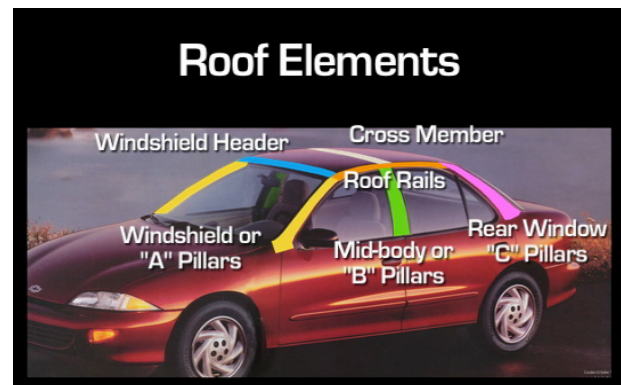


Figure 2. Roof elements are the typical structural members that interconnect to support the roof.

1950's: General Motors (GM) conducted dynamic rollover tests back in the 1950's, in *50 miles per hour rollovers* that GM referred to as the *“supreme test”* as noted in the adjacent GM illustration.

The 1955 Chevrolet's roof structure, with its closed-section or box-section windshield header, and its mid-body roof bow and center pillars, was shown by GM to be strong enough to prevent roof buckling and collapse. Sufficient roof strength and its performance in actual dynamic rollover testing was demonstrated.



1960: In 1960, Ford conducted Crash Test 116, a dynamic rollover test of a 1960 Ford Falcon passenger car. This ramp-type rollover test at 34 miles per hour was conducted in order to evaluate the Falcon's roof structure. The design of the Falcon's windshield header was a "hat section" – an open section design that's very similar to many of the windshield header designs in cars and SUVs throughout the 1970's to the present. *After two and one-half rolls, the Ford Falcon's roof had buckled and crushed downward... very much like what happened to the roofs in many rollover accidents over the past decades.*

In their report, Ford stated:

"The roof structure proved inadequate. The front of the roof collapsed. The hat section reinforcement at the very front of the roof was insufficient to withstand the load."



That kind of roof-buckling failure in a 34 miles-per-hour rollover certainly means the roof structure is inadequate and insufficient in its design and performance.

1971: The NHTSA report "*Test for Vehicle Rollover Procedure*" was based on a series of dynamic lateral rollover tests of a variety of vehicles. The abstract noted that "The tests proved the adequacy of this procedure to produce repeatable rollovers and to demonstrate the applicability over a large range of vehicle sizes and configurations."



1960s – 1970s: The state-of-the-art in the 1960's and 1970's was for roof structures that utilized closed-section or box-section members, as was often described in the automakers' literature.. General Motors said the roof was stronger, including "*its rugged box-section windshield header.*" Ford said the roof construction on all models has "*rigid box-section rails at the sides and at the front and back window headers.*" Chrysler said their "*uni-body construction was strong and tight, with its box-section windshield pillars and header.*"

The state-of-the-art for decades has been that windshield headers should be a closed-section or box-section design for sufficient strength.

1971: When NHTSA was in proposed rulemaking for Roof Intrusion Protection (Docket 2-6, Notice 4), General Motors was critical of the proposed static roof crush test up to 5,000 lbs. with a maximum ram travel of 5 inches, noting "*we know of no safety relationship correlating such a laboratory procedure with occupant protection in rollovers*" GM then proposed that the test be based on maintaining a vehicle interior "*non-encroachment zone*" of sufficient headroom that would not be intruded into by roof crush.

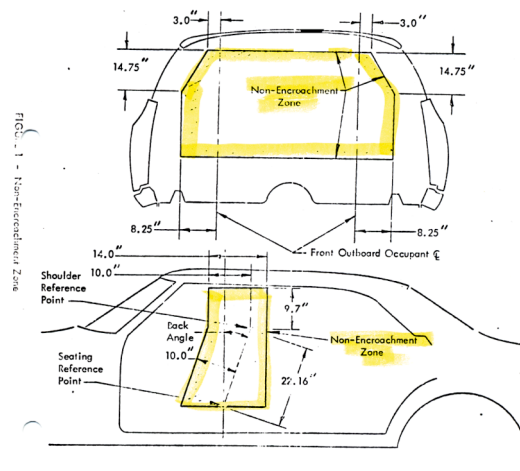


Figure 3. GM 1971 submission to NHTSA docket.

1974: Most of the world’s automakers actively participate in the International ESV Conference held every two years, beginning back in 1971. Many of the ESV papers over the years have shown how to design and test safer roofs for enhanced protection in rollovers. As an example, in 1974 Honda presented a technical report about ensuring “*Survival Space*” and showed how a strong roll cage construction, with roof cross-members, would help maintain the passenger compartment from being crushed during a rollover accident.

European automakers, especially, showed the merits of dynamic rollover testing to evaluate roof performance. They likely believed the NHTSA projection in 1973 that the FMVSS 216 “*slow push*” compliance test (as a *minimum*) would soon be superseded by a dynamic lateral rollover test at least at 30 mph, per FMVSS 208, beginning in 1977. However, the “*slow push*” test continued, and the rollover test requirement was not phased in.



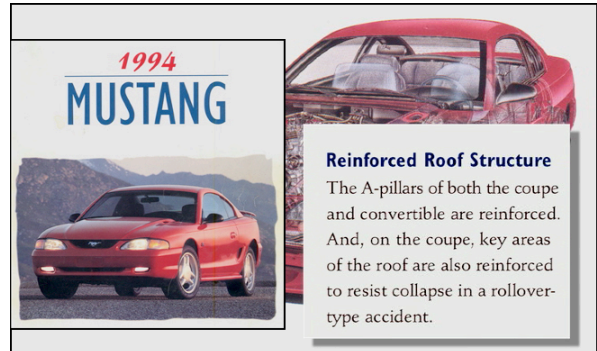
However, in too many vehicles through the late ‘70s into the ‘90s and early-2000’s, too many automakers opted to compromise and short-change roof strength, doing just enough to meet the FMVSS 216 minimum requirement of 1.5 times the weight of the vehicle. Thus, too many of their vehicles were designed with weaker open-section windshield headers with large hole cut-outs and A-pillars that were not fully reinforced. Yes, the roof complied, but performed terribly in real-world rollover accidents.

1994: Another example pointing out the need for closed-section windshield headers is found in Ford’s candid information when they introduced the 1994 Mustang:

“Reinforced Roof Structure ... key areas of the roof are also reinforced to resist collapse in a rollover-type accident.”

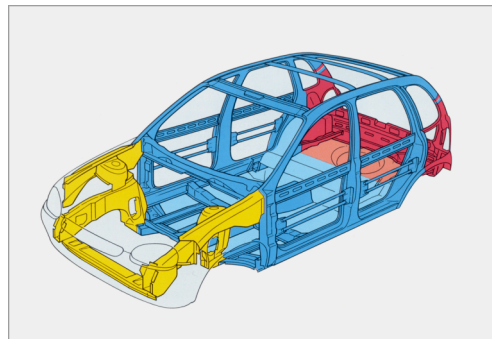
“In the previous-generation Mustang coupe, roof members were formed with open sections. Significant gains were made in the stiffness of the 1994 by

incorporating box-section roof headers and rails.”



1994: General Motors in Europe is known as Opel. Opel’s cars are designed with a full safety-cage construction. Here’s what GM-Opel said back in 1994 about rollover protection.

“Developments in safety at Opel also take into account occupant protection in roll-over accidents. The bodies of Opel cars are notable for their high degree of roll-over safety. Crash tests at the Technical Development Center prove the point: in a lateral rollover accident with a throw speed of 50 km/h the occupant cell suffers no critical deformation....”



1998: In 1998, a paper published by the Society of Automotive Engineers, or SAE, focused on “*Strength Improvements to Automotive Roof Components*”. Using various alternative structural designs for roof headers, the researchers conducted axial-load compression tests and three-point bending tests to

compare production roof elements versus reinforced designs. The comparisons included a production header of an open-section design, similar to the design in many production vehicles.

An open section roof member was modified by closing it along one flange to approximate a closed section, plus the insertion of an inner tubular support. Other alternative designs were also tested. In all cases, the alternative designs all proved significantly stiffer and stronger than the open-section production header... up to 5 times the peak strength in axial testing.

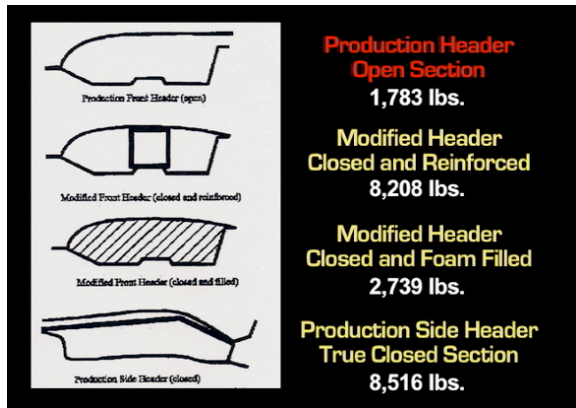


Figure 4. Simple upgrades increase roof strength.

In other words, there have been feasible and economical alternative designs that could have greatly strengthened the roof members, and such alternative roof element designs and the basic principles have been well-known for decades.

To further point out the failure of the Federal Safety Standard, FMVSS 216, to ensure safe roofs, note that the toll in rollover accidents in the U.S. has recently been in excess of 10,000 fatalities per year. In 2005, the United States Congress passed legislation that included a mandate to NHTSA to upgrade the roof crush standard to make it more effective. That resulted in NHTSA rulemaking from 2005 through 2009 that increased the strength-to-weight ratio (SWR) from an ineffective 1.5 to one, to become 3.0 to one.

It is important to note that FMVSS 216 is only a *minimum* requirement and, while somewhat of an improvement over its predecessor's terribly weak requirement, will likely not be strong enough nor require the dynamic testing that would more sufficiently ensure that vehicle roofs will perform safely in actual rollover accidents.

TEMPERED SIDE WINDOW GLASS SHATTERS COMPLETELY OUT AND ALLOWS UNSAFE OCCUPANT EJECTION IN ROLLOVERS

As commonly happens in rollover accidents, the side windows' tempered glass easily shatters into hundreds of small glass particles when the roof crushes down, or the occupant strikes it. This creates a large window opening through which the occupants, whether belted or unbelted, may be partially or completely ejected -- and suffer severe impact trauma with the road and the rolling vehicle.

In a rollover accident when the side window glass shattered out, a seat-belted woman in the rear seat was partially ejected and suffer fatal trauma. She was found with the seatbelt still fastened, with her legs protruding outward through the window opening.



Rather than tempered glass which shatters out much too easily, the side windows should have instead used the safer alternative of laminated glass.... a 3-layer laminate sandwich of glass-plastic-glass.

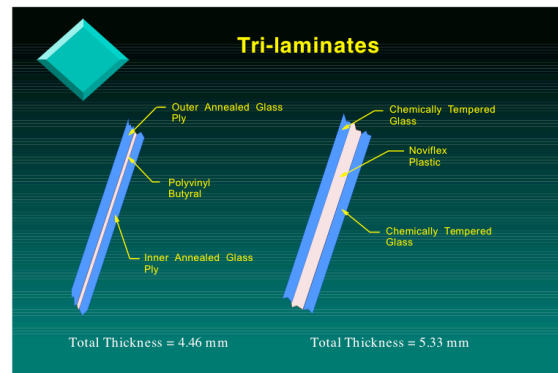


Figure 5. Laminated glass stays intact and serves as a "life net" to prevent occupant ejection.

As demonstrated in NHTSA's comparison tests, the *tempered* glass shatters out completely and allows the occupant to be ejected through the opening, while the

safer *laminated* glass may break but still stays intact and serves as a “life net” to keep occupants safely within the vehicle. Note that *the front windshield* of all vehicles is made of *laminated* glass, a three-layer sandwich of glass-plastic-glass that is analogous to what could and should have also been utilized for the side windows.



The U.S. National Highway Traffic Safety Administration (NHTSA) has regularly issued recommendations for vehicle manufacturers to utilize safer glass-plastic side windows to help prevent the occupant ejection hazard.



In 1996, NHTSA summed up the findings of its advanced glazing research team, which again examined the window glazing opportunities to reduce occupant ejection... a subject that had been on-again and off-again for 20 or more years. NHTSA showed that from 1988 through 1993, the annual average of severe injury for occupant ejection through window glazing was about 3,700 per year, plus over 3,500 fatalities.

Over the past 30 years and currently, some automakers have opted for laminated side windows in various models. Recent and current models that have laminated side windows, either as standard or optional, include: Buick LaCrosse, Chevy Malibu, Ford Taurus, Hyundai Genesis, Lexus GS, Volvo S-80, and many others. There continues to be a re-adoption and resurgence in using laminated side window glass for its many advantages, including the prevention of occupant ejection.

As just one accident case example, the right-rear tire of a Ford 15-passenger van lost its tread, and the van went out of control and rolled over. There were ten occupants in the van, and three were fully ejected when the large side window tempered glass completely shattered out.



Note the particles of tempered glass still embedded to the adhesive and rubber molding strip of the large side windows.

CASE EXAMPLES OF ROLLOVER ROOF CRUSH AND QUADRIPLEGIC INJURIES

In my analysis of many rollover accidents across the United States, I often inspect the vehicle at-issue and exemplar vehicles, to evaluate roof design characteristics, including how and why the roof buckled and crushed during the rollover. In most cases, the roof had been designed very poorly, with only minimum features that enabled the vehicle to comply with the “slow push” test of FMVSS 216. That test requires a slow push at a downward angle to

the side of the roof, with a force of 1.5 times the vehicle weight, or 5,000 lbs, whichever is less, with no more than 5 inches of roof crush allowed. This is known as a strength-to-weight ration (SWR) of 1.5 to one.

But in real-world accidents, the weak roof performed poorly, resulting in excessive crush into the driver's and passenger's survival space, often causing fatal or quadriplegic injuries. Yet, all of these poorly-designed and unsafely-performing vehicles had complied with the US Federal Motor Vehicle Safety Standard 216, which is only a minimum requirement by law. Such compliance with the "safety standard" did not ensure a reasonably safe roof. Yet, that FMVSS 216 "safety standard" had been in effect since 1973 through to the present, and has only recently been moderately strengthened to apply to future vehicles.

The following rollover accident case examples are intended to show the symptomatic weak roof designs and their failure in rollover accidents, illustrating ineffective roof structures that are all-too-common among many cars, pickups, vans, and SUVs made by many automakers over the past 40 years and currently.

Rollover Case A: 1989 Ford Escort Hatchback

This rollover accident occurred when the driver of a 1989 Ford Escort 2-door hatchback tried to avoid another vehicle that had cut into his lane, and rolled over at about 35 mph on a grassy center median. The seat-belted driver was rendered a quadriplegic.



The Escort's roof design was very minimal. The windshield pillar was internally reinforced with a baffle plate, but only in its lower 6 inches, and that's where it bent over in the rollover. The windshield header was a flat channel, a weak open-section, and was further weakened by many large hole cutouts, and the roof buckled in those predisposed weak

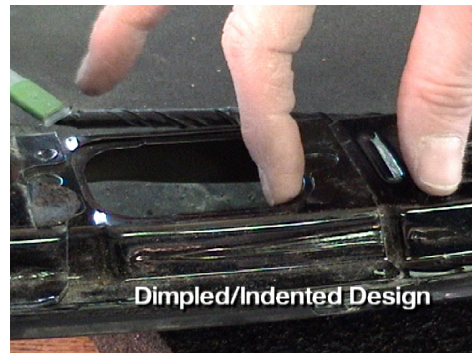
zones. Yet, despite its minimal design and poor performance, the Ford Escort's roof had complied with FMVSS 216.

Rollover Case B: 1999 Toyota SUV

This rollover accident occurred when a 1999 Toyota RAV4 SUV was impacted by an adjacent vehicle, and rolled over on the road. The seat-belted right-front passenger was subjected to the roof crush and was rendered a quadriplegic, while the driver was only moderately injured.



The RAV4 windshield header was an open-section shallow channel design, with many large hole cutouts and dimpled contours, and the corner gussets overlap only a short distance onto the header. In the rollover, the roof buckled and crushed down in these predictable weak areas.



The RAV4 had an “*open section*” design for the windshield header, basically a flat channel that’s spot-welded along the roof’s forward edge. In contrast, in the same 1999 model year, the Toyota Camry utilized a “*closed section*” design, a rectangular-shaped tube that was stiffer and stronger in resisting bending and compressive loads.

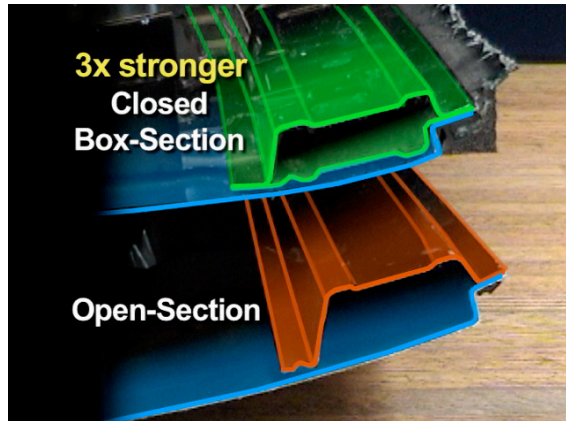


Figure 6. Closed box-section roof headers are about 3 times stronger than open-section headers.

Yet, despite its weak roof and poor performance, the RAV4 roof had complied with FMVSS 216, again indicating that compliance with the *minimum* force requirements of its unrealistic “*slow push*” test does not ensure a reasonably safe roof.

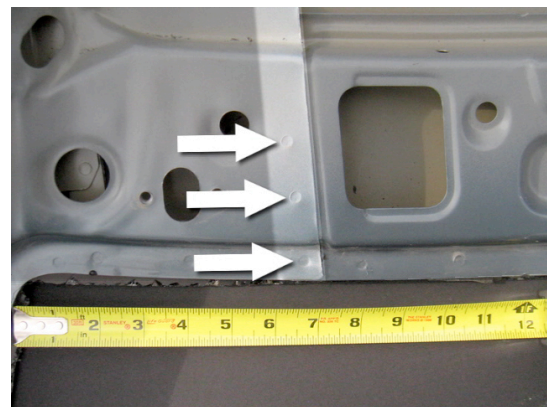
Rollover Case C: 2000 Daewoo Leganza

In the course of the vehicle rollover, the Daewoo Leganza sedan’s roof buckled and crushed down into the “survival space” of the driver. Photos at the scene show the seat-belted driver still positioned upright in the seat. He had suffered fractures of his cervical vertebrae, and was rendered a quadriplegic.



The windshield header was an “*open section*” shallow channel-type design, which is much weaker and less safe than a “*closed-section*” tubular design, which is about 3 times stiffer and stronger. The header design

had many “*Swiss cheese*” hole cut-outs and minimal overlaps, and was only .030-inch thin, all factors contributing to its weakness in rollovers.



Note the predictable weak zone where the roof buckled in the accident.... as shown in the photo below. It’s in this area about 6 to 8 inches inboard from the windshield pillar... where there’s only a minimal overlap of only about one inch, and just three spotwelds, where two pieces of thin sheetmetal overlap each other, adjacent to a large hole cutout. That’s the critical “*weak zone*” where the windshield header buckled, allowing the roof to distort laterally and downward.

Here again, even though the roof complied with FMVSS 216, its design was needlessly weak, and its performance in the rollover accident failed to protect the driver.

Rollover Case D: 1996 Chevrolet Cavalier Coupe

The rollover accident car was a 1996 Chevy Cavalier 2-door coupe, and the roof buckled and crushed down on the right-front passenger, a young man wearing his seatbelt. He suffered cervical spinal injuries that rendered him a quadriplegic, and paramedics cut off the roof in order to extricate him. The driver, seated where there was virtually no roof crush into her area, was essentially uninjured.



A key design defect in the Chevy Cavalier roof is the windshield header, a thin flat-channel design, an “open section” minimal design that is very weak that is easy to buckle and lacking in stiffness and strength.



The roof structure is further weakened by the short corner gusset that only overlaps about 5 inches, rather than continuing completely across the header from A-pillar to A-pillar, which would add more strength.



In contrast to this weak open-section design, the “closed section” or “box section” design... which looks like a rectangular tube, is about three times stiffer and stronger, and is much less likely to buckle. This design is used in many other production vehicles competitive to the Chevy Cavalier.

The opposite side windshield header also reacted by buckling upward in the weak area where the short corner gusset ended, about 5 inches inboard from its

junction with the A-pillar. When the windshield header buckles, whether upward or downward, it has thereby failed to maintain the structural stiffness that helps support the other interconnected elements.

Rollover Case E: 1994 Toyota 4Runner SUV

The Toyota 4Runner of the 1989-1995 era is known as Generation 2. The windshield header was an open-section flat-channel design with an additional strip of thin sheetmetal down the center. The header had many large hole cutouts, and the material was only about 30-thousandths. The corner gussets were very short, and ended adjacent to large hole cutouts, creating structural weak zones that are predisposed to buckling when loads are applied onto the roof in a rollover accident.



The windshield pillar had an internal reinforcement, but it only extended upward about 7 inches from the bottom. The roof siderail had a short reinforcement that ended about 8 inches back from the A-pillar. Thus there were weak zones where these structural discontinuities were located in the A-pillar and roof siderail, making them susceptible to deformation and buckling.

Inspection of the 4Runner showed that roof had buckled in those weak zones, including the A-pillar acting as a hinge at the location 7 inches from the bottom where the inner baffle reinforcement ended.



The open section flat-channel design of the windshield header, with its many large hole cutouts and minimal gusset overlaps, also proved inadequate in the rollover. Lacking in stiffness and strength, the windshield header deformed and buckled, predictably in the areas of large hole cutouts and structural discontinuities.

The combined buckling of the A-pillar and header and siderail allowed more extensive downward and lateral deformation and crush of the roof into the driver's "survival space" thereby causing cervical spinal loads that rendered the seatbelted driver into a quadriplegic.

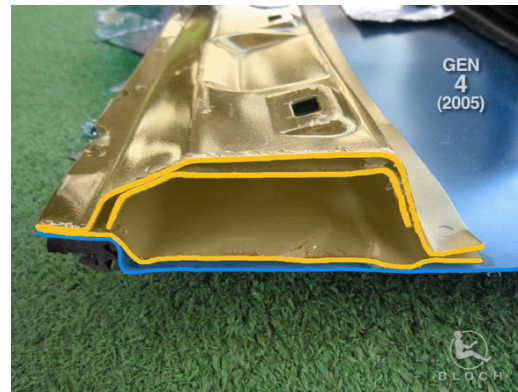


The 4Runner 3rd generation (1996-2002) adopted the well-known closed-section or box-section design for the windshield header. Though of the same thin 30 thousandths of an inch, the box-section design is about three times stiffer and stronger than the open-channel design that was used previously. Again, the short corner gussets and large hole cutouts were additional weaknesses that needlessly compromised the box-section design of the windshield header.



The 4Runner Generation 3 windshield pillar design was similar to the previous Generation 2 version, with the internal reinforcement too short, extending upward from the base only a few inches, rather than continuing the full length of the pillar.

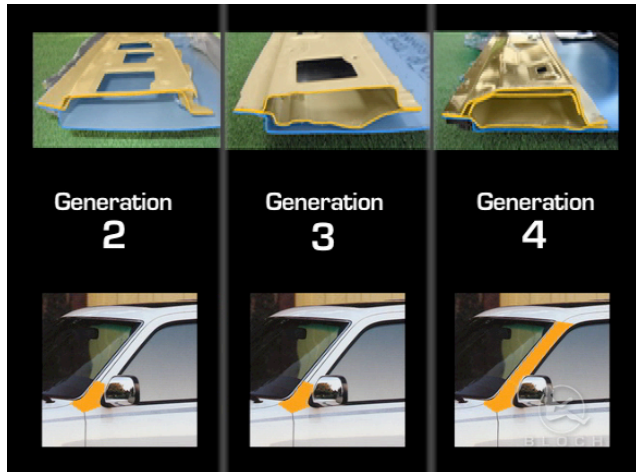
The 4Runner 4th generation (2003-2009) adopted a totally-new design for the roof structure. The previous thin sheetmetal of the windshield header was increased to 60 thousandths. A doubler plate of similar 60-thousandths thickness was also added, and there were notably less hole cutouts. The design was now a more robust thicker material, and had an internal reinforcement and taller vertical walls.



The Generation 4 windshield pillars were of thicker metal, with internal reinforcements continuing all the way from the base to the top of the pillar.



This comparison chart shows the successive revisions of the roof's structural elements from Gen 2 with its weak open-section windshield header with large hole cutouts, and only minimal lower reinforcement of the A-pillar... to Gen 3 which adopted the well-known box-section windshield header... to Gen 4 with a reinforced box-section header and full-length internal reinforcement of the A-pillar all the way from its base to the roof.



The roof structure of the 1994 Toyota 4Runner SUV was well-below the state-of-the-art. Critical roof elements were designed as minimum structures that would just comply with the minimum requirements of FMVSS 216 and its "slow push" test. But such a weak roof does not ensure a safe roof in real-world rollover accidents. The roof buckles and crushes down onto the occupants and cause fatal or severe injuries, including quadriplegia.

UNSAFE ROOF DESIGNS WERE NEEDLESS, WHILE SAFER ROOF DESIGNS HAVE BEEN KNOWN FOR DECADES

From my analysis of the roofs of vehicles that had been in rollover accidents, many with resulting fatalities and quadriplegics, there are patterns of needlessly-compromised designs that were well below the state-of-the-art that has existed for decades. Here's a review of the unsafe designs versus safer alternatives:

Windshield Header: If the windshield header is an open-section flat channel or shallow channel design, it will be much too flexible and subject to buckling. The header will be further weakened if there are large hole cutouts, as was often noted in production vehicles where the roof had buckled and crushed down. **Safer Designs:** The windshield header should be a closed-section or box-section design, with an internal baffle and/or doubler plate running

the entire length of the windshield header, from Left A-pillar to right A-pillar. To further stiffen and strengthen the header, rigid foam can be used, which can triple the compressive and bending strength of the closed-tube member.

Windshield Pillars: Too many windshield pillars (A-pillars) had an internal baffle-type reinforcement at only the bottom 5 to 8 inches of the pillar. After the rollover accident, the A-pillar was often seen to have buckled or bent at that location right where the internal reinforcement ended, with the pillar then acting much like a hinge that allowed the roof to matchbox and crush laterally and downward. **Safer Designs:** The windshield pillars (A-pillars) should be internally reinforced their full length, from the base all the way upward to where it meets the windshield header and roof side-rail. The use of rigid foam-filling and composite plastic inserts (bonded to the metal) are also effective and economical ways to increase stiffness and strength.

Roof Siderail: Too many siderails are hollow sections with a series of short internal baffles, some of which overlap each other. With hole cutouts and minimal overlaps, the side-rails often buckled downward and thereby failed to help support the roof structure. **Safer designs:** The roof siderails should have internal baffles and doubler plates that are longer and have more substantial overlaps. . As with other tubular roof members, the use of rigid foam filling and composite-plastic inserts can add to the strength of the roof structure.

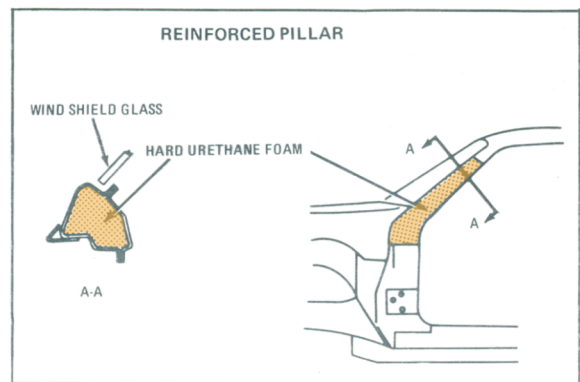


Figure 26

Figure 7. Nissan showed in the 1970's that hard urethane foam made roof pillars much stronger.

It is clear from analyzing the design and performance of roof structures that have failed in rollover accidents, that there are design characteristics that are weak and ineffective. It is apparent that too many automakers have failed to adequately test their vehicle roofs during development, to test to failure,

then analyze how and why those failures occurred... and then correct them with a stronger roof.

As a tragic result of such needless compromises in roof design, there has been an epidemic of death and quadriplegia and other severe injuries that have occurred in rollover accidents. In the United States alone, the death toll in rollovers has reached about 10,000 per year.

Yet, if the Federal Safety Standard had been sufficiently strong these past four decades, including a requirement for rollover testing at 50 mph, or at least requiring a strength-to-weight ration of at least 5.0, and with laminated glass for side windows, that toll of death and injury would have been dramatically reduced toward zero.

U.S. SUPREME COURT HAS RULED THAT COMPLIANCE WITH FMVSS IS NOT SUFFICIENT

In the United States, the National Traffic and Motor Vehicle Safety Act of 1966 created NHTSA and the Federal Safety Standards. That law defines safety standards as *minimum* standards for motor vehicle performance. A key provision states that *“Compliance with any Federal motor vehicle safety standard issued under this title does not exempt any person from any liability under common law.”*

The U.S. Supreme Court recently issued a unanimous 8 to 0 opinion (one justice was recused) in February 2011 in the case of *Williamson versus Mazda*. A key issue focused on whether a FMVSS 208 permissible option of a lap-belt-only for a middle-row aisle seat in a minivan was a significant objective of the federal safety standard. The Supreme Court ruled that it was not, so that Mazda could be potentially held liable in a state lawsuit for its failure to include a shoulder belt. NHTSA had encouraged inclusion of shoulder belts, which Mazda had failed to implement.

Applying this Supreme Court ruling to rollover roof crush cases, an automaker could be held liable even if its roof complied with FMVSS 216. Not only is the FMVSS 216 only a *minimum*, but NHTSA has consistently pointed out and encouraged that roofs be made stronger. So if a vehicle roof at-issue complied with the so-called *“safety standard”* yet was a weak roof structure with a *“defective design”* that was well below the state-of-the-art, the manufacturer could be held liable in a state court case. The risk of such potential liability also serves as a constructive incentive for automakers to make stronger roofs well beyond the minimum requirements, and that will help prevent future deaths and injuries.

Reflecting back on the case examples cited earlier, a roof that had a windshield header that was a weak open-section shallow channel design with large hole cutouts, and a partially reinforced A-pillar, could not escape liability by claiming the roof complied with FMVSS 216.

The directive for auto safety professionals and for automakers is to design roofs so they won't buckle and crush down in rollover accidents, to avoid causing injury-causing intrusion into the survival space of tall adult test dummies. This will require roofs well above a SWR of 1.5 or the latest 3.0 minimum (with many production roofs already well above 4.0 and some above 5.0).



Figure 8. Volvo illustrates how strong roof structural integrity, side curtain airbags, and seatbelt pre-tensioners enhance safe performance in dynamic rollover testing.

Automakers must also conduct dynamic rollover testing at sufficient levels (e.g., at least at 50 mph) to validate the safe performance of the roof, the seatbelts, the side window glass, the side curtain airbags, and other features. The issue is no longer whether there is precisely-exact repeatability in rollover testing, but rather reasonable repeatability in testing that simulates what happens in real-world accidents.

The compassionate goal must be to eliminate deaths and quadriplegic injuries in rollover accidents. As discussed above, including the illustrative case examples, this may well require roofs with a SWR well above 5.0 and dynamic rollover testing with instrumented test dummies at 50 mph or higher.

CONCLUSIONS

FMVSS 216 has been ineffective as a “safety standard” and does NOT ensure a safe roof to protect occupants in rollover accidents. Recent upgrading of the *“slow push”* compliance test requirement for a strength-to-weight ratio (SWR) from 1.5 to the new

requirement of 3.0 is far too minimal... with many production vehicles already well above 4.0 and some above 5.0.

Analysis of many roofs has shown that, for the past 40-plus years, automakers have been needlessly compromising roof strength by using open-section headers, partial reinforcement of A-pillars, minimal gussets, and other structural weaknesses.

Instead, roofs should use closed-section or box section headers with internal reinforcements, with A-pillars internally reinforced from bottom to top, with more substantial gussets, and with the use of rigid foam filling and composite plastic strengtheners, and other innovative designs and technologies that can significantly increase roof strength.

There is ample evidence that affirms that roof crush causes cervical spinal traumatic injuries and resulting quadriplegia, a cumulative body of authoritative research that is well supported by dynamic rollover tests with instrumented test dummies, and extensive bio-mechanical and bio-medical assessments.

In defending their weak roof that too easily buckle and collapse, some automakers and their defense experts have theorized a "diving theory" as the mechanism of injury, rather than such fatal and cervical spinal injuries being caused by roof crush.

What is needed is a strength-to-weight ratio (SWR) of at least 4.0 with a phased-in upgrade to 5.0, and a dynamic rollover test with instrumented dummies at 50 MPH and a phased-in upgrade to 60 MPH.

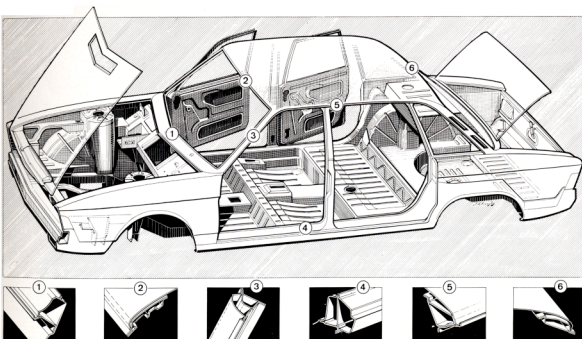


Figure 9. NSU-Volkswagen K-70 illustrated in 1969 how reinforced box-section roof members interconnect to help maintain structural integrity.

Safer designs have reinforced roof pillars with *full-length* internal baffle plates and/or are filled with *rigid foam* (which can *triple* their strength), and closed-section (like an "O") rather than open-section

(like a "C") tubular windshield headers and roof siderails, plus lateral side-to-side cross-members, and reinforcing gussets at the connections.

Thus, stronger roofs will help minimize the downward and lateral roof crush that causes head and cervical injuries, and will safely maintain the "survival space" or "non-encroachment zone" for the driver and passengers.

Safer roof designs have been documented since the 1950's when automakers conducted dynamic vehicle rollover tests and then again in the Experimental (Enhanced) Safety Vehicle Program that began in the early 1970's. In addition to stronger roofs, the use of laminated glass-plastic side-window glass, side curtain airbags, and energy-absorbing padded vehicle interiors can all reduce occupant injuries during rollovers.

In striving to attain the compassionate goal of Vision Zero... the elimination of fatal injuries due to the motor vehicle... it is imperative to innovate, design, develop, test, and produce vehicles that offer optimal crashworthiness in frontal, side, rear, and rollover accidents.

REFERENCES:

1. "Tomorrow's Look Today – Passenger Protection." General Motors Corp. 1955.
2. "Crash Test 116 – Roll Over Test of a 1960 Falcon 2-Door Sedan." Ford Motor Company, July 1960.
3. "Roof Strength Study", by J.R. Weaver. Ford Motor Company, July 1968.
4. "Roof and Windshield Header Constructions." by E.H. Klove and G.W. Ropers. General Motors Corp., January 13-17, 1969. SAE-690069.
5. "Comments of General Motors with Respect to Notice of Proposed Rule Making, Roof Intrusion Protection, Docket No. 2-6, Notice 4." General Motors Corp., April 5, 1971.
6. "Test for Vehicle Rollover Procedure." by R. Young and H. Scheuerman, Federal Aviation Administration, National Aviation Facilities Experimental Center. NHTSA Contract DOT-HS-032-1-036 (NAFEC-171). DOT-HS-800615. November 1971.

7. *“Roof Crush Resistance – Passenger Cars”* Preamble to Motor Vehicle Safety Standard No. 216, Docket No. 2-6, Notice 5. August 15, 1973.
8. *“Occupant Protection of 1,500 Pound ESV.”* Hideo Sugiura, Honda R&D. ESV Conference Proceedings, 1974.
9. *“Light Vehicle Occupant Protection – Top and Rear Structures and Interiors”* by Wm. Fann and Edward Jettner of NHTSA, 1982. SAAE 820244.
10. *“Vehicle and Occupant Response in Rollover Crash Tests”* by Louise Obergefell of Armstrong Laboratory, US Air Force, and Arnold Johnson of NHTSA.
11. *“Rollover Crash Study – Vehicle Design and Occupant Injuries”* by George Rechnitzer and John Lane of Monash University Accident Research Centre, Victoria, Australia, December 1994.
12. *“Vehicle Safety – Opel”* by General Motors (Europe) AG. March 1993.
13. *“Advanced Designs for Side Impact and Rollover Protection”* by Byron Bloch, Auto Safety Design, Potomac, Maryland, USA. Paper No. 98-S8-P-12, 16th International Technical Conference on the Enhanced Safety of Vehicles, Windsor, Ontario, Canada. 1998.
14. *“Strength Improvements to Automotive Roof Components”* by B. Herbst, S. Forrest, and S.E. Meyer, of Liability Research Group. Paper SP-1321, at Advances in Safety Technology, SAE International Congress, Detroit, Feb. 1998.
15. *“Alternative Roof Crush Resistance Testing with Production and Reinforced Roof Structures”* by B. Herbst, S. Forrest, S.E. Meyer and D. Hok, of SAFE, LLC. Proceedings of 2002 SAE International Body Engineering Conference, Paris, France, July 2002.
16. *“Roof Crush as a Source of Injury in Rollover Crashes”* by M.Bidez of Univ. of Alabama, J.E. Cochran of Auburn Univ., and Dottie King of Three Sigma.
17. *“Crashworthiness of Vehicle Structures: Passenger Car Roof Structures Program”* by Robert Carl and George Williams, of Lockheed-Georgia Co., for NHTSA. Contract No. FH-11-7549. March 1971.
18. *“Structural and Occupant Protection Systems of the Opel Safety Vehicle”* by E.S. Kiefer, of Adam Opel AG, Proceedings of 5th International ESV Conference, 1974.
19. *“Roof Strength and Injury Risk in Rollover Crashes”* by M.L. Brumbelow, E.R. Teoh, D.S. Zuby, and A.T. McCartt of the Insurance Institute for Highway Safety. Traffic Injury Prevention, January 2009.
20. *“Rollover Revolution”* by Byron Bloch, Auto Safety Design, USA. Crash Test Technology International, issue of May 2008.
21. *“Opinion re: Williamson versus Mazda Motor of America,”* Opinion by the Supreme Court of the United States. Case No. 08-1314. Decided February 23, 2011.

A Study of Occupant Ejection Mitigation

Jeff Dix

Koichi Sagawa, Lalitkumar Sahare

Nissan Technical Center North America

United States of America

Selim Hammoud, Alex Cardinali, Daniel Fulk

Nissan North America

United States of America

Abe Mitchell

Autoliv North America

United States of America

Paper Number 11-0368

ABSTRACT

The National Highway Traffic Safety Administration (NHTSA) has identified ejection mitigation as a top priority, issuing a notice of proposed ruling making (NPRM) for FMVSS 226, Ejection Mitigation, in December of 2009. The NPRM proposed a linear impact test that uses a featureless head-form with a mass of 18 kg to impact a vehicle's side windows' daylight opening at various positions. The test measures the excursion of the head-form beyond the plane of the window glazing. The intention is to evaluate the ability of a vehicle's ejection mitigation system, such as the curtain airbag or other vehicle features, to manage the impactor energy and limit excursion. The NPRM consists of two tests conducted 1.5 and six seconds after the ejection mitigation countermeasure is deployed at impactor speeds of 24 km/h (400 Joules) and 16 km/h (178 Joules) respectively. In January of 2011, the agency issued a final rule for FMVSS 226 revising the impact speed for the higher speed test from 24 km/h to 20 km/h, thus reducing the energy to 280 Joules. This paper will present the results of a case study using computer modeling to understand the roles of the seatbelts and curtain airbags in mitigating ejections, as well as studying a representative energy level that can be employed for evaluating ejection mitigation systems considering both rollover and side impact crashes. The results of the computer modeling will be compared with the energy levels outlined in the NPRM and final rule for FMVSS 226. Furthermore, the authors will also present the results of a parameter study in which the stiffness of a curtain airbag is optimized to balance the requirements of ejection mitigation with the injury prevention targeted by other side impact regulation such as FMVSS 214: Side Impact Protection.

INTRODUCTION

Ejections have a significant impact on occupant injuries in motor vehicle crashes, representing 8,605 fatalities as well as 20,000 injuries in 2007 [1]. For 2008, it has been reported that 20% of fatally injured passenger car occupants were ejected, either totally or partially [2]. For this reason, NHTSA has been studying ejections for a number of years. In November of 2006, NHTSA published details of a component test method being used for researching ejection mitigation, which was being considered for rule making [3]. The agency's test consists of a linearly guided impactor that projects an 18 kg impacting mass in the shape of a featureless head-form. This 18 kg mass is designed to be representative of the impacting mass of an AM50 occupant. Four impact locations are tested on each of the daylight openings to which the evaluated countermeasure is applied. Using a potentiometer, the impactor measures the excursion of the head-form beyond the inside glazing surface of the daylight opening. At the time NHTSA was researching two proposals summarized in Table 1. Both proposals consisted of two test conditions: the first test was conducted at a 1.5 second delay (time after curtain deployment); the second test was conducted at a 6 second delay. For the first test, there were two energy levels NHTSA considered, 280 Joules or 400 Joules. The proposed impact energy for the second test (6 second delay) was 178 Joules. These test conditions were determined on the basis of dummy pendulum testing, video analysis of full scale rollover tests, and sled testing, replicating rollover and side impact events, outlined by NHTSA in the Advanced Glazing First Status Report [4]. Figure 1 shows a typical setup for the ejection mitigation component test, and it outlines the method for determining the impact locations for each daylight opening.

Table 1.
NHTSA Linear Impactor Test Conditions

	Impact Mass	Test Energy	
		1.5 second delay	6.0 second delay
Proposal 1	18 kg	400 Joules Test Speed = 24 km/h	178 Joules Test Speed = 16 km/h
Proposal 2		280 Joules Test Speed = 20 km/h	

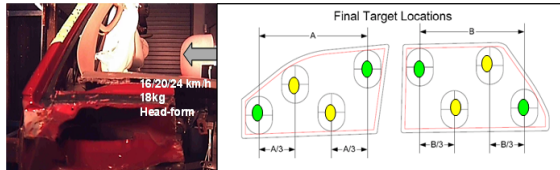


Figure 1. NHTSA ejection mitigation linear impact component test setup.

In December of 2009, NHTSA issued a notice of proposed rule making (NPRM) for Federal Motor Vehicle Safety Standard (FMVSS) No. 226 "Ejection Mitigation" [5]. In the NRPM the agency proposes a component test based on 'Proposal 1' of its research test method with the first test conducted at an impact energy of 400 Joules (24 km/h) 1.5 seconds after the curtain airbag is deployed. A second test is conducted at an impact energy of 178 Joules (16 km/h) with a 6 second delay after deployment. In January 2011, NHTSA published the final rule for FMVSS 226. In the final rule the agency reduced the test speed for the first test from 24 km/h to 20 km/h, thus the final rule is based on 'Proposal 2' [6].

During NHTSA's advanced glazing research, Willke et al. estimated that of 7,636 fatalities in 1999 involving partial or complete ejections through glazing, 2,864 of those occurred in planar crashes [7]. The NPRM for FMVSS 226 used 1997-2005 NASS CDS data adjusted to 2005 FARS level to estimate that 6,174 fatalities occurred in crashes involving ejections through side windows, including the first two seating rows [5]. Of these 6,174 fatalities, 1,568 occurred specifically in side impact planar collisions. In a more recent analysis, the NHTSA National Center for Statistics and Analysis (NCSA) examined vehicle occupants in fatal crashes from 2003 to 2007 (FARS data) to study ejection factors. In these crashes, 54,505 occupants were ejected, including both fatalities and survivors. Approximately 72% (39,312) of these 54,505 occupants were involved in rollovers. Approximately 21% (11,459) of these 54,505 occupants were ejected when the initial impact was on either the left or right side. While the data does not indicate how many of these side

impacts also involved a subsequent rollover, it is interesting to note that a larger percentage (13.1%) of occupants were ejected when the initial impact was against the side of the vehicle versus the front (9.8%) or rear (10.6%). The only other describable type of initial impact which resulted in a larger percentage of ejections at 42.9% is a non-collision. Non-collisions are thought to consist largely of rollovers; "...many rollovers occur without being initiated by an impact with other vehicles or fixed objects" [8] (ref: DOT HS 811 209).

The intent of the current study is to research representative energy levels for testing ejection mitigation systems considering rollover and side impact crashes in belted and unbelted conditions and compare these results with the test parameters outlined in the FMVSS 226 NPRM and final rule.

METHOD

Curtain airbags developed for ejection mitigation must serve two purposes: to help mitigate the risk of ejection in rollovers while also providing occupants protection in side impacts. As such, care should be taken to balance the performance requirements when developing the restraint systems. The purpose of this research was to study this balance in the development of curtain airbags. To accomplish this, this study was divided into two portions:

- Occupant Containment Energy Case Study
- Curtain Airbag Parameter Study

Occupant Containment Energy Case Study

Rollover case Four rollover tests were considered for analysis (reference Table 2). For the purposes of this study, the authors chose to use the number of quarter-turns as a comparative metric for rollover severity. This was deemed to be reasonable given Moore's finding that the risk of ejection increases from 5% and 20% for less than 4 quarter-turns to 10% and 80% for greater than 12 quarter-turns for belted and unbelted occupants, respectively [9]. Thus, as the number of quarter-turns increases so does the risk of ejection. Of the four tests considered, the FMVSS 208 Dolly rollover had the highest number of quarter-turns with a total of 12. Furthermore, the 12 quarter-turns value represents over 98% of field incidents with a MAIS 3 or greater injury (Figure 2). Therefore, it was concluded that the dolly rollover was the most severe of the tests considered, and while not a repeatable test, it

provides a reasonable representation of a severe rollover for the purposes of this particular study.

Table 2
Rollover testing summary

Test Mode	Test Speed (km/h)	No. of Quarter-Turns (Severity)	Peak Angular Rate (Degrees / second)	Duration (Seconds)
FMVSS 208 Dolly Rollover	50	12	450	4.5
Corkscrew Rollover	70	1	209	4.2
Curb Trip Rollover	27	2	168	3.7
Ditch Rollover	25	1	115	4.5

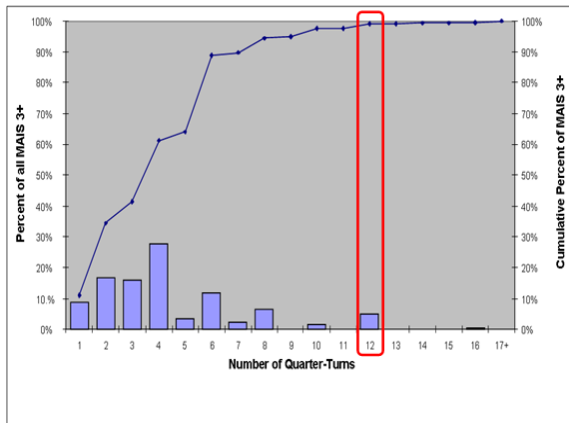


Figure 2. MAIS 3+ injuries vs. number of quarter turns [10].

The test vehicle was instrumented to measure the accelerations and angular velocities in the X, Y, and Z directions in the vehicle's local coordinate system. This data was then used as inputs for a MADYMO model using a prescribed motion technique as proposed by Yu, et al. [11]. The following conditions were used for the analysis:

1. AM50 occupants were used in the front outboard seating positions.
2. Both belted and unbelted conditions were considered for analysis.
3. All components which the dummy interacted with were included in the model (Figure 3).

Figure 4 shows the occupant kinematics from the MADYMO model. The vehicle orientation relative to the global coordinate system is also shown for reference. To estimate the maximum energy with which an occupant may impact an ejection mitigation countermeasure, the energy transfer between the

interior components and the dummy was measured in the simulation. In a rollover, occupants tend to move outward and upward interacting with the side window glazing and the headliner. The balance in the energy sharing between these two components will vary depending on the vehicle layout and occupant position. Therefore, it is difficult to predict an appropriate energy considering only the impact with the window glazing on these two vehicle layouts. For this reason, the sum of the energy transfers between the occupant and both the window glazing as well as the headliner were used.

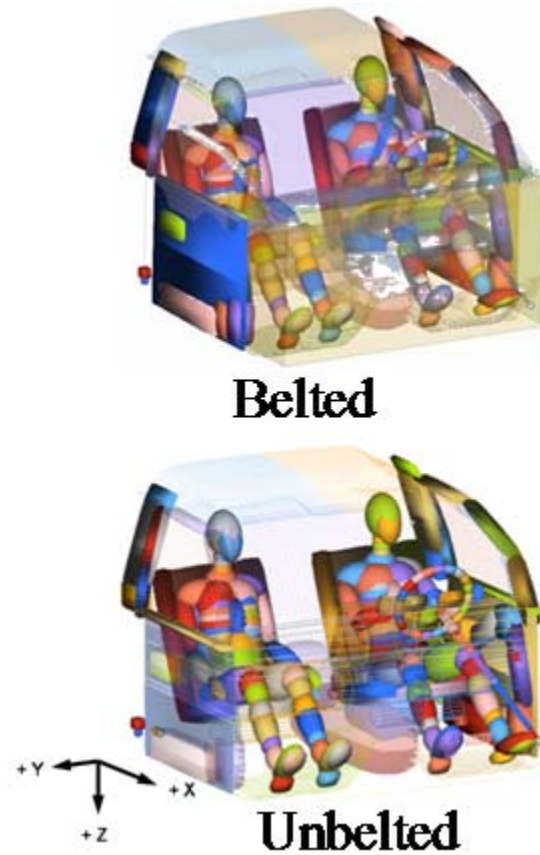


Figure 3. MADYMO ellipsoid model for rollover with belted and unbelted occupants.

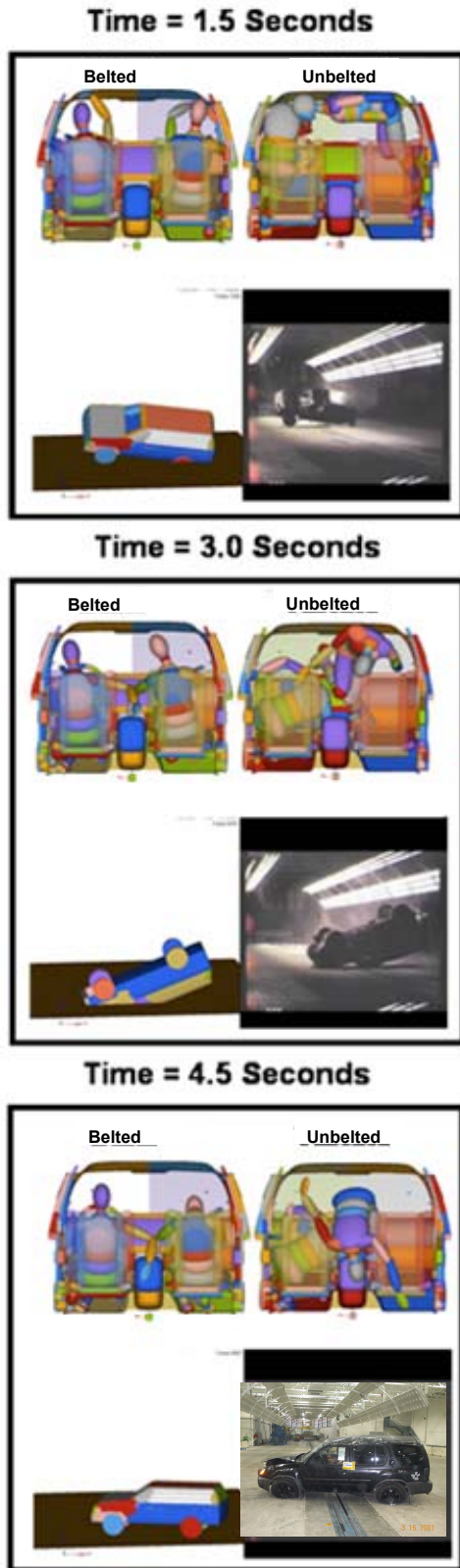


Figure 4. Occupant and vehicle kinematics for the dolly rollover test.

Side impact case In order to select a representative delta velocity for the simulations used in this study, two side impact tests conducted per the New Car Assessment Program (NCAP) moving barrier protocol were examined. One test was conducted on a passenger car and the second on a sport utility vehicle to cover a wide range of vehicle architectures. Both vehicles showed a delta velocity of approximately 24 km/h as measured at the vehicle center of gravity. While research which relates delta-velocities to ejection rates in planar crashes appears to be limited, NHTSA did publish such information in support of its Ejection Mitigation NPRM. Their study, which consisted of analyzing 1995-2004 NASS-CDS data, shows that 65.5% of side impact ejections occur at delta velocities less than 24 km/h (Figure 5) [5]. Also mentioned in the NPRM is that NHTSA simulated two conditions in tests it performed to develop the impactor mass – one representative of a rollover and one of a side impact. “For the test designed to be more representative of a side impact condition, the test was conducted at an impact speed of 24 km/h”. Thus, indicating that the vehicle tests chosen for this study provide a reasonable representation of side impact crashes in the field.

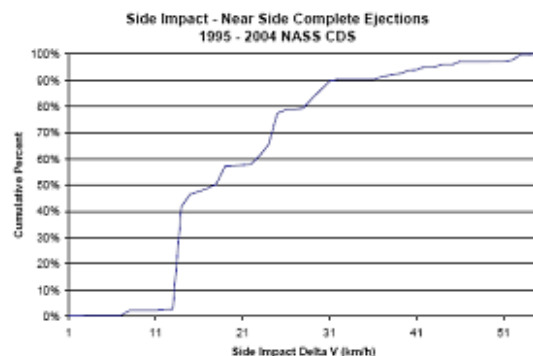


Figure 5. Completely Ejected Occupants vs. Delta-V in side impact crashes (Source: Notice of Proposed Rulemaking Ejection Mitigation (FMVSS 226), Figure 1.6 – generated from 704 unweighted ejections and 15,062 weighted ejections).

Both vehicles used in the NCAP tests were instrumented to measure the velocity at the test vehicle C.G., struck side door at the chest, abdomen, and pelvis; as well as the struck side roof rail above the occupant’s head. This set of data was used as the inputs in a MADYMO model using a prescribed motion technique. The model consisted of four sections: 1) Pelvis trim, 2) Abdomen trim, 3) Thorax trim and 4) Window Glazing, with an AM50 (ES2)

ellipsoid dummy positioned on the driver seat. The velocity measured at the vehicle C.G. was applied to the seat and floor pan of the model, while the chest, abdomen, and pelvis velocities were applied to the applicable trim ellipsoids. The trim stiffness, obtained from component testing, was provided to the translational joints of each of the ellipsoids to reflect the trim deformations due to dummy loading. The velocity of the top of the window glazing was set to match that of the roof rail measured in the vehicle test, with the bottom of the glazing attached to the chest trim ellipsoid by means of a revolute joint so that the side window glazing kinematics match that of the vehicle test. Figure 6 shows the MADYMO model used for this study.

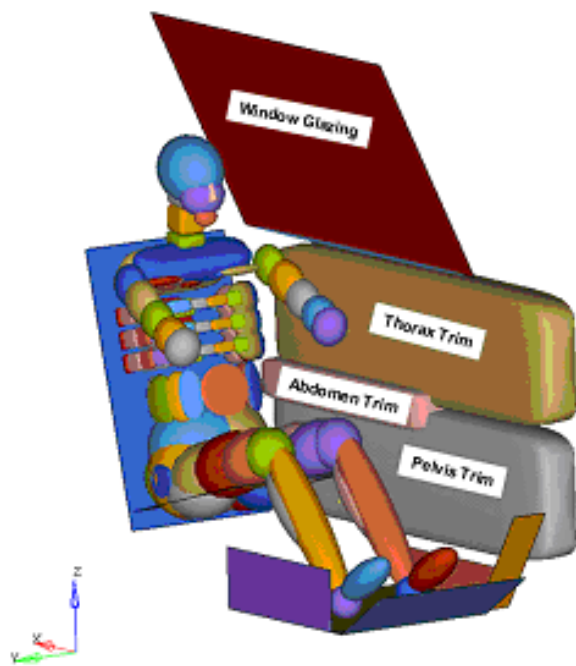


Figure 6. MADYMO ellipsoid model for side impact (unbelted model shown).

To ensure the occupant kinematics in the simulation correctly captured that of the vehicle test, the head, upper and lower spine (T1 and T12), and pelvis accelerations were correlated to the vehicle test. Figure 7 shows the kinematics of the occupant in the MADYMO model while Figure 8 displays the comparison of the correlated dummy responses for the passenger car vehicle and simulation. To estimate a representative occupant containment energy level that a curtain airbag may experience in a planar side impact crash, the energy transfer between the occupant and the side window glazing was measured. Figure 9 shows a comparison of the

energy transfer in the simulation compared with that measured in the vehicle test.

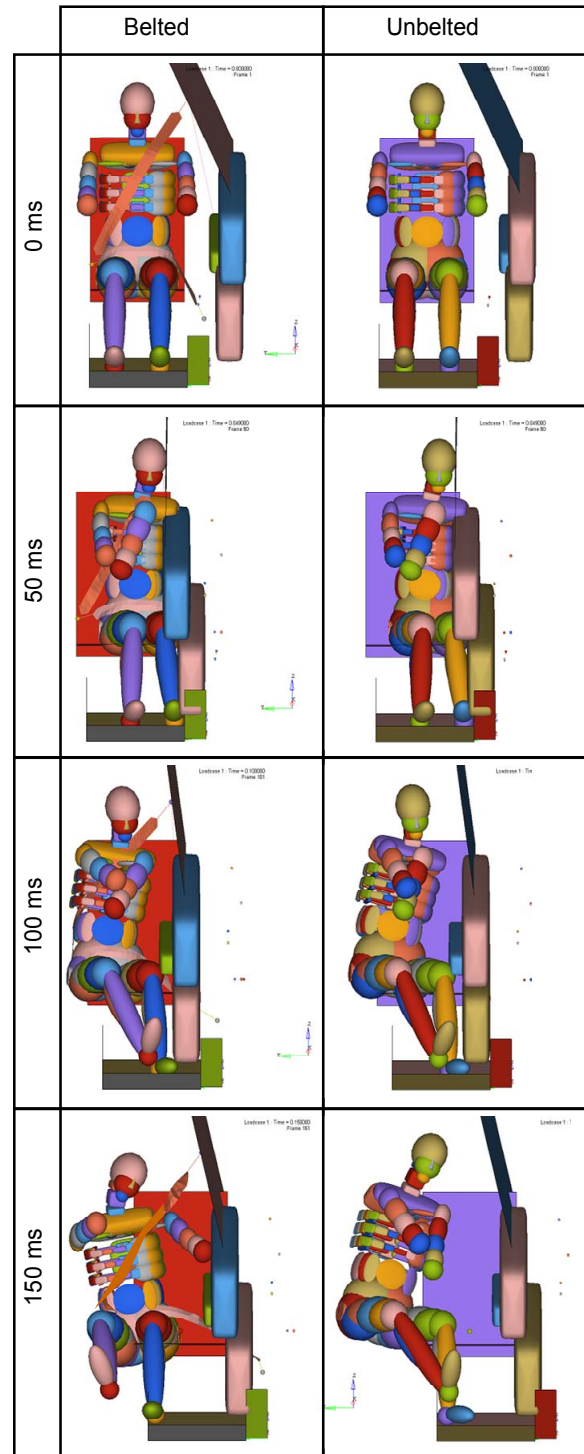


Figure 7. Typical Occupant Kinematics in the MADYMO model used for side impact.

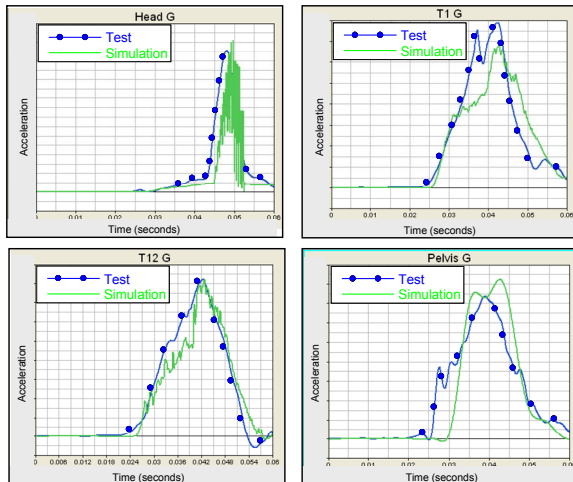


Figure 8. Occupant response comparison between the MADYMO side impact model and the vehicle test.

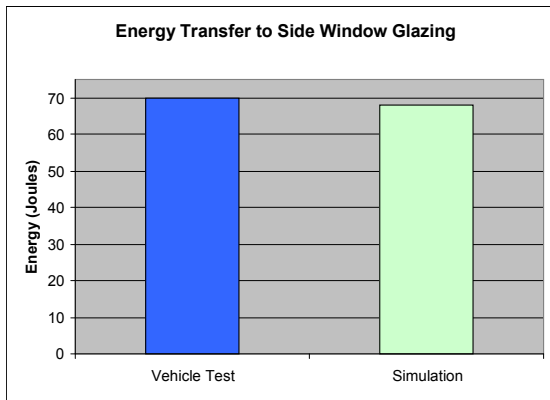


Figure 9. Comparison of the vehicle test and simulation occupant energy transfer to the side window glazing.

Once the correlation was completed, a parameter study was conducted to investigate the various interior layout parameters which may affect the energy transfer to the window glazing. A total of six interior dimensions were considered for this study:

1. Hip Point to armrest height
2. Chest to armrest offset
3. Armrest to pelvis offset
4. Hip Point to waistline height
5. Hip Point to door trim
6. Side window glazing angle

Figure 9 shows how each of the parameters were defined. A total of eight vehicles ranging from a sub compact car to a full size truck were analyzed to determine the range of values to consider for each

parameter in the study. Based on the observed ranges for each of the parameters, a sensitivity analysis was conducted at 3 levels for each to determine which interior layout parameters most affect the energy transfer to the glazing. Table 3 summarizes the levels used for the sensitivity analysis (reference Table 4 in the appendix for a detailed summary of each of the vehicles studied). Once the most sensitive interior layout parameters were determined, the most severe interior layout was evaluated in more detail to determine the maximum energy transferred to the window glazing.

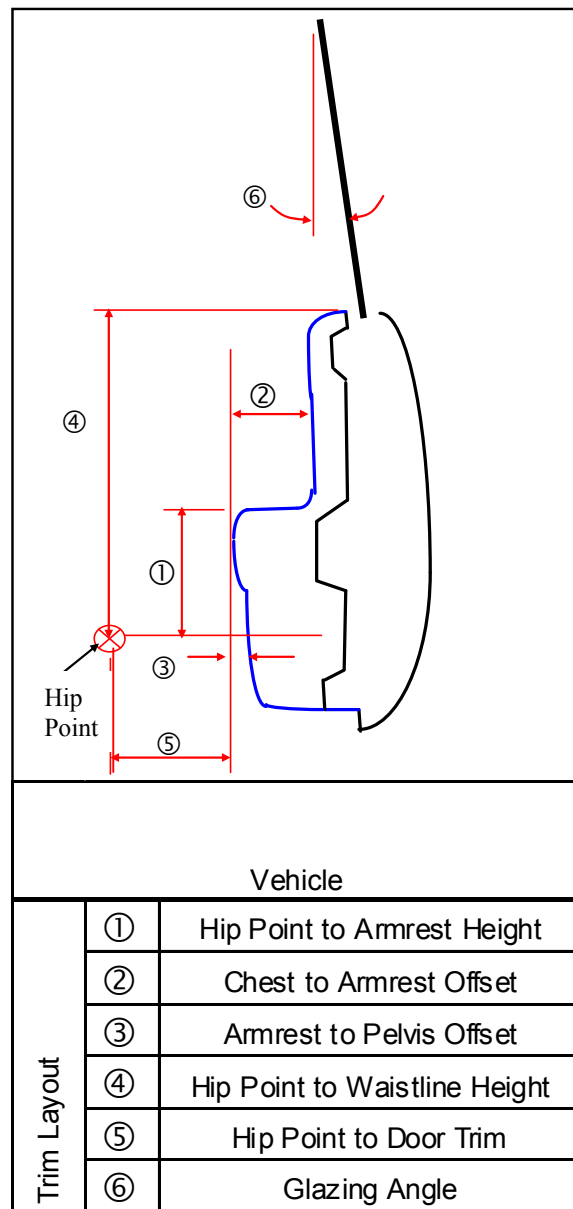


Figure 10. Interior layout parameters considered for this study

Table 3
Summary of interior dimensions and sensitivity analysis levels.

Measurement			Sensitivity Analysis			
			Level 1	Level 2	Level 3	
Trim Layout	①	Hip Point to Armrest Height	(mm)	168	198	227
	②	Chest to Armrest Offset		34	51	68
	③	Armrest to Pelvis Offset		1	41	81
	④	Hip Point to Waistline Height		314	408	502
	⑤	Hip Point to Door Trim		281	296	310
	⑥	Glazing Angle		(deg)	2.8	15.8

Curtain Airbag Parameter Study

A linear impact testing method was used to simulate an oblique pole side impact test at 32 km/h as outlined in FMVSS 214 [12]. A 254mm simulated rigid pole was positioned directly behind the Head C.G. impact location. The test setup is shown in Figure 11. A Hybrid III AM50 half head-form was mounted on a linear actuator with an effective mass of 5.5 kg. Testing was conducted for both the AM50 and AF05 seating positions. The impact speed was adjusted to achieve the desired impact energy for the AM50 or AF05 occupants depending on which position was tested. The head injury criterion (HIC) was predicted based on the peak force measured in the component test.

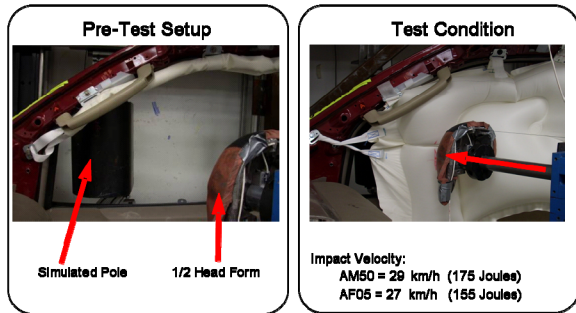


Figure 11. Linear impact test setup used to simulate the FMVSS 214 oblique pole test.

Ejection mitigation testing was conducted per the NHTSA proposed test procedure at the 1.5 second delay for both the 280 Joules and 400 Joules testing

conditions (20 and 24 km/h). Figure 1 shows the impact points used for this testing.

For this study a rollover curtain airbag with the following specifications was used (reference Figure 12 for a picture of the deployed airbag).

1. A stored gas inflator was used for this study.
2. The curtain airbag covered all impact locations for both the oblique pole test positions (AM50 and AF05) as well as the ejection mitigation test points.
3. There was full overlap with the B-Pillar.
4. The airbag was tethered to the base of the A-Pillar and overlapped the door waistline by approximately 100 mm.
5. The chamber depth was 200 mm.



Figure 12. Curtain airbag used for airbag pressure parameter study.

RESULTS AND DISCUSSION

Occupant Containment Energy Case Study

Rollover case In case of the belted condition, the seatbelt functioned to restrain the occupant in the seat during the duration of the event, and provided for much more controlled occupant kinematics as is shown in Figure 4. Furthermore, since the seatbelt restrained the occupant in their seat it will mitigate the risk of ejection regardless of the ejection path in this case, while the curtain airbag will only function to mitigate the ejection risk through the side windows. Therefore, the seatbelt should be considered the

primary countermeasure to help mitigate the risk of ejection.

Figure 13 and 14 summarizes the simulation results plotted as occupant contact energy versus time. Figure 13 displays the results for the unbelted occupant while Figure 14 show the results for the belted occupant. There were multiple contacts with the interior for both the driver and passenger occupants (both belted and unbelted) throughout the duration of the event. In the unbelted case, a peak contact energy of 207 Joules was observed for the driver at 0.75 seconds; as opposed to a peak contact energy of 8 Joules in the belted case at 1.5 seconds. The peak passenger energy in the unbelted case was 206 Joules, occurring at 1.75 seconds while the peak passenger contact energy in the belted case was 7 Joules at 3.8 seconds.

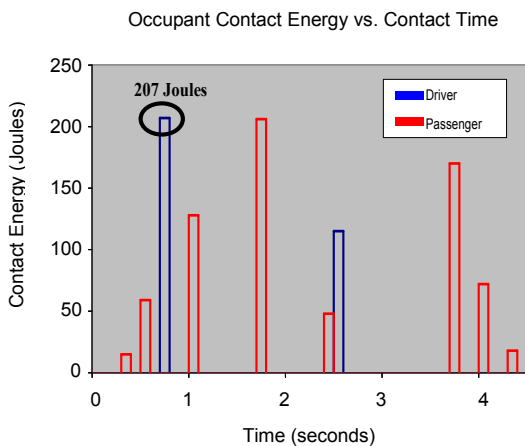


Figure 13. Occupant contact energy for the FMVSS 208 dolly rollover test simulation with unbelted occupants.

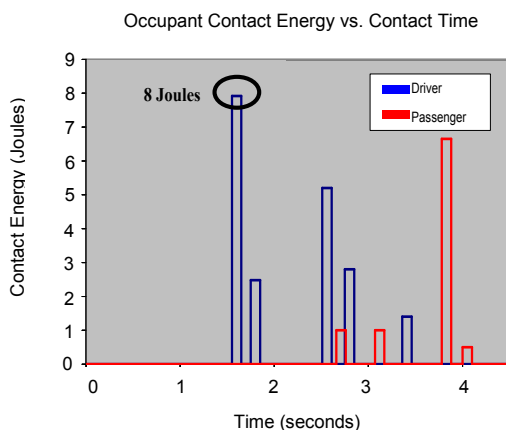


Figure 14. Occupant contact energy for the FMVSS 208 dolly rollover test simulation with belted occupants.

Figure 15 shows the results of the unbelted case (most severe case studied) compared to each of NHTSA’s proposals for ejection mitigation testing. The circles show the test energy at the appropriate delay times. A dashed line is drawn in to represent, in theory, the minimum performance that might be expected from a curtain airbag if developed to meet the performance requirements of each of the two proposals. It should be noted, however, that the dashed lines are provided for visualization purposes, and the actual performance of a curtain airbag may differ from this line. As can be seen, the occupant energy levels for both the driver and the passenger observed in the test analyzed fall below the thresholds of NHTSA’s proposals. Thus, either of NHTSA’s proposed energy levels appear adequate for the energy levels studied in this particular case.

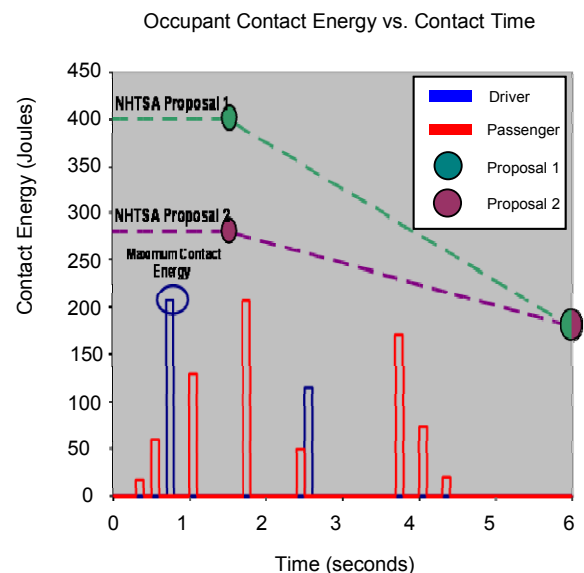


Figure 15. Occupant contact energy for the FMVSS 208 dolly rollover test simulation with belted occupants compared with each of the NHTSA proposals for ejection mitigation testing.

Side impact case In the side impact case there was not a discernible difference in the energy transferred to the window glazing between the belted and unbelted conditions. During the initial impact, the coupling between the occupant and the vehicle in the lateral direction through the seatbelt was negligible resulting in similar occupant kinematics during the initial impact for the unbelted and belted conditions. However, during the rebound the seatbelt functioned to restrain the occupant in the seat similar to the rollover case providing more controlled

occupant kinematics (Figure 7). Furthermore, all simulations were conducted with glazing in place; as result, it does not show the benefit of the seatbelt when the glazing is not present. As such, the authors feel the seatbelt is still the primary countermeasure for ejection mitigation in side impact crashes while the curtain may help further mitigate the risk of ejection through the side windows.

Figure 16 summarizes the results of the sensitivity analysis for the interior layout parameters. By far the most sensitive interior parameter affecting the energy transfer to the glazing was the waistline height. Window glazing angle did show some influence on the energy transfer, however, it was not nearly as significant as the waistline height. The other interior parameters showed very little effect on the energy transfer.

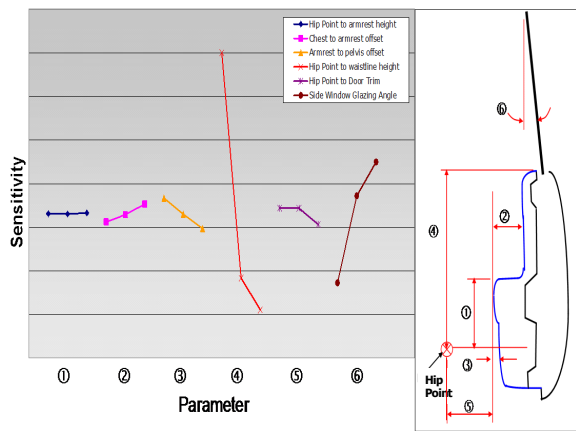


Figure 16. Sensitivity of the various interior layout parameters on the energy transfer to the window glazing.

Therefore, to better understand the effect of waistline height on the energy transfer to the side window glazing, a more detailed simulation study was conducted. This was done by setting all of the interior parameters to the most severe levels based on the sensitivity analysis, and then varying the waistline height. Figure 17 shows the energy transfer to the glazing versus the waistline height. As in the sensitivity analysis, the amount of energy transferred to the glazing increased as the waistline was lowered. In all cases the passenger car showed higher energy values for a given waistline height than did the SUV. This was due to the fact that while the delta velocity as measured at the vehicle center of gravity was similar for both vehicles, the SUV had substantially lower door intrusion velocities as measured at the occupant chest due to the fact that

the occupant was seated higher than the impacting barrier, whereas in the passenger car, the occupant is more inline with the barrier as shown in Figure 18.

The maximum energy transfer to the window glazing observed was 168 Joules, which occurred in the passenger car test condition at the lowest waistline height observed for the vehicles investigated (314mm Hip Point to waistline height) in this study. Furthermore, if the waistline height is further reduced to the point that it is flush with the top surface of the armrest (168 mm hip point to waistline height), the maximum energy transferred to the side window glazing was 258 Joules, still below the 280 Joules outlined in the final rule for FMVSS 226. Thus a curtain airbag developed to the 280 Joules test is expected to be adequate to mitigate the risk of an ejection in the side impact tests evaluated in this study.

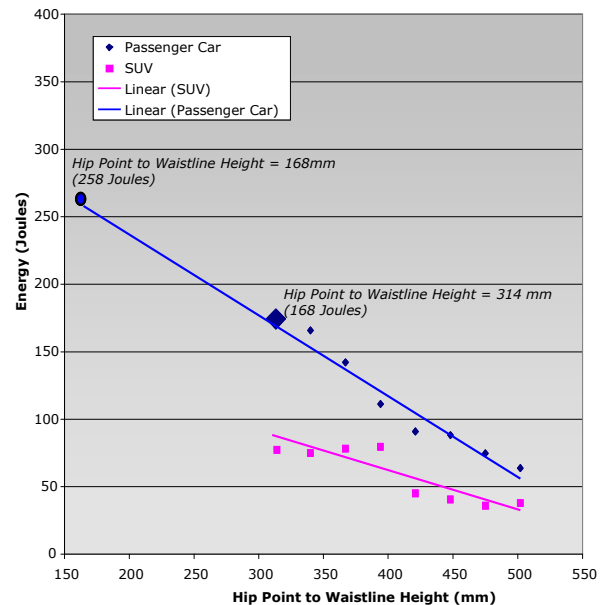


Figure 17. Energy Transfer to glazing versus Hip Point to waistline height

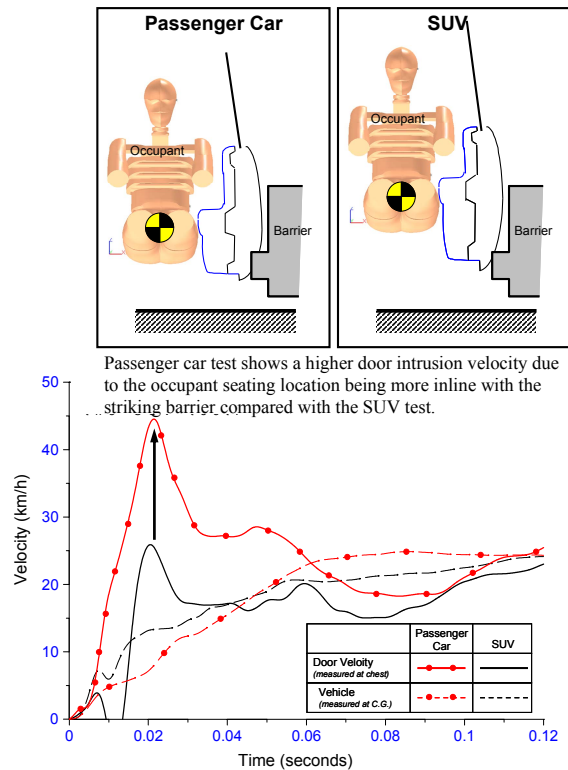


Figure 18 Comparison of Door and Vehicle C.G. velocities for the Passenger Car and SUV tests.

Curtain Airbag Parameter Study

Several airbag pressures were evaluated using the ejection mitigation component test. Pressures were determined which would achieve the excursion criteria proposed by NHTSA (100mm beyond the plane of the side window) for both the 280 and 400 Joules test conditions. Linear impact testing simulating the oblique pole condition was then conducted at each of the pressures. The results are summarized in Figure 19. The upper plot shows the maximum excursion from the ejection mitigation tests for both the 400 and 280 Joules test conditions versus the bag pressure. The excursion measured at location 1 was used for this plot, as it consistently showed the highest result (reference Figure 20 in the appendix for detailed results). The lower plot shows the predicted HIC from the simulated side impact as a function of the bag pressure. As would be expected, the excursion seen in the ejection mitigation test reduced as the bag pressure was increased. Furthermore, lower excursions were observed in the 280 Joules test as compared with those observed in the 400 Joules test at the same airbag pressures. However, in the side impact component testing, HIC levels increased by 37% and 42% for the AM50 and AF05 occupants, respectively, when the curtain

pressure was optimized to the 400 Joules ejection mitigation test as opposed to the 280 Joules test. Thus, there is a trade-off for side impact when optimizing for ejection mitigation at the higher energy level.

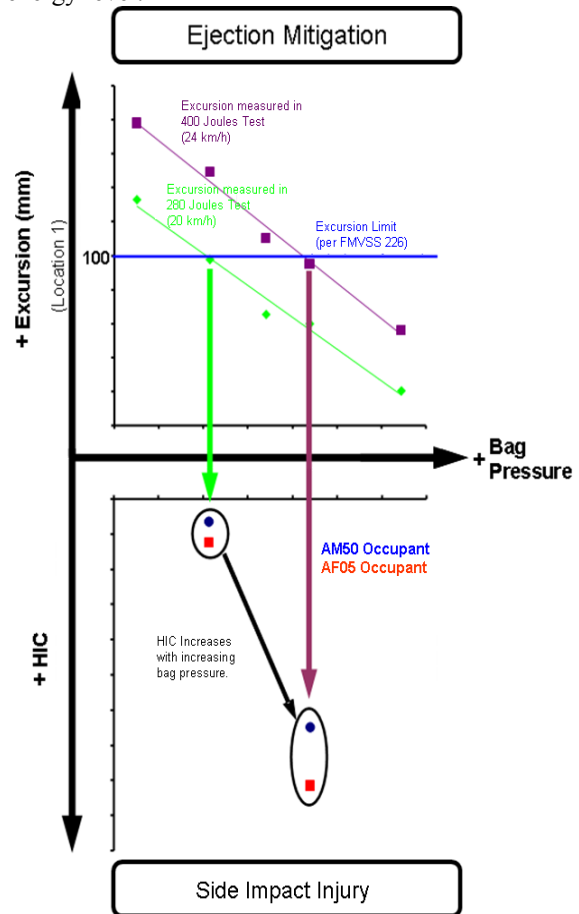


Figure 19. Curtain airbag pressure sensitivity considering rollover and side impact.

CONCLUSION

1. In the cases studied, the seatbelt was effective to help control the occupant kinematics functioning as the primary ejection mitigation countermeasure. The occupants remained restrained in the seat throughout the duration of the events studied. Furthermore, in the rollover cases the energy transferred to the side window glazing was substantially lower in the belted cases than in the unbelted cases. The curtain airbag may help further mitigate the risk of ejection through the side window glazing in the cases studied.

2. Either of NHTSA's proposals of 280 and 400 Joules would likely be adequate in both the rollover and side impact cases studied.
 - a) Maximum energy observed in the rollover case was 207 Joules for the unbelted AM50 occupants.
 - b) Maximum energy observed in the side impact case was 258 Joules for the unbelted AM50 occupants.
3. A curtain airbag optimized for the 400 Joules ejection mitigation test will likely have a higher HIC in side impact than one optimized for the 280 Joules test condition. Therefore, it is concluded that the 280 Joules ejection mitigation test condition allows for a better balance with side impact injury mitigation while likely still providing adequate protection for ejection mitigation in the events simulated. For this reason, the authors agree that NHTSA's direction to reduce the test speed for the 1.5 second delay ejection mitigation test to 20 km/h is preferred as compared to the previously proposed 24 km/h.

Administration, Docket No. NHTSA-2006-26467-0001, November 2006

4. "Ejection Mitigation Using Advanced Glazing A Status Report, November 1995", Advanced Glazing Research Team, National Highway Traffic Safety Administration, November 1995.
5. Notice of Proposed Rulemaking, Federal Motor Vehicle Safety Standard No. 226 "Ejection Mitigation", National Highway Traffic Safety Administration, Docket No. NHTSA-2009-0183, December 2, 2009
6. Department of Transportation, Standard No. 226 Ejection Mitigation, Part 571.226
7. Willke, Donald, et al., "Ejection Mitigation Using Advanced Glazing, Final Report", National Highway Traffic Safety Administration, August 2001.
8. "Factors Related to the Likelihood of a Passenger Vehicle Occupant Being Ejected in a Fatal Crash", National Center for Statistics and Analysis, National Highway Traffic Safety Administration, DOT-HS-811-209, December 2009.
9. Moore, Tara L.A., et. al "Biomechanical Factors and Injury Risk in High Severity Rollovers." 49th Annual Proceedings of the Association for the Advancement of Automotive Medicine (AAAM), pp. 133-150. 2005.
10. Hare, Barry M., et al. "Analysis of Rollover Restraint Performance with and without Seat Belt Pretensioner at Vehicle Trip." SAE 2002-01-0941.
11. Yu, H, C.E. Sturgess, A.M. Hassan, "Simulation of vehicle kinematics in rollover tests with quaternions", DOI: 0.1243/0954407JAUTO360, July 2006.
12. Department of Transportation, Standard No. 214 Side Impact Protection, Part 571.214

ACKNOWLEDGMENTS

The authors would like to thank our colleagues for their technical and analytical support. In particular we would like to thank the following people: Erik Robins, Stewart Richards, Brett Garner, Marc Folsom, Doug Stein, Andrew Wesolowski, Brian Roeser, and Analia Jarvis.

REFERENCES

1. "Motor Vehicle Traffic Crash Fatality Counts and Estimates of People Injured for 2007" National Center for Statistics and Analysis. National Highway Traffic Safety Administration. DOT-HS-811-034, Updated February 2009.
2. Traffic Safety Facts 2008: "Passenger Vehicles", National Center for Statistics and Analysis, National Highway Traffic Safety Administration, DOT-HS-811-368.
3. "Research Test Procedure for Ejection Mitigation Testing", Office of Crashworthiness Standards, National Highway Traffic Safety

APPENDIX

Table 4
Summary of interior dimensions for eight vehicles
studied for the side impact sensitivity analysis.

Measurement		Vehicle							
		A	B	C	D	E	F	G	H
Trim Layout	① Hip Point to Armrest Height	172	227	200	200	207	168	260	184
	② Chest to Armrest Offset	64	65	34	39	40	68	77	79
	③ Armrest to Pelvis Offset	1	26	31	29	28	67	81	27
	④ Hip Point to Waistline Height	429	457	502	473	475	342	427	314
	⑤ Hip Point to Door Trim	281	298	295	300	305	285	302	310
	⑥ Glazing Angle	(deg)	6.32	20.4	28.8	23.7	25.2	17.3	15.4

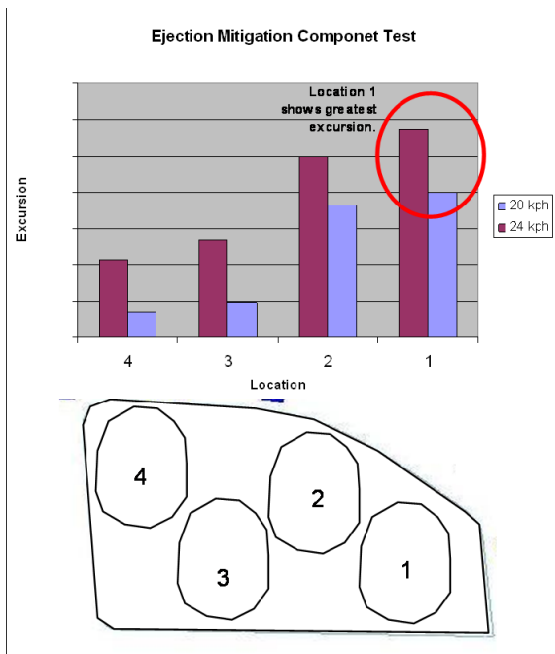


Figure 20. Typical excursion plot in the ejection mitigation test showing location '1' with the highest excursion.